AD NUMBER
AD338339
CLASSIFICATION CHANGES
TO: unclassified
FROM: confidential
LIMITATION CHANGES
TO: Approved for public release, distribution unlimited
FROM: Distribution authorized to U.S. Gov't. agencies and their contractors; Administrative/Operational Use; 27 MAY 1957. Other requests shall be referred to Naval Ordnance Lab., Silver Spring, MD.
AUTHORITY
NOL ltr, 6 Jun 1980; NOL ltr, 6 Jun 1980

AD 338 339L

DEFENSE DOCUMENTATION CENTER

FOR

SCIENTIFIC AND TECHNICAL INFORMATION

CAMERON STATION, ALEXANDRIA, VIRGINIA

DISCLAIMER NOTICE

THIS DOCUMENT IS BEST QUALITY PRACTICABLE. THE COPY FURNISHED TO DTIC CONTAINED A SIGNIFICANT NUMBER OF PAGES WHICH DO NOT REPRODUCE LEGIBLY.

NOTICE: When government or other drawings, specifications or other data are used for any purpose other than in connection with a definitely related government procurement operation, the U. S. Government thereby incurs no responsibility, nor any obligation whatsoever; and the fact that the Government may have formulated, furnished, or in any way supplied the said drawings, specifications, or other data is not to be regarded by implication or otherwise as in any manner licensing the holder or any other person or corporation, or conveying any rights or permission to manufacture, use or sell any patented invention that may in any way be related thereto.

NOTICE:

THIS DOCUMENT CONTAINS INFORMATION AFFECTING THE NATIONAL DEFENSE OF THE UNITED STATES WITHIN THE MEANING OF THE ESPIONAGE LAWS, TITLE 18, U.S.C., SECTIONS 793 and 794. THE TRANSMISSION OR THE REVELATION OF ITS CONTENTS IN ANY MANNER TO AN UNAUTHORIZED PERSON IS PROHIBITED BY LAW.

(S) 625 400

WT-1005 (NOLR-1215)
(ITR-1055)

161 A

Operation VIGWAM

Military Only

1955

t 1.2

...WATER FREE-FIELD PRESSURES TO JUST BEYOND TARGET LOCATIONS

(Chief Security Div DASA
Auth 7 Mar 1958)

Issuance Date: May 27, 1957

This document contains restricted data as defined in the Atomic Energy Act of 1954. Its transmittal or the disclosure of its contents in any manner to an unauthorized person is prohibited.

Formerly Restricted Data

COMMANDER TASK GROUP 7.3

UNCLASSIFIED

"This document contains information affecting the National Defense of the United States within the meaning of the Espionage Laws, Title 18, U. S. C., Section 793 and 794. Its transmission or the revelation of its contents in any manner to an unauthorized person is prohibited by law."

If this report is no longer needed, return it to
AEC Technical Information Service Extension
P. O. Box 401
Oak Ridge, Tennessee

"This document contains information affecting the National Defense of the United States within the meaning of the Espionage Laws, Title 18, U. S. C., Section 793 and 794. Its transmission or the revelation of its contents in any manner to an unauthorized person is prohibited by law."

UNCLASSIFIED

④ NA ⑤ 625 200 UNCLASSIFIED

MT-491
cy 1

REG. NO. 15593
LOG. NO. 11625
WDSOT

WT-1005 (NOLR-1215)
(Supersedes ITR-1055)

This document consists of 254 pages
No. 161 of 225 copies, Series A

Report to the Scientific Director

⑥ UNDERWATER FREE-FIELD PRESSURES TO JUST BEYOND TARGET LOCATIONS

MT, ⑦ NA
⑧
⑨ NA

⑩ By

C. J. Aronson,
J. F. Bampfield,
E. A. Christian,
E. J. Culling,
V. F. DeVost,
F. J. Oliver,
R. S. Price,
J. P. Slifko and
M. A. Thiel,

Approved by: C. J. ARONSON
Project Officer
Project 1.2

Lt Col G. F. WATKINS, USAF
Director, Program I

Approved by: A. B. FOCKE
Scientific Director
Operation Wigwam

⑪ 27 May 56, ⑫ 254p. ⑬ - ⑰ NA

Explosives Research Department
Naval Ordnance Laboratory
White Oak, Silver Spring, Maryland
May 1956

⑱ NOL; DASA
⑲ 1215; WT/1005
⑳ S ㉑ NA

RESTRICTED DATA

This document contains restricted data as defined in the Atomic Energy Act of 1954. Its transmittal or the disclosure of its contents in any manner to an unauthorized person is prohibited.

UNCLASSIFIED

CONFIDENTIAL UNCLASSIFIED

ABSTRACT

Mechanical, piezoelectric, and Wiancko pressure-time gages and ball-crusher peak-pressure gages were used to measure the underwater free-field pressures from the deep explosion of an atomic bomb predicted to have the energy of 66 × 10^6 lb of TNT. Gages were located at distances from Surface Zero from about 2000 to 12,000 ft ~~(it was necessary to determine final gage locations by computations based on shock arrival times)~~ and were suspended at depths down to 2000 ft from buoys, LCM hulls, and YFNB barges. Although many of the gages and records were lost, there was an adequate number of backup systems that provided a wealth of detailed pressure data. The principal results of this experiment were:

1. The peak pressure vs distance curve for free water in the region measured was essentially as predicted by Project 1.1 and was similar to one which would have resulted from an explosion of TNT having a yield equivalent to $\frac{2}{3}$ the radiochemical yield of 32 metric kt.

2. The best estimate of the first bubble period was 2.878 sec, from which was calculated a TNT yield equivalent to $\frac{3}{4}$ the radiochemical yield. This can be compared with the Project 1.1 prediction of 2.88 sec. The second and third bubble periods were 2.6 and 1.9 sec, respectively. Migration of the bubble to about the time of the first minimum was 400 ft.

3. The effect of the temperature structure in the water in refracting the shock wave was essentially as predicted—increasing the pressures and decreasing the duration of the shock wave.

4. Shock-wave energy flux and impulse varied with distance differently from TNT in a homogeneous medium when corrections were made to account for the time of integration. The differences are believed to have arisen from a basic difference between the shock waves produced at Operation Wigwam and those from TNT or from refraction effects.

5. There were at least three bottom reflections, all attributable to the primary shock's being reflected from successively deep bottom layers.

CONFIDENTIAL UNCLASSIFIED

PREFACE

Project 1.2 was one of three projects to measure underwater pressures on Operation Wigwam, each covering separate regions with some overlaps. The other projects were Project 1.2.1, conducted by the Naval Research Laboratory, which measured pressures closer to the bomb, and Project 1.3, conducted by the Navy Electronics Laboratory, which measured pressures farther from the bomb. Project 1.2 represented the major effort of the Naval Ordnance Laboratory (NOL) on this operation and, together with information from the other NOL projects (1.1, Energy Distribution Studies; 1.4, Bubble Phenomena; and 1.5, Gross Surface Phenomena), was to obtain an over-all picture of the free-field effects of an underwater atomic burst. Techniques used by Project 1.2 were developed from allied techniques used on previous operations, principally Operation Castle, and on routine research on high explosives conducted over a period of several years by the NOL and the Underwater Explosives Research Laboratory of the Office of Scientific Research and Development. Although most of the funding for this project was supplied by the Armed Forces Special Weapons Project, a substantial fraction was supplied by the Bureau of Ordnance.

This report contains the results of Project 1.2 completed up to the time of writing, although further analyses of the data may be worth while at later times.

Since there are so many facets to this project, there is some repetition so that readers concerned with one phase to the exclusion of others will not have to read portions beyond their immediate interest. For example, the basic results are discussed in detail in Chaps. 1 and 7 to 9 and are summarized in Sec. 10.2. Instrumentation is discussed in detail in Chaps. 2 to 6 and is summarized in Sec. 10.1. Although it was beyond the scope of Project 1.2, Appendix A, which is a discussion of the effects of the Wigwam shot on ships' sonar apparatus, is included since it is a subject of considerable military interest on which little information is available elsewhere.

ACKNOWLEDGMENTS

The authors and their associates on Project 1.2 gratefully acknowledge the outstanding cooperation and assistance rendered them by the officers and men of the USS Comstock, USS LST-1048, USS LST-975, USS Tawasa, USS Butternut, USS Bolster, Task Group 7.3 Boat Pool, and HRM-362 during the seagoing phases of Operation Wigwam.

Further acknowledgment is made to E. O. Arnold and his men of the Naval Repair Facility, San Diego, LT CDR E. J. Kratochvil, CDR D. R. Saveker, F. J. Friel, and J. N. Shellabarger, whose efforts contributed immeasurably to the successful preparation of this project for the Operation. The prompt, willing, and excellent assistance of CAPT J. P. Z. Reynolds, CDR F. D. Muir, and LT CDR O. A. Johnson and their men in solving logistics and supply problems and in devising operating procedures to expedite the work is also gratefully acknowledged.

Appreciation is expressed to the personnel of the Navy Electronics Laboratory and the Naval Station, San Diego, for their hospitality, cooperation, and assistance throughout all phases of this Operation.

The over-all planning of this project was largely the result of the work of Dr. Paul M. Fye, Dr. G. K. Hartmann, Dr. J. E. Ablard, and Dr. E. Swift, Jr., of the Naval Ordnance Laboratory, and of Dr. A. B. Focke, CAPT J. H. Lofland, and Lt Col G. F. Watkins of the Armed Forces Special Weapons Project.

The Project Officer especially thanks James R. Mitchell, who ably handled the logistics and administrative details for him; Mrs. Ethel L. Rankin, for the artwork in this report; and Mrs. Caroline Fasig and Mrs. Donna Schindler, who contributed greatly to the preparation of this report in both its final and preliminary versions.

CONTENTS

SECRET – RESTRICTED DATA

CONTENTS (Continued)

CONTENTS (Continued)

CONTENTS (Continued) CONFIDENTIAL

SECRET — RESTRICTED DATA

CONFIDENTIAL

CONTENTS (Continued) CONFIDENTIAL

ILLUSTRATIONS

SECRET—RESTRICTED DATA

CONFIDENTIAL

ILLUSTRATIONS (Continued) CONFIDENTIAL

SECRET — RESTRICTED DATA
CONFIDENTIAL

ILLUSTRATIONS (Continued) CONFIDENTIAL

ILLUSTRATIONS (Continued) CONFIDENTIAL

TABLES

SECRET — RESTRICTED DATA

CONFIDENTIAL

TABLES (Continued)

CONFIDENTIAL

SECRET—RESTRICTED DATA

CONFIDENTIAL

CHAPTER 1

INTRODUCTION

1.1 OBJECTIVE

The objective of Project 1.2, Operation Wigwam, was to measure peak pressures and pressure vs time under water in the region from about 1500 ft to about 12,000 ft from Surface Zero (SZ) arising from the explosion of a nominal 30-kt atomic bomb fired at a depth of 2000 ft in about 15,000 ft of water. Table 1.1 gives some of the basic data describing the Wigwam shot. Measurements were to be made from depths of 25 ft to 2000 ft, including the region where large scaled models of submarines were located as targets.

1.2 GENERAL CONFIGURATION OF ARRAY AND METHOD

The general array of bomb, targets, instrumentation platforms, and gage strings has been described in detail in other Wigwam reports. For purposes of this report, it is probably sufficient to say that the array comprised a tow about 30,000 ft long, at one end of which the bomb was suspended from the bomb-support barge (YC-473). Free-field underwater pressures were measured by the Naval Research Laboratory (NRL) from this barge to a depth of 1200 ft as described in reference 1, and arrival times were measured to within about 15 ft of the bomb by the Armour Research Foundation (ARF) as described in reference 2. Between the YC-473 and the nearest target (SQUAW-12) at about 5200 ft from SZ, Project 1.2 suspended pressure-gage strings of three types: ball-crusher peak-pressure gages, Naval Ordnance Laboratory (NOL) mechanical pressure-time gages, and electronic piezoelectric and electromechanical pressure-time gages. The ball-crusher gages were suspended from towline floats with separate rubber recovery buoys. The mechanical pressure-time gages were suspended from wooden floats held off the towline by 150-ft spars; the electronic gages were suspended from two modified LCM's (0-1 and 0-2). The ball-crusher and mechanical gages were completely self-recording, whereas the electronic gages were to have their signals recorded on magnetic tape in buoys which were to be freed from the LCM's by the arrival of the shock. Each of the three instrumentation barges (YFNB's 12, 13, and 29) was to have two gage lines on the portside for this Project and one gage line on the starboard for Project 1.3 (see reference 3). The gage line from the port bow was to support electronic gages, and the one from the port stern was to support the ball-crusher and mechanical pressure-time gages. On the YFNB's 12 and 13, an underwater camera for the bubble-displacement measurements of Project 1.4 (reference 4) was also to have been on the mechanical gage line. Measurement of the free-field underwater pressures in the region between the YFNB-29 and the towing tug, with the exception of a single string of Project 1.2 ball-crusher gages, was to have been made by Project 1.3.

Table 1.1 —WIGWAM SHOT CHARACTERISTICS

Location:	28° 39.6' N ± 0.25 mile	126° 10.5' W ± 0.5 mile (SOFAR)
	28° 44' N	126° 16' W (NAVIGATIONAL)
Time:	1300 PDT 14 May 1955	
Surface Conditions:	Wind:	NNE 18 Knots
	Humidity:	65 per cent (Relative)
	Temperature:	15°C
	Barometric Pressure:	1025 millibars
	Sea State:	5-ft sea, 7-ft swell, and 8.3 ft combined (average of highest one-third waves)
Depth of Water:	About 15,300 ft	
Depth of Charge:	2,000 ft	
Time of Actual Zero After Fiducial:		29 msec (EG&G) 12.5 msec (NRL) 13.0 msec (Used in this Report, unless otherwise noted)
Metric Kilo ton:	Measure of Energy Equal to 4.18×10^{19} ergs $\approx 10^{12}$ gm-cal	
Yield (RC):	32 ± 10% Metric KT (LASL October 1955) 35 $^{+10}_{-3.5}$ Metric KT (NRL October 1955) 30.5 ± 1 Metric KT (ARF HYDRODYNAMIC October 1955) 70.6×10^6 lbs of TNT at 1000 gm-cal/gm (from 32 metric KT)	

The over-all guiding principle for Project 1.2 was to back up all instrumentation in one or more ways to be sure that at least the minimum required information was obtained. This was done to an extent not often achieved even on an operation of the scope of Wigwam; and, as it resulted, most of these precautions were actually needed. In the instances where backup instrumentation systems were not essential, they provided enough check data to give considerable weight to the values obtained and a basis for estimating the accuracy and precision of the results.

1.3 OPERATIONS

1.3.1 Preshot Operations

Instrumentation was designed and built at NOL, White Oak and Indian Head, Md. Preliminary testing was conducted there and at the Navy Electronics Laboratory, San Diego, Calif. LCM modifications and other comparatively heavy construction work were done by the Naval Repair Facility, San Diego. Sea trials were made off the California coast on several occasions during the period January to April 1955.

1.3.2 Shot-time Operations

To prepare for the actual shot, personnel (see Table 1.2) were split into three main groups—one aboard the USS Comstock to prepare and set into operation the LCM instrument stations, one aboard each of the three YFNB's to prepare instrumentation located thereon, and one aboard the LST's 975 and 1048, to install the free-floating ball-crusher and mechanical pressure-time gages. The latter group actually made the gage installations from the USS Butternut (AN-9), the USS Bolster (ARS-38), and the LCM's operated by the Task Group 7.3 (TG 7.3) Boat Pool.

By D−2 all systems were considered ready to be installed and operated, and boats 0-1 and 0-2 were attached to the towline. The spars for the mechanical pressure-time gages were also attached to the tow. It was planned to lower the gage strings as soon as the tow was completed, which was scheduled for 1030 on D−1. Actually, the four ball-crusher-gage strings, one of the mechanical gage strings, and the gage strings from 0-1 and 0-2 were put into the water rather late in the afternoon on D−1, although the tow was not completed even by that time. The YFNB strings, except the port stern gage line on the YFNB-12 which was never installed, and the remaining mechanical pressure-time string were put into the water on D-day, the former in the predawn hours and the latter shortly after daylight. During the morning of D-day, both 0-1 and 0-2 buoys broke free from the modified LCM's as a result of sea action. The 0-2 buoy broke free at about H−6, and the 0-1 buoy, at about H−4. Since the apparatus in the buoys required starting signals from radios in the LCM's, but external to the buoys, no data were obtained from these two systems.

1.3.3 Recovery Operations

After the shot and after permission was granted, recovery commenced on the night of D-day with the hauling up of the two NOL gage strings on the YFNB-13. The remaining YFNB strings were recovered during the morning of D+1. It was not until the afternoon of D+1 that it was possible to start recovery work on the equipment which had been attached to the towline. Searching was done by two helicopter surveys of two craft each and by the USS Tawasa (ATF-92). By evening the latter had recovered the 0-1 buoy, both spar gage lines, and two of the ball-crusher-gage buoys from which the gage strings had been lost. The 0-2 buoy was recovered the next day, and two of the ball-crusher-gage lines and buoys were never seen.

Tables 1.3 and 1.4 summarize the Project 1.2 data that were recovered and used as a basis for the preparation of this report. Chapter 10 summarizes the results of this report.

Table 1.2—NOL FIELD GROUP, PROJECT 1.2 OF OPERATION WIGWAM

I. Aboard USS COMSTOCK to prepare and set in operation the ex-LCM's, O-1 and O-2

C. J. Aronson - Project Officer
R. S. Price - Crew Chief, O-1
J. P. Slifko - Crew Chief, O-2

R. L. Knodle - O-1	J. R. Mitchell - O-2
C. E. Hopkins - O-1	H. J. Stattel - O-2
D. H. Mitowitz - O-1	E. G. Nacke - O-2
L. D. Cooley - O-1	D. B. Wilhite - O-2

II. Aboard YFNB's

E. J. Culling - Chief, Electronics Gage Systems
F. J. Oliver - Chief, Mechanical Gage Systems
P. S. Bengston - Crew Chief, YFNB-12
J. F. Bampfield - Crew Chief, YFNB-13
V. F. DeVost - Crew Chief, YFNB-29
B. E. Cox - YFNB-12, Electronic Gages
H. W. Baggott - YFNB-12, Ball-Crushers
W. G. Zuke - YFNB-12, Mechanical Gages
J. F. Fitz - YFNB-13, Electronic Gages
H. H. Haug - YFNB-13, Ball Crushers
J. B. Dempsey - YFNB-13, Electronic Gages
H. B. Benefiel - YFNB-29, Mechanical Gages
A. E. Jones - YFNB-29, Ball Crushers
C. W. Mangold - YFNB-29, Electronic Gages
C. H. Somers - YFNB-29, Electronic Gages

III. Aboard LST's to put down free floating ball-crusher and mechanical pressure-time gages

M. A. Thiel - Chief, Ball-Crusher Group
W. F. Carver - Mechanical Gages
D. L. Marks - Ball-Crushers
C. F. Vogt - Mechanical Gages
J. W. Thompson - Ball-Crushers
J. H. Baker - Ball-Crushers

Table 1.3—PROJECT 1.2 DATA-RECOVERY SUMMATION

Station	Horizontal Distance (ft)	Type of Gage	No. of Gages	No. of Channels [b]	No. of Channels Recovered	No. of Data Channels	Remarks
	1520[a]	B/C	176	44	0	0	
O-1	1920[a]	B/C	216	54	0	0	Buoy recovered but all gages lost.
O-1	2150	EPT	12	18	0	0	Buoy broke free before zero time.
	2900	MPT	7	7	5	4+1	(4 P vs t; 1 peak press. only)
O-2	3520[a]	B/C	216	54	0	0	Buoy recovered but all gages lost.
O-2	3650	EPT	12	18	0	0	Buoy broke free before zero time.
	8700[a]	MPT	7	7	7	3+3	(3 P vs t; 3 peak press. only)
YFNB 12	5440[c]	MPT	7	7	–[c]	–[c]	
YFNB 12	5440[c]	B/C	172	43	–[c]	–[c]	
YFNB 12	5500	EPT	15	18	18	15	
YFNB 13	7860	MPT	7	7	7	6	
YFNB 13	7860	B/C	172	43	43	43	
YFNB 13	8035	EPT	16	18	18	15	
YFNB 29	10,865	MPT	7	7	7	0+7	(Peak pressure only)
YFNB 29	10,865	B/C	64	16	16	16	
YFNB 29	11,030	EPT	16	18	18	16	
	11,900[a]	B/C	176	44	0	0	

[a] Nominal distance.
[b] In the case of B/C gages - four gages were averaged to give a single pressure value. In the case of Wiancko and of MPT pressure gages 1 gage = 1 channel. In the case of some PE gages; data from a single gage was recorded twice at different amplifications.
[c] This line never installed.

Table 1.4—PROJECT 1.2 NOMINAL GAGE DEPTHS FOR USABLE PRESSURE-DATA CHANNELS

Horizontal Nominal Distance (ft)								
2900 Mech P vs t	8700 Mech P vs t	5600 PE P vs t	7860 B/C P_{max}	7860 Mech P vs t	8035 PE P vs t	10,865 Mech P_{max}	10,865 B/C P_{max}	11,030 PE P vs t
50	50	25	5,15,25	50	25	50	259	25
100	300	25[a]	35,45	100	25[a]	100	309	25[a]
300	750	50	55,65	300	50	200	358	25[a]
500	-	100	75,85	500	200	300	408	50
-	-	200	95,105	750	200[a]	500	458	200
Mech	Mech	200[a]	115,125	1000	500	750	508	500
P_{max}	P_{max}	500	135,145	-	1000	1000	556	1000
200	-	1000	155,165	-	1000	-	606	1000
-	200	1000[a]	175,185	-	Wiancko	-	655	Wiancko
-	500	Wiancko	195,205	-	P vs t	-	705	P vs t
-	1000	P vs t	215,225	-	100	-	754	100
-	-	200	235,245	-	200	-	804	200
-	-	200	255,265	-	200	-	853	200
-	-	300	275,322	-	300	-	903	300
-	-	500	369,417	-	500	-	952	500
-	-	500	464,512	-	500	-	1002	500
-	-	1000	561,611	-	1000	-	-	1000
-	-	-	660,709	-	-	-	-	1000
-	-	-	758,807	-	-	-	-	-
-	-	-	856,905	-	-	-	-	-
-	-	-	953,1002	-	-	-	-	-

[a]PE Gages which recorded on two channels.

CONFIDENTIAL

REFERENCES

1. C. B. Cunningham, Free-field Pressures, Station Zero, Naval Research Laboratory, Operation Wigwam Project 1.2.1 Report, WT-1006, December 1955.
2. F. B. Porzel, Close-in Time of Arrival of Underwater Shock Wave, Operation Wigwam Project 4.4 Report, WT-1034 (in preparation).
3. T. McMillian, Free-field Pressure Measurements, Project 1.3, Operation Wigwam Project 1.3 Report, WT-1007.
4. G. R. Hamilton et al., Bubble Phenomena, Operation Wigwam Project 1.4 Report, WT-1008.

CHAPTER 2

BALL-CRUSHER PEAK-PRESSURE MEASUREMENTS

2.1 PURPOSES

The principal purposes for making ball-crusher-gage underwater peak-pressure measurements were to provide a simple, reliable backup measurement system for the pressure-time gages and to obtain peak-pressure measurements at a large number of positions.

2.2 DESCRIPTION OF BALL-CRUSHER GAGE

2.2.1 History

The ball-crusher gage consists essentially of a steel piston, a copper ball, and a steel anvil as shown in Figs. 2.1 and 2.2. One end of the piston is in contact with the small copper sphere which rests on the anvil. The other end of the piston is subjected to the shock wave from an explosion. These gages, in groups of four, are clamped to lines suspended from floats. Such gages have been used extensively to obtain peak-pressure data from underwater explosions of charges weighing from 50 lb to 45 tons. A discussion of some such experiments is given by Cole.[1]

On shot Baker of Operation Crossroads and on shots 1, 2, 4, 5, and 6 of Operation Castle, the peak pressure vs depth and peak pressure vs distance relations were obtained by the use of ball-crusher gages.

As on Operations Crossroads and Castle, ball-crusher gages were used on Operation Wigwam to obtain peak pressure vs depth and peak pressure vs distance relations as a supplement to the pressure-time recording.

2.2.2 General Gage Details

Figure 2.1 shows the gage components, a waterproofed gage assembled with a $\frac{3}{8}$-in.-diameter sphere, and a block of four gages.

Figure 2.2 is a cross-sectional drawing of an assembled gage. Two sizes of spheres, $\frac{5}{32}$ and $\frac{3}{8}$ in. in diameter, can be used in these gages. The $\frac{3}{8}$-in. sphere is used with the spacer ring, as shown, and the $\frac{5}{32}$-in. sphere is used without the spacer ring. The purpose of having two sizes is to widen the pressure range covered by the gages.

The dynamic calibration curve for the $\frac{5}{32}$-in. spheres is nearly linear for deformations from 0.01 to 0.05 in., and for the $\frac{3}{8}$-in. spheres it is nearly linear for deformations from 0.01 to 0.09 in. These deformations correspond to a range of peak pressures for a step wave of about 300 to 1500 psi ($\frac{5}{32}$-in. spheres) and about 700 to 6000 psi ($\frac{3}{8}$-in. spheres).

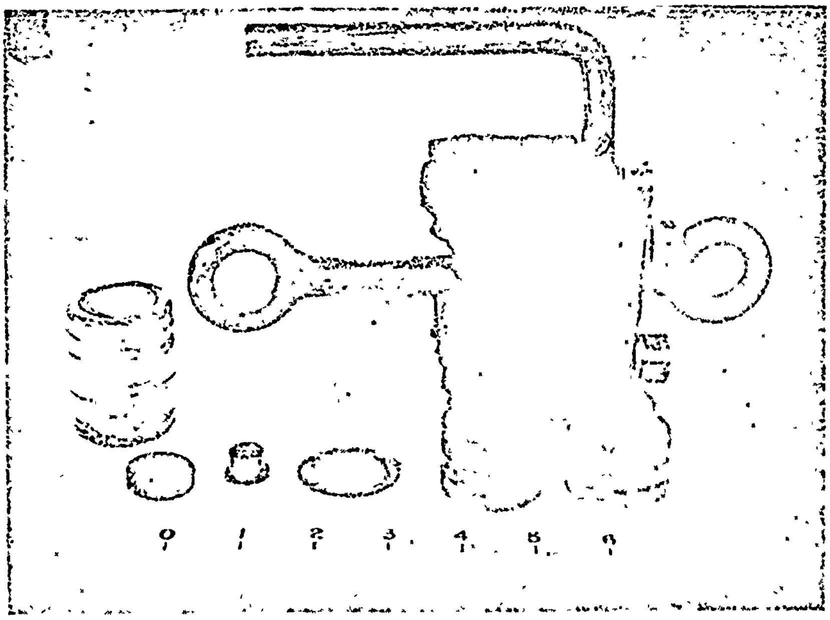

Fig. 2.1—Ball-crusher gage components, waterproofed gage, and gage block.

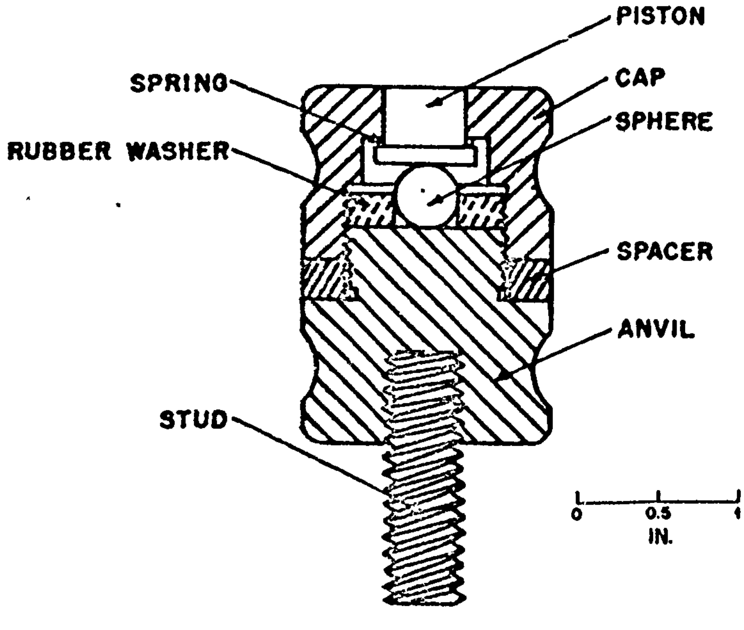

Fig. 2.2—Cross section of a ball-crusher gage.

Errors in measured deformations are estimated to be ±0.0005 in.; hence, for a final deformation of 0.01 in., the error in measurement alone is about ±5 per cent. Thus, for deformations smaller than 0.01 in., the errors due to measuring the spheres become extremely serious.

2.2.3 Theory

The theory of the ball-crusher gage has been discussed elsewhere.[2-4,6] In brief, it has been shown that the response of the gage up to the time of maximum deformation is equivalent to that of a mass and spring subjected to a force applied to the mass and that the differential equation of a linear oscillator results for the motion of the piston. This equation can then be integrated for any assumed pressure variation. In the use of the gage, therefore, it is necessary to know the shape of the pressure-time curve and certain other factors. In small-charge work most of these factors have been well known; in the instance of the Crossroads Baker work, pressures were calculated on the assumption that the shock wave was a step function. A limited number of pressure-time records indicated that this approximation was good to 10 per cent or better. On Operation Castle the ball-crusher gages were subjected to a slowly increasing pressure wave rather than a shock wave. The gage acted then as a static pressure gage, and peak pressures were calculated by using only the final deformations of the spheres and their static calibrations.

Since the ball-crusher gages were waterproofed and were to have been used to depths as great as 2000 ft on Operation Wigwam, the effect introduced by the predeformation of the sphere by the hydrostatic pressure must be considered. The theory of the ball-crusher gage in which the sphere has been predeformed by the hydrostatic pressure has been discussed in references 5 and 6. The deformations discussed in reference 6 have been used to calculate peak pressures by the method of reference 5, and a comparison showed that the two theories, references 5 and 6, gave the same values of peak pressures for the region of measurement.

2.2.4 Analysis

Ball-crusher peak pressures were calculated by the method outlined in reference 6, using

$$P_D = \left[\frac{K_D}{24A}(x_m + x_0) - P_0\right]\left(1 + \frac{\pi}{2}\frac{\mu}{\omega}\right) \tag{1.1}$$

where P_D = the peak pressure above hydrostatic pressure, pounds per square inch
K_D = the dynamic force constant, pounds per foot
K_s = the static force constant, pounds per foot
A = the area of the piston (0.197 sq in.)
x_m = the final deformation, inches
x_0 = the initial deformation, in inches, caused by the hydrostatic pressure; it is equivalent to $(12 \times 0.444D_0A)/K_s$
P_0 = the hydrostatic pressure, in pounds per square inch, to which the gage is subjected; it equals $0.444D_0$
D_0 = the depth, in feet, to which the gage is lowered
$\mu = 1/\theta$, where θ is the time constant of the shock wave, seconds
ω = the $\sqrt{K_D/m}$, where m is the equivalent mass of the moving system

The dynamic force constants were obtained by the NOL from drop test equipment as usual[7] and were

$K_D = 1.40 \times 10^5$ lb/ft (for $\frac{5}{32}$-in. spheres)

$K_D = 3.38 \times 10^5$ lb/ft (for $\frac{3}{8}$-in. spheres)

The static force constant for the $\frac{5}{32}$-in. spheres was obtained by placing waterproofed gages in a pressure pot and measuring deformations produced over a range of pressures. The static calibration for the $\frac{3}{8}$-in. spheres was taken from reference 6. The lot of spheres used in the work described in reference 6 is the same lot of spheres used in Wigwam. The static force constants were

$$K_s = 1.21 \times 10^5 \text{ lb/ft} \qquad \text{(for } {}^5\!/_{32}\text{-in. spheres)}$$

$$K_s = 2.84 \times 10^5 \text{ lb/ft} \qquad \text{(for } {}^3\!/_8\text{-in. spheres)}$$

The correction for the decay of the shock wave, $1 + (\pi/2)(\mu/\omega)$, was less than 0.5 per cent for an exponentially decaying shock wave with a time constant of about 30 msec, and hence it is omitted in what follows.

Substitution of numerical values in Eq. 1.1 and simple algebraic rearrangement give:

$$P_D = (7.15 \times 10^4 \, x_m) - 0.178 D_s \qquad \text{(for } {}^3\!/_8\text{-in. spheres)}$$

$$P_D = (2.96 \times 10^4 \, x_m) - 0.186 D_s \qquad \text{(for } {}^5\!/_{32}\text{-in. spheres)}$$

2.2.5 Gage Preparation

The copper spheres were measured using micrometer calipers. The tolerances were ±0.0003 in. from a nominal diameter for the ³⁄₈-in. spheres and ±0.0002 in. for the ⁵⁄₃₂-in. spheres. The spheres were checked at three diameters, and any sphere which fell outside the tolerance was discarded.

The gage components were washed in carbon tetrachloride to remove oil and grease from the outside surfaces to ensure adhesion of Tygon primer and paint (Tygon paint and primer are manufactured by The United States Stoneware Co., Akron 9, Ohio). The piston, with spring in place, was checked in the cap. The gages were then assembled with the desired size of sphere.

Tests conducted with 8- and 50-lb charges showed that the method of waterproofing that was used on Operations Crossroads (see also Sec. 9.9) and Castle affected the response of the ball-crusher gage at least when the gage was subjected to a short-duration shock wave.[5] Further tests were conducted to obtain a waterproofed gage that would have the same response as a nonwaterproofed gage.[5] The method that was developed and was used on Operation Wigwam is outlined below:

To waterproof the gages, a rubber cot (the finger cots were manufactured by Killashun Sales Division, Akron, Ohio) was pulled tightly over the piston end of the gages and held in place with a rubber band. Each gage was checked to ensure that no air was trapped under the cot at the piston end of the gage. The sides of the gages were wrapped with Uskorona tape (Uskorona tape is manufactured by The United States Rubber Company, New York 20, N. Y.), and Bostik No. 1015 cement (Bostik cements are manufactured by the B. B. Chemical Co., Cambridge and South Middleton, Mass.) was applied to the point between the tape and the cot at the piston end of the gage and between the tape and the gage at the other end. Two coats of Tygon primer, TP-107B, were painted over the tape and the Bostik cement.

The sides of the waterproofed gages were wrapped with two layers of friction tape and inserted into the blocks (Fig. 2.1).

2.3 GAGE RIGGING AND MOORING

2.3.1 Gage Rigging

The ball-crusher gages were to be suspended in vertical strings at nominal horizontal distances from SZ of 1520, 1920, 3520, 5440, 7860, 10,865, and 11,900 ft. The gage strings at 5440, 7860, and 10,865 ft were to be hung from the YFNB's; however, the ball-crusher gages at 5440 ft were never installed. The remaining four were supported by flotation buoys on the tow cable.

Figure 2.3 is a schematic drawing of the ball-crusher-gage strings which were suspended from the flotation buoys. The gage blocks were suspended between wire-rope pendants. From the surface to 300 ft they were spaced at 10-ft intervals; from 300 ft to 1000 ft they were at

CONFIDENTIAL

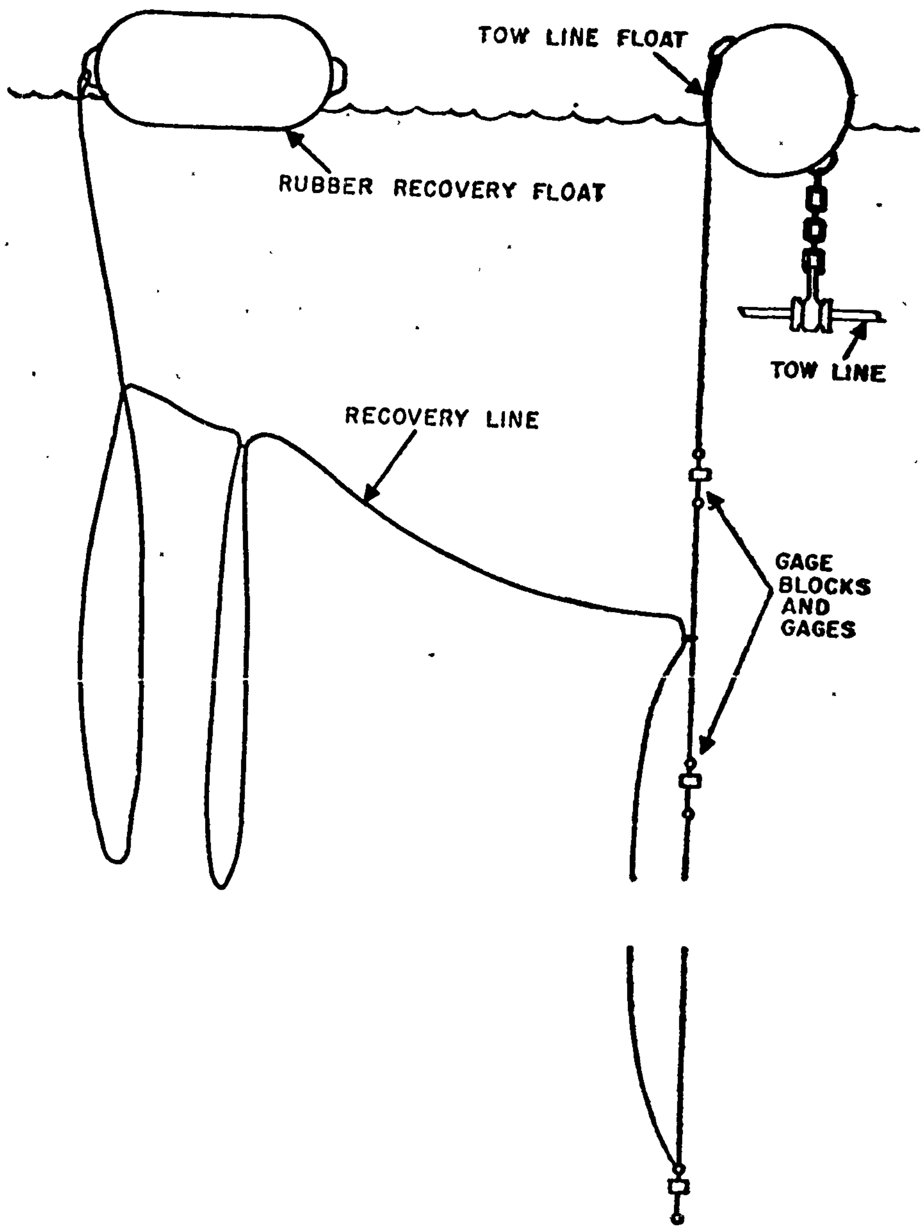

Fig. 2.3—Ball-crusher-gage line and supporting rig hung from towline.

SECRET – RESTRICTED DATA

CONFIDENTIAL

50-ft intervals. The gage strings at 1920 and 3520 ft were 2000 ft long. Gage blocks were at 100-ft intervals from the 1000- to the 2000-ft depth on these two strings.

The gage strings at 1520, 1920, and 3520 ft from SZ had a weak link, a $\frac{1}{4}$-in. shackle, between the top gage block and the flotation buoy. (This weak link was expected to break at the time of the shock-wave arrival.) A $\frac{3}{8}$-in.-diameter wire-rope safety or recovery line ran alongside the gage strings. The recovery line was slack and was clipped to the gage string every 50 ft. At the surface the recovery line was connected to a safety float, a 600-gal rubber buoy, with about 80 ft of slack cable. The safety float was not connected to the towline. Gage depths were determined from the lengths of the wire-rope pendants and the gage blocks.

The ball-crusher strings which were hung from the YFNB's were combined with the mechanical gage strings. The main support cable was $\frac{3}{4}$-in.-diameter wire rope to which seven mechanical gages were attached (see Chap. 3). Each ball-crusher string, a series of gage blocks and pendants, was clipped to the $\frac{3}{4}$-in. wire rope by means of $\frac{1}{2}$-in. steel rods (see Fig. 2.1), which were welded to each ball-crusher-gage block. The pendants between the ball-crusher-gage blocks were slack since the mechanical gage string supported all the weight. To make up for this slack, an extra ball-crusher-gage block and 50-ft pendant were added to these strings. The depths of the gage blocks which were near mechanical gages were obtained from the depths of the mechanical gages. Depths of the remaining gage blocks were estimated by assuming that the ball-crusher-gage blocks were spaced evenly between mechanical gages.

2.3.2 Installation and Recovery of Gages

On the YFNB's the $\frac{3}{4}$-in. wire rope was lowered from a drum on a winch. It was run over a block at the end of a boom which projected over the side of the barge. The mechanical gages and the ball-crusher blocks were attached to the cable as it was lowered. The weight of each combined string was supported by its winch. A pendant from the ball-crusher string was secured to a bit on the deck of each YFNB to serve as a safety cable.

A complete gage string was lowered from the YFNB-13, and a partial string was lowered from the YFNB-29. The string on the YFNB-12 was not lowered.

The ball-crusher-gage strings that were hung on the flotation buoys were lowered from the USS Butternut (AN-9) or the USS Bolster (ARS-38). The gage strings were connected together on deck and lowered over the side by means of tumbling hooks. The gage strings were taken by M-boat to the towline. Because of heavy seas it was not possible to secure the gage strings to wire-rope pendants hung from beneath the buoys as planned. At most of the positions the gage strings had to be connected to the ring on top of the flotation buoys.

On the YFNB's all the gages that were installed were recovered. None of the ball-crusher gages which were hung on the flotation buoys were recovered. At the 1520-ft position, neither the flotation nor the safety buoy was recovered. At the 1920-ft position the flotation buoy was not found, but the safety buoy was retrieved; however, the recovery line had parted between the buoy and the first gage block. At the 3520- and 11,900-ft positions the flotation buoys were recovered. Neither of these positions had a safety buoy.

REFERENCES

1. R. H. Cole, "Underwater Explosions," Princeton University Press, 1948.
2. G. K. Hartmann, Memorandum for File, A16(OND) (Re6b) Navy Department, BuOrd, 25 September 1942.
3. R. Finkelstein, The Theory of Piston Gages, Explosives Research Report No. 5, Navy Department, BuOrd, April 1944.
4. J. S. Coles, Appendix I by Arons, The Measurement of Underwater Explosions near the Surface and Bottom of the Ocean, BuOrd NAVORD Report 105-46, 1947.
5. C. R. Niffenegger and M. A. Thiel, The Ball Crusher Gage; Modified Gage Designs, Predeformation, and Waterproofing Tests, NAVORD Report 4224, U. S. Naval Ordnance Laboratory, White Oak, Md. (in preparation).

CONFIDENTIAL

6. A. D. Hirsch and C. D. Martin, Measurements of Peak Pressure from 5350-pound Cylindrical Charges of HBX-1 with Ball Crusher Gages, DTMB Report C-682, 1955.
7. J. S. Coles et al., The Measurement of Underwater Explosions from Service Weapons at the Underwater Explosives Research Laboratory (UERL), NDRC Report A-362, OSRD Report 6240, March 1946.

SECRET — RESTRICTED DATA

CONFIDENTIAL

CHAPTER 3

MECHANICAL PRESSURE-TIME GAGES AND SYSTEMS

3.1 INTRODUCTION

3.1.1 Objectives

The development of a self-contained mechanical-recording pressure-time gage was initiated for use on Wigwam to provide a backup system for the NOL electronic systems.

The objectives and requirements were:

1. Pressure sensing and recording using techniques different from those of the electronic systems.
2. Starting of the recorders to be independent of the Edgerton, Germeshausen & Grier (EG&G) timing system.
3. Independent attachment to the towline.
4. Principal shock peak-pressure measurement accuracy of ±10 per cent over a range from 500 to 3000 psi.
5. Time resolution of 2 msec or better for events lasting up to 100 msec.
6. Time accuracy of 1 per cent for intervals ½ sec long.

3.1.2 Background

Measurement of underwater shock pressures by means of a self-contained pressure-time recorder was first accomplished on an atomic burst by the University of Washington on Crossroads.[1-5] Two designs were used, a linear recorder and a banjo or logarithmic recorder (Fig. 3.1).

The linear recorder was housed in a 1200-lb cylindrical container, 30 in. long and 25 in. in diameter. It could measure pressures up to 1000 psi and could withstand shock up to 1000 g without damage. It could be started in advance electrically by a blast switch or timing signal. Its sensing element was a 10-in. diaphragm acoustically damped so that it did not overshoot more than 5 per cent for a step pressure pulse. A stylus fastened to the diaphragm scratched a chrome-plated disc 3 in. in diameter which rotated a fixed number of turns at 4 rpm.

The banjo or logarithmic recorder was 8 in. in diameter and 3 in. thick. It also used a diaphragm as a sensing element; however, the diaphragm was effectively damped by sponge rubber, which gave characteristics about the same as those of the linear recorder. The stylus of this gage recorded by scratching on a flat surface of a rod which moved in a straight line under the action of a spring. The initial recording speed was about 1 in./sec. The rod was restrained by a piston moving in oil so that its displacement varied logarithmically with time. Starting was accomplished at shock arrival. Neither gage used any time marker system, which meant that time measurements were obtained from a calibration of the recording speed which was conducted under the circumstances of no shock.

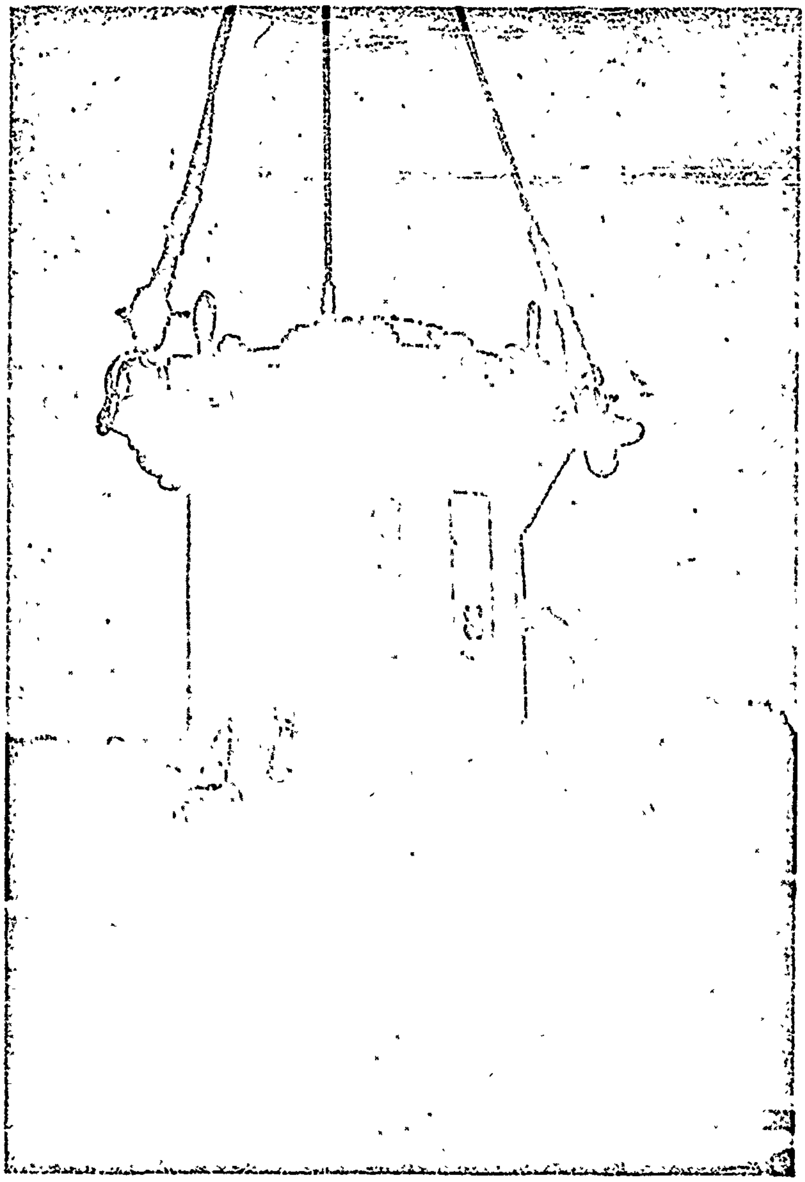

Fig. 3.1—University of Washington linear and log recorders.

Photographs of some of the better University of Washington original pressure-time records of the principal shock phase are shown in Figs. 3.2 and 3.3. The complete records may be seen in the analysis study made by the University of California.[6] The time scale shown was constructed using recording speed and enlargement information furnished by the University of Washington. The marks do not represent positive durations and are provided only as an approximate time scale.

It is obvious that there was considerable time distortion present in the principal pulses from both types of recorders. This distortion in the log or banjo recorder must have been due to the fact that the recording surface was sensitive to linear acceleration. In the case of the linear recorder, the University of Washington stated that the probable cause was stoppage of the motor or gear train, slipping of the recording disc, or gear backlash.

Pressure distortion was also present, but the amount is difficult to determine. If the principal pulse was made up of two to five very short duration pulses as concluded by the University of California,[6] the gages may have been too slow to fully respond. In addition it seems that some pressure-sensitivity to linear acceleration should have been present.

From the foregoing the reader can obtain an idea of some of the difficulties to be overcome in making a self-contained recorder capable of withstanding 500- to 1000-g shock and at the same time giving an undistorted record. For the Wigwam shot a new design was necessary because:

1. The linear recorder was too heavy for handling with seven gages on a string dropping to a 1000-ft depth.
2. The linear-recorder case was too weak for expected shock pressures.
3. The logarithmic recorder could not be readily modified to give sufficient recording time for Wigwam without sacrificing time resolution.
4. Neither recorder had any provision for a timing trace, which was felt necessary to determine what speed changes, if any, occurred during periods of heavy acceleration.
5. There was some doubt about the acceleration sensitivity of the pressure-sensing diaphragm under shock.

3.2 GENERAL DESCRIPTION

The mechanical pressure-time recorder (Figs. 3.4 to 3.6) developed by NOL recorded small rotary displacements of the sensing element directly on a rotating smoked-glass drum.

The sensing element was a hollow twisted tube which rotated so as to untwist when internal pressure was applied. There was a stylus on the moving end of the element. The moving end of the element was supported in a bearing, and the stylus arm was balanced to reduce linear acceleration effects. The stylus weight was held to a minimum to keep the rotational inertia down and the natural frequency high. Shock pressure entered the water-filled twisted tube through a water-filled spiraled lead-in tube having an orifice at its entrance. The system was theoretically quite insensitive to linear acceleration.

The deflection of the stylus was roughly 0.017 in. for the rated pressure of the element; however, it was found that the rated pressures of the element could safely be increased by two or three times. The range of the sensing element was further increased by means of a negative bias obtained by charging the inside of the gage housing with air pressure ranging from 400 to 1000 psi.

The drum was driven through worm gearing by a modified Army M-500 fuze movement, which for this recorder was called a clock or spring motor. This unit was used because it could withstand heavy shock loads and because it could start in 2 or 3 msec. Power was taken off a gear fastened to the escapement wheel of the motor.

The escapement was released by a trigger energized by a National Bureau of Standards explosive motor, BS 25, which was energized electrically.

The shock-excited reed provided a timing trace. The record was reproduced by photographing the trace through the eyepiece of a 40 power microscope or by wrapping film around the transparent recording drum and exposing it to an internal light.

CONFIDENTIAL

Range 878 yd,
Record No. B-8-1

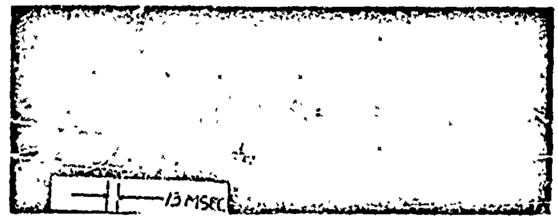

Range 935 yd,
Record No. B-3-1

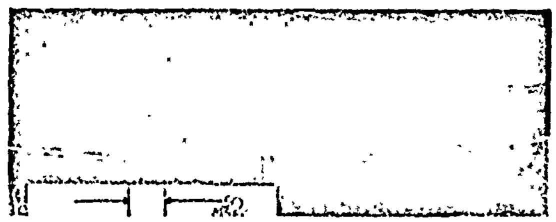

Range 1040 yd,
Record No. B-38-1

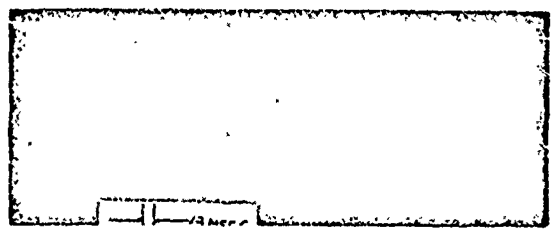

Range 1250 yd,
Record No. B-21-1

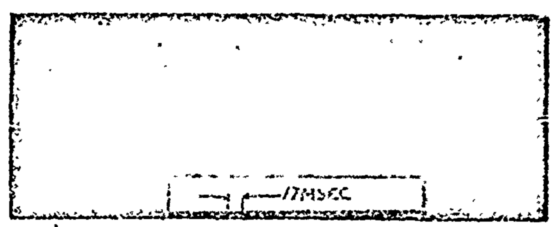

Fig. 3.2—University of Washington linear recorder: original Crossroads records at 100-ft depth.

SECRET – RESTRICTED DATA

CONFIDENTIAL

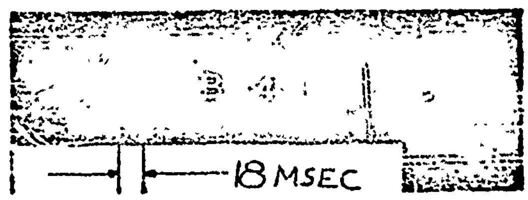

Range 878 yd,
Record No. B-14-1

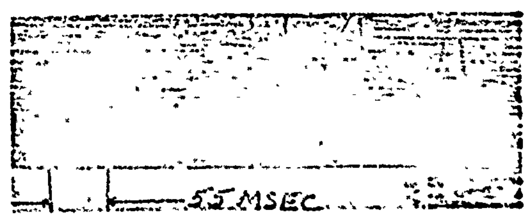

Range 935 yd,
Record No. B-31-1

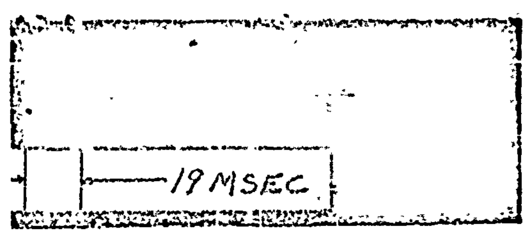

Range 1040 yd,
Record No. B-43-1

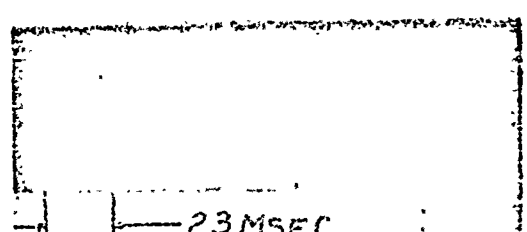

Range 1250 yd,
Record No. B-48-1

Fig. 3.3—University of Washington log recorder: original Crossroads records at 110-ft depth.

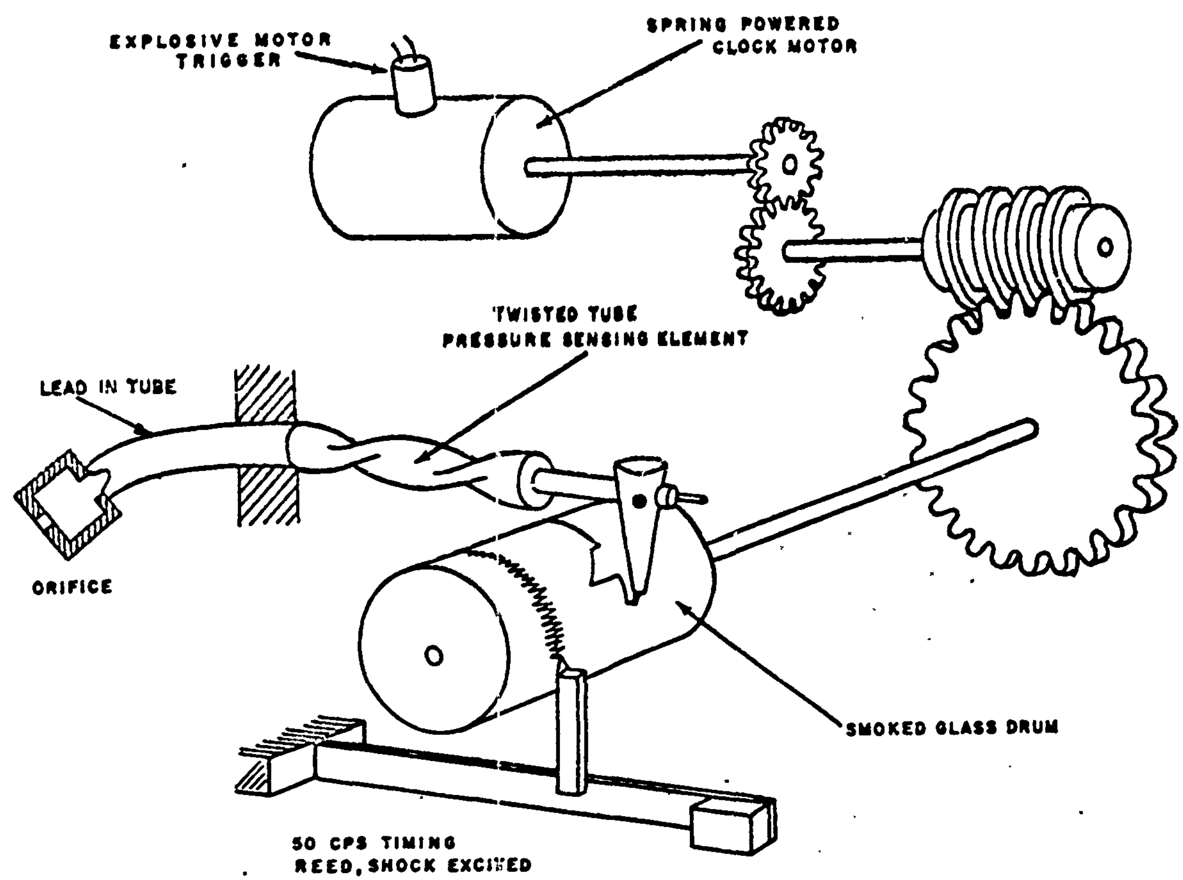

Fig. 3.4—Schematic diagram of the NOL mechanical pressure-time gage.

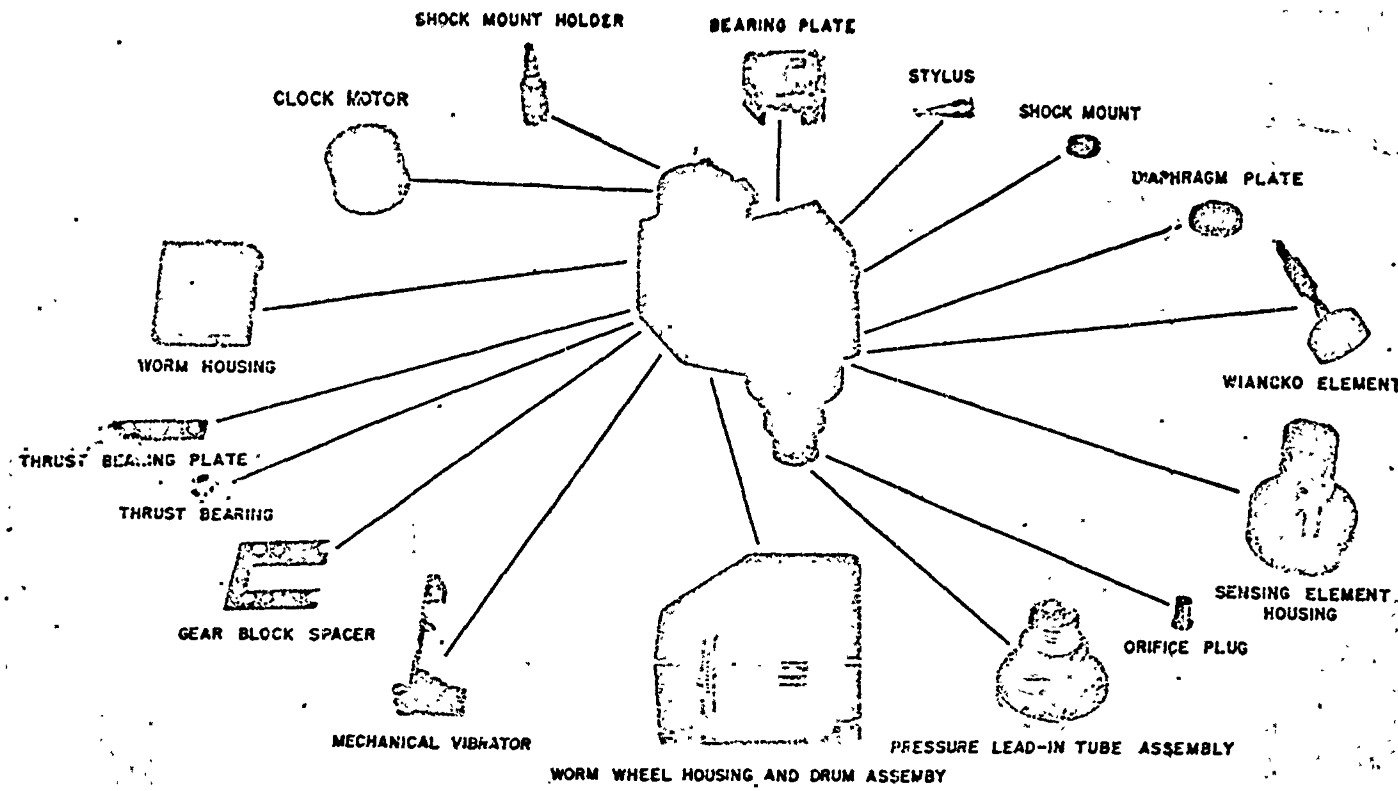

Fig. 3.5—NOL mechanical pressure-time gage and parts.

CONFIDENTIAL

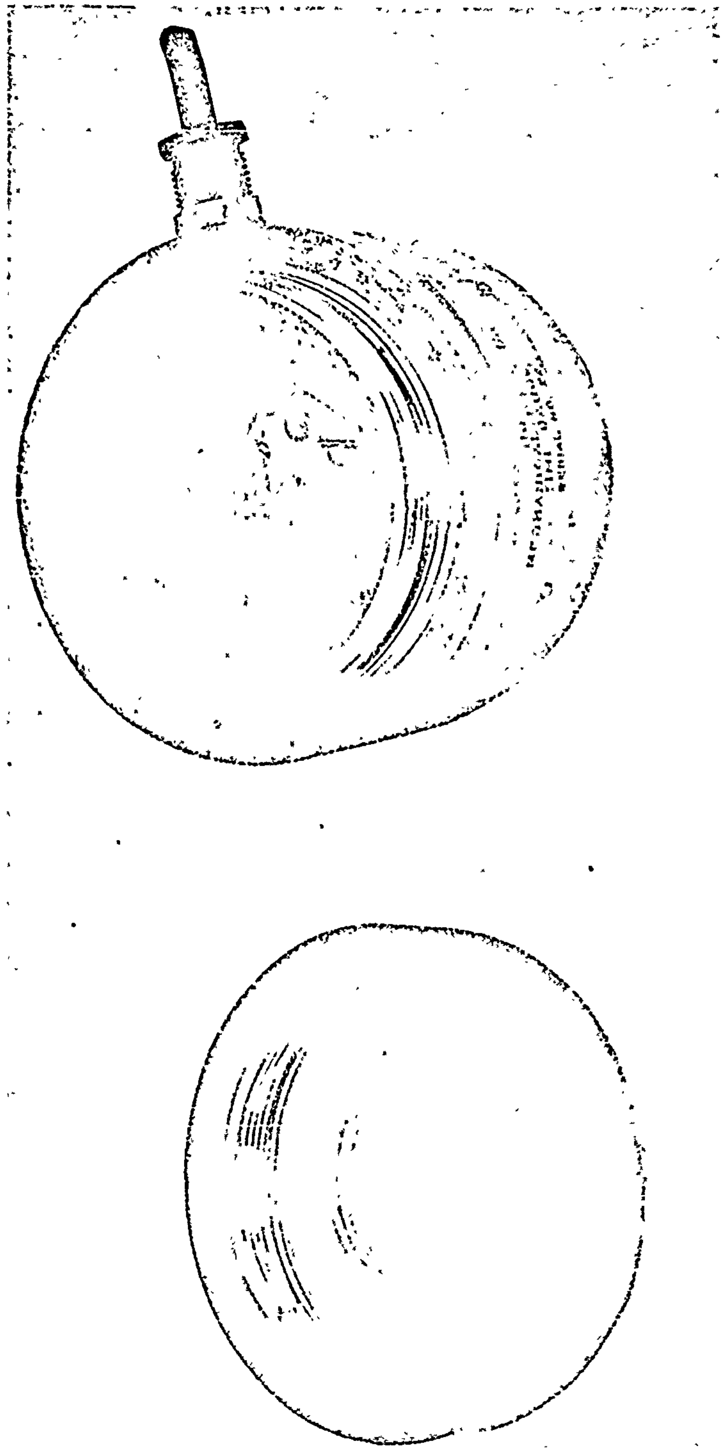

Fig. 3.6—NOL mechanical pressure-time gage in housing.

SECRET—REST ICTED DATA

CONFIDENTIAL

The recorder was housed in a 7-in.-diameter bronze ball. It was separated from the housing by eight lead plugs and eight rubber washers which acted as shock absorbers.

For the Wigwam test, two methods of starting were employed. The first utilized a blast switch of novel design (Figs. 3.7 and 3.8) which closed by shock pressure several milliseconds before shock arrival at the recorder. The second method utilized a relay closed by the EG&G system.

3.3 DEVELOPMENT

The principal problems encountered by NOL during the development period arose from the lack of a calibrating facility which could provide a step pressure rise of known amplitude and a rectangular pulse of known duration.

The first was solved by constructing a pressure vessel in which one or more ND-24 detonators could be fired. A diaphragm strain gage (Fig. 3.9) made by Control Engineering Corporation of Norwood, Mass., having a 20,000-cycle/sec natural frequency, was used for the measurement of pressure. Before the shot this apparatus had only been developed to the point where it could be used for damping studies. After the test the apparatus (Fig. 3.10) was refined so that pressure comparison between mechanical and strain gage records was sufficiently accurate.

A rectangular pulse of known duration was provided by the use of a conical charge of TNT, 25 ft long.[7] This was fired in the Potomac River, and it produced a rectangular pulse 6 msec long at 6000 psi. Only two such tests were made. Some additional information was obtained by the use of small conical charges giving a rectangular pulse 1 msec long; however, these were of little use because the recording speed was too slow to make it possible to read time to 1 msec.

In the course of developing and checking out 40 gages, many time-consuming problems arose. In brief some of these were:

1. Leakage of sensing elements at points which were silver soldered.
2. Sensing element friction.
3. Stylus design.
4. Escapement wear and breakage.
5. Shock mounting.
6. Stuffing-gland leakage.
7. Trigger design.
8. Worm-gearing backlash.
9. Starter leakage.
10. Damping.

Although solutions to all these problems were found, it became apparent during the program that there was not sufficient time to make all the usual tests before the shot and still have time for corrective design. It was decided that it was better to have all the gages in use, although some deficiencies were expected, rather than to perfect a few gages.

3.4 DETAILED CHARACTERISTICS

The following is a brief summary of the characteristics of the gage and the blast switch.

3.4.1 Sensing Element

Type: Wiancko twisted tube, which rotated a 1-in.-long balanced magnesium stylus arm with a diamond stylus of 0.002-in. tip radius

Maximum displacement: ± 0.050 in.

Response: Frequency undamped, about 1000 cycles/sec; critically damped response time, about 1.0 msec for the step pulse

Nominal sensitivities used: 150 to 1000 psi

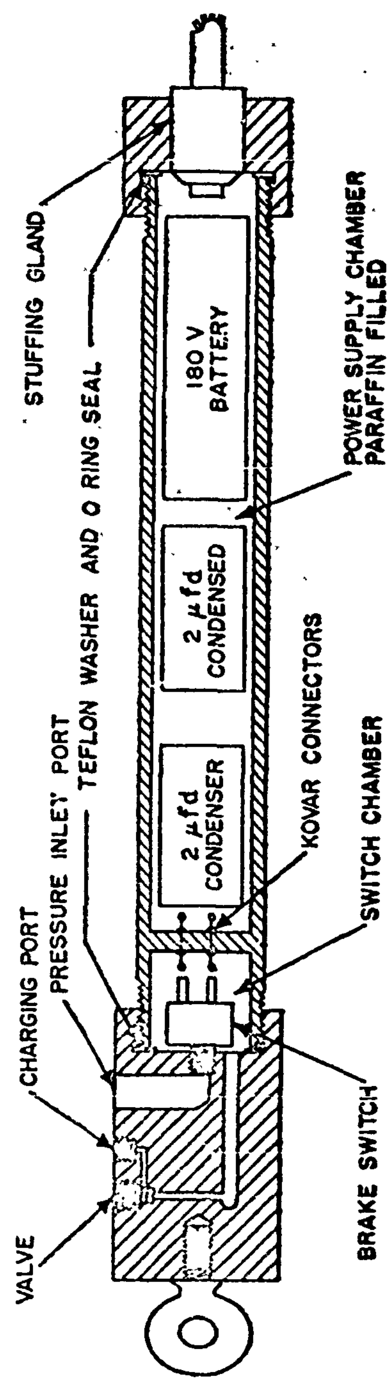

Fig. 3.7—Schematic diagram of starter for mechanical pressure-time gages.

CONFIDENTIAL

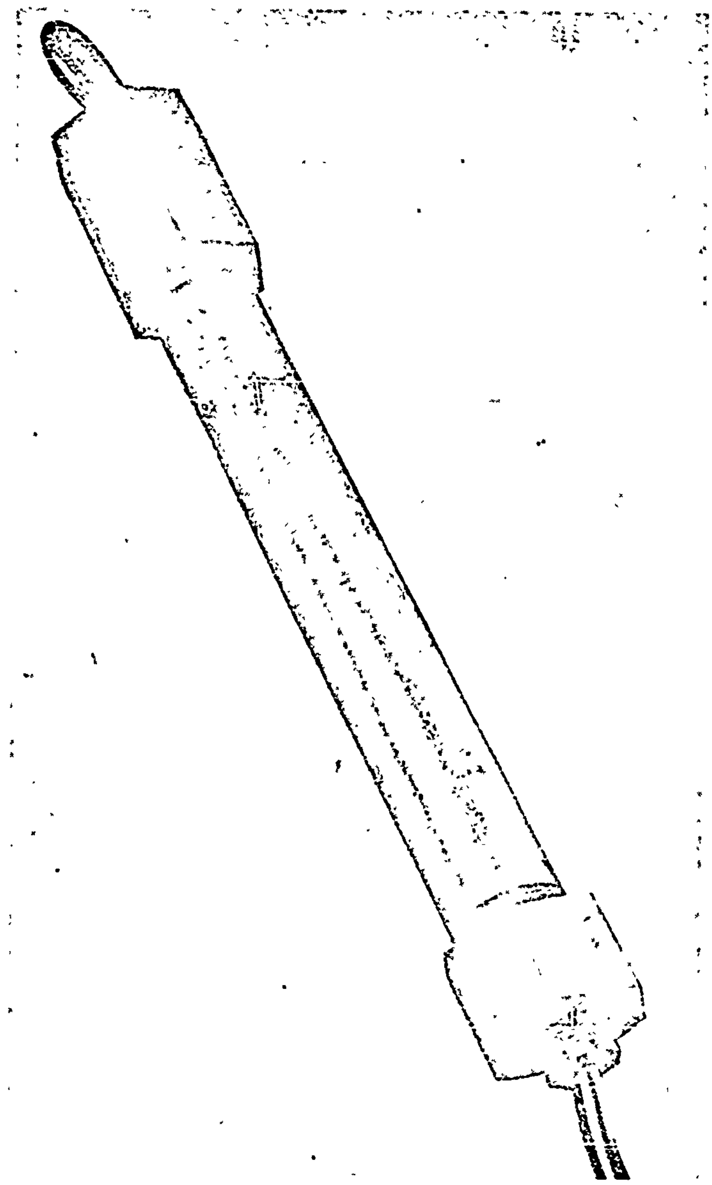

Fig. 3.8—Starter for mechanical pressure-time gages.

SECRET—RESTRICTED DATA

CONFIDENTIAL

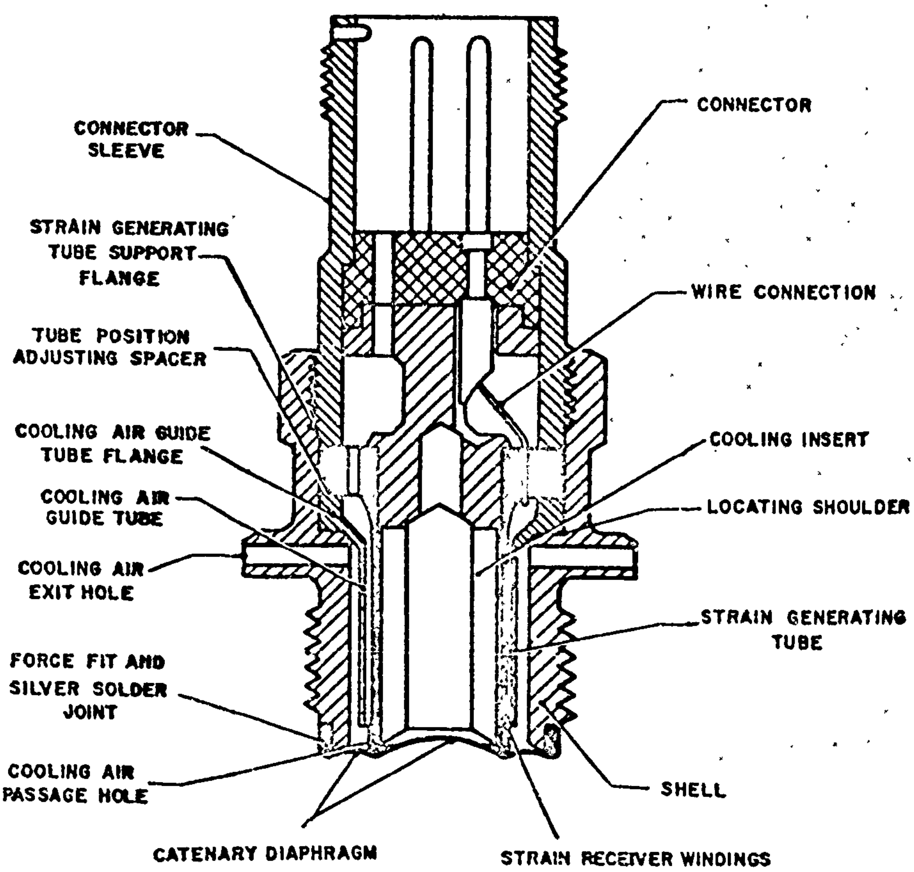

Fig. 3.9—Control Engineering Corporation strain gage used for calibrating mechanical pressure-time gages.

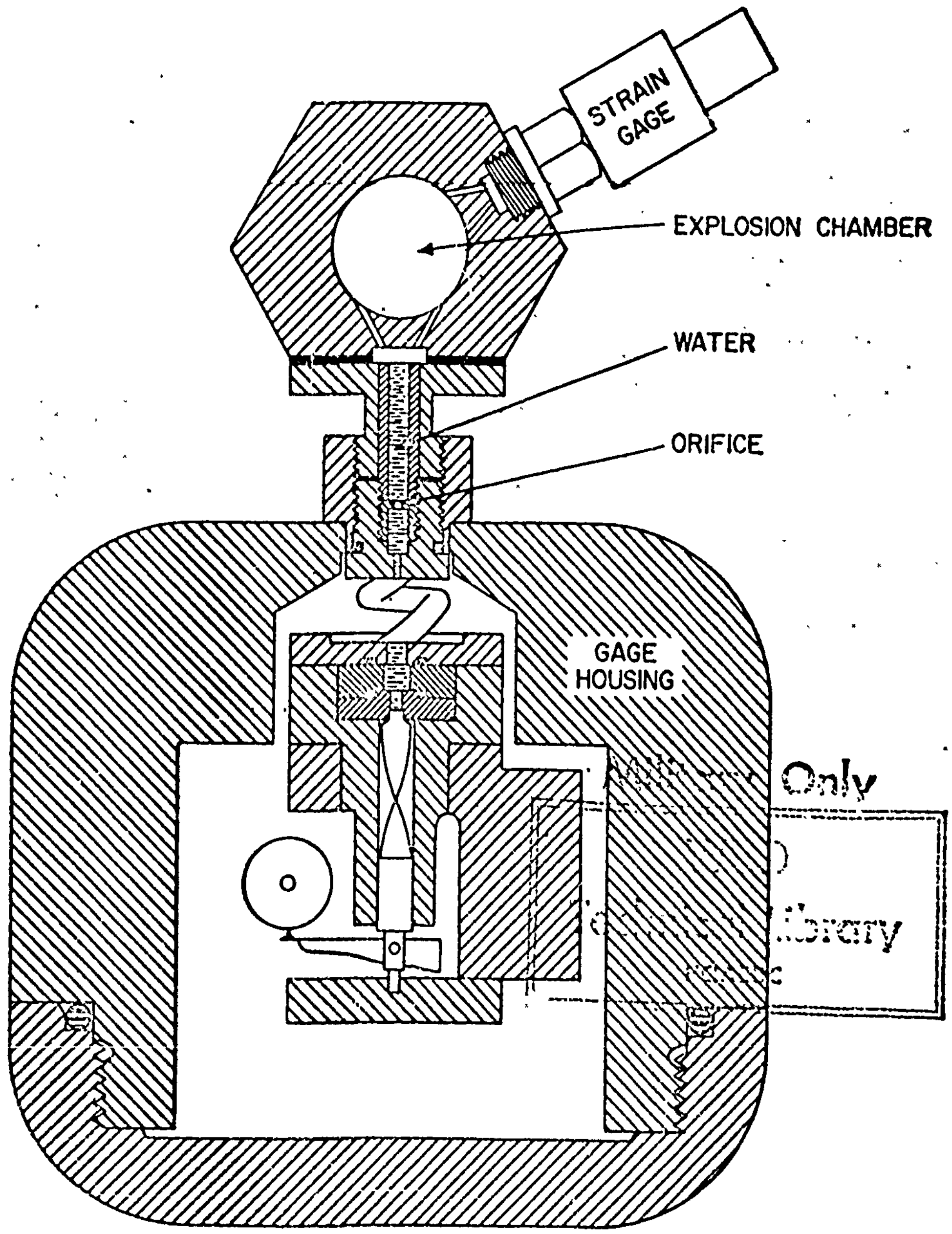

Fig. 3.10—Calibration arrangement for mechanical pressure-time gage.

3.4.2 Recorder

Type: Microrecording, on a 1.0-in.-diameter smoked-glass drum, with spring-powered motor, escapement speed control, and worm gearing
Recording time: 10 to 15 sec
Drum speed: About 0.2 rps or 0.0006 in./msec
Timing trace: By shock-excited 50-cycle/sec cantilever reed and stylus
Line width: 0.0005 in. (0.5 mil), representing 0.5 per cent maximum pressure displacement and about 1 msec in time
Recorder starting: Explosive-motor-actuated escapement release lever; power requirements, 2 volts and 0.2 ma; available force, 10 lb; stroke, $\frac{1}{8}$ in.
Starting time: 2 msec
Weight of recorder: 5 lb
Weight of recorder housing: 75 lb

3.4.3 Blast Switch

Operating pressure: 75 to 100 psi
Operating time: 0.1 msec
Depth range: 0 to 2000 ft
Power pack: 180-volt battery paralleled by a 4-μf condenser
Size: 2.5 in. in diameter by 18 in. in length
Weight: 10 lb

3.5 INSTALLATION

Plans were made to install five strings of gages in the region straddling the SQUAW targets, as follows:

1. Buoy string No. 1, 2800 ft from the YC
2. Buoy string No. 2, 4500 ft from the YC
3. YFNB-12
4. YFNB-13
5. YFNB-29

(3–5) On the after port quarter about 170 ft aft of the piezoelectric and Wiancko gage string

Each buoy string was designed to be suspended by a 4- by 4- by 4-ft solid wood buoy (Fig. 3.11) which was towed at the end of a 150-ft spar (Fig. 3.12) by a 100-ft wire-rope pendant, as shown in Fig. 3.13.

The buoys were made of solid wood to withstand the water shock without collapsing. The purpose of the spars was to keep the gage strings away from the towline, which was expected to sink after the blast and which might carry the gage string down with it. The spars were designed to release the buoy pendant when the towline end of the spar was 50 ft deep. The buoys also were designed to release the tow pendant should the buoy be dragged under by 50 ft. Each gage on the buoy line was suspended in an antifouling frame designed to shed the tow cable should it drag by (see Fig. 3.14).

Because of the heavy weather and the resultant difficulty in connecting up the tow, lowering of the gage strings was delayed as long as possible. During the afternoon of D−1, buoy string No. 1 was lowered and connected to its 150-ft spar. The spar for buoy string No. 2 was not spread out that night. On the morning of D-day, buoy string No. 2 was lowered from the USS Bolster (ARS-38). This string was towed to the spar location, but the spar had parted its forward pendant and had fouled up the tow bridle. As there was insufficient time to free this, the wooden buoy was secured to the 4700-ft towline buoy by means of a 40-ft pendant. The spar and buoy of buoy string No. 1 were riding satisfactorily on the morning of D-day (H−4).

Lowering of the YFNB strings was done after midnight before D-day. This work was hampered by darkness, misuse of handling equipment, and activity on the YFNB stern, where repairs were being made to the SQUAW pontoon lashings. Strings were lowered, however, on the YFNB's 13 and 29. Figure 3.15 shows the gages packed, prepared for lowering, and just before entering the water.

CONFIDENTIAL

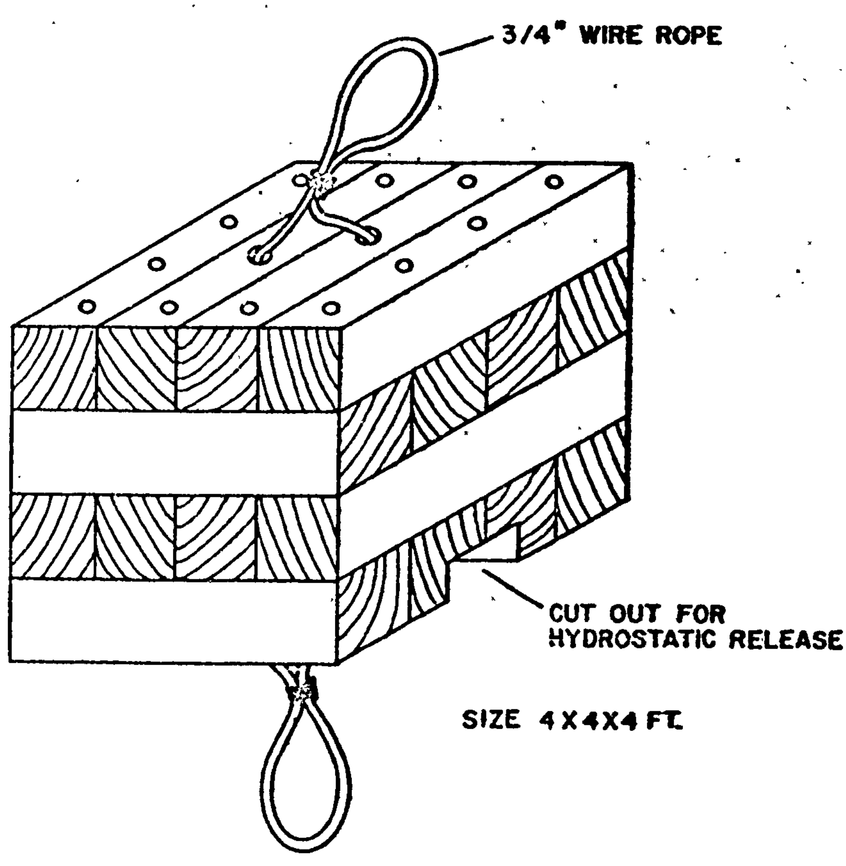

Fig. 3.11 — Wooden buoy for mechanical pressure-time gage string.

CONFIDENTIAL

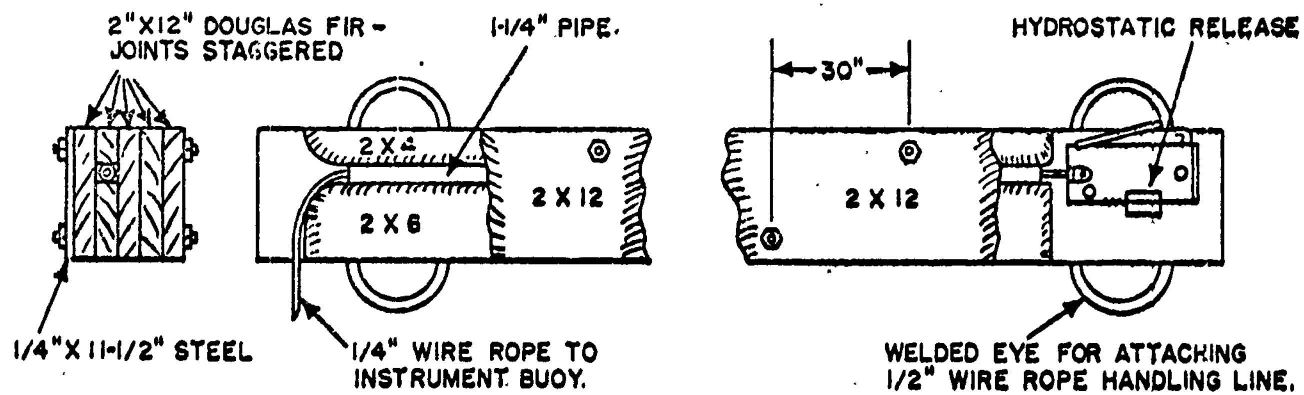

Fig. 3.12—150-ft-spar details.

SECRET – RESTRICTED DATA

CONFIDENTIAL

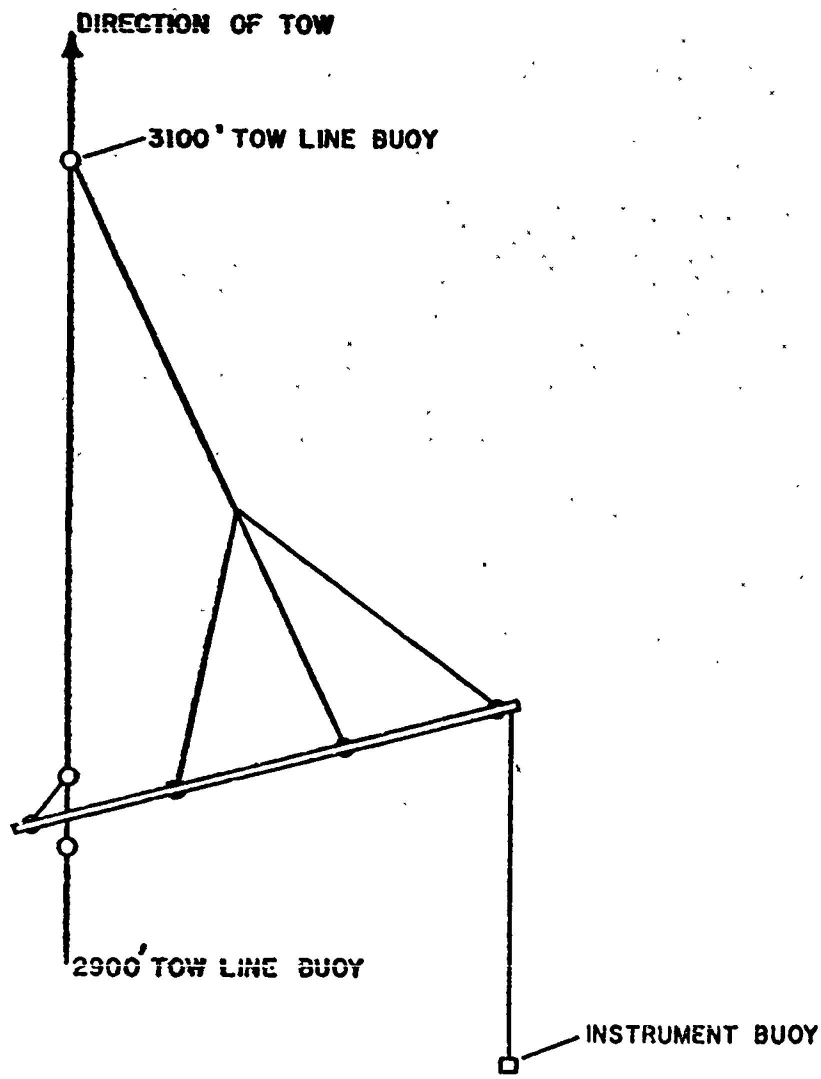

Fig. 3.13—150-ft spar and bridle.

CONFIDENTIAL

CONFIDENTIAL

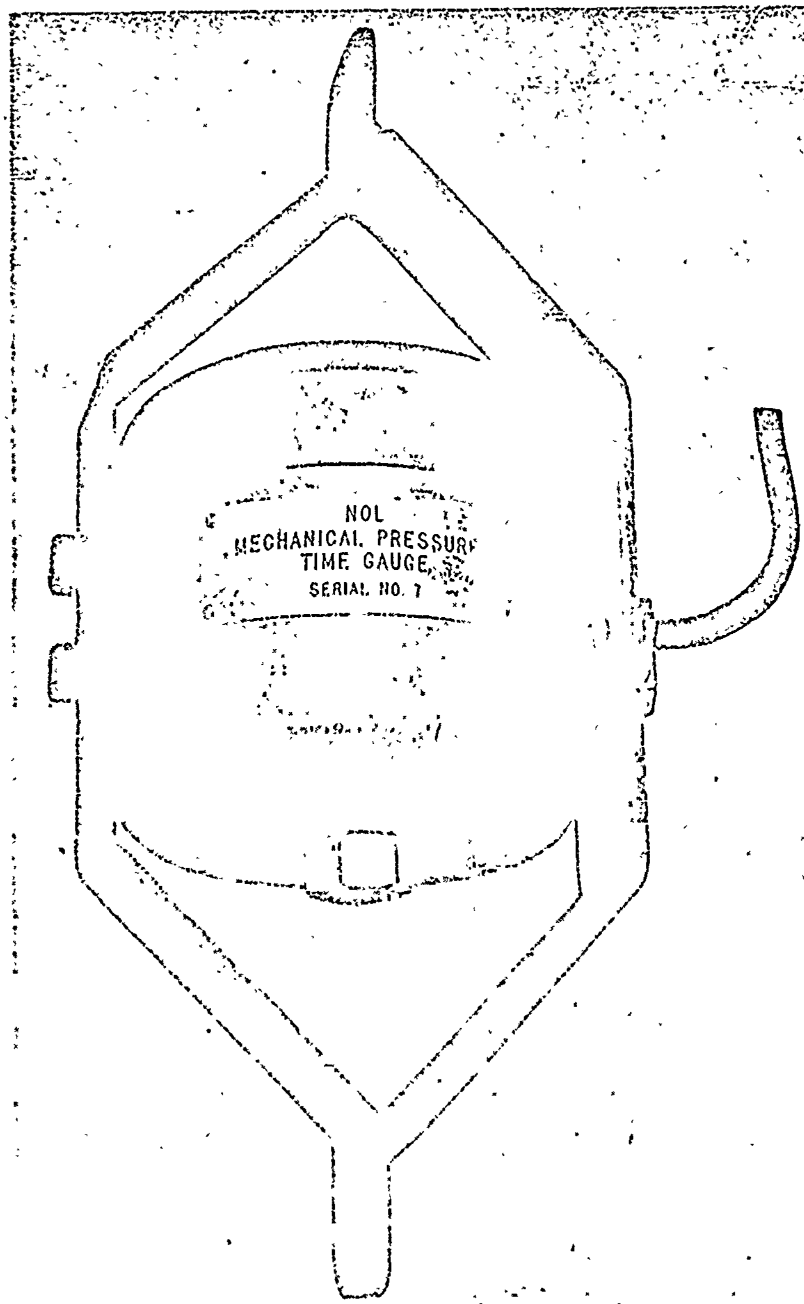

Fig. 3.14—Antifouling frame for mechanical pressure-time gage.

SECRET – RESTRICTED DATA

CONFIDENTIAL

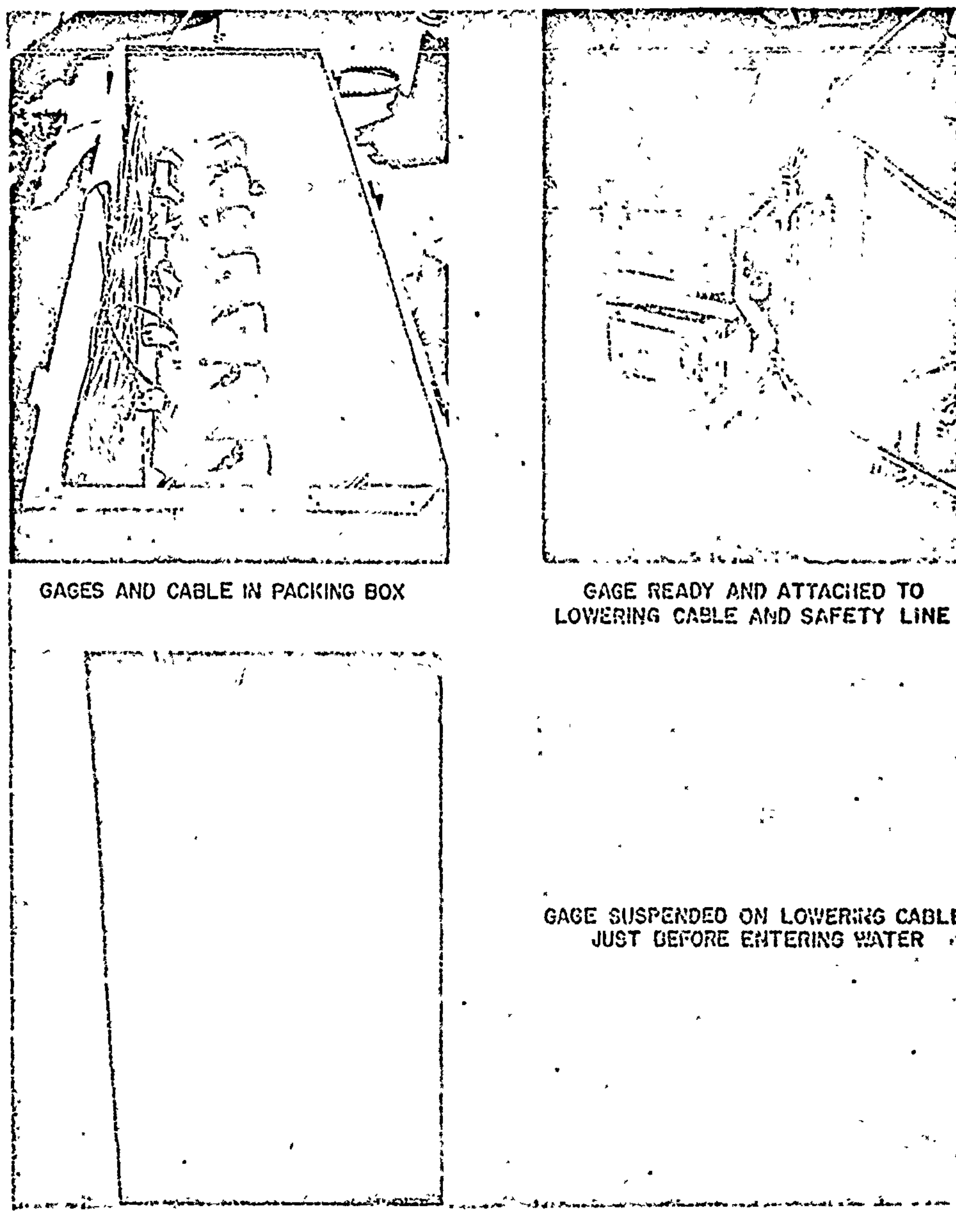

Fig. 3.15—Sea trials.

CONFIDENTIAL

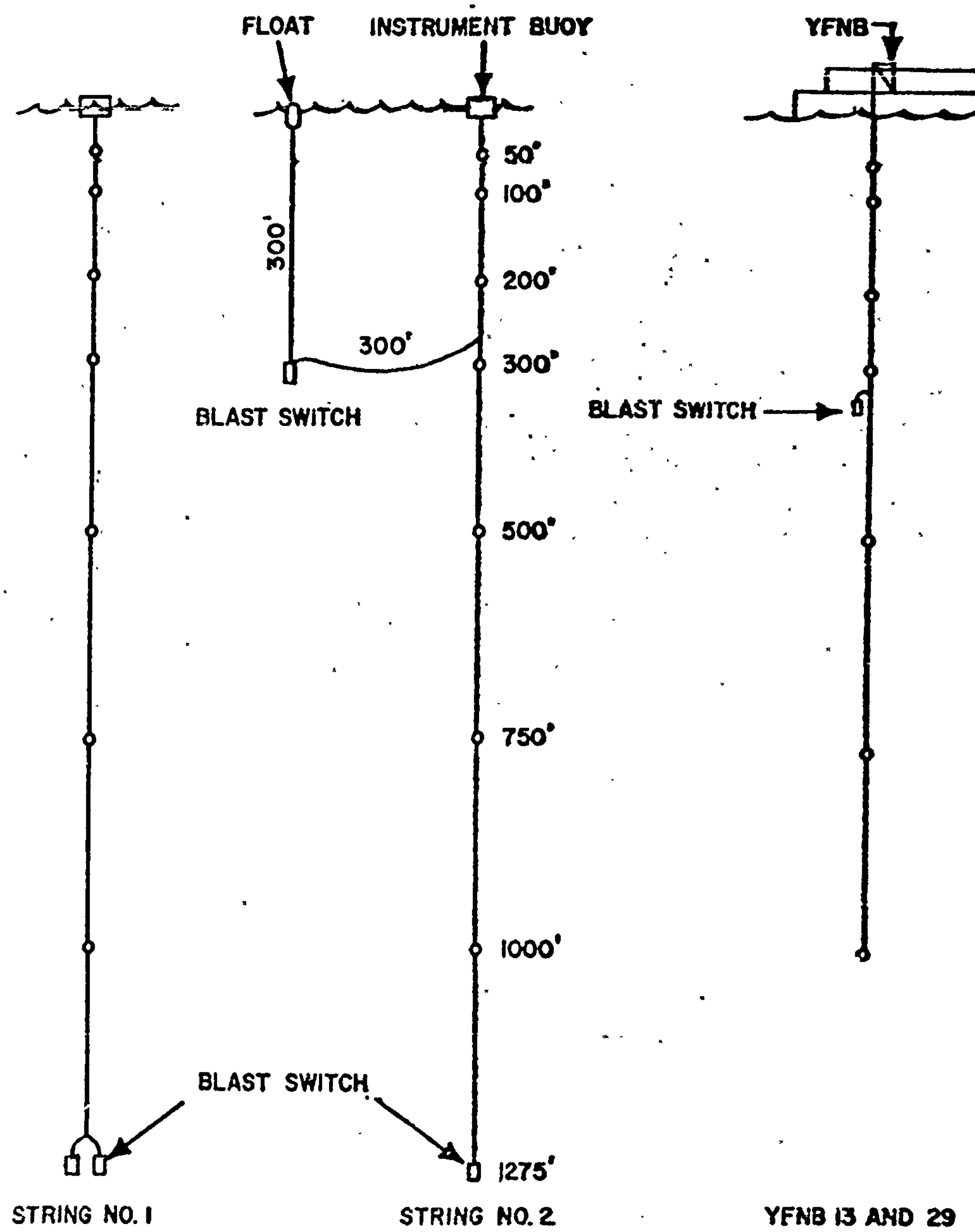

Fig. 3.16—Underwater arrangement of mechanical pressure-time gages.

SECRET – RESTRICTED DATA

CONFIDENTIAL

The buoy strings were installed as follows:

1. Buoy string No. 1 at 2800 ft from zero, secured at the end of the 150-ft spar.
2. Buoy string No. 2 at 4700 ft from zero, secured to the towline buoy.

The vertical arrangement was as shown in Fig. 3.16.

On each string, two independent starting circuits were used, four gages on one circuit and three on the other. A blast switch was connected to each circuit at the 2800- and 4700-ft stations. On the YFNB strings, three gages were connected to a blast switch, and the other four gages were connected to a power supply in series with the EG&G relay set for closing at zero time. These latter relays were connected after the strings were lowered.

At 2800 ft both switches were located 275 ft below the 1000-ft gage because the shock front was predicted to approach from below. At the 4700-ft station the prediction was uncertain, so one switch was suspended at 1275 ft and the other at 300-ft depth, by means of a trailing float. However, because of heavy seas and rough handling the trailing float parted from the switch and the starter settled to approximately 600 ft below the surface.

On the YFNB's the 50-, 100-, and 750-ft gages were connected to a blast switch located at the 300-ft depth. This was based on the prediction that thermal refraction would cause the shock to arrive at intermediate positions of the gage string before it arrived at the top and bottom positions and would thus give plenty of starting time.

The following operations were done on each gage string before lowering it into the water:

1. The inside of each gage housing was charged with air between 300 and 1000 psi, depending on the element rating. This procedure increased the range of the gage, kept water out if leaks developed, and gave a method of checking for leaks.
2. Frames were bolted onto housings.
3. The lead-in tubes were vacuum-filled with water. This was done to remove all air bubbles.
4. Blast switches were spliced into the line.
5. Blast switches were closed, and voltage checks were made at each gage.
6. Circuits were closed, and continuity checks were made.

3.6 RECOVERY

Late in the morning of D+1, the USS Tawasa (ATF-92) was made available for hunting instrument floats. Neither the Bolster nor the Butternut (AN-9) was available as originally planned because of other assignments.

The YFNB-13 string was raised during the night of D-day. The YFNB-29 string was raised on the morning of D+1.

The wooden buoy with string No. 2 was located and raised first. The mine release had not operated. The 75 ft of ¼-in. wire rope which had been attached to the mine release in the buoy was missing, indicating failure at the spliced eye. The starters were found where expected—one at the 600-ft depth and the other at the 1275-ft depth. The wire rope and electrical cable were radioactive at depths above 300 ft. Measurements were taken of radioactivity as the wire was raised. It was then cut free and thrown overboard.

The wooden buoy with string No. 1 was recovered next. The instrument cable had parted somewhere around the 600-ft depth, resulting in the loss of the 750- and 1000-ft gages and the starters. This buoy showed more radioactivity than the other, as did the wire rope and the electrical cable. The mine release had not opened, and attached to it was a 30-ft length of the ¼-in. wire rope, with a frayed end.

Both buoys were in perfect condition and were returned to San Diego. Neither 150-ft spar was found. They were presumed to have sunk with the towline to which they were attached.

REFERENCES

1. J. E. Henderson et al., Crossroads Technical Instrumentation Report, Tests Able and Baker, Vol. I, Administrative History, Instruments and Instrument Preparation, University of Washington, 1947.

2. Ibid., Vol. II, Rigging and Instrumentation of the Target Ships.
3. Ibid., Vol. III, Time-Pressure Measurements, Results.
4. Ibid., Vol. IV, Original Data, Linear Time Axis Recorder.
5. Ibid., Vol. V, Original Data, Logarithmic Time Axis Recorder.
6. C. W. Nelson and C. F. Garland, Analysis of Underwater Explosion Data—Test Baker, Progress Report No. 5, University of California, Contract NObs-47436, June 1951.
7. C. R. Niffeneger, A Study of the Production of Step Shock Waves in Water, NAVORD Report 2624, U. S. Naval Ordnance Laboratory, White Oak, Md., September 1952.

CHAPTER 4

ELECTRONIC PRESSURE-TIME SYSTEMS

4.1 INTRODUCTION

Electronic pressure-time recording equipment was located on two LCM's (the 0-1 and 0-2) and the three YFNB's. The basic pressure-sensing elements used at each of the five stations were of two types—the tourmaline piezoelectric gage and an electromechanical gage manufactured by the Wiancko Engineering Co., Pasadena, Calif. The piezoelectric gages were suspended in the water on low-noise coaxial cables which were, in turn, supported throughout their length by a steel cable. The Wiancko gages did not require the use of special low-noise cables. At each of the two LCM stations the signal cables terminated in an instrument buoy suspended over the water at the stern of the LCM, whereas at the YFNB stations the signal cables were fed through a port in the side of the ship and then into an instrument trailer located within the YFNB. At each of the five recording stations the mechanical configuration of the equipment was dictated by the prime requirement of having the electronics as isolated as possible from any accelerations which might have interfered with the recording of the data.

4.2 MECHANICAL WORK ON LCM'S

4.2.1 LCM Hulls

The LCM-based recording instruments were within the limits of what was considered to be the area of total destruction and consequently necessitated a special housing and shock-mounting procedure for the electronic recording equipment. Since the LCM's served only as a floating base from which a buoy containing the recording equipment was suspended, the modifications to the LCM hulls were centered around the buoy and its suspension system.

The basic modifications to each 50-ft LCM hull were as follows:

1. The two engines, screws, and drive shafts were removed.
2. The engine-room casing was removed.
3. The conning tower, rudder, and rudder linkages were removed.
4. The ramp at the bow of the LCM's was welded shut instead of having the water seals repaired around its edges.
5. An elevated platform with a cradle for nesting the buoy when in the "servicing" position, along with a sheave for lowering the signal cable string, was constructed on the quarter-deck of each LCM, Fig. 4.1.
6. A boom, supported by an A-frame, was designed and built to serve as the supporting structure for the instrument buoy. Additional interior bracing was installed along the sides and the stern of the LCM's to distribute the load imposed by the A-frame, boom, and buoy.

In addition to the above-mentioned modifications to the LCM's, a metal shelf for supporting the EG&G radio receivers was constructed in the well of each LCM.

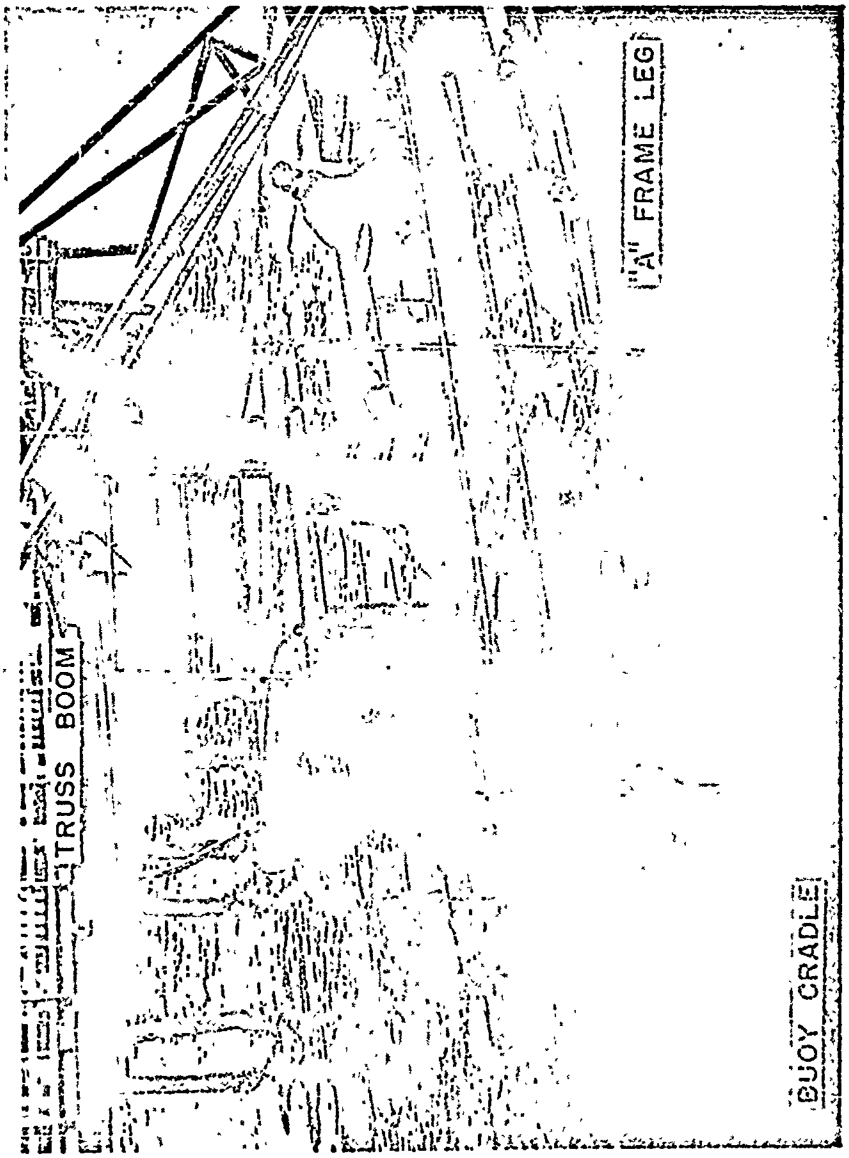

Fig. 4.1 — Buoy cradle and A-frame mount.

4.2.2 LCM Tow-cable Attachment

The LCM's were held in position in the target array by the tow cable which connected all the array ships together. Initial towing of the LCM's was accomplished by connecting a "secondary" cable from the bow of the LCM's to a floating marker buoy which was, in turn, fastened into the main towline. To keep the longitudinal axis of the LCM's parallel to the direction of the tow, the main towline was passed through two eyelets on the portside of each LCM. The line was free to slip in the eyelets but was restrained from too much fore and aft movement by clips which were attached to the towline. After the main tow cable had been secured in the eyelets, the actual towing operation was transferred to the main cable.

The eyelet was part of a bracket which slid into a vertical track welded to the side of the LCM and was intended to break loose under an extreme vertical force or, should the LCM sink, by a hydrostatic release.

Figure 4.2 shows the bracket through which the main tow cable was passed.

4.2.3 A-frame and Boom

The A-frame with its associated boom was the major structural addition made to the LCM's and was the structure around which most of the other LCM modifications were made.

The A-frame was built of two pieces of 6-in. steel pipe and welded together at one end to form the apex of the A. The base of the A fitted into two brackets—one on either side of the stern of the LCM—and hinged on pins which permitted the A-framework to be raised or lowered. Reference to Fig. 4.1 shows how the legs of the A-frame straddled the buoy cradle and were attached to the deck of the LCM.

A triangular truss boom was constructed of 3-in. steel pipe and rested on and pivoted around the cross bar of the A-framework and thus served as the immediate supporting structure from which the buoy was hung. The lower end of the truss boom was fastened to a slider which was, in turn, able to be moved along the length of a greased 6-in.-pipe guide rail which was rigidly fastened to the deck of the LCM. Figure 4.3 shows the relation between the truss boom, A-frame, and the guide rail.

In practice, the position of the slider on the guide rail was set by pulling it along the rail by means of a rope and block-and-tackle arrangement. This action determined the position of the triangular truss boom and thus that of the buoy. For reliability, the A-frame, boom, and foundations into the LCM hull were designed to withstand and transmit, without mechanically failing, a 10-g acceleration to the buoy–signal-cable assembly.

4.2.4 Winch and Generator Power

There was a need for two sources of mechanical power on each LCM, one to drive a generator for charging the nickle-cadmium batteries installed in the instrumentation buoy and the other to supply power for electricity and a winch. The mechanical power requirements were met by installing two surplus four-cylinder engines in the original engine compartment of each LCM. Cooling for one of the two 15-hp water-cooled engines was accomplished by installing "keel coolers," a gridwork of cooling pipes located below the keel of each LCM; the other engine made use of a conventional radiator and fan for its cooling.

Each of the two engines was directly connected to a three-phase 3-kva 110-volt alternator, and the port engine on each LCM was, in addition to driving an alternator, connected through a reverse gear unit to a worm-gear winch located on the tank deck. The winch was used primarily for handling the gage-support cable and secondarily to aid in attaching the tow cable to the LCM's.

The portside engine and alternator supplied electric power into the wiring system of each LCM, and the output of the other engine-alternator unit was fed directly into a three-phase electric motor which was, in turn, mechanically connected to a standard 50-amp-capacity aircraft type generator. This aircraft generator had been modified slightly by adjusting its carbon-pile voltage regulator in order to produce a regulated output of 35 volts (instead of the normal 28 volts). The 35-volt output was used to charge the nickel-cadmium batteries used in the instrumention buoy. It was found that this method of charging the buoy batteries permitted

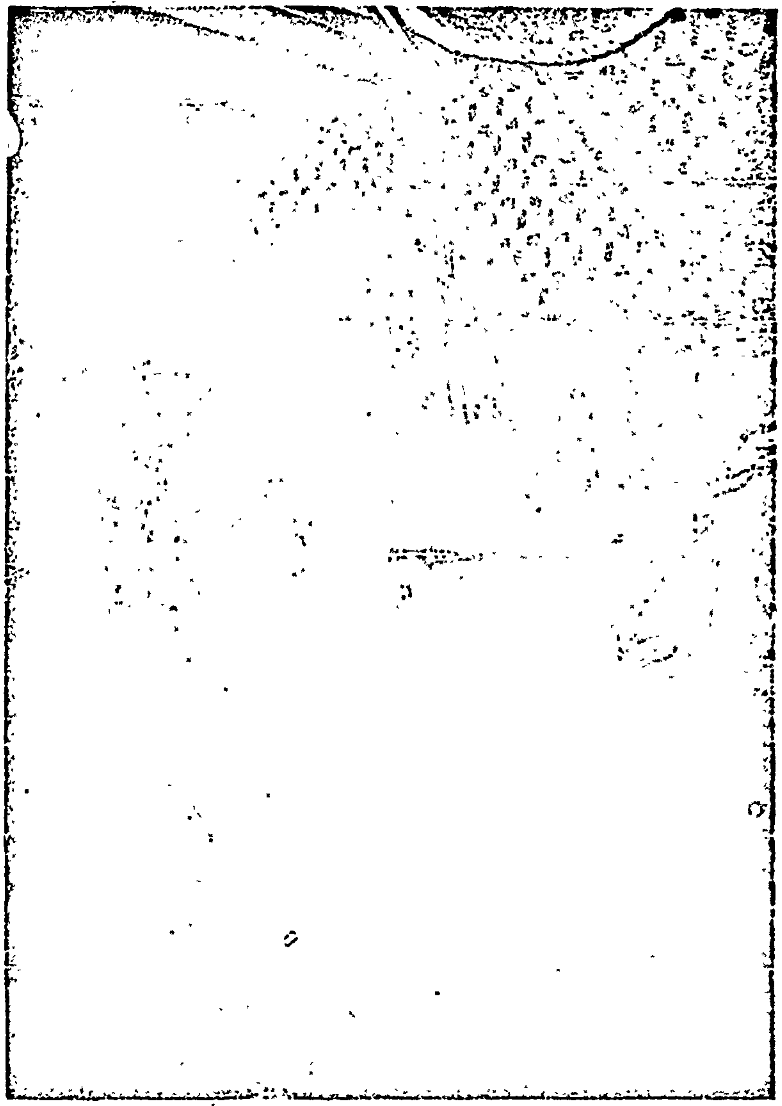

Fig. 4.2—LCM tow-cable attachment.

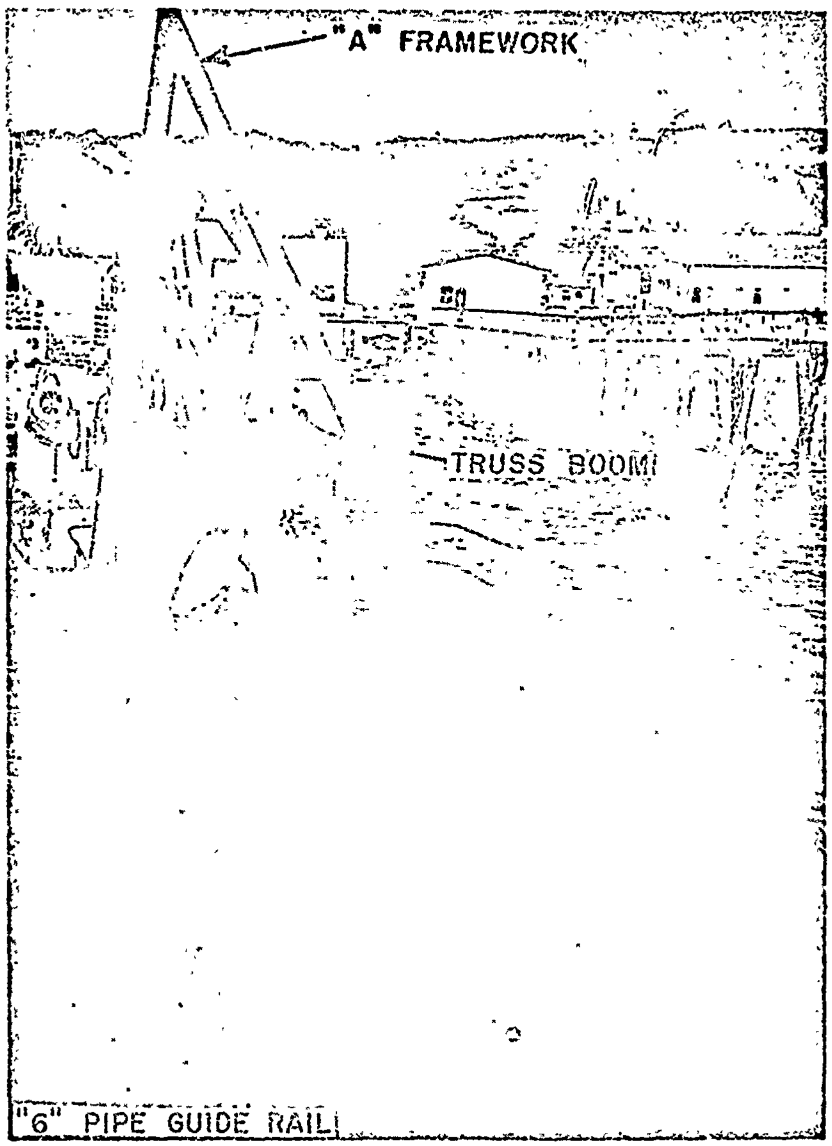

Fig. 4.3—A-frame and truss boom.

them to be recharged in the shortest time and without any danger of damaging the batteries or of excessive gassing. The complete charging time could be limited to about 30 min with this system.

4.3 MECHANICAL DESIGN OF INSTRUMENT BUOYS

4.3.1 Buoy-design Considerations

To ensure uninterrupted recording at shock-wave arrival time and a minimum of damage to the electronic recording equipment during the recovery interval, the buoy housing the recording equipment at locations 0-1 and 0-2 had to meet the following design conditions:

1. Be suspended from an expendable floating unit and be clear of the water during the critical phase of the underwater shock.
2. A means of releasing the buoy from the LCM should the suspension point for the buoy experience a vertical acceleration of more than 4 g.
3. The buoy had to withstand both dynamic and static pressures of 100 psi as well as to maintain leak integrity throughout the test and for an anticipated recovery delay of three weeks.
4. Safety releases had to be provided to prevent the buoy from being dragged down should it or its attached cables become entangled with other sinking equipment.
5. The total weight of the buoy had to be kept to a minimum in order to facilitate its handling and servicing under sea conditions. It was also required that the buoy be buoyant enough to remain afloat while supporting the extra weight of its associated cables and gages.

4.3.2 Buoy

The basic buoy was a modified 550-gal gas tank manufactured by the Buffalo Tank Corp., Dunellen, N. J. It was constructed of a $\frac{1}{4}$-in.-sheet-steel cylinder and two $\frac{5}{16}$-in. elliptical ends. The outside diameter of the tank was 41 in., and the over-all length was 108 in. The net weight of the tank was 1300 lb.

To provide a support for the tank while on land, legs were made of 4- by 4-in. I-beams and dog-legged away from the buoy for added stability. Each leg was fitted individually into a socket near the top for torsional stability and then bolted in a tongue-in-groove fashion to a guard near the base of the tank.

The basic layout of the individual parts of the buoy, including the following NOL modifications, can be visualized by reference to the buoy schematic, Fig. 4.4.

1. Upper access port: The upper end of the tank was cut away 4 in. below the top edge of the cylindrical section, and a reinforced flat top with an elliptical 30-in.-diameter port section was welded in place. A flanged head served as a lid to seal off the port.
2. Internal bracing: Reinforcing ribs were welded to the inside of the tank to increase its resistance to external crushing forces after a hydrostatic pressure test performed on the tank showed it to be necessary. The results of this test showed buckling along a lap weld at 65 psi, indicating a marginal strength and a need for the reinforcing ribs. After reinforcing with the ribs, the tank withstood a test pressure of 100 psi without any leaks or other damage.
3. Lower access port: The bottom end of the tank was fitted with a flanged 12-in. port in order to provide an access to the recording-equipment cables (located inside the tank) which were to be connected to the gage cables prior to the lowering of the gage string.

To maintain water tightness at the base of the buoy where the signal cables passed through, a gage-cable connector plate was designed for bolting over the cable-port opening. The design of the connector plate was dictated by the requirement of maintaining a high electrical impedance of the gage cables and by the necessity of making the connections through the bottom of the buoy after the electronics had been installed. The plate consisted of a $14\frac{1}{2}$-in.-diameter aluminum disk $1\frac{1}{2}$ in. thick, with 12 cable entries as shown in Fig. 4.5. The plate had special elongated bolt holes which were designed to permit its removal without removing the Allen bolts from the port flange. This design eliminated the danger of dropping either the bolts or the gasket into the water while servicing the buoy at sea. A cable snubber was incorporated into the plate to prevent the gage cables from being accidentally pulled out at the stuffing glands and thus causing

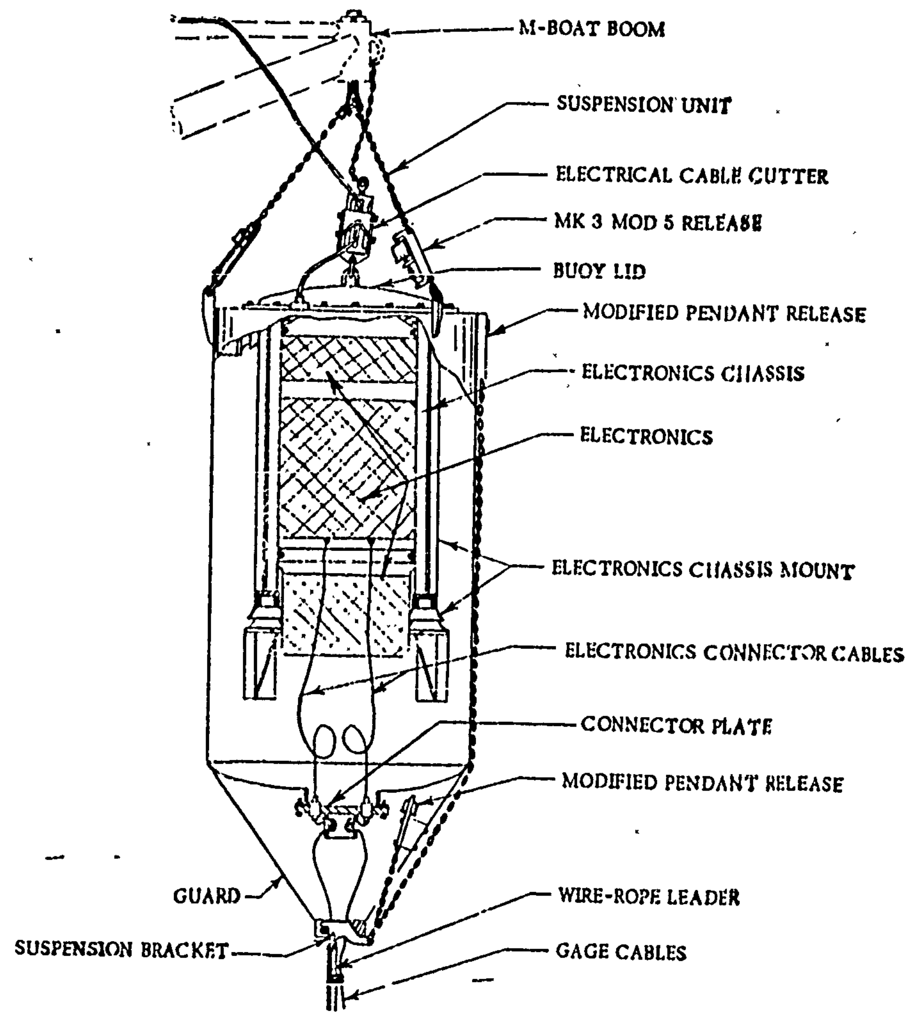

Fig. 4.4—Schematic diagram of the instrument buoy.

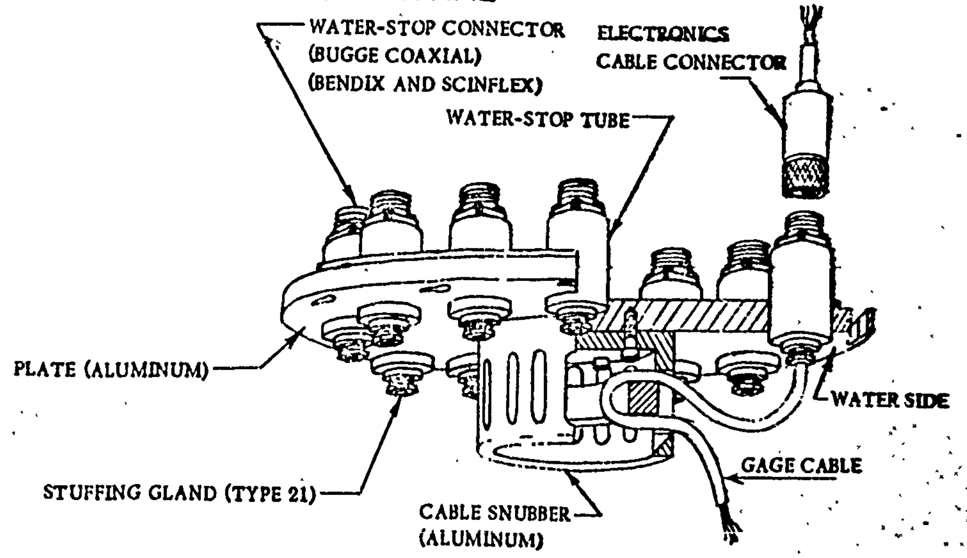

Fig. 4.5—Connector plate.

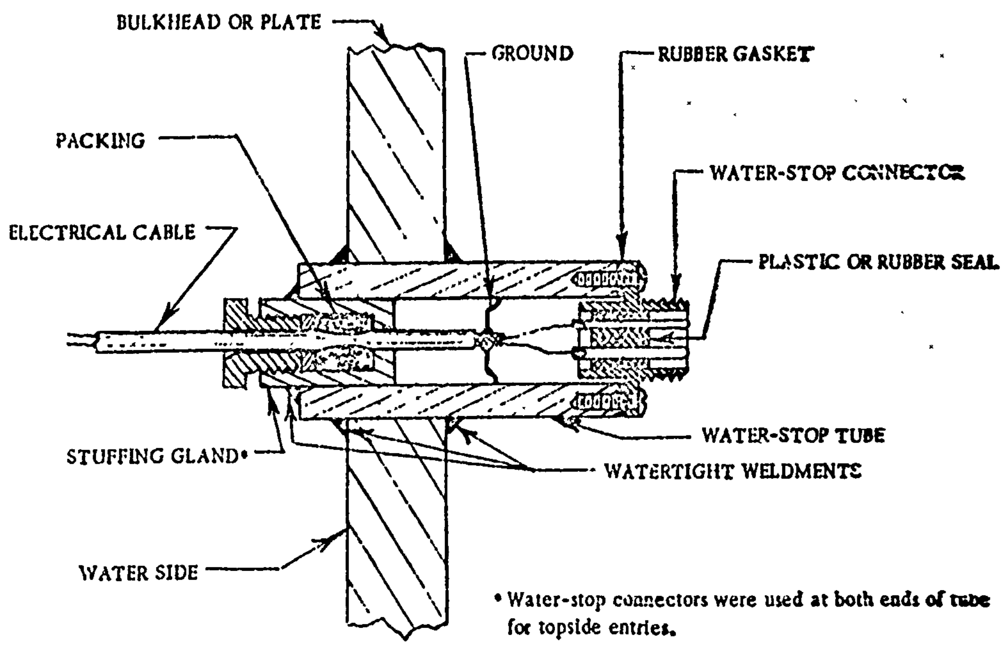

Fig. 4.6—Water-stop cable entry.

damage to the water-stop connector. The use of the cable snubber and the tests applied to it are covered more fully in Sec. 4.3.6.

The pressure plate was tested hydrostatically to check for water tightness. Leaks developed around the weldments and the Bendix gaskets ($\frac{1}{32}$ in. thick) but were remedied after reworking the weldments and increasing the thickness of the gaskets to $\frac{1}{16}$ in.

Previous experience in the use of buoys for underwater tests showed that conventional stuffing glands were inadequate for maintaining water tightness at the cable-entry points. When cables parted, either in handling or under shock, the water would seep through the cable casing past the stuffing gland and into the buoy. For this reason the cable entries to the buoy were specially designed to provide a secondary water stop in the event the cables parted. Each cable entry consisted of a 2-in.-O.D. by 1-in.-I.D. tube fitted at one end with a stuffing gland and at the other end with a water-stop connector. Each connector and connector-plate assembly was pressure tested hydrostatically at 100 psi. Details of the cable entry are shown in Fig. 4.6.

4. The conical guard: A conical-shaped guard was welded to the bottom of the buoy to protect the vulnerable connector plate and the cables coming from it and also to reduce the water-entry shock to the buoy and its electronics when it dropped into the water. In addition, the guard served as a frame to which the steel cable, used to support the gage string, was attached and as a support point for the buoy legs. An effort was made to avoid securing any equipment under load directly to the buoy shell. Details of the conical guard and the leg-attachment points can be seen in Figs. 4.7 and 4.8.

4.3.3 Electronics Chassis and Buoy Chassis Mount

To support the electronics within the buoy, a lightweight aluminum structure was designed which consisted essentially of four channel uprights, two plug-in plates, and two battery boxes. The unit was 43 in. high, 20 in. wide, and 24 in. deep. Four 3-in. aluminum channels were bolted in pairs, flange to flange, and formed the uprights and the main structure to which the tape recorders, the panels, and the battery boxes were bolted. The matched flanges provided two diametrically opposite keys which guided the completed assembly into the chassis mount located within the buoy. The panels, $\frac{1}{4}$-in. aluminum plate, were fitted with special quick locks and plugs to facilitate the electronic component replacement and installation. The two battery boxes, 14 in. wide by 10 in. high by 10 in. deep, were made of $\frac{1}{4}$-in. aluminum plate and housed 23 nickel-cadmium storage batteries each. The boxes were bolted back to back to the bottom of the channel uprights and also served as a stand to support the electronics assembly when it was removed from the buoy. The tape recorders were bolted back to back at the top of the uprights. By loosening six bolts the aluminum framework could be split into two independent sections, each containing a complete recording installation. Details of how the component parts are fitted together can be seen in Fig. 4.9.

To support the electronics within the buoy and isolate it from shocks and high-frequency oscillations, a rack, shown in Fig. 4.10, resting on shock mounts was fitted in the upper half of the buoy. The rack consisted of two slotted vertical rails, 43 in. high, that were bolted to two braced horizontal channels. The vertical rails served as guide tracks for the electronics chassis, and the channels served as a base on which the chassis rested. The rack assembly was isolated from the buoy framework by two shock mounts at the top and four at the bottom. To install the electronics, the vertical rails were pulled up against the mounts by tightening bolts in them which served to compress the shock mounts and thus permitted the electronics chassis to slide in freely. When the chassis rested on the base channels, the vertical rails were released, thus clamping the chassis securely. A retaining bar, bolted to the top of the rails, further locked the chassis in place.

4.3.4 Buoy-suspension Unit

The buoy was suspended over the water by a one-point suspension system to reduce the possibility of angular acceleration to the buoy during its release; this was important because the recorder tape reels, within the buoy, were sensitive to angular accelerations. The buoy-suspension unit, shown in Fig. 4.11, consisted of a tensile bar, a collet, and a three-strand bridle.

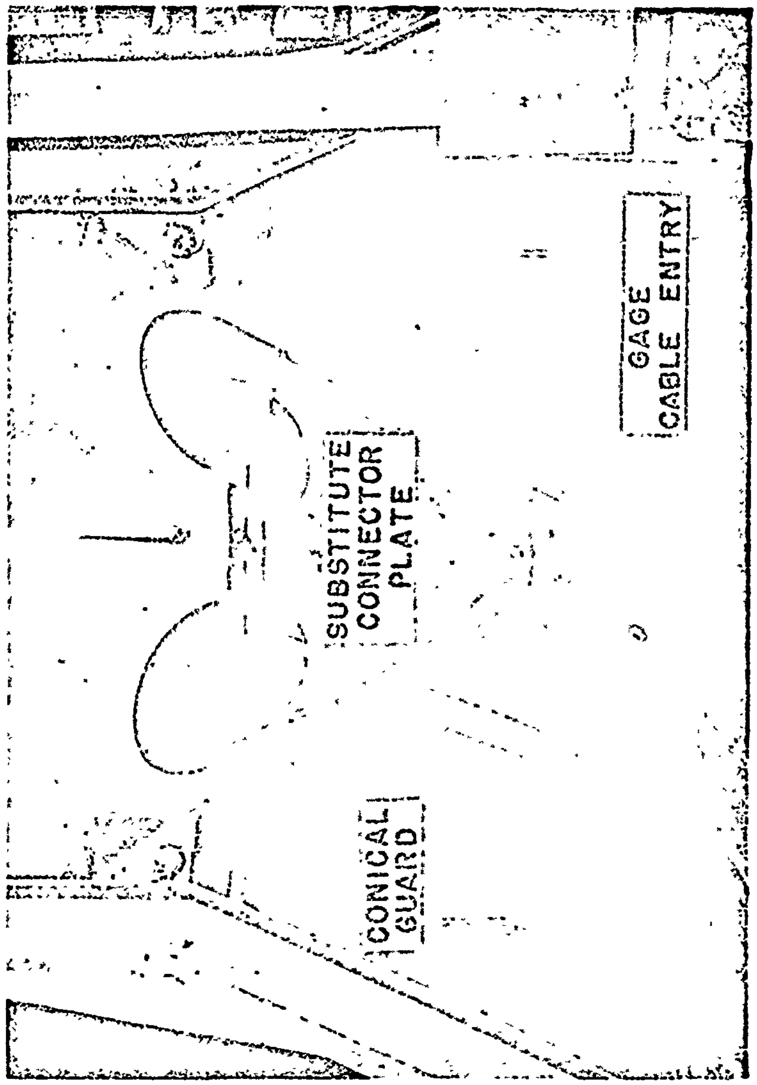

Fig. 4.7—Base of buoy, showing leg attachment and conical guard.

CONFIDENTIAL

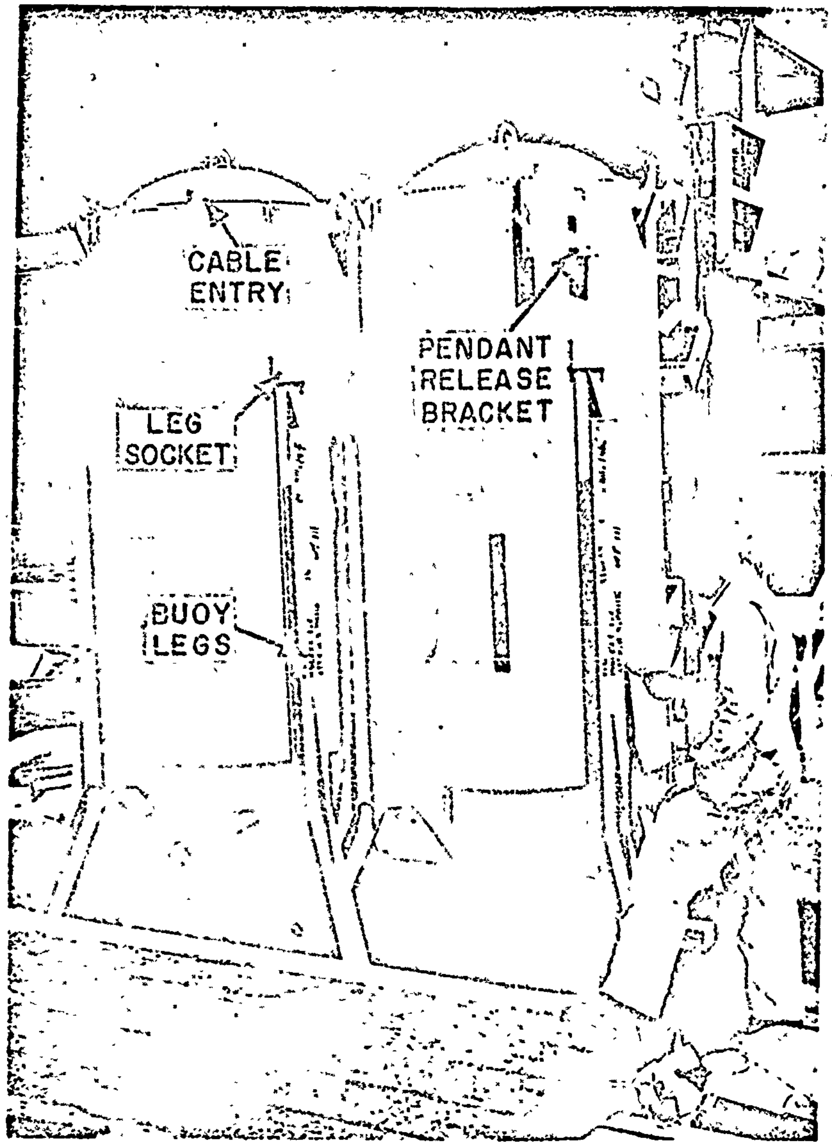

Fig. 4.8—Completed buoys.

SECRET—RESTRICTED DATA

CONFIDENTIAL

CONFIDENTIAL

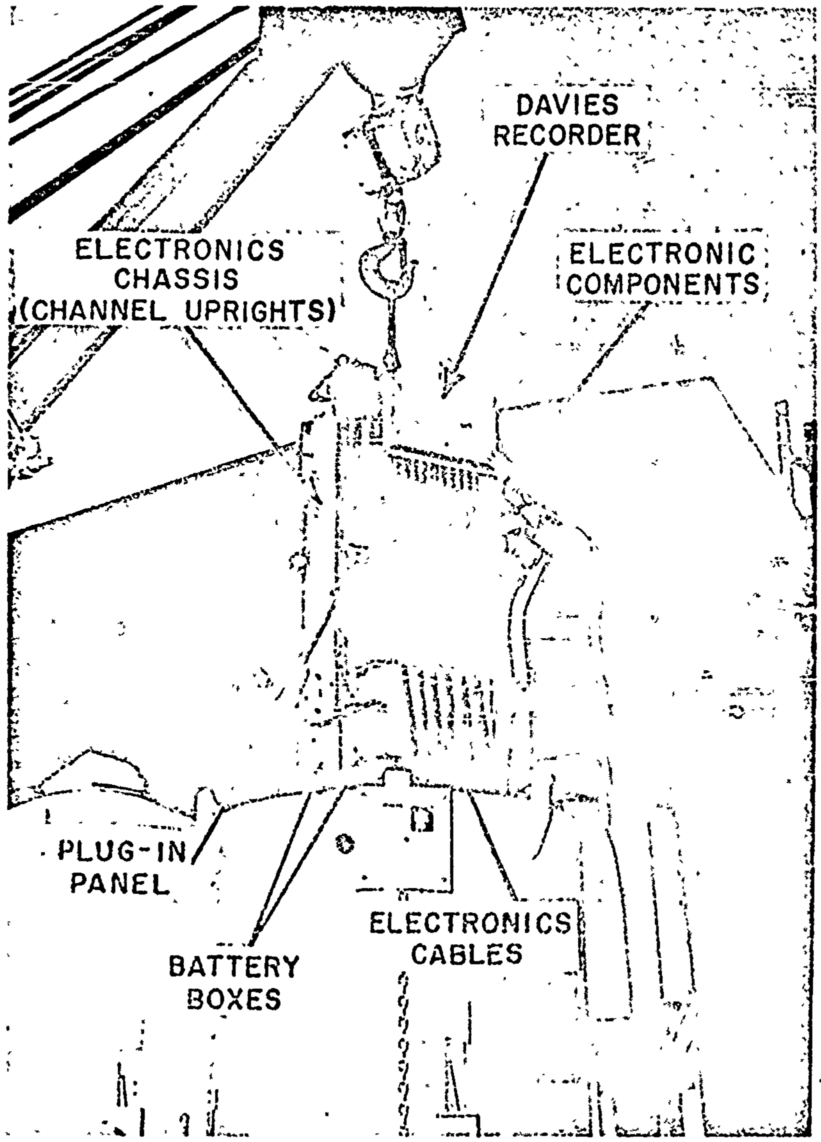

Fig. 4.9—Installing electronics in buoy.

SECRET – RESTRICTED DATA

CONFIDENTIAL

CONFIDENTIAL

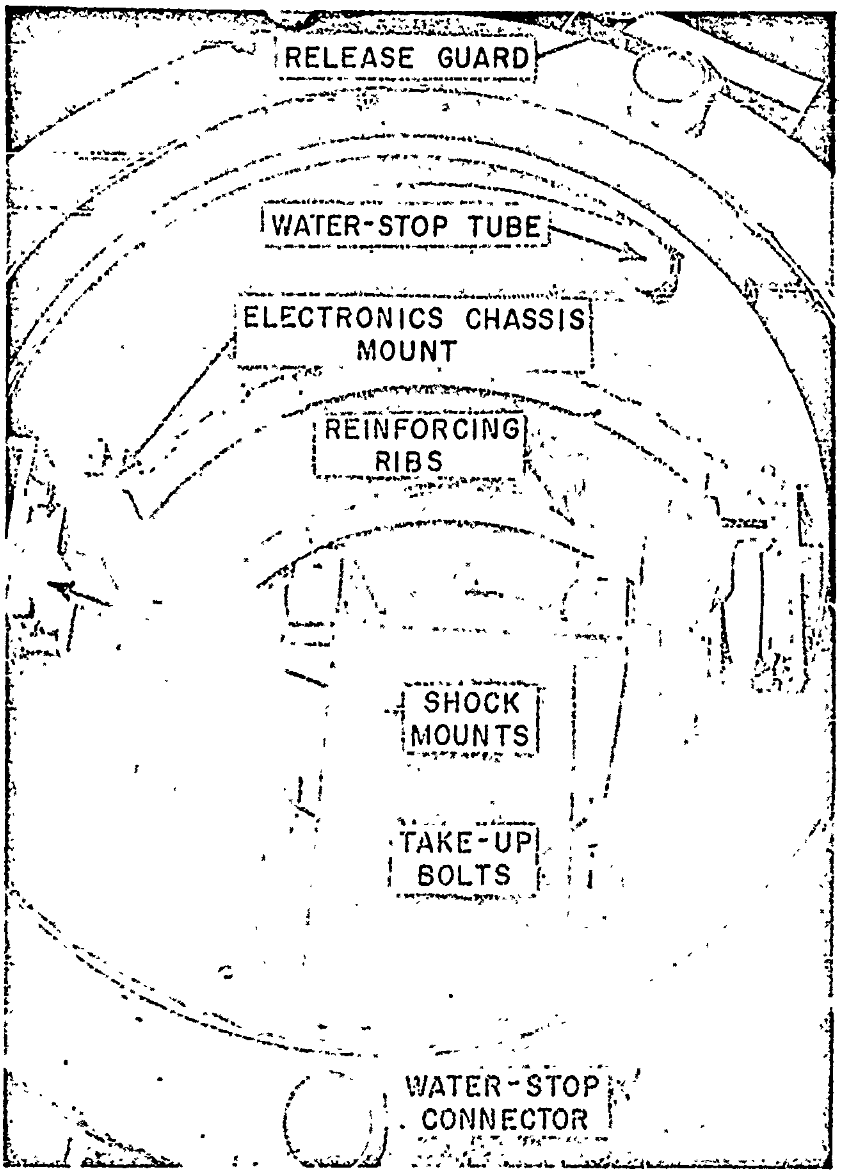

Fig. 4.10—Interior of buoy.

SECRET—RESTRICTED DATA

CONFIDENTIAL

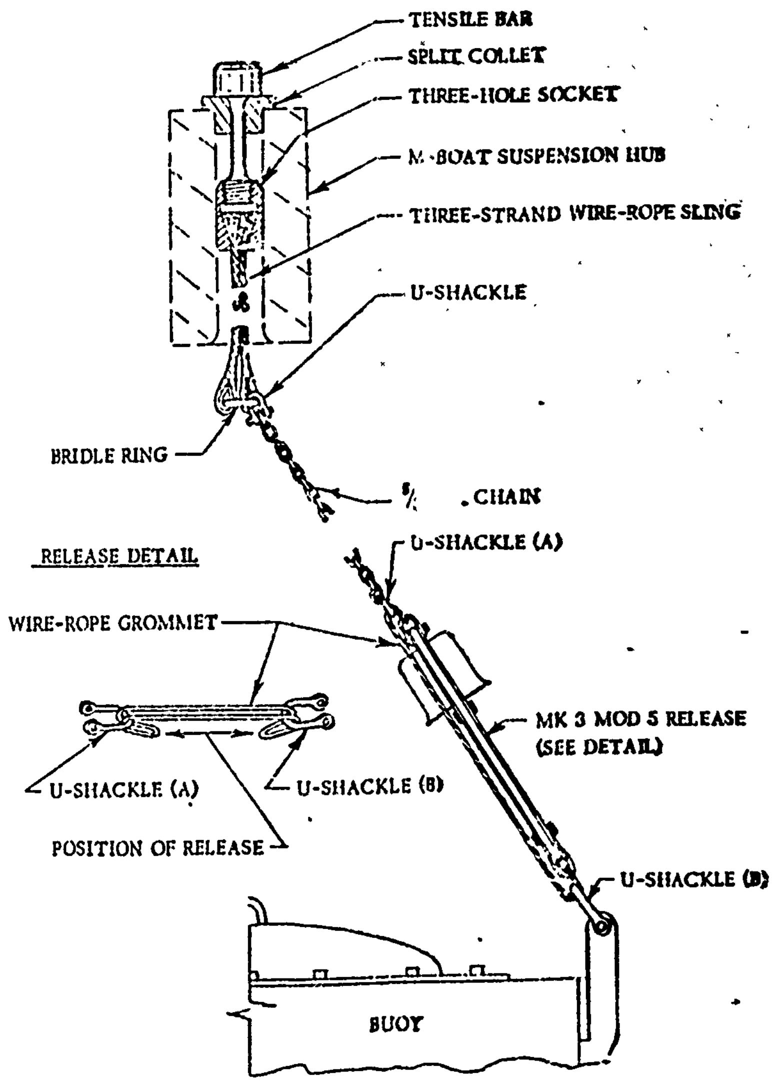

Fig. 4.11—Buoy-suspension unit.

Tensile and shock tests were run on sample tensile bars to compare the strength characteristics under shock and static loading. Annealed copper and both 2S-0 and 61S-T6 aluminum were tested, and it was found that the breaking strength of each material, under short-duration shock loads, was greater by an amount approximately equal to the per cent elongation of the material than its breaking strength under a static load. Aluminum (61S-T6) was selected for the tensile bar to reduce the load on the M-boat boom when under shock and was designed primarily to release the buoy under a minimum of 4 g of acceleration. The tensile bar consisted of a 6-in.-long bar with a 2-in.-diameter shoulder, a $^5/_8$-in.-diameter neck-down shaft, and a $1^1/_4$-in.-diameter threaded stud. The bar was supported in the boom hub by means of a split collet and screwed into the wire-rope socket. The wire-rope socket was similar to conventional sockets with the exception that three strands of wire were bonded into a three-hole socket. Each strand was made up of $^3/_8$-in. wire, 10 in. long, with a $^3/_8$-in. thimble eye. A $1^1/_2$-in.-I.D. bridle ring made up of $^1/_2$-in.-diameter rod ran through the wire-cable thimble eyes and provided an attachment for the bridle. The bridle itself consisted of three 2-ft lengths of chain, joined to the bridle ring with $^3/_8$-in. U-shackles, and three Mk 3 Mod 5 hydrostatic releases fitted with $^3/_8$-in. wire-rope grommets.

The split collet—the supporting member for the tensile bar—provided a quick and simple means of securing the entire buoy assembly to the boom hub. The tensile bar was simply thrust up through a 2-in.-diameter hole in the hub, the collets were dropped into place at the top of the hub, and the bar was then pulled down until the shoulder rested on the collets.

The three-strand socket was designed to provide a flexible link between the tensile member and the bridle which, by pulleylike action, directed the shock load axial to the bar regardless of the orientation of the M-boat. The bridle, in turn, and through three hydrostatic releases, supported the buoy from three suspension ears which were spaced equally around the rim of the buoy. This arrangement allowed ample space between the bridle members for removing the 35-in.-diameter buoy lid and afforded enough headroom to lift the electronic recording equipment in the event component replacement became necessary.

A tensile test, using a 6-g tensile bar, was run on the complete suspension unit to evaluate the assembly, and it was found, after a few modifications (such as increasing the diameter of the wire-rope grommet to $^5/_{16}$ in.), that no mechanical failures occurred even when a shock sufficient to break the 6-g tensile bar was applied.

4.3.5 Buoy and Pendant Releases

The suspension system used for each of the buoys made use of three hydrostatic releases which formed a connecting link between each of the supporting ears on the buoy and the bridle ring (Fig. 4.11). Their purpose was to free the buoy from the M-boat if the initial shock should fail to break the tensile bar, in which case the M-boat would sink and drag the buoy down with it. The releases were slightly modified by installing heavier springs in them to prevent them from being triggered by the shock. However, if the tensile bar did not break and the M-boat did drag the buoy under, the releases would have freed the buoy at a depth of 200 ft.

In addition to the three releases in the suspension harness of each buoy, there were two other hydrostatic releases used to ensure the flotation of the buoy. Reference to Fig. 4.4 will show two hydrostatic pendant releases, one fastened to the side of the buoy near its top and the other within the conical guard at the base of the buoy. These two releases were connected in parallel to ensure against a premature release during handling and were intended to release the steel cable supporting the signal cables from the buoy should sinking equipment become entangled in the cables and pull the buoy down.

The pendant release consisted of two modified Mk 3 Mod 5 hydrostatic releases and a suspension bracket linked together with a $^5/_{16}$-in. chain. As a result of laboratory tests with an air gun for checking the response of the releases to pressure pulses, the release bellows were modified to delay their actuation time from 0.1 to 15 sec. This was necessary to prevent their actuation by anticipated pressure pulses following the entry of the buoy into the water. After modifying the releases to prevent them from being triggered by long-duration (of the order of 100 msec) pressure pulses, they were essentially tested under hydrostatic conditions to determine their actuation time. It was found that the orifice type of release actuated in 10 to 30 sec and the stem-leakage type actuated in 5 to 30 sec. It was decided to use the latter type since there was less chance of its becoming clogged while in service. The modifications to the pendant release are shown in Fig. 4.12.

To test the complete suspension unit for wear, the buoy was left hanging from the M-boat truss boom in the ready position and allowed to swing free for a one-week period. The test was run at dockside with no load or pendant on the buoy. It was found that no appreciable chafing was observed on any of the strands in the wire-rope socket; only the marline winding had worn away. Then, with the buoy still in the ready position and with a 4500-lb weight hanging 25 ft below in the water and attached to the suspension bracket of the buoy, the M-boat was towed at 8 knots to test the bridle for resistance to drag loads. No apparent damage was observed to any of the components in the suspension system.

4.3.6 Upper and Lower Cable Cutters

Control cables for the buoy and the NRL gage cables, secured to the top of the buoy and to electronics aboard the M-boat, had to be cut away if the buoy dropped from the boom.* Cutting had to be done without putting strain on the cable connectors in the buoy or accelerating the buoy angularly. The upper cable cutter, shown in Fig. 4.13, was designed to utilize the energy of the falling buoy for cutting free both the electrical control cables and the NRL cables and to apply the cutting load axial to the buoy. The unit consisted of two thin-walled cylinders, one fitting within the other. Essentially, the inner cylinder held the cables fast in specially milled slots while the outer cylinder cut them free. One cylinder was fastened to the boom, and the other was fastened to the center of the buoy lid. As the buoy fell, the cylinders were pulled apart, and thus the cables were cut.

In addition to severing the buoy control cables and the NRL gage cables when the buoy dropped away from the supporting boom, there were gage signal cables coming from the bottom of the buoy which had to be cut if they became entangled with other sinking equipment and dragged the buoy down. The hydrostatic pendant release (described in Sec. 4.3.5) would have actuated at a depth of 100 ft and released the steel supporting cable to which the gage signal cables were fastened, thus putting the entire weight of the signal cables on the connector plate (described in Sec. 4.3.2) and still endangering the buoy. Because of this possibility, a cable snubber unit was designed and made a part of the connector plate (Fig. 4.5). The edges of the slots in the snubber unit were designed to cut rather than simply restrain the cables. Also, the cables were assembled so that six pairs of cables differed in length by 2 in.; therefore the entire weight of the pendant (1500 lb) would be brought to bear in turn on each of the cables. Tests conducted with dummy loads connected to relatively short pieces of signal cables to simulate the weight of the total length of the signal cables showed that none of the cables pulled out at the stuffing glands when the hydrostatic pendant release was actuated and that the cables were severed neatly at the cutting edge of the snubber as intended.

4.4 OPERATION OF INSTRUMENT BUOY

4.4.1 Plan of Operation

The two LCM's (the 0-1 and 0-2) were ferried out to the Pacific testing grounds in the LSD-19; and, before being launched, the following operations were completed: The buoys were hung from their respective booms, the gage signal cables were connected, the electronic recording equipment and sensing gages were checked, the buoy batteries were charged, the EG&G radios were tested, and the hydrostatic releases were set. On the LST-1048 the tow-cable attachment fittings were installed and checked.

*At −1 min, the buoy was to have been armed and operating independently of the M-boat controls, and the NRL data were to have been recorded prior to the arrival of the shock wave at the LCM.

CONFIDENTIAL

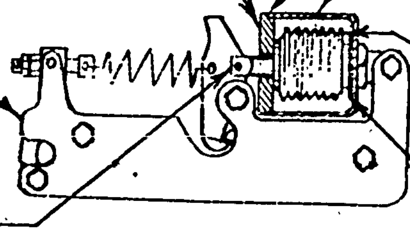

Fig. 4.12—Modified Mk 3 Mod 5 release.

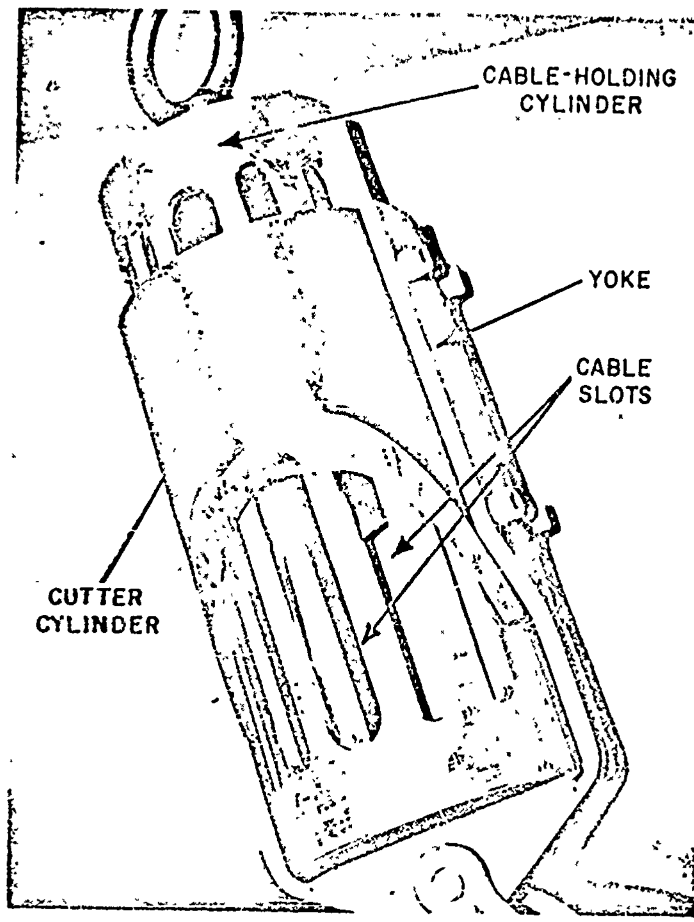

Fig. 4.13—Upper cable cutter.

SECRET—RESTRICTED DATA

CONFIDENTIAL

Each LCM was towed to the tow wire by a powered LCM on D−2, and 60-ft wire pendants were used to attach it temporarily to the main tow cable. The winches on board the LCM's were then used to raise the tow cable and place it in the side brackets (Sec. 4.2.2), first the forward bracket and then the one near the stern. Safety chains were attached, and the boats were then considered secure in the main tow.

On D−1, the ¾-in. nontwisting steel supporting cable was payed out over the stern sheave on each LCM, and the signal cables with the pressure-sensing gages (Figs. 4.14 and 4.15) were fastened to the steel supporting cable at intervals varying from 12 to 50 ft. After the steel supporting cable with its attached signal cables had been let out, the end of the steel cable was attached to the bottom of the buoy. Then the buoy, with the use of the winches, the A-frame, and the truss boom (with the buoy), was moved to its outboard position to complete the setting operation. The EG&G radio control receivers were again checked, and a visual inspection of all the gear was made to check for points of wear to ensure its proper operation. All machinery and loose gear were then secured.

At H−1 min the buoys were to have been operating independently of their LCM's. It was planned that each buoy, at that time, would be ready for the following sequence of events:

1. The arrival of the shock wave and the resultant movement of the LCM would break the tensile bar supporting the buoy.

2. As the buoy fell away from the LCM, the topside electrical cables would be cut by the cable cutter.

3. In the event that the buoy did not fall free (owing to insufficient g units to break the tensile bar) and the LCM sank dragging the buoy down, the gage cables would be cut free at a 100-ft depth and the buoy would be released from its support bridle at a 200-ft depth and then float up free.

4.4.2 Results of Tests (D-day)

Despite unfavorable sea conditions, the general plan of operation was followed. However, on D−1, emergency chains were used to support the towline bracket since the hydrostatic releases, originally intended for this purpose, mechanically failed in the heavy seas prevailing at that time.

A few hours before zero time both buoys prematurely dropped free of the LCM's because of chafing or failure of the wire-rope socket units of the suspension bridles. This resulted in cutting the buoys off from the radio arming signal, thus rendering them inoperative. Consequently, no data were obtained. A survey of the equipment after recovery of the two buoys on D+1 and D+2 revealed no further failures or damage despite the severe shock sustained during handling in rough seas. No leaks were observed even after the buoys had been in the water for well over 24 hr, including the shot time. In general, servicing and handling of the buoys presented but few problems and were relatively simple. Both LCM's survived the shot but were not recovered.

4.4.3 Recommendations

The buoys, with minor modifications, could be used adequately in similar tests or where it was required to place the buoys in the water. However, the following modifications are recommended:

1. The M-boat boom should be raised sufficiently to permit installation of the tensile bar between flexible linkages and outside the hub.

2. The cables from the electronics instruments should be made longer—preferably long enough to reach at least 3 ft beyond the flanged port at the base of the buoy to facilitate making the connections.

3. Design the suspension hub to release the bridle hydrostatically with just one Mk 3 Mod 5 release instead of the three which were used in the present system.

4. The three-strand wire-rope sling in the bridle assembly should be materially strengthened.

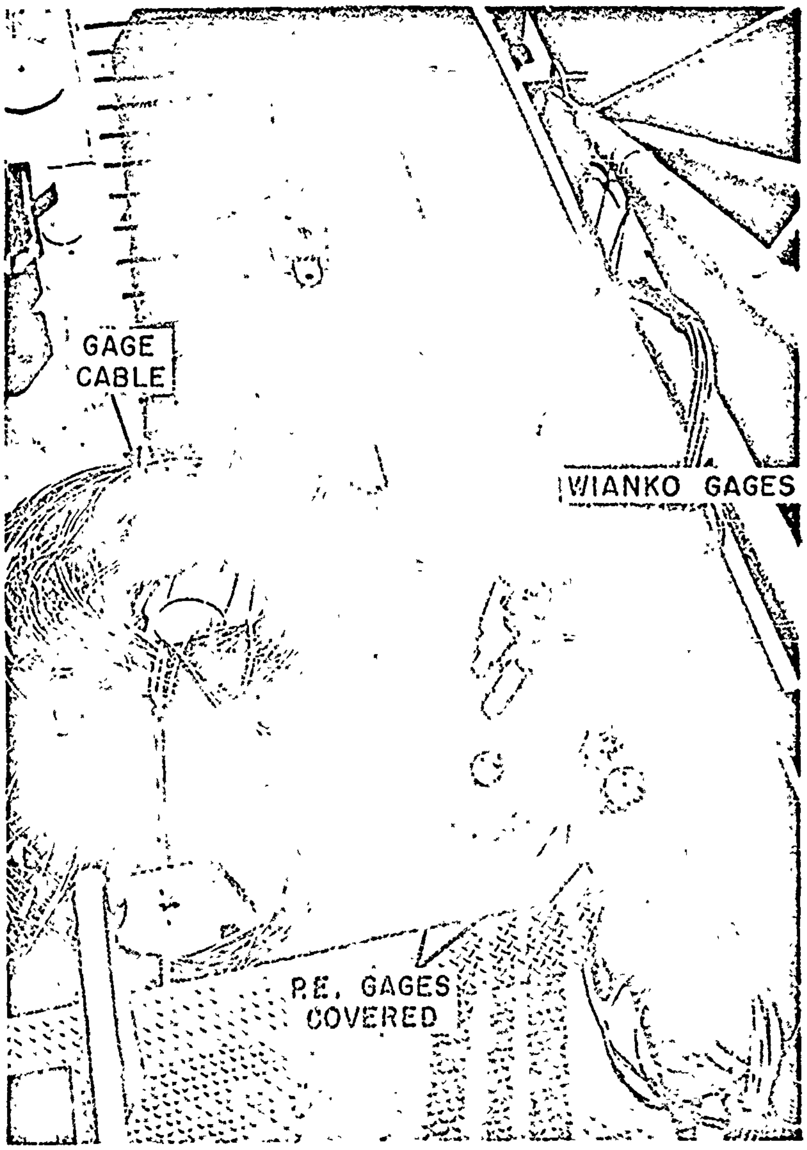

Fig. 4.14—Storage of signal cables and sensing gages on LCM's.

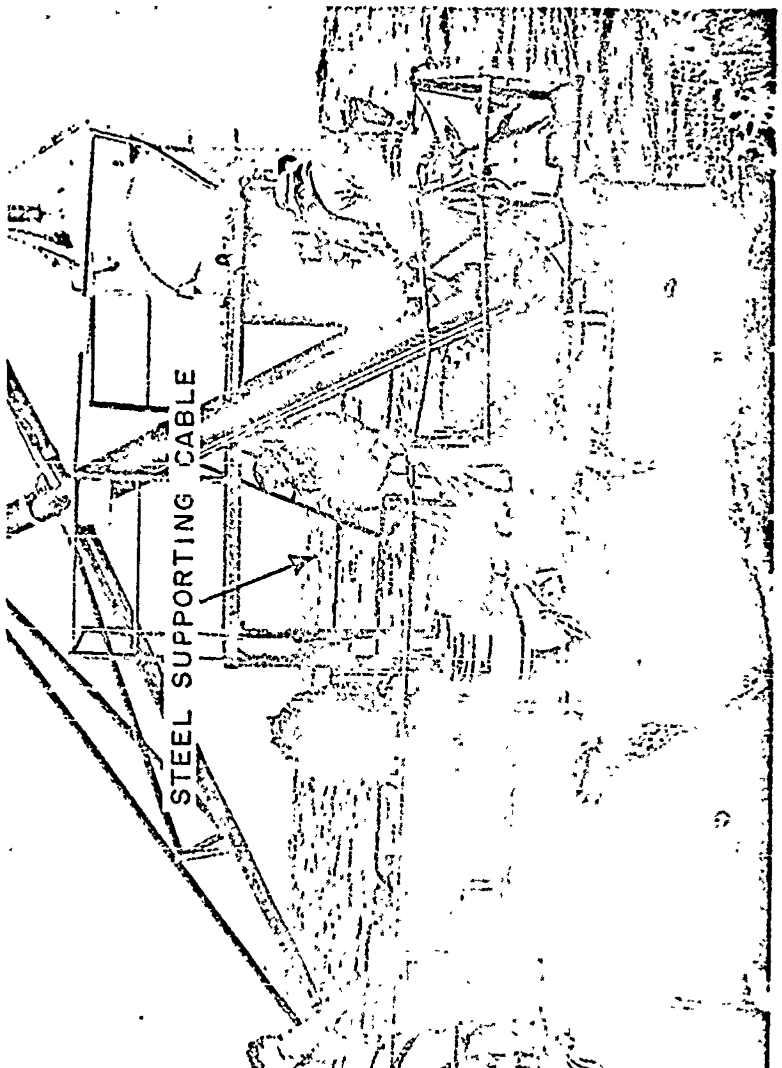

Fig. 4.15 — Signal-cable setting.

4.5 MECHANICAL WORK ASSOCIATED WITH YFNB'S

4.5.1 Trailers

Three trailers were provided for the use of Project 1.2 to accommodate the recording instrumentation and test equipment necessary on the YFNB's. One trailer was rigidly mounted in the forward section of each of the three barges. To have enough clearance between the top of the trailers and the overhead crossbeams of the YFNB's, the trailers had their wheels, springs, and undercarriage removed. Figure 4.16 shows how the chassis of each of the trailers rested directly on, and was welded to, two 10-in. I-beams placed crossways at each end of the trailers. The I-beams were, in turn, welded to the deck of the ship. Extra flanges were welded to the ends of the I-beams to increase their effective width so that there would be less chance of the trailers "rocking" off. The I-beams on which the trailers rested were centered as well as possible over the supporting cross members under the YFNB decks to distribute the load imposed by the trailers better and to provide an even more rigid support.

Two of the trailers used were standard refrigerated meat-transport trailers, and the other was a conventional cargo carrier; the meat trailers were placed aboard the YFNB's 12 and 29, and the cargo trailer was placed on the YFNB-13.

Power for the recording electronics was supplied from within the trailers by standard Navy type storage batteries which were clamped into an angle-iron framework and bolted solidly to the frame of the trailer. It was not considered necessary to shock mount the batteries in any way.

A wooden box with a hinged top served as a compartment for the batteries and also formed a working shelf when the lid was closed. Air-entrance holes were drilled at one end of the compartment to permit the exhaust fan, placed at the opposite end, to discharge any accumulated gases formed during the charging cycle to the outside of the trailer. Tungar rectifiers were mounted on the side wall of the trailers above the battery compartment for the purpose of recharging the batteries.

Wooden workbenches with padded pigeonholes were designed and built to house the test equipment and other spare parts associated with the recording equipment and were secured to the trailer floor with wood screws. It was not considered necessary that the workbenches be able to survive the shock but rather that they simply afford some measure of protection to the test equipment.

A first-aid kit and two fire extinguishers, with reduced charges to compensate for an anticipated large temperature rise, were mounted in the rear of each trailer.

4.5.2 Trailer Instrumentation Mounts

The meat-transport trailers were constructed with heavy reinforcing members in the roof and sides but with little relative strength in the flooring. The cargo type carrier, on the other hand, had its main strength in the flooring, and its sides and roof were thin and weak. This built-in ceiling and wall strength of the meat trailers was utilized by bolting four steel plates, with hooks welded to them, directly to the cross braces in the ceiling and four similar plates to the side walls near the floor. It was from these hooks that the recording instrumentation was suspended by means of shock cords. A metal boxlike framework had to be built inside the cargo trailer to increase its strength and to hold the eight suspension hooks, but otherwise it was similar to the other two trailers. Figure 4.17 shows the type of corner construction used in the cargo trailer, and Fig. 4.18 shows a general view of the type of suspension used in the meat trailers.

In all cases the equipment was suspended in the forward section of the trailer by multiple strands of $^5/_8$-in. shock cord radiating from the equipment to the hooks fastened near the ceiling and floor. The suspension used in the YFNB-13 (the cargo trailer) was "softer" than that used in the meat trailers and resulted in a natural vertical period of about 1 sec vs $^1/_3$ sec for the other type system. The YFNB-13 system also had a much lower rotational period about its vertical axis (1 sec) since a center-point suspension system was used (Fig. 4.19), as compared to about $^1/_2$ sec for the other two. This was necessary because the recording equipment used at

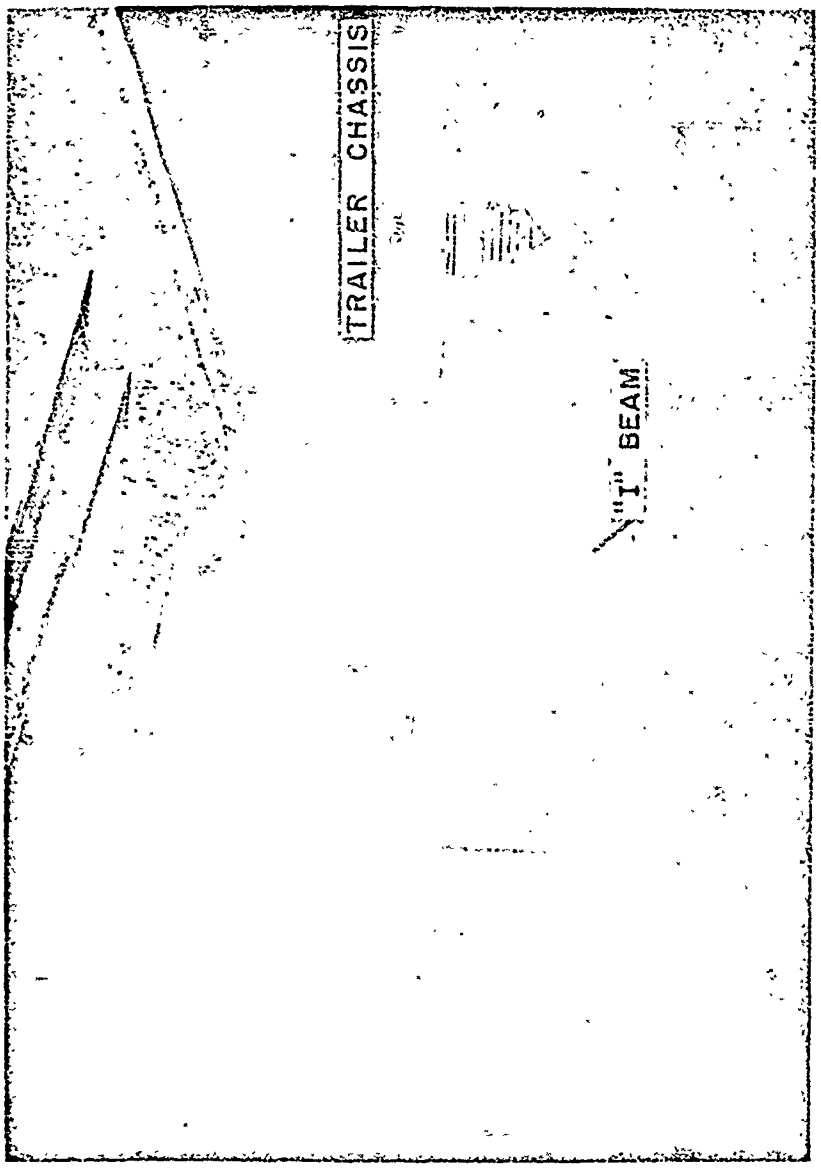

Fig. 4.16—Trailer mounting.

CONFIDENTIAL

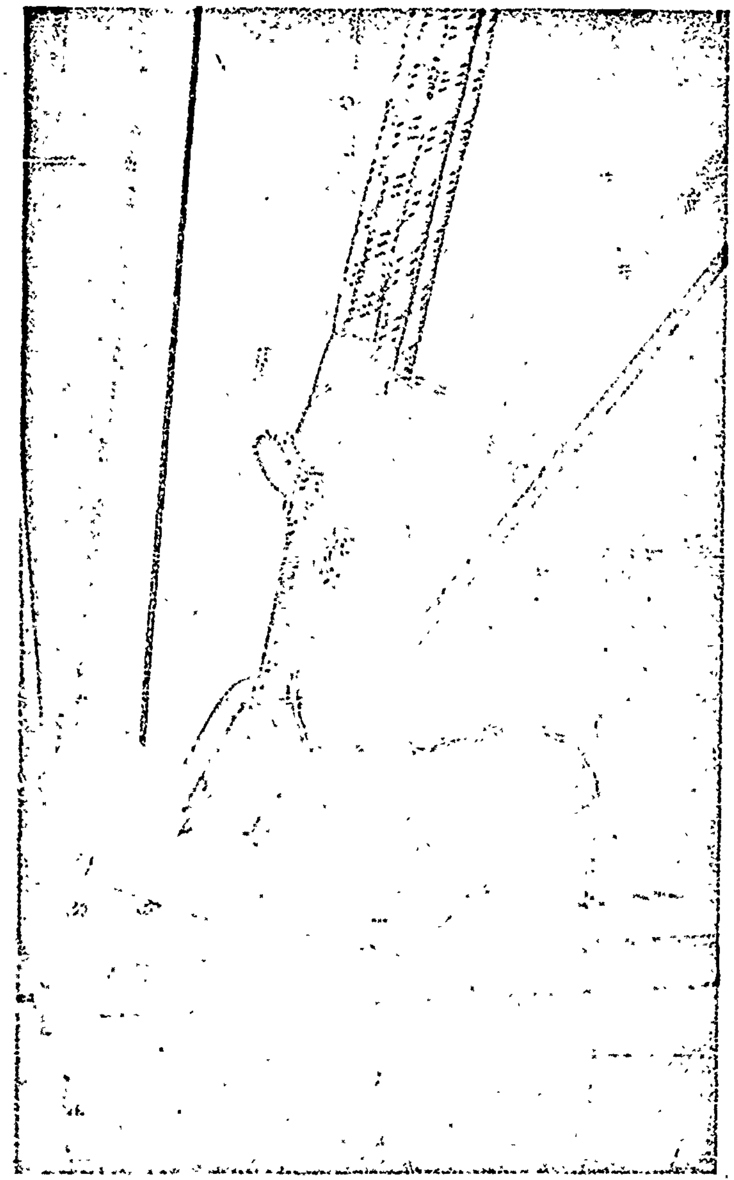

Fig. 4.17—Corner construction of suspension cage in cargo trailer.

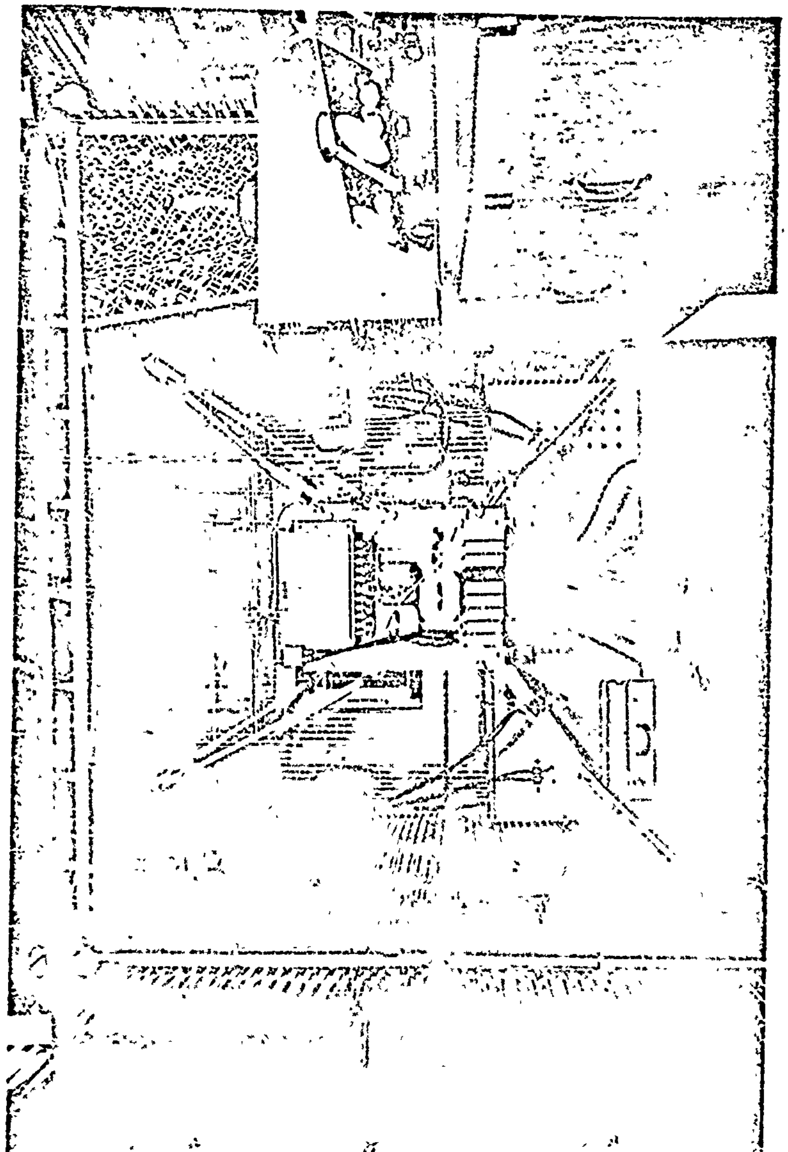

Fig. 4.18—Suspended recording equipment in meat trailer.

CONFIDENTIAL

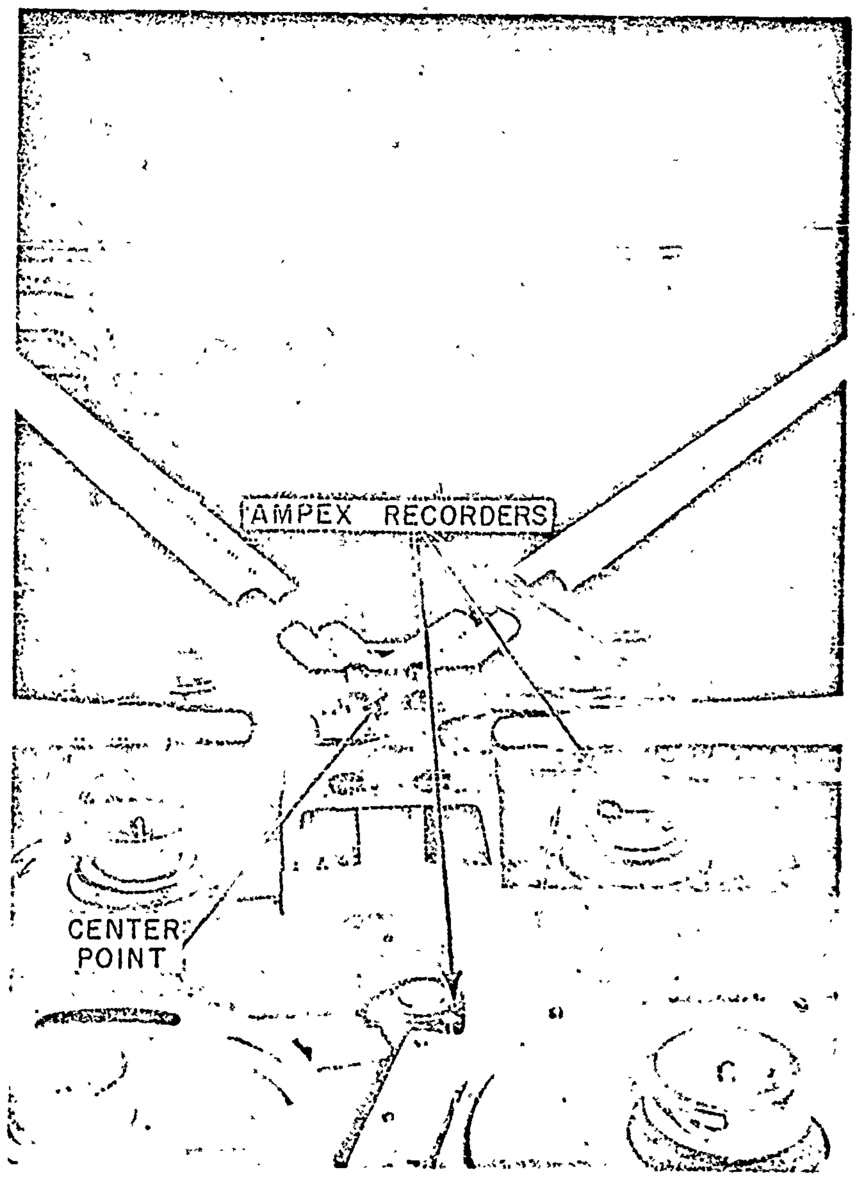

Fig. 4.19—Center-point suspension used with Ampex recorders.

SECRET—RESTRICTED DATA

CONFIDENTIAL

the YFNB-13 station was more susceptible to tape-speed changes during the recording period if the equipment experienced excessive torsional accelerations.

The design of the suspension system was such that should the displacement of the suspended recording equipment ever reach its limit (touch either the side or the floor of the trailer) the restoring forces tending to bring the instrumentation equipment back to its center position would have been about eight times gravity. The maximum elongation experienced by any of the shock cords under such a condition would have been a 100 per cent increase in its initial (unstretched) length, still some 20 per cent below its breaking point.

4.5.3 Signal-cable Flow

The instrumentation signal-cable flow was similar at each of the YFNB stations; the cable bundle, consisting of about 15 signal cables with the attached gages, was fed over the side of the ship and attached at intervals of 12 to 20 ft to a steel supporting cable as it was slowly lowered into the water. The steel cable was guided from the controlling winch on the top deck of the YFNB by running it through several pulleys welded to the deck and then out to a boom located near the port bow of the ship. Upon completion of the cable-lowering operation, the signal-cable bundle was lashed to the horizontal member of the boom to prevent chafing of the cables and then fed into an 8-in. pipe protruding through the bulkhead and slightly lower than the top of the boom.

Inside, the cable bundle was clamped every 2 ft to a vertical steel plate which ran from the pipe opening down to the deck of the YFNB. The bundle was then run along the deck beside the trailer and clamped down every few feet until it reached to within about 5 ft of the front of the trailer. At this point the cable bundle was split, one half rising vertically to a port on the right side of the trailer and the other half being fed under the trailer and then up and through a similar cable port on the left side of the trailer. Inside the trailer each of the two groups of cables was "snaked" up one of the shock cords which extended from the floor to the suspended recording equipment and then lashed into place.

Power cables for the instrumentation equipment were also "snaked" down, lashed at each of the crossover points on the lower shock cords, and then fed into the battery rack.

4.5.4 Instrument Booms and Winches

Three instrument booms were installed on each of the YFNB's. The forward port boom on each ship was for the Project 1.2 electrical pressure-time measuring gages, the starboard boom was for the Project 1.3 equipment, and the after port boom was for the combined use of Project 1.2 mechanical pressure-time gages and ball-crusher gages. On the YFNB's 12 and 13 the after port boom was also used for the Project 1.4 camera unit.

The booms were designed so that when swung outboard they would hold the steel support cable with the attached signal cables and sensing elements far enough from the side of the barge to prevent rubbing on the hull if the YFNB rolled as much as 30°. One boom was tested with a static load of 9300 lb, although it was expected that it would hold twice this amount of weight before failing. Some of the booms had ladders and other special attachments added to facilitate the cable rigging.

The winches used were those previously removed from the after cranes of the YFNB's, the double drum winches being used for the starboard and forward port booms. The single drum slewing winches had their drum flanges built up to hold 2200 ft of $\frac{3}{8}$-in. wire rope and were used with the after port booms.

The standard d-c electric control with magnetic braking was found to be excellent for lowering the instrument cables. The manual controls for the clutch and brake normally used in cargo handling were not used.

4.5.5 Plan of Operation

A few days before the YFNB's were towed out to sea, the instrumentation system for each trailer was suspended on the shock cords. The task of stretching the cords to reach the mounting hooks in the ceiling and near the floor was done by tying nylon rope to the free ends of the shock cords with a girth hitch, passing the nylon through a pulley fastened within a few inches of the hook and then through a block and tackle arrangement which was, in turn, anchored to another of the eight hooks. By stretching each of the shock cords in turn and looping its "eye" over its respective hook, the complete job of shock mounting each recording station could be completed by two men in about 3 hr. The units placed in the meat trailers (on the YFNB's 12 and 29) weighed about 400 lb each, and those placed in the cargo-trailer unit (on the YFNB-13) weighed nearly 525 lb. Power and control cables for the equipment were installed and checked while in transit to the testing grounds.

It was intended that the signal cables be lowered into the water on the afternoon of D−1 but was postponed until nearly 1 A.M. of D-day because of the rough weather. It was decided that this was the latest possible time the operation of lowering the cables could begin and still be completed in time to have the necessary last-minute equipment checks. The operation of lowering the cables was hampered by darkness and slippery decks but was, however, completed in about 4½ hr, leaving only 2 hr for clamping the cables to the deck, securing loose gear, and making the final adjustments on the recording equipment.

After the lowering of the signal cables had been completed, the cable boom on the YFNB-13 was extended at a right angle to the axis of the ship (contrary to the original plan and design of the boom) in an attempt to keep the cables from chafing on the hull of the ship; the YFNB was drifting sideways and over the cables. Since the original steel bracing cables for the boom were too short when the boom was extended at a right angle, a rope sling was used to secure the boom.

A preplanned and detailed check-off list was found to be extremely useful for the last-minute preparations and reduced the final equipment adjustments to a purely mechanical operation.

At H−1 min the controlling signals from the EG&G radio on each of the YFNB's had served its purpose, and all control was transferred to the timing and control circuits within the recording equipment; the tape-transport mechanism was energized; calibration signals were recorded on the tape; and the equipment was made ready to record the initial and any succeeding shock waves.

4.5.6 Results of Shock on Trailers and Recording Equipment

Weldments bonding the I-beams to the trailer chassis and to the decks of the YFNB's were inspected on D+1; no cracks or other indications of failure were noticed. Inside, the commercial air-conditioning equipment on the YFNB's 12 and 13 had been shifted about 0.5 in. from their original mounts. Operability after the test was not checked, but there is reason to believe that the unit in each of the trailers was in relatively good condition.

The workbench located in the trailer on the YFNB-12 was found overturned in the center of the floor, whereas the workbench on the YFNB-13 merely tore loose the small wood screws holding it to the floor. There was a broken light bulb found in one of the light sockets at the rear of the YFNB-12 trailer (all bulbs near the recording equipment in each trailer were removed from their sockets prior to the test as a precautionary measure). There was essentially no damage at all in the trailer located on the YFNB-29, the location farthest from SZ.

Displacement measurements taken in each trailer by means of strings having one end tied to the recording equipment and the other end fixed to a rigid support in the trailer indicated that the maximum relative vertical motions of the trailers with respect to the suspended equipment were as follows: YFNB-12, 5½ in.; YFNB-13, 4¼ in.; and YFNB-29, 2¼ in. There were no indications that the equipment at any of the stations experienced a lateral displacement with respect to the trailer.

4.5.7 Conclusions

The installation of the trailers in the YFNB's and the design of the instrumentation-suspension systems proved to be quite satisfactory; no unforeseen problems arose which necessitated a change in procedure or plan of operation and the same type of mounting could be used very well on a similar type of test.

The winches on the YFNB's performed smoothly and afforded good control over the steel cable supporting the gage signal lines at all times.

It is recommended that the booms be made longer—by perhaps 5 ft—to hold the signal cables farther from the sides of the ships and lessen the danger of their chafing on the hull.

CHAPTER 5

ELECTRONIC PRESSURE-TIME GAGE

5.1 WIANCKO PRESSURE GAGE

5.1.1 Introduction

Wiancko gages, using type P9-1005 transducers, and tourmaline gages were used by NOL to measure underwater pressures vs time in Operation Wigwam. Mechanical pressure-time gages (discussed in Chap. 3 of this report) were also used by NOL in Operation Wigwam. In brief, the operation of the Wiancko transducer was such that when pressure was applied to one end of a flat Bourdon tube twisted about its longitudinal axis, a rectangular pad (mounted on the other end of the tube) rotated about the tube axis away from the pole faces of two E-shaped cores. Two coils, mounted on the cores, were used as inductances in a modified Hartley oscillator. Thus, as the pressure in the Bourdon tube increased, the oscillator frequency increased. The Wiancko transducer and oscillator were mounted inside a watertight case, and a cable was used to deliver power from the surface to the oscillator and to transmit the f-m signal from the gage to a magnetic-tape recorder on the surface.

This gage was evolved from the NOL Wiancko gage which was used to measure underwater pressures in Operation Castle.[1] Some of the difficulties encountered in the development of the NOL Wiancko gage were in the pressure transducer which, when subjected to underwater shock waves, produced a permanent change in frequency and a distorted signal (usually oscillatory) in the demodulated output. Although these effects were somewhat reduced in time for use in Operation Castle by the expedient of shock mounting the transducer from the gage case, it was apparent that more development work was necessary to produce a reliable gage for Operation Wigwam.

In January 1954, after the Castle gages were shipped to the field, this work was resumed at NOL, and two prototype gages were produced, the results of which were good as determined by laboratory pressure tests and one underwater shock-wave test.

In these gages the two transducers were modified by securing one end of a short shaft to the pivot point of the rectangular pad, the shaft being aligned with the extended axis of the twisted Bourdon tube, and terminating the other end in a bearing mounted to the gage case. In one transducer, damping fluid was inserted in the bearing, and in the other the fluid was inserted between a disk mounted on the shaft and a flat plate which was secured to the gage frame and aligned parallel to the disk. Thus optimum damping was possible by adjustment of the length of the bearing, the adjustment of the gap between the disk and plate, and by the use of different viscosity damping fluids. Furthermore, the bearing was to reduce translational movement of the pad — the cause of spurious signals.

The Wiancko Engineering Company was then requested to produce similar prototype gages incorporating the above transducer modifications and other improvements suggested by representatives of both NOL and the Wiancko Engineering Company. The results of tests at NOL showed that the response of the prototype gages was fast and essentially free of spurious oscillations. However, large "permanent" frequency changes were obtained, and after four underwater shock-wave tests the damping mechanism was so badly damaged that this modification of the transducer was considered impractical to be a pressure gage for use in Operation Wigwam. The Wiancko Engineering Company then introduced a type P9-1005 transducer in which spurious movements of the rectangular pad were restricted by two cross wires[1] that secured the pad to the gage frame. Six prototype gages using type P9-1005 transducers were produced, and slight modifications were made by the manufacturer since acceleration and shock-wave tests conducted by NOL indicated a need for improvement. An additional 34 of the improved gages in pressure ratings of 750, 1000, 1500, 2000, 2500, and 3000 psi were then purchased for Operation Wigwam. These gages were calibrated in a pressure chamber and subjected to underwater shock-wave tests at NOL for evaluation for Operation Wigwam. The description of the Wiancko gage as used in Wigwam and the development and performance of the gage are described in this chapter.

5.1.2 Description of Wiancko Type P9-1005 Gage

The gage was contained in a stainless-steel hollow cylinder (see Fig. 5.1) 5 in. in diameter and $3\frac{1}{2}$ in. in height. A recessed groove $1\frac{1}{2}$ in. high and $\frac{1}{16}$ in. deep was cut around the lower end of the cylinder for mounting the gage to the gage array. All gage components were mounted on the inside of the top plate (Fig. 5.2), and the cable packing gland with cable terminating pins and pressure inlet with damping fitting was mounted on the outside of the top plate. The top plate was screwed in flush with the top of the cylindrical case, and a watertight seal was obtained with an O-ring.

The oscillator tube (type CK 6111) was shock mounted on one end of a flat spring which was spiraled about the tube. The other end of the spring was rigidly secured to a metal block on the top plate. A hole in the top plate ($2\frac{1}{4}$ in. in diameter and $\frac{15}{16}$ in. in depth) permitted large movements of the tube without bottoming. The wire leads from the tube were tied to the flat spring and terminated in three small holes drilled (under the cover plate, Fig. 5.2) in the top plate. The oscillator components, the output transformers, and the cable terminal pins were also mounted in these holes, which were filled with wax.

Each of the two F-shaped cores was rigidly clamped to the top plate with four hardened steel screws, and the contact surfaces of the top plate and cores were increased and roughened to increase the friction. Two straight wires, which crossed at the midpoints to form an X, were firmly secured at their junction to the center of the rectangular pad (Fig. 5.3) at the point where the pad was welded to the twisted Bourdon tube. These wires, under tension, were terminated in four solid posts protruding from the top plate. The Bourdon tube was inserted in an enlarged hole in the top plate (Fig. 5.4), and at the pressure-inlet end the wall of the tube was welded to the top end of this hole. Thus both ends of the Bourdon tube were secured to the top plate, and the cantilever movement of the tube and pad was greatly reduced, resulting in almost purely rotational movement about the tube axis as pressure was applied or released. An additional improvement in the P9-1005 transducer was the removal of part of the F-shaped cores at the center gap (Fig. 5.3), thus eliminating contact with the pad during its rotational movement. The mass of the pad, which was made of 0.025-in.-thick mu-metal, was reduced by tapering both ends, thus improving the gage response. Furthermore, the pole faces were milled flat and aligned parallel to the armature pad. The latter improvement resulted in a more uniform magnetic field in the gaps and made possible the construction of gages with more uniform characteristics.

A damping fitting (Fig. 5.4) was attached on the upper side of the top plate on the extension of the axis of the Bourdon tube. A small orifice about 0.35 in. in length and 0.0315 in. in diameter, but enlarged to 0.090 in. in diameter for a length of about 0.15 in., was used to connect the pressure inlet of the Bourdon tube to an enlarged opening (reservoir). A small wire, 0.009 in. in diameter to 0.025 in. in diameter, depending upon the pressure range of the gage, was inserted in this orifice to decrease further the rate of flow of oil to the Bourdon tube. The reservoir was divided into approximately two equal volumes by means of a thin neoprene diaphragm, the

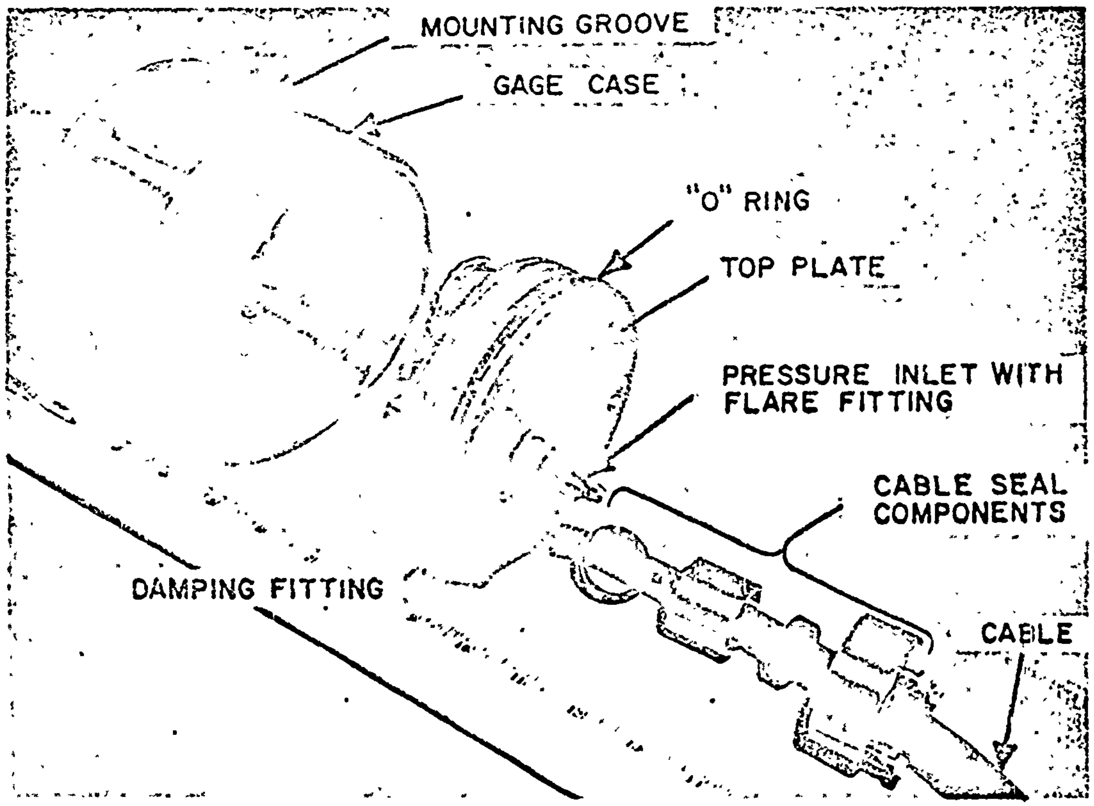

Fig. 5.1—Wiancko gage, type P9-1005, expanded view.

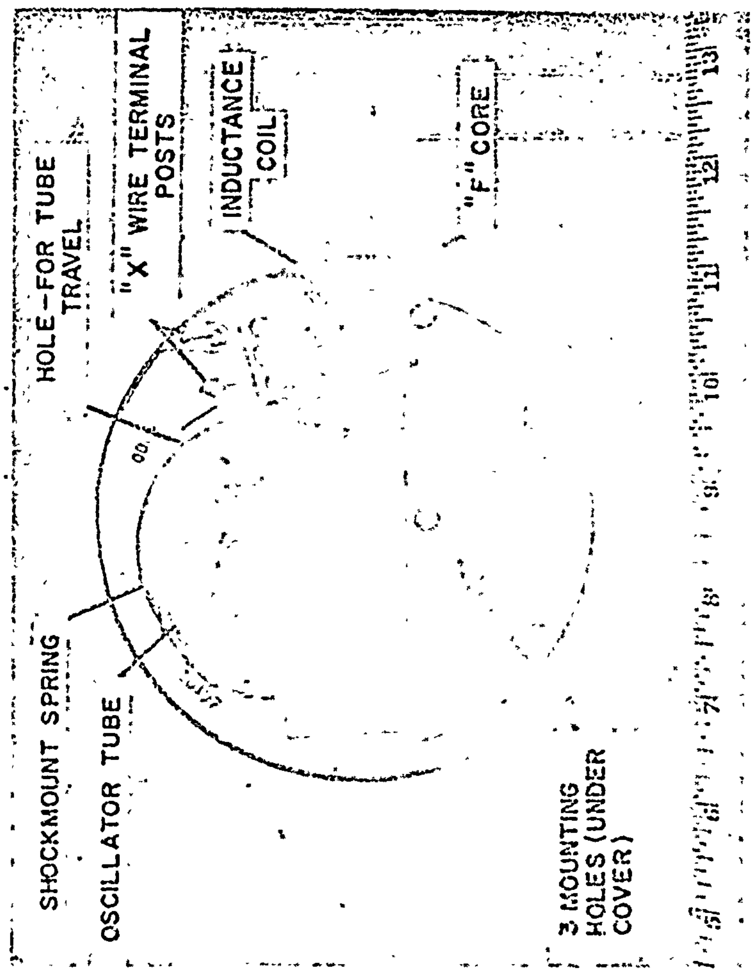

Fig. 5.2—Wiancko gage, type P9-1005, inside view of top plate.

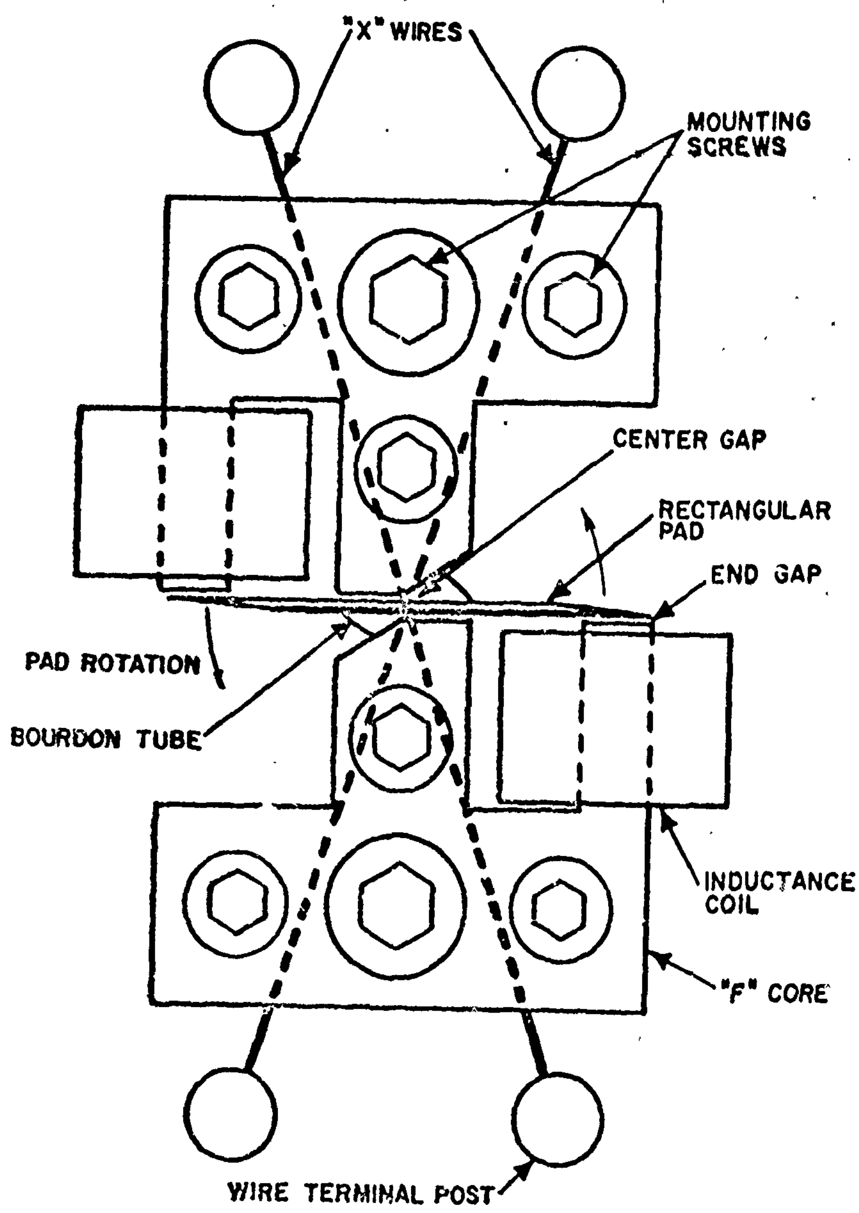

Fig. 5.3—Wiancko transducer, type P9-1005.

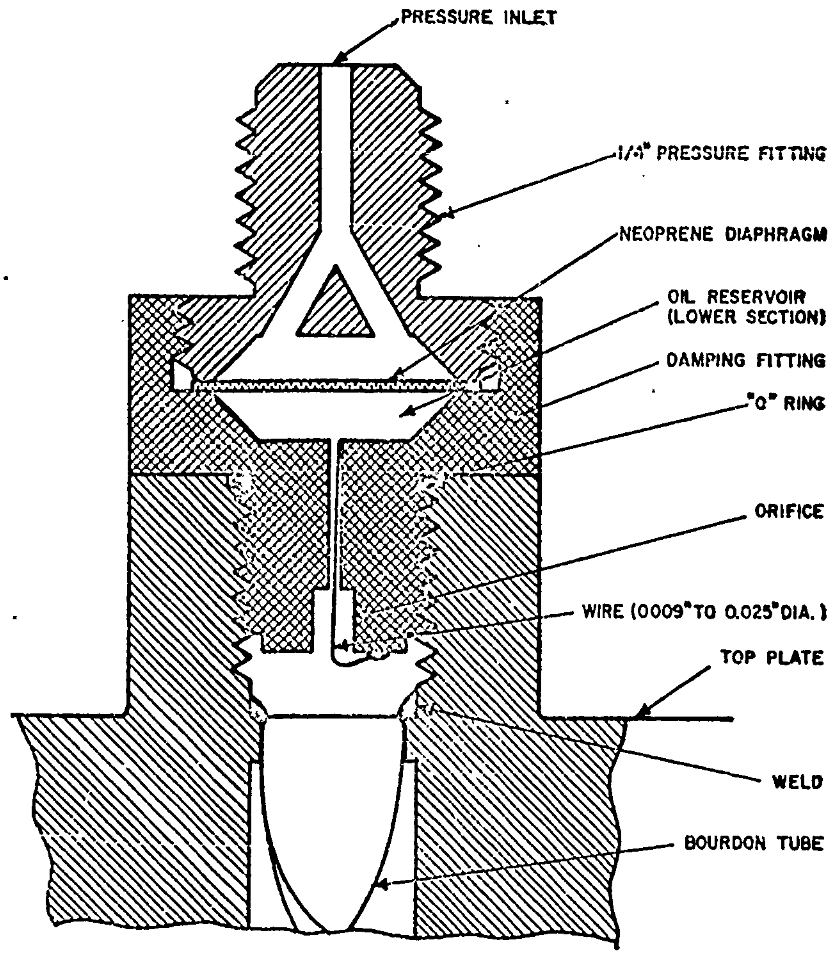

Fig. 5. —Damping fitting for Wiancko transducer.

purpose of which was to prevent loss of oil in the Bourdon tube and the damping orifice and to prevent foreign particles from getting in the fine damping hole. The upper chamber of the reservoir was connected to the pressure source by means of three holes which merged into a single hole about 0.10 in. in diameter at the pressure inlet. A ¼-in. copper-tube flare fitting was constructed on the pressure inlet for static calibration. The damping fitting and the Bourdon tube were filled with 100-centistoke oil (DC200), under a vacuum, to eliminate air bubbles.

5.1.3 Development

Large accelerations are imparted to recording gages used in the measurement of large underwater shock-wave pressures. Values of 12,000 g were measured on a cylindrical gage case from a step shock wave of about 1700 psi.[1] The forces were so great that vacuum tubes (in the oscillator circuit) were damaged, wires in the inductance coils were broken, and the flat Bourdon elements were distorted. These acceleration effects, however, can be reduced by proper shock mounting of the components of the gage and by using rugged components. The approach to this problem in the NOL Wiancko gage used on Castle was to "shock mount" the transducer (type P-2007) from the gage case by means of soft-copper tube which also transmitted pressure to the Bourdon element in the transducer. Thus the acceleration of the transducer was reduced; however, the transducer was not designed for rugged use, and hence the output signals were still somewhat distorted. (See Chap. 3 of reference 1 for typical pressure-time signals.)

The approach to this problem chosen by the representatives of the Wiancko Engineering Company was to use a rugged transducer (see description above) mounted directly to the gage case. The full effects of the shock wave were imposed upon the transducer. The first two prototype gages received from the manufacturer for evaluation from underwater shock-wave tests* were completely covered with foam rubber about ¼ in. thick, supposedly to reduce the effects of acceleration on the gage. The results from one underwater acceleration test, however, showed that large signals, roughly similar in shape to the shock-wave signals, and a large permanent change in oscillator frequency were obtained. In the underwater acceleration tests, the gage and gage case were subjected to the shock wave; however, the normal operation of the rectangular pad was restricted by replacing the oil with air in the flat Bourdon tube and in the pressure inlet and then sealing off the pressure inlet from the water. Upon examination of these gages at NOL, it was found that the permanent frequency change could be reproduced by tapping the F-shaped cores with a hammer. Furthermore, the permanent change in frequency was greatly reduced when the contact surfaces of the F-shaped cores and the top plate were roughened and glued. Unfortunately, that particular glue (or the method of application) was unsatisfactory, for the bond failed after several simulated shocks with a hammer. The manufacturer, also cognizant of the cause of the undesired frequency change, modified the subsequent transducers by roughening the contact surfaces of the F-shaped cores and the top plate, by increasing the area of the contact surfaces, and by clamping the F-shaped cores to the top plate with two additional (total of four for each core) hardened steel screws (see Fig. 5.3). Three 3000-lb prototype gages, with the modified F-shaped cores but without the foam rubber coating which was not used again on the Wigwam Wiancko gages, were then subjected to several underwater shock-wave acceleration tests, with the result that a maximum permanent frequency change of about 5 per cent of the shock-wave pressure was obtained on two gages and about 1½ per cent on the other. The recorded acceleration signals, however, were quite large and

---

*Truncated-shaped charges[2] 4 and 6 ft long were used in the underwater acceleration and performance tests. The shock-wave pressures for the 4- and 6-ft charges were essentially constant for about 1 and 1½ msec, respectively, and then decayed with time. The pressure amplitude, also measured with ⅛-in.-diameter tourmaline gages at the same distance, was varied by adjusting the charge-to-gage distance and by using different size charges so that the pressures would not exceed the pressure rating of the Wiancko gages. In some instances the charges were lengthened from 4 to 4½ ft.

were similar in wave form to the shock-wave pressure-time signals but with a superimposed ring of about 5 kc. The amplitude of the acceleration signals from the three gages was between 10 and 28 per cent of the shock-wave signals. Similar acceleration tests were also performed on three prototype gages rated for 750 psi with similar modifications to the F-shaped cores. The results were encouraging since the maximum permanent change in oscillator frequency was only 1 per cent of the shock-wave pressure and the amplitude of the recorded acceleration signal was between 3 and 7 per cent of the shock-wave pressure. The recorded acceleration signal was also similar in wave form to the shock-wave pressure except for a superimposed ring of about 3.8 kc. These superimposed oscillations were caused by the movement of the ends of the rectangular pad, relative to the F-shaped cores, as the shock excited the flat Bourdon tube and the pad into resonance. These oscillations were eliminated by using 1000-centistoke oil in the end gaps. The manufacturer made a significant development in the securing of the X wires to the rectangular pad, thereby reducing spurious movements (and signals) of the pad. The oscillator tube mount was also effective, for only two tubes failed during the development tests: one after two shots and the other after 10 shots. Therefore the results with the improved prototype gages showed that the permanent frequency change was sufficiently reduced for acceptance for Operation Wigwam. However, the acceleration signals were still too large, but further development and investigation were impossible because of the lack of time in preparation for Operation Wigwam. The 34 similarly improved gages were then calibrated in a pressure chamber and subjected to the underwater shock-wave performance tests for evaluation for Operation Wigwam. These results are discussed below.

5.1.4 Performance Tests of Wiancko Gages

The purpose of the performance tests was to determine how faithfully and quickly the Wiancko gage (type P9-1005) responded to an underwater shock wave and to determine whether the gage was sufficiently rugged to withstand the shock wave and hydrostatic pressures expected in Operation Wigwam. Since the gages were rated for pressures which were only slightly less than those that would probably impair the performance of the gages, the shock wave and calibration pressures never exceeded the pressure ratings established by the manufacturer. These tests differed from the shock-wave acceleration tests described above in that normal operation of the transducer was permitted by filling the flat Bourdon tube and pressure inlet with 100-centistoke oil under vacuum and by removing the seal at the pressure inlet. Although the durations of the shock-wave pressures were short compared with the durations expected from the Wigwam shot, nevertheless the amplitudes were about equal, and these tests showed that the Wiancko gages were in general ruggedly constructed. The gage cases, the cable packing glands, and the O-ring seal in the top plate were sufficiently rugged to withstand hydrostatic pressures of at least 3000 psi. In a few gages, however, the pins used to connect the cable leads to the gage oscillator were loosely secured in the glass seal. Examination of the few gages that performed erratically during the shock-wave tests showed that a wire lead was broken at a terminal, the screws on the F-shaped cores were loosened, the glass seal at the cable termination was fractured, and the oscillator tube was microphonic. These defects, however, were readily corrected before use in Operation Wigwam, thus assuring a higher percentage of dependable and reliable gages. The underwater shock-wave acceleration tests, although desirable, were not made on these 34 improved gages because of lack of time. For the same reason, only one shock-wave response test was made on each gage. However, in some cases where the response was not satisfactory on the first test, a modification, when possible, was made to the gage and the test was repeated. (The primary modifications were the addition of 1000-centistoke oil to the end gaps of the transducers when necessary to eliminate oscillatory signals superimposed upon the shock-wave signals and the replacement of the oscillator tube or repair of broken wires when discontinuous signals were obtained.)

The arrangement of the charge and gages used in the underwater shock-wave performance tests (Fig. 5.5) was as follows: The charge and gages were set about mid-depth in 22 ft of water. Two tourmaline gages ($^3/_4$ in. in diameter) were mounted the same distance from the small end of the truncated charge as were the pressure inlets of the Wiancko gages. All gages were arranged symmetrically about the extended axis of the truncated charges so that the

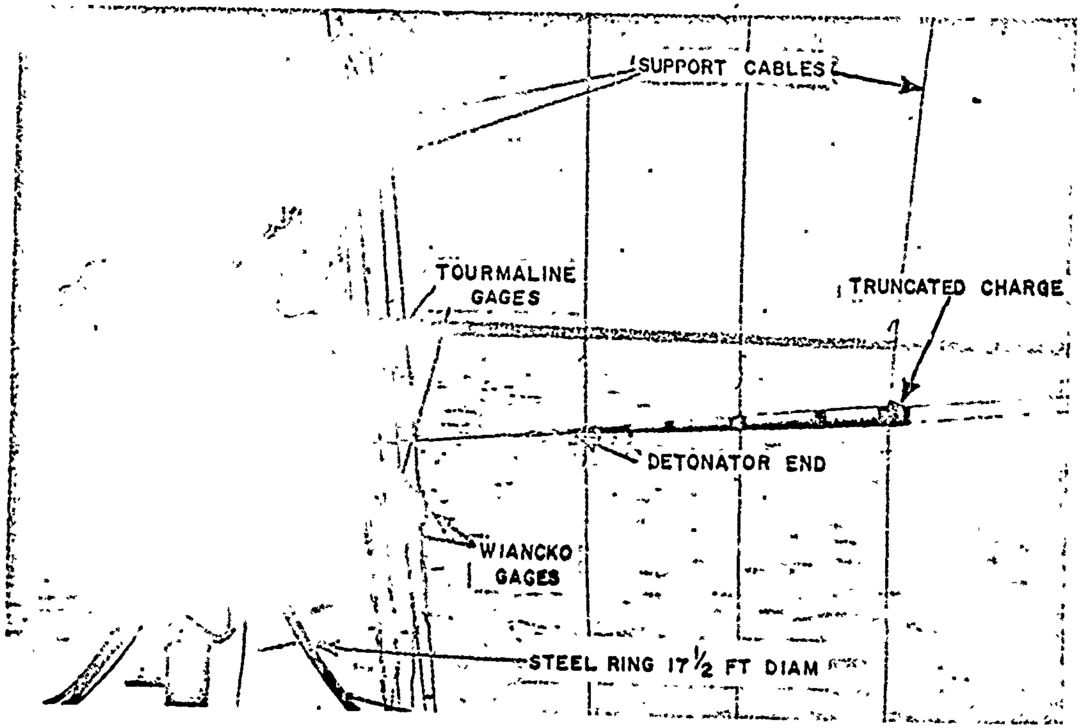

Fig. 5.5—Charge and gage arrangement for shock-wave performance tests.

pressure vs time was the same at all gage positions. To obtain large frequency deviations and to determine whether the gage was sufficiently rugged to withstand its design pressures, the shock-wave pressures used were approximately 60 to 90 per cent of the pressure rating of most of the gages tested. The various values of shock-wave pressures were obtained by using different sized charges and by changing the charge-to-gage distance. The duration of the nearly constant pressure of the shock wave was 1 or 1½ msec, depending on which charge length was used. This was sufficiently long for the response of the Wiancko gage and the associated recording equipment since the rise time of the Wiancko gage and the frequency discriminator was about ½ msec. Typical pressure-time curves obtained with tourmaline and Wiancko gages are reproduced in Fig. 5.6. The frequency of each gage oscillator was measured immediately before and after each shock-wave test to determine the permanent change in frequency.

5.1.5 Calibration of Wiancko Gages

Before the shock-wave pressures could be evaluated from the record obtained with Wiancko gages, it was first necessary to know the pressure frequency relation of each gage. This relation was obtained from two types of hydrostatic calibrations performed on each gage for use in the shock-wave test. In one calibration the pressure was applied to the flat Bourdon tube in the transducer by means of an oil-filled tubing which connected the flare tube fitting on the pressure inlet to a high-pressure pump. In the other calibration, the entire gage was immersed in an oil-filled pressure chamber (9 in. in diameter and about 24 in. in length) with the gage cable let out of the chamber through a packing gland. In the latter calibration the pressure was applied simultaneously to the gage case and the pressure inlet as it would be in the measurement of underwater shock-wave pressures. This calibration was performed with increasing and decreasing pressures to determine the hysteresis. In both calibrations the same EPUT meter (the EPUT meter is an Events-Per-Unit-Time Meter manufactured by the Berkeley Scientific Corp., Richmond, Calif.; the Bourdon pressure gage was calibrated several times with a dead-weight tester and was found to be accurate and reproducible) and Bourdon pressure gage were used to measure, respectively, the frequency of the gage oscillator and the pressure on the Wiancko gage. Approximately 10 calibration points at equal increments of pressure were obtained on each gage in the range from hydrostatic pressure to the rated pressure of the gage. A smooth curve connecting these points was called the calibration curve, and one is shown in Fig. 5.7.

In the second procedure, where the dynamic response to shock loading was measured, the f-m gage signal was applied directly to the input of the discriminator, the demodulated output of which was fed into an oscilloscope. The signals on the cathode-ray tube were photographed on a 10-in. strip of 35-mm film moving at right angles to the tube signal deflections. Since the responses of the oscilloscopes and demodulators were linear, the tube signal deflections were proportional to the frequency produced by the gages, and the trace in the direction of the movement of the film was proportional to the time. In addition, the following calibration signals were photographed: an accurate time signal applied simultaneously with the shock-wave signal and a discriminator calibration signal obtained by applying a frequency "step" signal to the discriminator input. The latter signal was produced by a frequency step-signal generator which was essentially an oscillator that was capable of changing the frequency of oscillation from one value to another value within a cycle (about 0.1 msec) without changing the amplitude. The two values of frequency were preset before the shock-wave test and were measured with an EPUT meter. Hence the discriminator calibration signal (photographed from the cathode-ray tube as a square step with a rise time of about 0.3 msec) represented a known change in frequency. To convert the photographed shock-wave signal into a pressure-time signal, the amplitudes of the shock-wave signal were first measured at desired time increments, and each amplitude was compared with the amplitude of the discriminator calibration signal to obtain the corresponding change in frequency produced by the gage. Since the frequency-pressure relation of the gage was non-linear, the hydrostatic calibration curve (curve A, Fig. 5.7) was used to convert each of the above changes in frequency into corresponding changes in pressure. A sufficient number of such pressure points were thus obtained to construct a pressure-time curve (Fig. 5.6). It should be

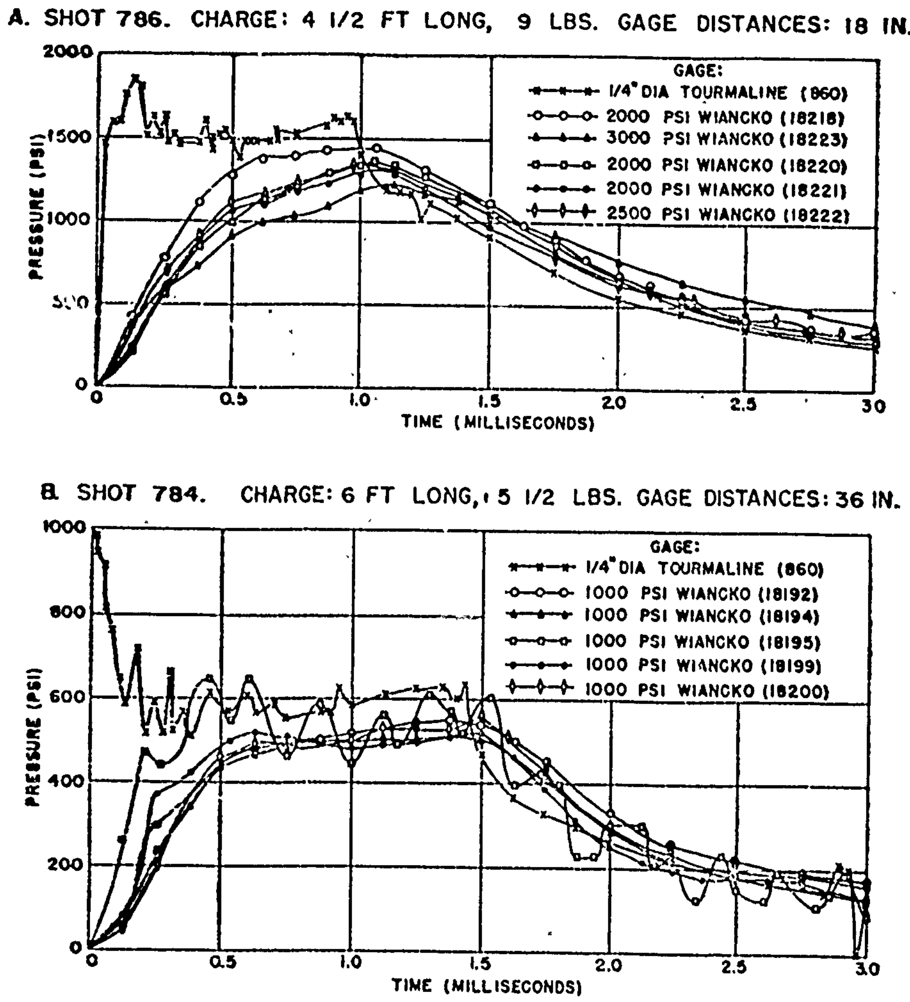

Fig. 5.6—Pressure-time curves from truncated charges fired under water.

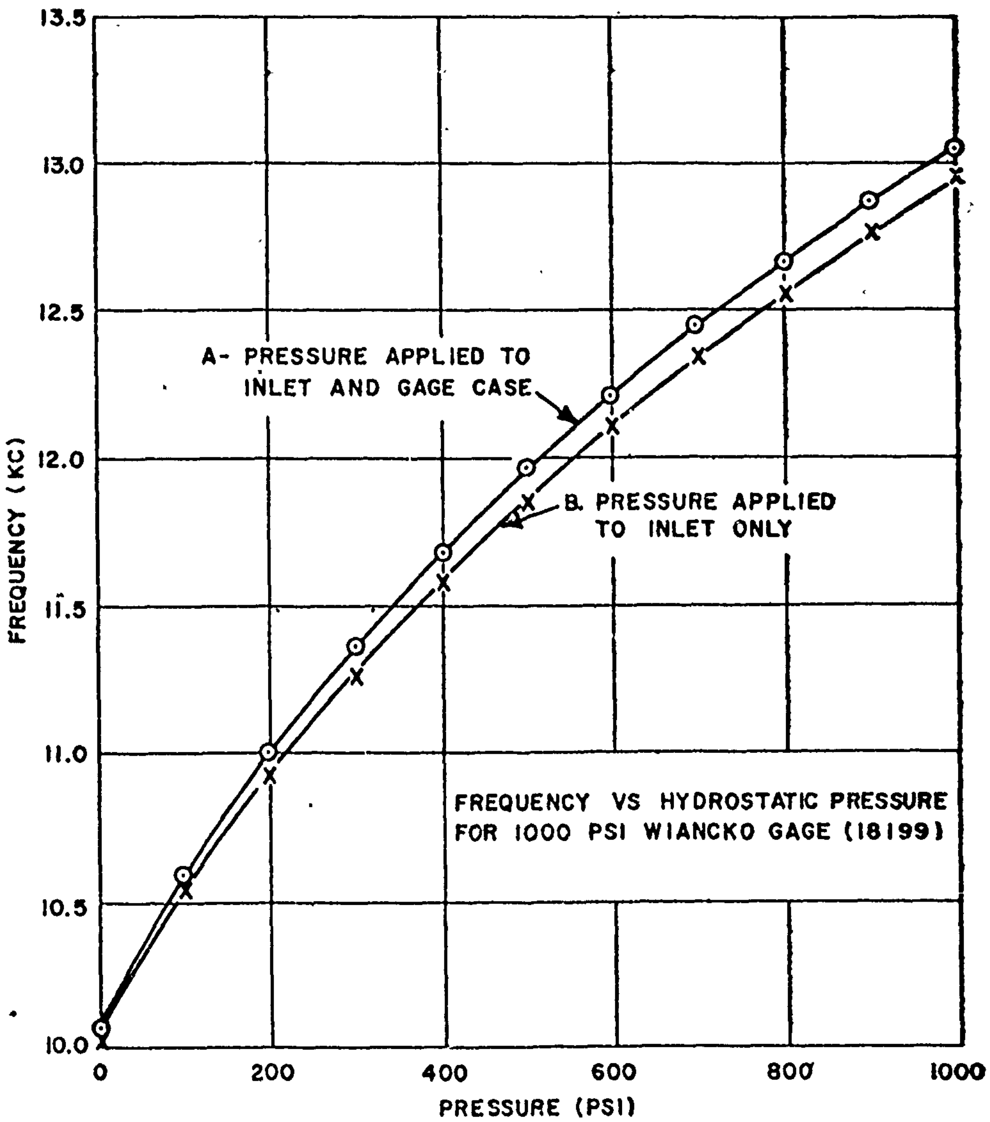

Fig. 5.7—Wiancko gage calibration curves.

noted that the instrumentation described above as being used in these shock-wave performance tests differed considerably from that used during the Wigwam shot where, for example, recording was done on magnetic tape.

5.1.6 Comparison of Wiancko and Piezoelectric Gages in Shock-wave Tests

The results of the shock-wave performance tests showed that the pressures recorded with the Wiancko gages were smaller than the pressures recorded with the two ¼-in.-diameter tourmaline gages. The Wiancko gage pressures were evaluated from the gage-calibration curve obtained by applying hydrostatic pressure simultaneously to the pressure inlet and the gage case. The average value of the ratio (R) of the Wiancko gage pressure to the tourmaline gage pressure* was 0.89 with a standard deviation of the mean (σ_m) of 0.01 for gages rated for 1000 psi in the 23 measurements obtained. The values of R for gages with various pressure ratings are shown in Table 5.1. Application of Table 5.1 to particular gages was made by using the gage ranges listed in Tables 6.1 to 6.3.

Table 5.1 — RATIO OF WIANCKO GAGE TO TOURMALINE GAGE PRESSURES

Gage Rating (psi)	Pressure Ratio (R)	σ_m	Number of Measurements
1000	0.89	0.01	23
1500	0.88	0.02	12
2000	0.90	—	7
3000	0.79	—	4

5.1.7 Hysteresis and Permanent Frequency Change of Wiancko Gages

Measurements of the gage-oscillator frequency before and after each shock-wave test showed that a small "permanent" change in frequency was obtained on most of the 34 improved gages tested for Operation Wigwam. The results showed that the permanent frequency change, expressed in pressures, was equivalent to, or less than, 1 per cent of the maximum shock-wave pressure recorded (about 600 psi) by the gages rated for 1000 psi in the 23 measurements made. The errors due to the permanent change in frequency for gages rated for 1500 psi were 1 per cent or less of the maximum shock-wave pressure (about 1200 psi) recorded in 10 measurements and between 1 and 2 per cent in two measurements. The errors were somewhat larger for gages rated for 2000 and 3000 psi; six values were obtained at less than 1 per cent, four between 1 and 2½ per cent, and a value each at 7 and 8½ per cent of the maximum shock-wave pressure recorded, which for these gages was about 1500 psi. In general, it was found that the gage-oscillator frequency was smaller after the shot than before the shot, at atmospheric pressure.

The results from the hydrostatic calibration showed that the gages possessed hysteresis. Larger values of gage-oscillator frequency were obtained, for a particular pressure, when the pressure was being decreased than when it was being increased. The value of hysteresis was obtained for each gage size by expressing the difference in frequency, for several particular values of hydrostatic pressure, in percentage of the frequency deviation obtained at rated pressure. The values of hysteresis averaged approximately 1, 1½, 2, and 3 per cent for gages

*In order to account for the slow response of the Wiancko gages and the discriminators, the pressures used in these ratios were taken on the constant-pressure part of the pressure-time curve just before the pressure began to decay, i.e., at times of about 1 and 1½ msec.

rated for 1000, 1500, 2000, and 3000 psi,* respectively. In general, the maximum deviation of the increasing- and the decreasing-pressure calibration curves occurred at approximately $\frac{2}{3}$ the gage-rated pressure, and the two curves coincided at atmospheric pressure. The Bourdon pressure gage which was used to measure the pressure in the above hydrostatic calibrations was itself calibrated with increasing and decreasing pressures from a dead-weight tester, and no measurable hysteresis effect was observed.

5.1.8 Frequency Deviation, Stability, Temperature Effect, and Reproducibility of Wiancko Gages

The manufacturer of the Wiancko gages succeeded in obtaining large frequency deviations. This was an important factor since the accuracy of the results was enhanced by an increase in the signal-to-noise ratio. Although, in general, the frequency increased from a gage mean frequency of about 10 kc at atmospheric pressure to about 13 kc at the rated gage pressures, in many gages frequency deviations were larger, being between 30 and 40 per cent of the mean frequency. The stability of the frequency of the gage oscillators was good if a short warm-up time to reach equilibrium was allowed. Most gage oscillators maintained the mean frequency within ±10 cycles/sec during the few minutes required to calibrate the gages. However, many gages maintained the mean frequency within ±15 cycles/sec for over a month, even after being shipped across the country. Several gages that were to be used at a depth of 1000 ft in Operation Wigwam were calibrated at temperatures of about 9°C and also at room temperature (21°C). The maximum difference between the two calibrations for any gage was only 35 cycles/sec or about 1 per cent when referred to the full range of the gage. No tests were made for the specific purpose of determining the reproducibility of the gage calibrations. However, comparison of the calibrations obtained before and after an underwater explosion test on gages that exhibited a permanent change in frequency of less than 1 per cent showed that the reproducibility of the frequency was better than ±40 cycles at any particular pressure. Another effect noticed during the calibration of these gages was that the amplitude of the oscillator signal increased as the frequency increased. On some gages the amplitude increased by a factor of 2, but the wave form remained nearly sinusoidal.

5.1.9 Rise Time of Wiancko Gages

The response of the Wiancko gages and the frequency discriminators used is shown in Fig. 5.6. The rise time was approximately 0.6 msec for the discriminators and gages rated for 1000 psi and 1500 psi and longer for gages with higher pressure ratings. The rise time of the discriminators alone, however, was about 0.3 msec, as determined by applying a frequency step signal to the discriminator. The rise time of the gage alone, therefore, was about 0.3 msec. This was shown to be the case when a few pressure–time records evaluated from f-m signals recorded directly on film were compared with the demodulated shock-wave signals obtained from the discriminators. The rise time of the gages was perhaps increased by the use of 1000-centistoke damping oil placed between end gaps of the transducer to eliminate the superimposed 4- to 5-kc oscillator signals.

5.2 TOURMALINE GAGES

5.2.1 Introduction

The tourmaline gage is a piezoelectric transducer in which the hydrostatically sensitive tourmaline crystals produce an electrical charge proportional to the applied pressure and to the area of the crystal faces.[3] This charge, when distributed over the connecting cable and shunting capacitance, results in a voltage which is readily measured and recorded with a voltage-sensitive device such as the oscilloscope. Tourmaline gages have been used in England

*Similarly, the hysteresis could be stated as the difference in pressure, for several particular values of frequency, expressed in percentage of the rated pressure of the gage. The results would be approximately the same as those stated above.

since 1921 to record pressures produced by charges fired under water.[4] These gages, which consisted of many tourmaline crystals arranged in a mosaic pattern, were quite large[5] and hence were suited to the measurement of shock-wave pressures produced only by large charges. Development of considerably smaller tourmaline gages for more precise measurements of shock-wave pressures from charges smaller than service weapons was begun in this country about 1941. More detailed information concerning the history and development of the tourmaline gage is presented in reference 6.

Several materials exhibit piezoelectric properties, and some have sensitivities greater than tourmaline.[3] However, for quantitative underwater shock-wave measurements, tourmaline gages are generally used because of the hydrostatic sensitivity, ruggedness, linear response to pressure, freedom from hysteresis, and simplicity in construction and use. Nevertheless, the advantage of tourmaline does not preclude the use of the higher sensitivity crystals in gages, particularly in the measurement of small-amplitude shock-wave pressures in which the sensitivity of the recorder is too low for recording with tourmaline gages.

The use of tourmaline gages (and piezoelectric gages in general) in shock-wave recording has limitations, however, which must be considered before the gages are used. The limitations of the tourmaline gage imposed by high-frequency distortion and cable-signal and spurious electrical signal effects[3,6] were either negligible or were not discernible with the Wigwam instrumentation and hence will not be discussed here. Low-frequency distortion, however, is of particular interest in the recording of pressures in the Wigwam shot since the shock-wave durations were quite long. This distortion is caused by the high internal impedance of the gage, pyroelectric effect, and the "first-time gage effect." For practical purposes the piezoelectric gage may be considered to be an ideal voltage generator in series with a capacitance; when the gage is connected to a cable, the voltage developed by the sudden application of constant pressure will decrease exponentially at a rate determined by the product (RC) of the total capacitance in the gage-cable circuit and the shunting resistance. Hence a large error will be incurred in the momentum of a recorded negative exponential shock wave (or any pressure wave in which the positive or negative duration is long) if the integration is carried out to long times (several times the shock-wave time constant) unless the gage-cable time constant (RC) is considerably larger than the shock-wave time constant. In the shock-wave records obtained on the Wigwam shot the RC time constant was about 10 sec (about 300 times the shock-wave time constant), and the error in momentum due to this effect was estimated to be less than 1 per cent in the worst case, i.e., the 1000-ft-depth gage at the YFNB-12 station.

Pyroelectric effect is the result of a polarization charge developed by the change in temperature in hydrostatically sensitive piezoelectric crystals. An increase in the temperature of tourmaline crystals of 1°C will produce a charge equivalent to a decrease in pressure of about 200 psi. The increase in temperature by adiabatic compression of the tourmaline crystals is negligible,[7] but the increase in temperature of the surrounding water by adiabatic compression is about 0.3°C per 1000 psi and would result in distortion in the recorded shock wave were it not for the fact that the insulation of the gage coating transmits only a small fraction of the temperature increase during the time of recording of short-duration shock waves.

Since the positive duration of the shock wave recorded on the Wigwam shot was considerably longer than the duration in any previous measurements, tests were performed to determine the effectiveness of the insulation of the gage coating by measuring the response of the coated gage (the coating is described in Sec. 5.2.2) when the temperature of the water surrounding the gage was suddenly increased and maintained while the pressure remained constant. The result was that at 20 sec the response was only 0.1 per cent of the response expected from a pressure required to produce an equivalent temperature increase by adiabatic compression of the water. The pyroelectric effect due to adiabatic compression of the gage coating was simulated in a similar test in which a bare gage (edge insulation was also removed) was used in an oil medium; the oil represented the gage coating of wax. The gage response was considerably faster (ultimate response was obtained in 30 sec) than in the above test and in 1 sec was about 2 per cent of the response expected from a pressure that would produce an equivalent temperature increase. Therefore, considering the time constant and the positive duration of the shock wave recorded on the Wigwam shot, the above tests indicate that the distortion caused by the increase in temperature in the tourmaline gages by adiabatic compression of the surrounding water and the gage coating may be neglected for practical purposes.

The first-time gage effect results in a low-frequency distortion the first time a new tourmaline gage or a newly coated gage is exposed to shock waves. This effect is characterized by a larger negative displacement of the recorded pressure-time curve from a standard pressure-time curve than can be accounted for by the RC time constant of the gage-cable circuit. Furthermore, this effect is greatly reduced or disappears entirely on the second and later exposures to shock waves[8] of the same or smaller amplitude. The reason for this is not known, but it is perhaps a pyroelectric effect caused by the compression of the gas bubbles in the gage coating at the interface of the tourmaline. Since the gas bubbles are dissolved, the effect is not so pronounced on subsequent exposures to shock waves. Nevertheless, the first-time gage effect is believed to have been eliminated on the tourmaline gages used in the Wigwam shot since the gages were "pre-aged" with detonators and afterward were exposed to at least two shock-wave tests in which the pressures were larger than those in the Wigwam shot. These tests are described in Sec. 5.2.4.

Experimental evidence of the magnitude of the errors caused by low-frequency distortion is shown in the comparison of the Wiancko gage results with the tourmaline gage results (Secs. 8.3.2 and 8.3.3), where the small differences obtained in the momentum comparison and the peak-pressure comparison indicate that the combined effects of the hysteresis of the Wiancko gages and the low-frequency distortion of the tourmaline gages were small.

5.2.2 Description of the Wigwam Tourmaline Gages

The tourmaline gages used in Operation Wigwam were constructed from thin disks of tourmaline crystals, the faces of which were cut perpendicular to the optical axis (see reference 9 for construction of tourmaline gages). A silver electrode was baked on each crystal face, and the diameters of the disks for the three gage sizes used were $\frac{7}{8}$ in., $1\frac{1}{8}$ in., and 2 in. Eight crystals were used in the $1\frac{1}{8}$-in.-diameter gages, and only four were used in the $\frac{7}{8}$- and 2-in. gages. In each gage, $\frac{1}{2}$ of the crystals used were arranged in a stack (with proper regard to the polarity of the faces) on either side of a steel ground tab to form a gage that was symmetrical electrically and mechanically about the ground tab. In this assembly thin silver tabs were sandwiched between the crystals with the "arms" of the tabs extending out of the stack, and the assembly was sweated together. Araldite (Araldite Epoxy Resin AN 101 with hardener HN 951 was used; the manufacturer of these products is Ciba Company, Inc., Plastics Division, 627 Greenwich St., New York 14, N. Y.) was applied around the edges of the crystals to reduce leakage that could result from handling bare tourmaline crystals. Silver paint was then applied over the entire gage assembly (except at the exit of the positive leads) to provide an electrical connection from the outside electrodes of the two outer crystals to the ground tab and to provide an electrostatic shield for the gage (see Fig. 5.8).

The essential difference between the $\frac{7}{8}$-in. gages and the larger gages was in the type of ground tab used and the method of mounting to the transmission cable. In the $1\frac{1}{8}$- and 2-in. gages a split ground tab (see Fig. 5.11 of reference 6) was used to facilitate the mounting of the relatively massive gages to a flexible cable. A copper tube $\frac{3}{8}$ in. in outside diameter and about $2\frac{1}{2}$ in. in length was soldered between the two tapered arms of the split ground tab, and the core of the cable was inserted inside the tube. The high leads of the gage were then soldered to the central conductor of the coaxial cable, and the braided shield was soldered to the copper tube for a ground connection. A fairly rigid gage mount was thus obtained, and the stress was relieved from the relatively weak gage leads and the cable central conductor (see Fig. 5.8). In the $\frac{7}{8}$-in.-diameter and smaller gages the steel ground tab was shaped like a flattened frying pan (similar to the split tab but with only one arm) and was soldered directly to the cable shield. Another steel tab similar to the ground tab in construction was sandwiched between one outside crystal and the adjoining crystal, and it was soldered to the central conductor of the cable. The strain was thus equally distributed between the two rugged steel tabs (see Fig. 5.8). A waterproof coat was obtained on all gages by dipping the mounted gages about four times in melted mineral wax (Zophar wax C-276 was used at a temperature of about 235°F; the wax is

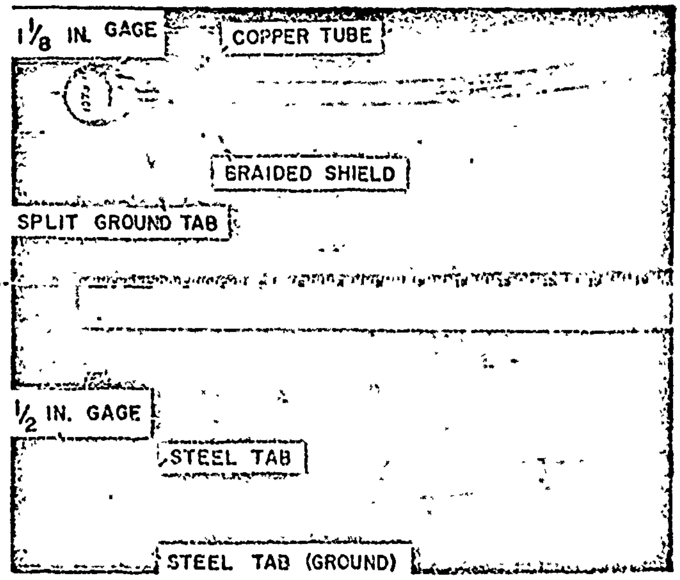

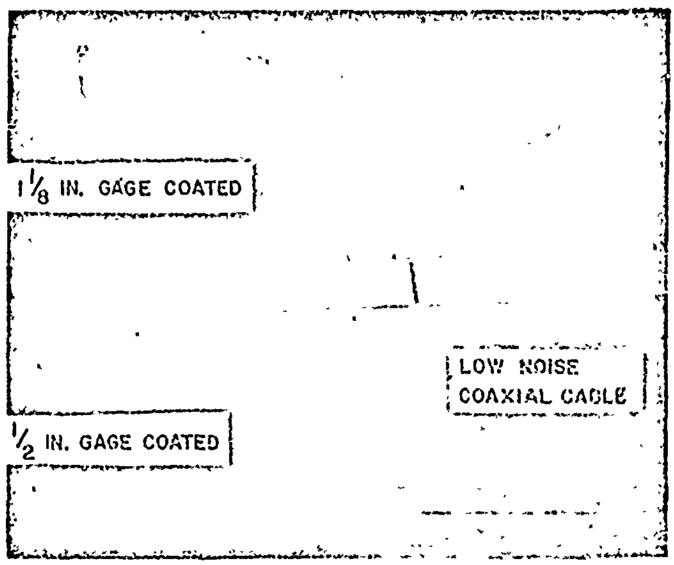

Fig. 5.8—Tourmaline gages mounted on low-noise cable before and after coating.

manufactured by Zophar Mills, Inc., 112-130 26th St., Brooklyn 32, N. Y.) to a point about 1 in. above the terminus of the cable jacket until the thickness of the wax was about $\frac{1}{8}$ in. at the edges of the gages and about $\frac{1}{16}$ in. at the center of the faces of the gages. One layer of Uskorona splicing compound (Uskorona splicing compound is manufactured by The United States Rubber Company) was applied under tension over the wax, after it cooled, to a point on the cable jacket about 1 in. above the wax terminus. Next a thin layer of Bostik cement (Bostik cement No. 5002 is manufactured by B. B. Chemical Co., Cambridge, Mass.) was applied; this was followed by another layer of splicing compound and, finally, by a thin coat of acrylic spray (acrylic spray is manufactured by Krylon, Inc., Philadelphia 46, Pa.). The waterproof coat was carefully applied to reduce the number and the size of air bubbles. The effectiveness of the waterproof coating was determined by hydrostatic tests that are described below. Figure 5.8 shows two gages mounted on cable before and after waterproofing.

5.2.3 Tourmaline Gage and Gage-cable Tests

These tests were designed to simulate some conditions of Operation Wigwam not normally encountered in the routine underwater shock-wave measurements at NOL. The object of these tests was to determine what effect, if any, these conditions would have on the performance of the gages and cables used on the Wigwam shot and also to obtain only reliable gages and cables for the Wigwam shot by eliminating those that performed poorly or doubtfully in these tests. These tests were performed in two parts, the first of which was to determine the imperviousness of the gage coating and the cable jacket to water under large hydrostatic pressures. The second part was to determine the effectiveness of the special transmission cables used in reducing the signals generated by the shock-wave pressures on the cables themselves.

In the first test the mounted gages and cables were placed in a water-filled pressure chamber (8 ft in diameter and 30 ft in length), and the cable ends extended out of the pressure chamber for about 2 ft so that the leakage resistance could be measured while the pressure was applied. A special packing gland which would accommodate seven cables was used to seal off the cable ends from the applied pressures, thereby reducing the time required to perform these tests. The gages were mounted on cables which were cut to the exact lengths required for the gage arrays on the five NOL recording stations on Operation Wigwam. Chamber pressures of 600 psi were used on gages and cables expected to be used at depths from 300 to 1000 ft. To simulate lowering the gages in water and to determine the pressure at which failure occurred, the pressure was increased from atmospheric pressure by steps of 150 psi every 15 min until 600 psi was obtained. The latter pressure was maintained for about 3 hr. Leakage resistance was obtained with a megohmmeter (megohmmeter type 2423, manufactured by Brüel & Kjoer, Copenhagen, Denmark, and distributed by The Brush Development Company, 3405 Perkins Avenue, Cleveland 14, Ohio) at each pressure, and several readings were obtained at 600 psi. The eight gages and cables expected to be used at depths greater than 1000 ft were subjected to a maximum hydrostatic pressure of 1000 psi. The pressure was likewise increased by increments and maintained at 1000 psi for $1\frac{1}{2}$ hr. These tests for imperviousness were performed on a total of 49 gage-cable assemblies, some of which were for the use of NRL on Project 1.2.1 of Operation Wigwam and a few of which were repeats. In the total of 49 tests, seven failures occurred, all of which were caused by a short circuit in the gages and by the imperfections in the gage coatings. In general, the leakage resistance of the gage-cable assembly was of the order of 10^5 megohms.

The electrical cables used on Wigwam between the tourmaline gages and the recording equipment were especially constructed to reduce the "cable signals" generated by the shock-wave pressures. (The cable was manufactured by the Simplex Wire and Cable Co., Cambridge, Mass.) The cable signals from this cable are negligible as far as underwater shock-wave measurements such as those conducted at NOL on high explosives are concerned. In Operation Wigwam, however, the geometry of the gage and cable array was such that large portions of the submerged cable lengths were continuously stressed by the shock-wave pressure during the time of recording the shock-wave pressures by the tourmaline gages. Since the cable signal is proportional to the amount of cable stressed and to the pressure applied on the cable,[10,11] the cable signals generated could conceivably be large. Therefore, underwater shock-wave tests were performed on these cables at NOL to determine the effectiveness of these cables in reducing the cable signal and to determine what errors would be incurred in the recording of the Wigwam shot.

In these tests, approximately 200 ft of cable was arranged in a compact coil (about $2\frac{1}{2}$ ft in outside diameter, 1 ft in inside diameter, and 5 in. in length) and set at mid-depth in 22 ft of water with the mounted gage protruding out of the water. The axis of the truncated-shaped charges (see reference 2 and Sec. 5.1.3) coincided with the coil axis, and the nearest end (small end) of the charge was about 2 ft from the coil. In this manner the entire 200 ft of cable was subjected to the shock-wave pressure of the order of 2000 psi almost simultaneously so that a measurable signal would be obtained.

The actual cable lengths varied from about 220 ft to about 2025 ft, depending upon the gage depth on the Wigwam shot, although only about 200 ft of each cable was subjected to the shock-wave pressures in these tests. It was assumed that the cable-signal properties of the remainder of the cable were the same as those of the 200-ft section tested.

Tests were performed on about 60 per cent of the cables used on the three YFNB stations; these cables were attached to gages located at depths between 200 and 1000 ft. The largest signal recorded on any one cable was 1.7×10^{-4} $\mu\mu c$/psi (micromicrocoulombs per pound per square inch) per foot of the cable exposed to the pressure. Assuming that the same amplitude of shock-wave pressure was applied simultaneously to the gage and the entire submerged length of cable, the cable signal from this cable was estimated to be about 0.2 per cent of the recorded shock-wave signal on the Wigwam shot. (The actual cable-signal error should be smaller since this hypothetical case was not realized on the Wigwam shot.) However, the results from the test performed on the remainder of the YFNB cables showed that the cable signals relative to the recorded shock-wave signals on the Wigwam shot were several times smaller than the 0.2 per cent value. Therefore, unless the cable signal per foot of cable obtained from each 200-ft section tested was much smaller than that from the remainder of the cable, the cable-signal errors caused by the cables used on the three YFNB stations may be neglected.

5.2.4 Tourmaline Gage Calibrations

All tourmaline gages used on the Wigwam shot were first calibrated by the manufacturer (Crystal Research, Inc., 42 Concord Lane, Cambridge, Mass.) and again by NOL. In these static calibrations the unmounted gage (bare gage, without a waterproof coat) was placed in an oil-filled chamber in which the pressure was gradually increased with a hand pump to a predetermined value that was measured with a calibrated Bourdon gage. The pressure was then suddenly dropped to atmospheric pressure (within about 30 msec by means of a quick-release valve), and the gage output signal was obtained on a microcoulometer.[12] A comparison of this signal with the signal obtained by applying an accurately measured voltage step to the gage circuit was used to obtain the gage KA (gage sensitivity expressed in micromicrocoulombs per pound per square inch). Each gage was thus calibrated about five times at one value of pressure. The reproducibility was about $\pm\frac{1}{2}$ per cent, and the KA value used was the average of these calibrations. The pressure values used on each gage were 500, 100, and 2000 psi. Not only did this cover the pressure range of interest to NOL on the Wigwam shot but the calibrations at the three pressures served to determine the linearity of the gage KA.

Additional static calibrations were performed on a few gages mounted on low-noise cable and coated as described in Sec. 5.2.2. In this calibration the mounted gage and about 1 ft of cable were placed in a water-filled chamber and calibrated as described above. Because of the limitations in the design of this pressure chamber, pressures of only 500 psi were used. It was expected that the comparison of the static calibrations on the mounted and unmounted gages would determine whether the gage coating had any effect on the gage KA. It was found that the bare-gage KA was larger in general than the coated (and mounted) gage KA but that the difference in the KA's was small, ranging from −0.25 to +3.7 per cent. These results, however, are not conclusive since the number of comparisons (five) was small. Therefore a dynamic calibration was performed on all gages used on the Wigwam shot to study this effect further, particularly since gages of these sizes ($^7/_8$, $1^1/_8$, and 2 in. in diameter) have seldom been used in quantitative underwater shock-wave pressure measurements.

In the dynamic calibration, three $^3/_8$-in.-diameter and six Wigwam gages were equally spaced along the circumference of a 1-ft-diameter ring, and the gages were arranged edge-on toward the small end of a truncated charge.[2] The gages were arranged equidistant from the small end of the charge and symmetrically about the extended charge axis so that the shock-wave pressure at any instant was the same at the midpoint of all gages. The responses of all gages were recorded simultaneously on the nine channels of shock-wave recording equipment

Table 5.2—SUMMARY OF TOURMALINE GAGE CALIBRATIONS

YFNB-12				YFNB-13			
Gage No.	Depth (ft)	Dynamic KA	Static KA	Gage No.	Depth (ft)	Dynamic KA	Static KA
891	25	84.0	82.0	1032	25	23.8	24.0
1067	25	79.9	77.8	1064	25	82.3	76.2
1026	50	23.9	23.9	810	50	82.9	80.0
1029	100	24.3	23.9	1033	200	23.4	23.8
1031	200	26.1	25.1	1065	200	83.1	77.6
823	200	79.7	81.4	1	500	144.0	139.3
825	500	--	119.3	811	1000	79.0	81.8
623	1000	80.4	82.2	815	1000	83.2	83.8
893	1000	77.6	82.1				

YFNB-29			
Gage No.	Depth (ft)	Dynamic KA	Static KA
1034	25	24.1	24.2
817	25	82.8	81.1
1036	50	25.2	(23.5)* 24.4
1035	200	23.2	23.7
821	200	76.7	(70.5) 71.9
902	500	126.5	(126.5) 127.2
1066	1000	78.3	(78.9) 78.7
896	1000	76.8	(78.4) 80.7

* Static KA values of coated gages are enclosed in parentheses.

that is used by the EH division at NOL[13] in the measurement of the shock-wave pressures in explosives-comparison programs.

The pressure-time records from these calibration shots showed that the pressure was essentially constant, at about 1500 psi, from about 0.4 to 0.9 msec after the arrival of the shock wave at all gages. (See Fig. 5.6 for the general shape of pressure-time curves produced by truncated charges.) The shock-wave pressures were calculated from the response of the $^3/_8$-in.-diameter gages at four different times in the 0.4- to 0.9-msec interval and from the static (bare-gage) KA values of the respective $^3/_8$-in. gages. The dynamic KA values for each Wigwam gage were then calculated from the response of the Wigwam gages at each of the four times and from the average pressure obtained from the three $^3/_8$-in.-diameter gages at the corresponding time. For each gage the KA value used in determining the pressures recorded on the Wigwam shot was the average of eight dynamic KA values obtained from two calibration shots. The dynamic and static KA values are summarized in Table 5.2. All gages were "aged" prior to the calibration shots by firing detonators at close range.[8]

The precision in the dynamic KA calibration was not so good as the precision in the measurement of the static (bare-gage) KA values. In the dynamic calibrations of the 25 tourmaline gages used on the three YFNB recording stations, the reproducibility of the eight measurements on each gage was better than ±3 per cent of the average KA value, whereas the reproducibility of the static KA measurements was about ±0.5 per cent of the mean value. A fair agreement was obtained between the dynamic and static KA's (see Table 5.2); the dynamic values ranged between +7 and −5.5 per cent of the respective static values. It was difficult to determine whether the coating on the Wigwam gages (compared with the effect of the coating of the ¾-in. gages) had any effect on the gage sensitivity. The indications, however, are that the dynamic KA values, on the average, are slightly larger than the static KA values of the Wigwam gages. Although the precision was not so good in the dynamic measurements as in the static measurements, the dynamic KA values nevertheless were used in the analysis of the Wigwam results because a direct comparison was obtained with small gages, which are used exclusively in explosion-comparison work at NOL and other laboratories.

REFERENCES

1. C. J. Aronson, E. J. Culling, and J. P. Slifko, Underwater Pressure Measurements, Operation Castle Project 1.4 Report, WT-908 (NOL portion), NOLR-1209, October 1955.
2. C. R. Niffenegger, A Study of the Production of Step Shock Waves in Water, NAVORD Report 2624, U. S. Naval Ordnance Laboratory, White Oak, Md., September 1952.
3. A. B. Arons and R. H. Cole, Design and Use of Piezoelectric Gages for Measurement of Large Transient Pressures, Rev. Sci. Instr., 21: 31-38 (1950).
4. D. A. Keys, Phil. Mag., 42: 473-488 (1921).
5. A. B. Wood, Nature of the Pressure Impulse Produced by the Detonation of Explosives Under Water—An Investigation by the Piezoelectric Cathode-ray Oscillograph Method, Admiralty Research Laboratory, November 1924.
6. R. H. Cole, "Underwater Explosions," Princeton University Press, 1948.
7. D. A. Keys, Phil. Mag., 46: 999 (1923).
8. E. A. Christian and C. R. Niffenegger, The Aging of Tourmaline Gages by Underwater Shock Waves, NAVORD Report 2938, U. S. Naval Ordnance Laboratory, White Oak, Md., July 15, 1953.
9. C. Frondel, Construction of Tourmaline Gages for Piezoelectric Measurement of Explosion Pressure Waves, The Underwater Explosives Research Laboratory, Woods Hole Oceanographic Institution, NDRC Report A-378, OSRD Report 6256, January 1946.
10. A. H. Bebb and R. V. Bundy, The Electrical Potentials Produced in the Conductors of a Submerged Cable by Underwater Explosions, Naval Construction Research Establishment, Rosyth, Scotland, October 1945.
11. T. A. Perls, Electrical Noise from Instrument Cables Subjected to Shock and Vibration, Office of Basic Instrumentation, U. S. Dept. of Commerce, National Bureau of Standards, NBS Report 1388, January 1952.
12. R. W. Astheimer, Piezoelectric Gages for Underwater Pressure-Time Measurements. II. A Preliminary Evaluation of Barium Titanate, NAVORD Report 2929, U. S. Naval Ordnance Laboratory, White Oak, Md., July 1953.
13. H. H. Hall, Instrumentation for Measurement of Underwater Pressures Generated by Explosives, NAVORD Report 477, U. S. Naval Ordnance Laboratory, White Oak, Md., Mar. 24, 1949.

CHAPTER 6

ELECTRONIC INSTRUMENTATION

6.1 INTRODUCTION

Five magnetic-tape recording installations were set up by Project 1.2 for electrical pressure-time measurements using piezoelectric and electromechanical gages: One was located in each of the trailers mounted on the YFNB's, and two were mounted in buoys suspended from the LCM 0-1 and LCM 0-2 (sites 1B and 2B). Electrically, all the systems were similar; mechanically, however, the equipment at the YFNB-13 differed in that the Ampex tape-transport systems were used there instead of the Davies tape recorders which were used at the other locations.

For protection against a complete loss of data at any one station, the recording at each location was divided into two systems as far as practical. Each system consisted of a tape-transport mechanism with all the associated electronic equipment. The two complete systems for each location were rigidly bolted together and suspended as a unit.

6.2 DIFFERENCES BETWEEN CASTLE AND WIGWAM

Designs for the Wigwam electronic pressure-time instrumentation circuits were based on the premise that the basic Castle system would be used where possible and would be changed only when either the requirements for Wigwam or the experience gained with the Castle system dictated the advisability of a change. (The Castle system is described in reference 1.)

It was found that the changes necessitated by the different conditions and requirements of Wigwam were:

1. Higher gain amplifiers to increase the signal levels from the piezoelectric gages used.
2. Parallel operation of amplifiers having different gains to make possible the measurement of the initial shock wave as well as the bubble pressures while using the same gage.
3. Addition of a radio-transmitted fiducial signal at zero time since there would be no bomb flash.
4. The addition of a recorded timing track to improve timing accuracy.
5. The addition of a negative power supply.
6. Wigwam required about twice the number of data channels used in Castle.
7. Reduction of the size and weight of the system for its use at the two buoy stations.

In addition to the above changes, unsatisfactory Castle experiences necessitated the following modifications:

1. Addition of multiple calibration steps to ensure that at least one calibration step would be near the data point being read.
2. The addition of equal negative calibration steps to shorten the recovery time of the calibration circuits.

3. Direct coupling of all amplifiers to shorten their recovery time and make it possible to apply time-constant corrections if necessary.

4. Complete parallel operation of power supplies for improved reliability.

5. Longer warm-up time for the Logaten heaters.

6. Changes in the sequence timer to prevent the rundown of batteries and the overheating of equipment.

7. Redesign of the primary activation circuits to protect against a possible premature failure of individual timing signals.

8. More extensive use of unitized construction, check points, and system test sets to reduce servicing and check-out times.

In general, a complete mechanical, as well as a major electrical, redesign was undertaken to improve the over-all operation and reliability of the equipment. However, the basic recording techniques as used in Castle remained the same.

Figure 6.1 shows a simplified block diagram of the Wigwam recording equipment. There are only six of the 10 recording channels per system shown here since the remaining four are but duplicates of one or more of these. Each of the units within the recording system is described in the following sections.

6.3 TAPE TRANSPORTS

6.3.1 Davies Recorders

The four Davies recorders originally used on Castle were left unchanged mechanically except for minor rewiring and the replacement of some electrical connectors. The single power supply normally in the recorder was removed to make room for a redesigned dual supply which furnished all the power requirements for both the recorder and the associated electronics. The power supply will be covered in more detail in Sec. 6.11.

In addition to the four Davies recorders already on hand, four more Davies recorders (part of the Horizons, Inc., data-recording system developed under a contract with the Office of Naval Research) were modified to be identical to those used on Castle. This modification consisted in changing the original ½-in. tape-transport mechanisms and the four-channel heads to accommodate a 1¼-in. tape and 10-channel heads.

6.3.2 Ampex Recorders

The three Ampex top plates were changed only to the extent of replacing the capstan idler solenoid with a model providing a greater pulling force. Since the Wigwam design incorporated a more elaborate timing and flutter compensation system than was used on Castle, the precision capstan drive source was eliminated. Instead, the capstan drive motors were supplied with 110-volt 60-cycle power from two 28-volt d-c rotary converters mounted below the recorders. Since all three Ampex top plates were required at one location to obtain enough recording capacity (each Ampex recorder had a seven-channel recording head), they were integrated into one mechanical unit.

6.4 CONTROL SYSTEM

Previous experience with the Castle control system indicated a need for improved reliability to ensure operation at the correct time as well as to prevent premature operation. Additional characteristics to permit resetting and return of the equipment to its initial state in various call-off situations were also desirable. This was accomplished in two separate units, the two-out-of-three box and the sequence timer.

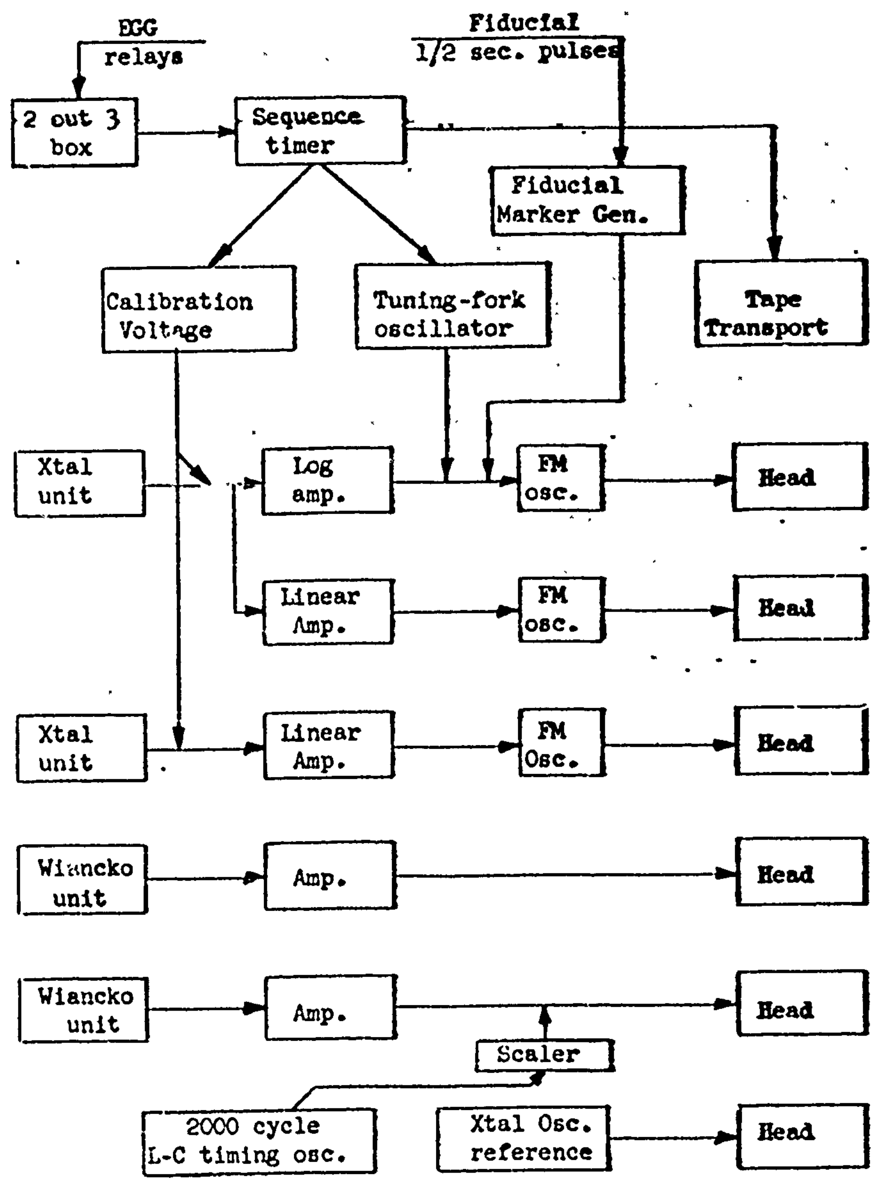

Fig. 6.1—Block diagram of Wigwam recording system.

6.4.1 Two-out-of-three Box

The Wigwam equipment was designed to be activated by three radio time signals given at −45, −15, and −1 min. To ensure that the equipment would run at the proper time, a coding system was devised which would activate it if any two of the possible three predetermined signals were received. These three signals consisted in the closure of three relays at the times just mentioned and were under the control of EG&G. Specifically, the first of the signals served only to turn on a heater in the Logaten amplifiers to provide as much time as possible for them to become stable since they were sensitive to thermal changes. The second signal (−15 min) turned on the power supplies and filaments in the recording equipment (15 min was considered enough time for the amplifiers to become stable). The last signal (−1 min) served simply as a "transfer" signal and took all control away from the radio receiver. If any one of these three radio signals had been missing, the two-out-of-three box would have supplied the missing signal at the proper time; the functions normally occurring at −45 min would have been combined with those at −15 min if the −45-min signal had not been received. However, if the test had been canceled even a few seconds before the scheduled arrival of the −1-min signal, the timing equipment would have been recycled and readied for another run. Furthermore, if a single early spurious signal had been received, such as is believed to have occurred on Operation Castle, it would not have activated the recording equipment but would have been rejected by the two-out-of-three box.

The schematic diagram of the two-out-of-three box is shown in Fig. 6.2, and the mechanical configuration of the waterproof model used at the buoy locations is shown in Fig. 6.3. Figure 6.4 shows the box as used at the trailer installations.

Prior to leaving the instrumentation stations on D-day, the "arm" switch of the two-out-of-three box was closed to enable the signals from the radio to actuate it. The "ready" light served only to indicate that the motor within the two-out-of-three box had homed, i.e., returned to its initial setting, and was then ready to begin a new sequence of events.

A clock-controlled timer was used at the two buoy locations to control the "on" time of the radio receivers. However, in contrast to their location in the buoys as on Operation Castle, they were located within the canister containing the radio and were under the control of EG&G.

6.4.2 Sequence Timer

The sequence timer, in conjunction with the two-out-of-three box, controlled both the order and duration of events within the recording equipment. The reception of the −15-min radio signal (through the two-out-of-three box) served to apply power to the 20-min timer motor within the sequence timer as well as to the filament circuits within the recording equipment. Also at this time, partial power was applied to the power-supply dynamotors; then, after a 20-sec delay provided by a thermal relay, full power was applied. This was done to prevent arcing in the power-supply regulator tubes since they would have been operating under no-load conditions.

Once the −1-min radio signal had been received (or its substitute from the two-out-of-three box), all control was taken away from the radio and the two-out-of-three box. Then the timing functions were controlled completely by the sequence timer, a motor-driven switch which determined the proper sequence of events during the recording cycle of the equipment.

At this time (−1 min) both the tape-transport mechanism and a $\frac{1}{5}$-rpm timing motor within the sequence timer were energized. After an interval of 10 sec, switches activated by cams coupled to the $\frac{1}{5}$-rpm motor caused the calibration-voltage generator to inject a series of calibration-voltage steps into the recording system. After 20 sec the Q-step circuit within the calibration generator was energized, and at 30 sec a 10-sec gate was opened for the tuning-fork oscillator. After $2\frac{1}{2}$ min this complete cycle was repeated, thus providing a complete series of calibrating and timing signals immediately after as well as before the arrival of the data. After a total running time of 3 min, cams on the $\frac{1}{5}$-rpm motor caused a relay to close, which, in turn, blew a master fuse and prevented the equipment from running a second time and destroying the tape. However, the $\frac{1}{5}$-rpm motor continued to run until it homed, at which time power was automatically removed from the motor.

CONFIDENTIAL

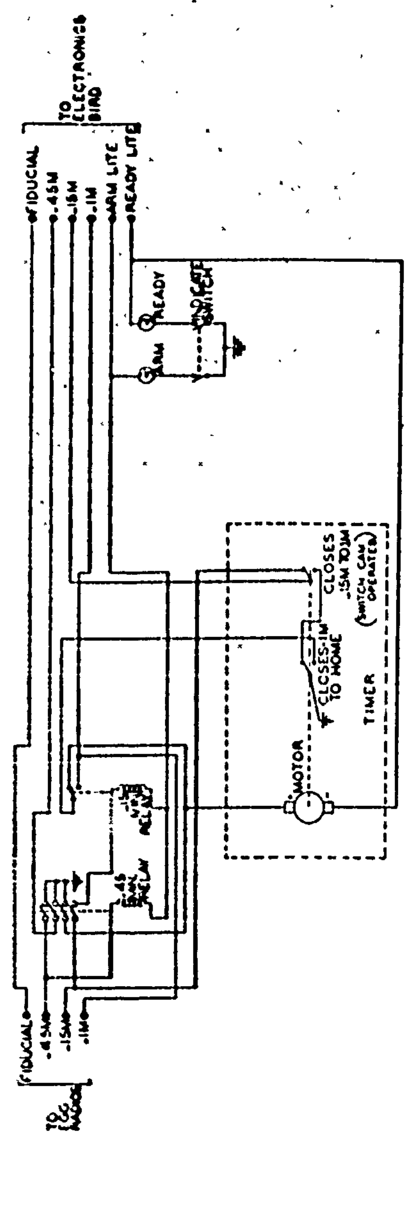

Fig. 6.2—Schematic diagram of the two-out-of-three box.

SECRET—REST[illegible]ICTED DATA

CONFIDENTIAL

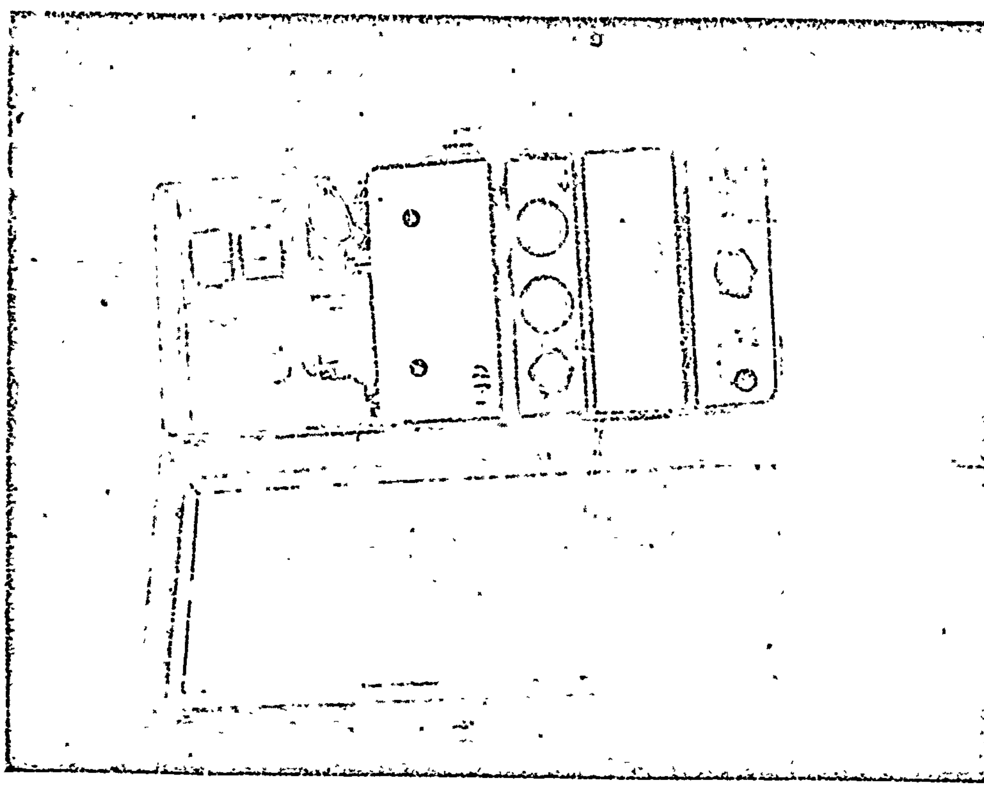

Fig. 6.3—Two-out-of-three box (waterproof model).

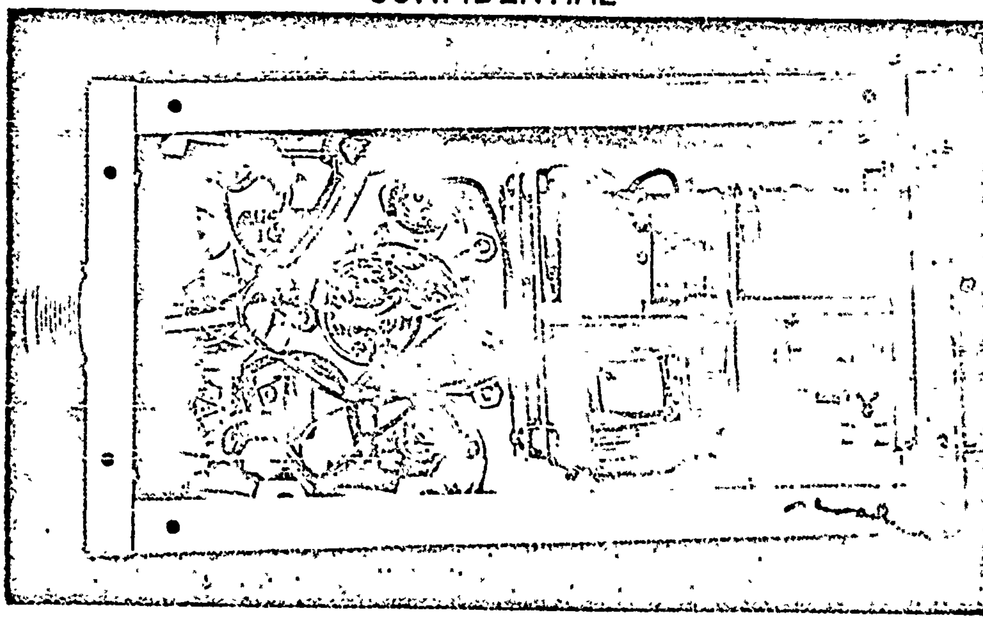

Fig. 6.4—Two-out-of-three box (trailer model).

If neither a −1-min signal from the radio nor its substitute from the two-out-of-three box had been received, the equipment would have continued to run (with the exception of the tape transport and the sequence timer's $\frac{1}{3}$-rpm motor) until the batteries were depleted. The function of the 20-min timer motor in the sequence timer was to prevent just such an occurrence by breaking momentarily the arming circuit after 20 min.

A summary of the sequence of events is shown below. The sequence-timer schematic diagram is shown in Fig. 6.5, and its physical construction is shown in Fig. 6.6.

SUMMARY OF TIMING AND CALIBRATION SIGNALS

−45 min	Turns on 28 volts to Logaten heaters. In the event that the −45-min signal is not received, the same function is accomplished by the −15-min signal.
−15 min	Turns on 28 volts to all heaters and power supplies (20-sec delay for full power to dynamotors). Starts 20-min timer motor in sequence timer.
−1 min	Turns on 28 volts to recorder transport and starts $\frac{1}{3}$-rpm timer motor in sequence timer.
−50 sec	Sequence timer causes calibration-voltage generator to inject a series of 10 reference voltages into each piezoelectric channel.
−40 sec	Sequence timer causes calibration-voltage generator to inject a 2-sec positive Q-step into each piezoelectric channel.
−38 sec	Sequence timer causes calibration-voltage generator to inject a 2-sec negative Q-step into each piezoelectric channel.
−30 sec	Sequence timer opens gate, allowing 2-kc signal from tuning-fork oscillator to be recorded for 10 sec.
Zero time	Equipment ready to record signals produced by shock-wave and bubble pulses.
+1 min 30 sec	Sequence timer causes calibration-voltage generator to repeat series of 10 reference voltages into each piezoelectric channel.
+1 min 40 sec	Sequence timer causes calibration-voltage generator to repeat 2-sec positive Q-step.
+1 min 42 sec	Sequence timer causes calibration-voltage generator to repeat 2-sec negative Q-step.
+1 min 50 sec	Sequence timer opens gate, allowing 2-kc signal from tuning-fork oscillator to be recorded for 10 sec.
+2 min	All power is turned off (fuse blown), with the exception of the $\frac{1}{3}$-rpm sequence-timer motor.
+4 min	Sequence-timer motor homes and stops.

6.5 CALIBRATION-VOLTAGE GENERATOR

6.5.1 Calibration-generator Operation

In contrast to the use of just two calibration voltages (a high and low calibration voltage) as in Castle, the Wigwam calibration system made use of a stepping relay which injected a series of 10 logarithmically spaced voltages into each piezoelectric-gage channel. The voltage steps were applied 10 sec after the arrival of the −1-min signal and within a period of about $\frac{1}{2}$ sec. The use of 10 voltage steps ensured the placement of a calibration voltage near a data point.

CONFIDENTIAL

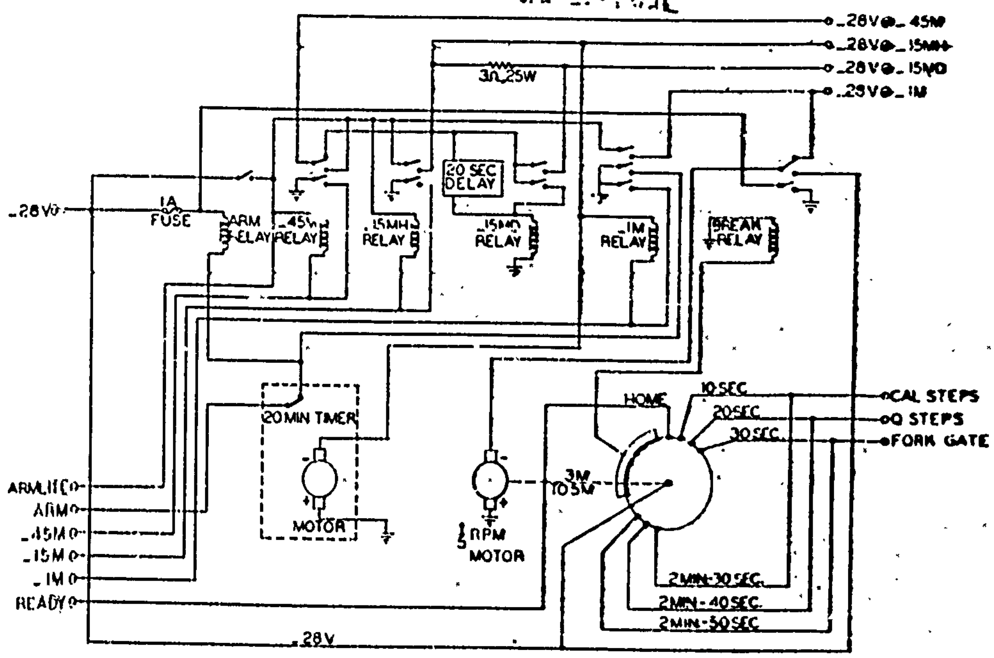

Fig. 6.5—Schematic diagram of the sequence timer.

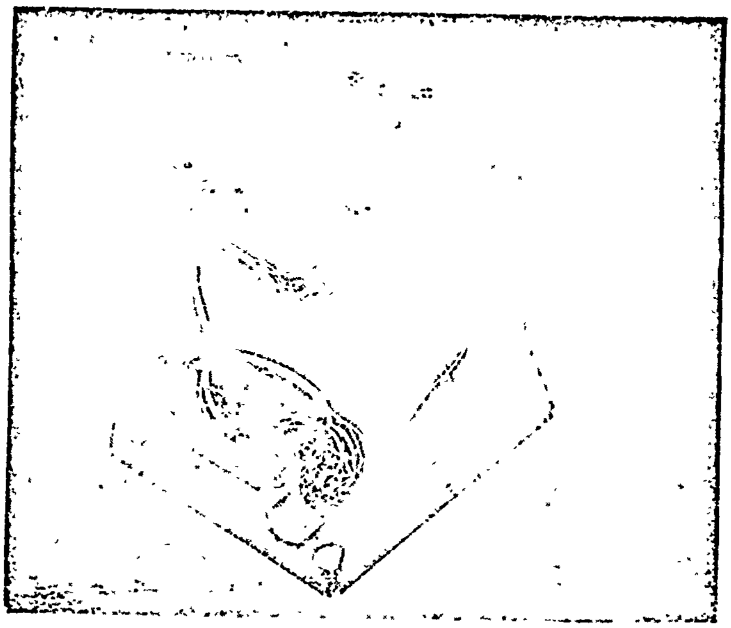

Fig. 6.6—Sequence timer.

SECRET - RESTRICTED DATA
CONFIDENTIAL

Twenty seconds after the arrival of the −1-min signal (−40 sec), a 2-sec positive voltage step and then (at −30 sec) a 2-sec negative voltage step were placed on each of the two calibration lines, termed lines 1 and 2. Line 1 received 4-volt positive and negative steps, and line 2 received 0.8-volt positive and negative steps. The positive step (Q-step) served as a check on the time constant of the input circuits of each of the crystal pickup amplifiers, and the negative step was used to hasten amplifier recovery after receiving the positive step. Line 1 was used to calibrate all type K amplifiers, and line 2 fed all G amplifiers. The amplifiers are discussed more fully in Sec. 6.7. The theory behind the calibration system using the Q-step method is fully developed in Secs. 4.6.1 to 4.6.3 of the Castle report.[1]

6.5.2 Calibration-generator Voltages

The standard voltages for the 10 steps were generated from two sets of voltage dividers using a type 5651 reference tube. All even-numbered steps were fed from one divider, and the odd-numbered steps were fed from the other. The two dividers, each with its associated reference tube, were, in turn, fed from separate power supplies for protection against a complete loss of calibration steps if one of the power sources should fail. If one of the power supplies failed, half the calibration steps still covering the range would have been available. The schematic diagram of the calibration-voltage generator is shown in Fig. 6.7.

The voltage appearing at each of the 10 steps was:

Step	Voltage	Step	Voltage
1	10.0	6	0.88
2	6.0	7	0.50
3	4.0	8	0.30
4	2.4	9	0.20
5	1.4	10	0.12

The 2-sec positive voltages used for the Q-step were obtained from the same dividers that supplied the precision step voltages, and the negative 2-sec Q-step was obtained from a divider connected across the 28-volt supply line. No attempt was made to regulate the negative Q-step since its only purpose was to shorten amplifier recovery time.

The resistors used in the precision voltage dividers were all chosen to be within ±1 per cent of the design values. The first and second step voltages were adjusted during a standard "check run" of the equipment while using an infinite-impedance type of voltmeter designed especially for the purpose. The remaining voltage steps were then measured (as a check) to an accuracy of ±1 per cent.

To ensure that the type 5651 voltage reference tubes would fire in the darkness (tests showed that the striking characteristics of the 5651 were erratic when placed in the dark for long periods), a small 6-volt pilot light was installed near the tubes and lighted by the −1-min voltage. A picture of the calibration-voltage generator is shown in Fig. 6.8.

6.6 TIMING SYSTEM

6.6.1 Tuning-fork Oscillator

For purposes of clarity, there were two separate oscillators used in the Wigwam instrumentation for the measurement of time intervals. One, a tuning-fork oscillator, was used as a frequency standard and as a check on the base frequency of the other oscillator, an L-C oscillator which had its output amplitude modulated. Both oscillators were constructed on the same chassis and were referred to as the timing oscillators. The amplitude modulation of the L-C oscillator output was, however, performed by a separate unit, the scaler. The L-C oscillator and the scaler will be covered in more detail in Secs. 6.6.2 and 6.6.3.

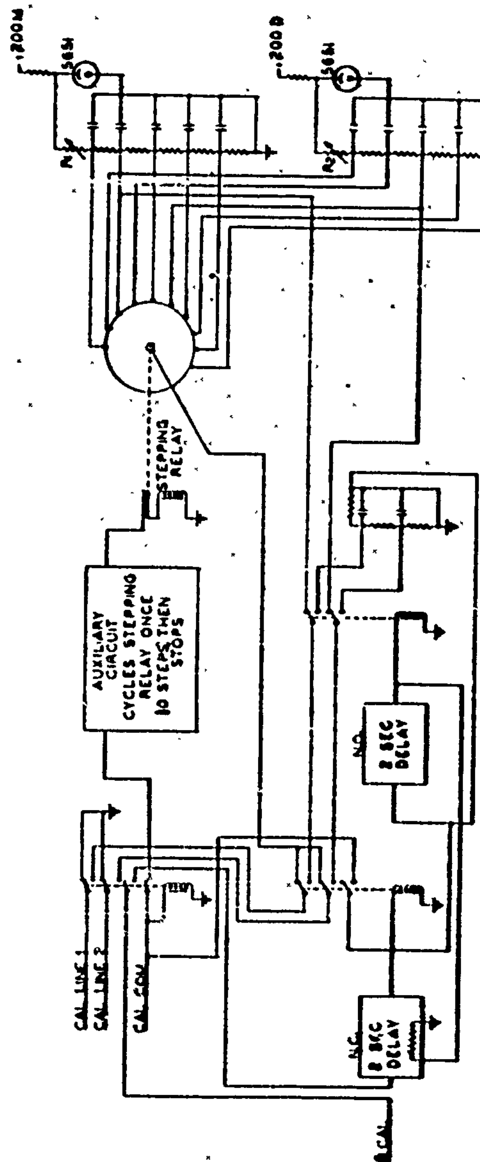

Fig. 6.7—Schematic diagram of the calibration-voltage generator.

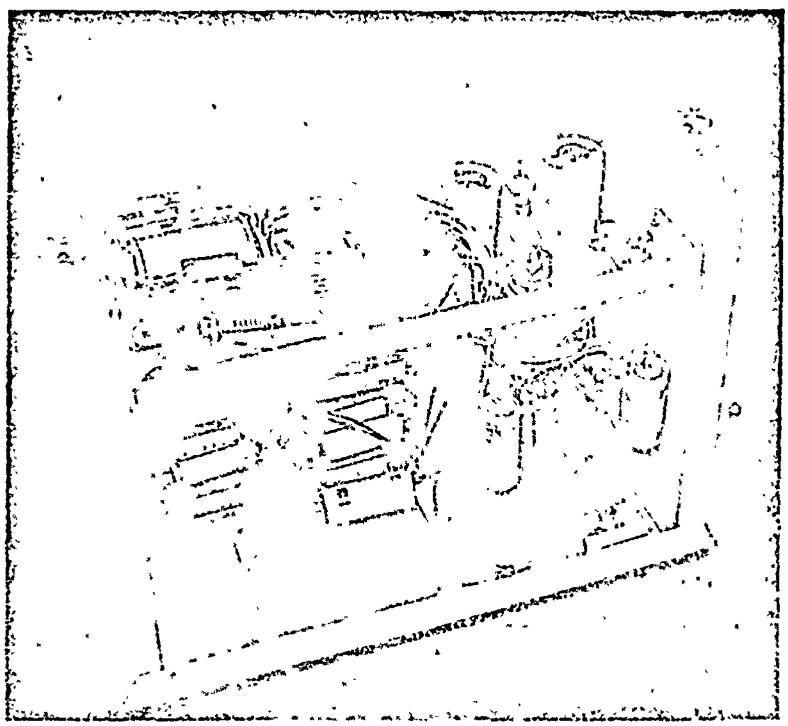

Fig. 6.8—Calibration-voltage generator.

Shortly before the data-reception period and then again immediately afterward (see the summary of timing and calibration signals in Sec. 6.4.2), a 10-sec signal from the tuning-fork oscillator was recorded on channel 1 of each recording system. The signal from the tuning-fork oscillator could not be relied upon during the data-recording period since both its frequency and amplitude were sensitive to accelerations. During this time the L-C oscillator was used because it was considered more dependable, although it was slightly less accurate.

The tuning-fork oscillator was a commercially available item manufactured by American Time Products and similar to those used on Castle. The Wigwam requirements, however, necessitated the use of a 2000-cycle signal to meet the timing accuracies specified in the original planning of the instrumentation. Since there were a few 500-cycle tuning-fork oscillators available which had been used on Castle and since the Wigwam requirements called for a 2000-cycle signal, a quadrupler circuit was built into all the timing units. The additional tuning-fork oscillators purchased for the project had a frequency of 2 kc, and thus the quadrupling circuit was not needed with these. The elimination of the quadrupling circuit was accomplished by simply inserting a jumper into the circuit and bypassing it when the higher frequency tuning-fork oscillators were used.

6.6.2 L-C Oscillator

The heart of the timing system used on Wigwam was a specially designed 2000-cycle L-C oscillator using resistance stabilization. Laboratory tests showed that the frequency drift of the Hartley-circuit oscillator did not exceed more than a few tenths of a cycle from a cold turn-on until it had reached its final operating temperature. In addition, the amount of drift was always the same, thus facilitating any frequency compensations which may have been necessary later.

The output of the L-C 2000-cycle oscillator was fed directly into the scaler, which, in turn, amplitude modulated the signal before it was recorded. Unlike the tuning-fork oscillator, the L-C oscillator was recorded continually.

Figure 6.9 shows the schematic diagram of the quadrupler circuit used with the tuning-fork oscillator as well as the L-C oscillator circuit. A picture of the assembled unit is shown in Fig. 6.10.

6.6.3 Scaler

The output of the 2000-cycle L-C oscillator was coded by a series of a-m fluctuations and served to ensure timing continuity through a period of high acceleration of the recording equipment. This change in carrier amplitude was expected to facilitate the counting of the individual cycles when the records were later analyzed. The coding was also a precautionary measure to serve as a check for the total time in which the tape may have lost contact with the recording heads during periods of high acceleration (up to 10 g). The coding of the L-C oscillator, performed by the scaler, was repeated every 0.3 sec; it was unlikely that the time of a "drop-out" would exceed this time of one complete coding cycle.

Basically, the coding was performed by modulating the 2000-cycle signal from the L-C oscillator by a signal derived from a series of Berkeley counters. The counters, too, were fed by the initial 2000-cycle frequency to keep the two signals—the L-C oscillator signal and the modulating signal from the counters—in synchronization. The desired output of the scaler is shown in Fig. 6.11.

Analysis of the final records showed, however, that the code counters did not always count properly; it is thought that the amplitude and wave shape of the L-C oscillator that fed the counters were not matched properly to the counter input requirements. A picture of the scaler is shown in Fig. 6.12.

6.6.4 Fiducial Marker System

Supplementing the L-C oscillator–scaler units was a radio marker system which served as a backup provision for the other timing units in the system. Since, in Wigwam, there was no visible bomb flash at zero time from which a signal could be derived, a radio link was used to provide the necessary zero-time information.

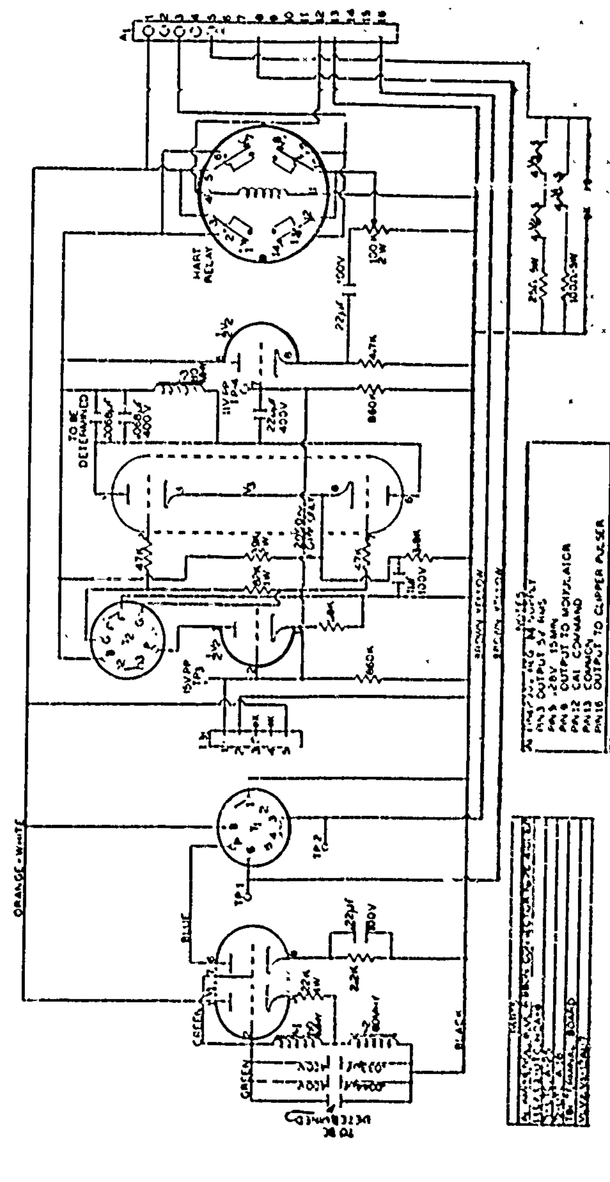

Fig. 6.9—L-C oscillator and quadrupler circuit.

CONFIDENTIAL

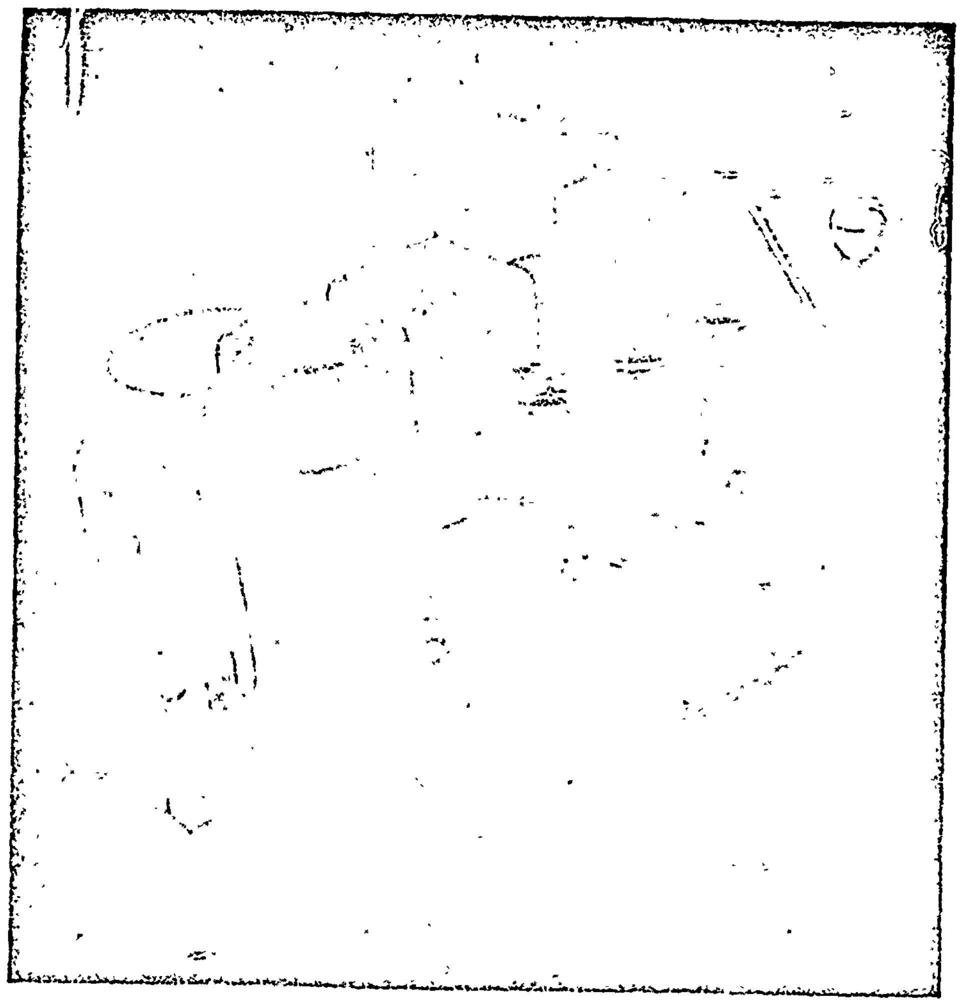

Fig. 6.10—Timing oscillators.

SECRET—RESTRICTED DATA

CONFIDENTIAL

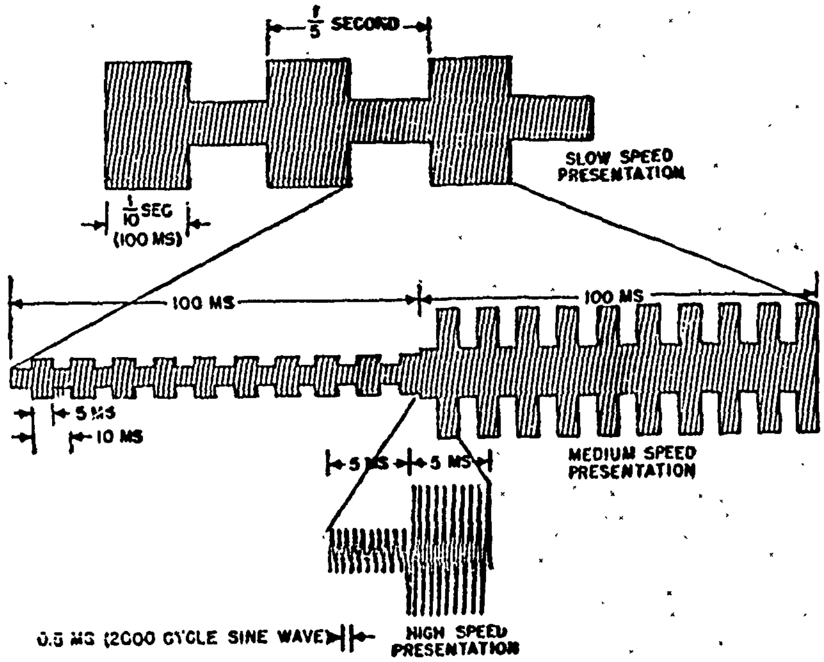

Fig. 6.11—Scaler presentation.

Fig. 6.12—Scaler unit.

At zero time, and every ½ sec thereafter for 9 sec, a radio signal was received and superimposed on the same channel as the tuning-fork oscillator (refer to the block diagram of the recording system, Fig. 6.1). However, the short-duration high-voltage marker signals as received by the radio link were unacceptable, as such, and had to be "matched" to the recording instrumentation system. This was accomplished by the fiducial marker generator.

The operation of the fiducial generator was centered around two thyratrons that were fired by the radio pulse at zero time. After the reception of the zero-time pulse, one thyratron remained in a conducting state and the other was quickly extinguished. Consequently, each succeeding pulse (every ½ sec) had no effect on the thyratron that was already conducting but did serve to fire the other momentarily. At zero time the fiducial generator produced an output of a positive-going 1-volt pulse with a duration of about 0.1 sec, and each succeeding ½-sec timing pulse produced a negative and much shorter duration pulse (about 1 msec). The rise times of both the positive fiducial marker pulse and the negative ½-sec marker pulses were, for practical purposes, instantaneous; the over-all timing accuracy of the fiducial and the following ½-sec timing marks were dependent upon delays within the radio transmitting and receiving equipment.

The schematic diagram for the fiducial marker generator is shown in Fig. 6.13, and a picture of the completed unit is shown in Fig. 6.14.

6.7 CHANNEL AMPLIFIERS

As the shock wave passed the piezoelectric gages, a voltage was generated, amplified, and converted to an f-m signal, which was then recorded. The conditions of the test necessitated the use of amplifiers having widely differing gains to ensure the adequate bracketing of the pressure levels predicted for the various gage depths and locations. This amplifier gain bracketing served also as a safeguard against major prediction errors. In addition, since the amplitude of the bubble pulse following the initial shock wave was expected to be as small as $\frac{1}{20}$ that of the initial shock pressure, a high-gain amplifier was often placed in parallel with one having a low gain (refer to the block diagram of the recording system, Fig. 6.1).

In contrast to the two kinds of amplifiers used on Castle, the Wigwam instrumentation made use of five amplifiers of various types for the crystal pickup channels. For purposes of identification, they were code named as follows: the K, G, B, C, and L or log amplifiers. These five amplifiers, in turn, can be subdivided into two main groups: linear and logarithmic. The linear amplifiers differ only in their gain characteristics. In addition to, and in contrast to, the Castle instrumentation, each Wiancko channel made use of a buffer amplifier (the W amplifier). Each is described in the following sections.

6.7.1 K Amplifier

When the signal voltage from the piezoelectric pickup was sufficient to modulate the f-m oscillator fully (Fig. 6.1), it was necessary to have only an impedance transformer to match the piezoelectric sensing unit to the input of the oscillator. The K amplifier was designed to serve this purpose and was, essentially, nothing more than a specialized cathode follower that provided an input impedance for the piezoelectric pickups of up to 1000 megohms, making possible time constants of the order of 10 sec.

Unlike the cathode follower used on Castle, the K amplifier (refer to schematic diagram, Fig. 6.15) made use of both sections of the WE-5755/420A input tube and employed d-c feedback. In addition to the much higher stability provided by the new K circuit, its frequency response was flat from zero cycles to well over 10 kc. The K amplifiers provided a gain of about 0.97 and a linearity of better than 1 per cent for positive signals up to 10 volts.

The values of C_P and C_S (Fig. 6.16) were computed from the known values of: the KA of the piezoelectric unit with which the amplifier was to be used; C_C, the cable capacity; P, the predicted peak pressure; and E, the desired peak voltage which the pressure, P, was to produce at the amplifier input. For ease of manipulation, C_S was made to equal $C_C + C_P$; hence the calibration voltage appearing at the amplifier input was equal to half that produced by the calibration generator.

CONFIDENTIAL

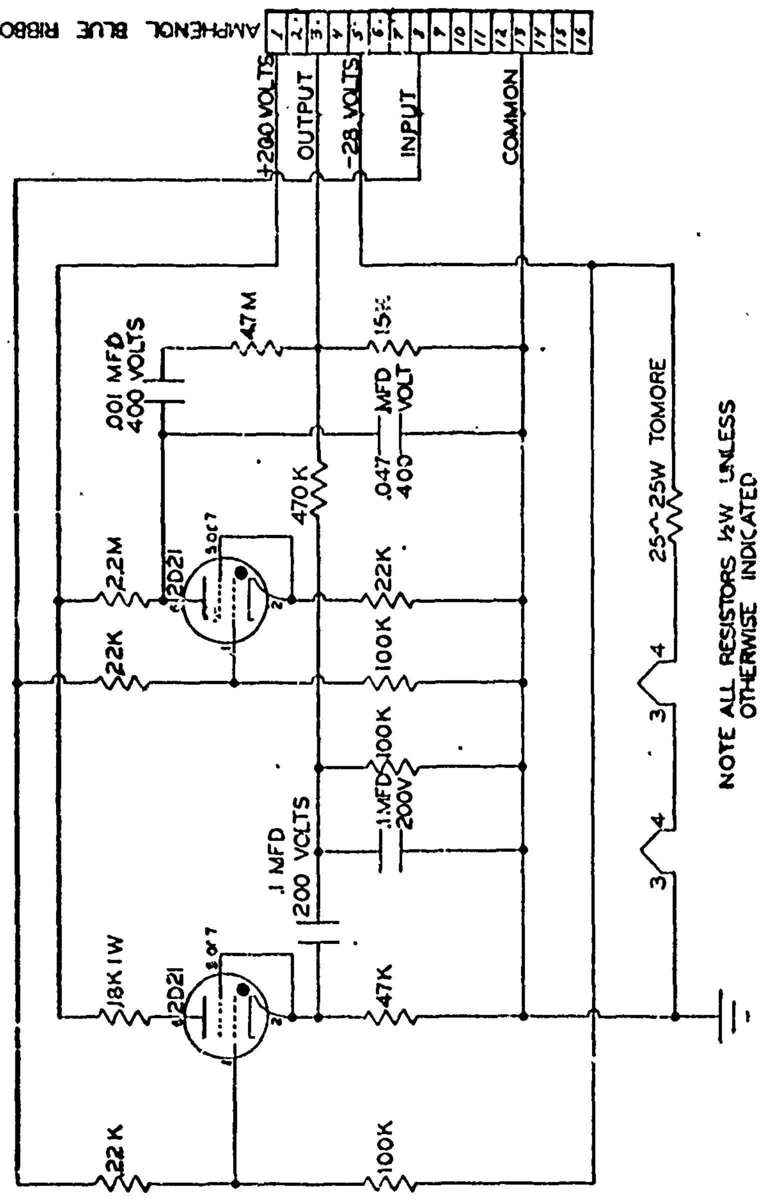

Fig. 6.13—Schematic diagram of the fiducial generator.

CONFIDENTIAL

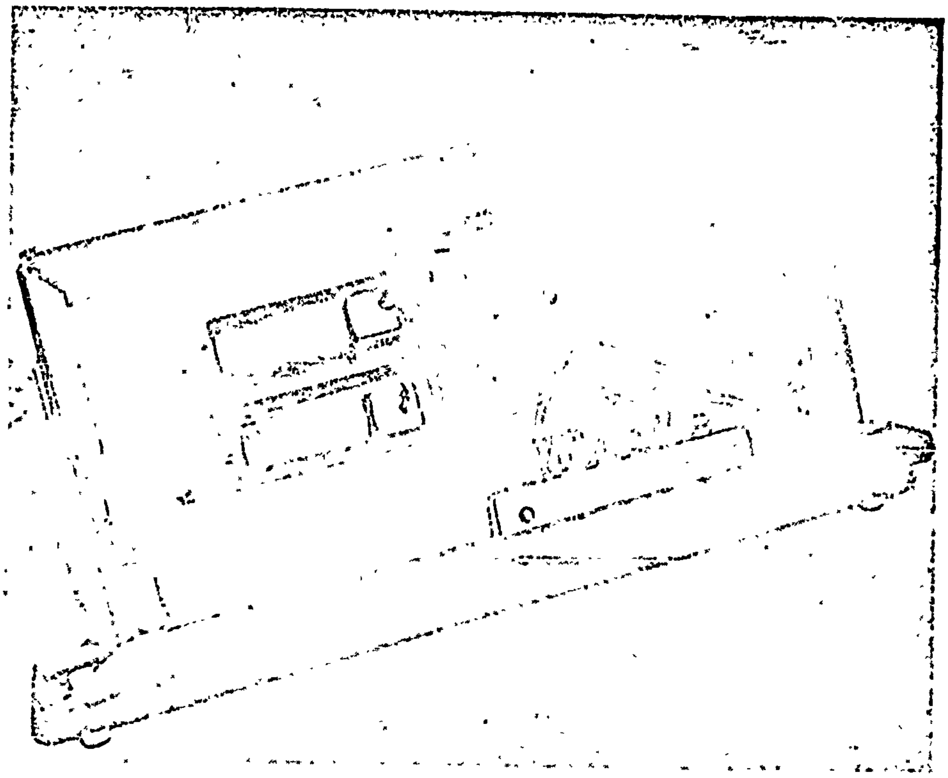

Fig. 6.14—Fiducial generator unit.

SECRET – RES[illegible]ICTED DATA

CONFIDENTIAL

CONFIDENTIAL

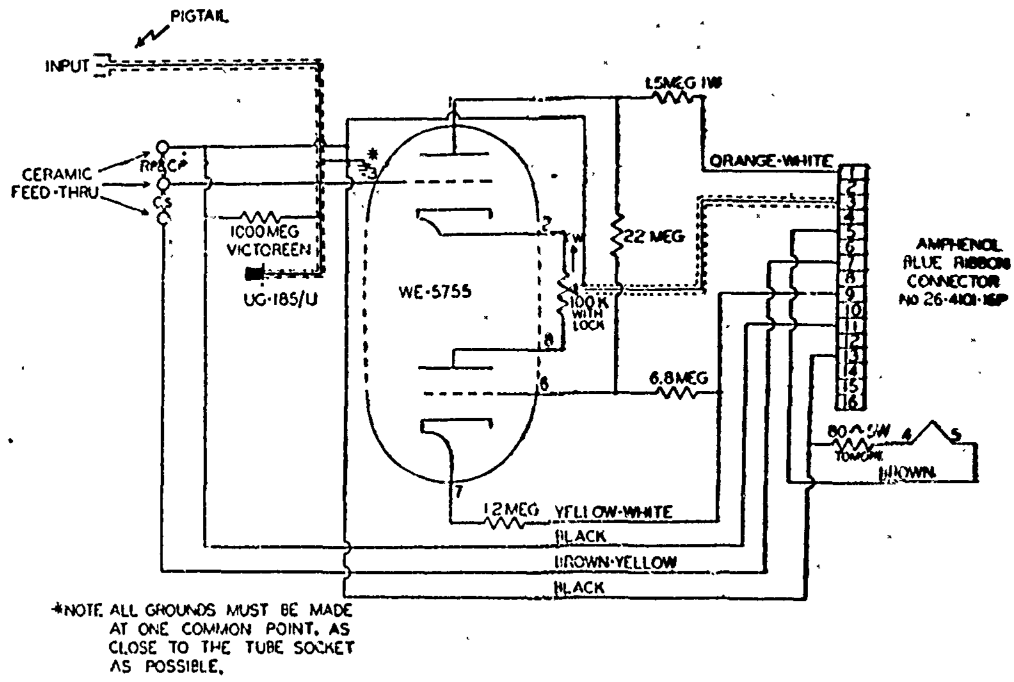

Fig. 6.15—Schematic diagram of the type K amplifier.

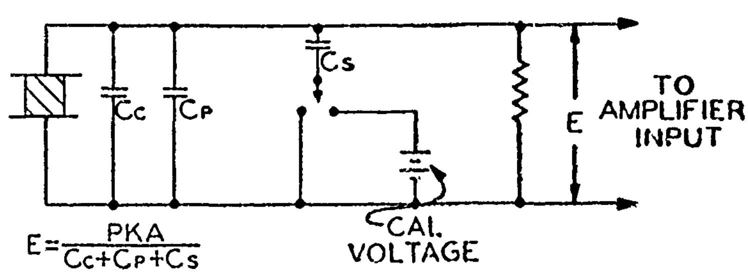

$$E = \frac{PKA}{C_c + C_P + C_s}$$

LET: $C_s = C_c + C_P$

Fig. 6.16—Determination of C_s and C_p.

A picture of the K amplifier is shown in Fig. 6.17.

6.7.2 G, B, and C Amplifiers

The necessity of having several higher gain linear amplifiers led to the development of but a single "master" amplifier. By altering slightly the master-amplifier circuit, the various gain requirements were met. The code G, B, and C simply referred to the gain settings of the "master" amplifier and were adjusted for an average gain of 3, 5, and 15, respectively. Reference to the schematic diagram in Fig. 6.18 shows that the over-all gain of the amplifier was set by changing the value of R_1, which controlled the amount of negative feedback. Observe, too, that the input circuit is similar to that of the K amplifier and thus affords the same high input impedance necessary with the use of crystal pickups. The B and C amplifiers were always used in parallel with either the K or G type amplifier and hence did not need the insertion of a C_P or C_S as was mentioned in the previous section. The G amplifier, however, had an input circuit which was an exact duplication of the K amplifier, and therefore it did require the addition of the two condensers C_P and C_S, as well as a grid resistor.

Direct coupling was used throughout the amplifiers; a momentary overload in the higher gain units, produced by either a signal or calibration step, did not cause blocking. The time constant was determined solely by the input-circuit impedance and the associated capacities of the crystal unit and cable and the values of C_P and C_S.

The output circuits of the G, B, and C amplifiers were similar, in many respects, to the output circuit used with the K amplifier. The d-c level, in all cases, was controlled by a potentiometer and adjusted for −1.4 volts to satisfy the input requirements of the f-m oscillator into which they fed.

Figure 6.19 shows the mechanical construction of the G, B, and C amplifiers. Mechanically they were identical, with the exception of the addition of standoff terminals in the G amplifier for the insertion of C_P, C_S, and the input grid resistor.

6.7.3 Logarithmic Amplifier

The primary function of the logarithmic amplifier was to supply, in one unit, a variable-gain amplifier capable of handling the signals (both large and small) which did not fall within the range of the linear amplifiers. Consequently, it was used only in conjunction with a linear amplifier. Essentially, it consisted of a modified B amplifier (gain of 5) which drove a Kay Lab model 511CE Logaten (Kalbfell Laboratories, Inc., San Diego, Calif.). The output of the Logaten, in turn, fed another "master" amplifier having a gain of 10. Figure 6.20 shows the complete schematic diagram of the logarithmic amplifier, and Fig. 6.21 shows the over-all gain characteristics of the amplifier. The characteristics of the Logaten unit alone are shown in Fig. 4.13 of the Castle report.[1]

Although the heater within the Logaten was turned on at −45 min and the amplifier filaments were energized at −15 min to enable the amplifier to become thermally stable, there was still considerable difficulty in maintaining a zero d-c voltage level at the Logaten input. In practice, the input amplifier feeding the Logaten was "zeroed" at −1 min during trial runs, and then only after the complete unit had been subjected to the same heat cycling it was expected to receive during the data run. As was done with the linear amplifiers, the d-c level of the output was adjusted to −1.4 volts. This value was hard to maintain, however, because of the high gain of the logarithmic amplifier and the inability to keep the input of the Logaten unit at zero voltage.

Figure 6.22 is a picture of the completed amplifier.

6.8 DAVIES MODULATOR

The output of the piezoelectric channel amplifiers (Sec. 6.7) was converted from an amplitude signal to an f-m signal before being recorded. This was accomplished by feeding the output of the amplifiers directly into commercially available f-m oscillators (Davies modulators) and then to the recording head.

(Text continues on page 130.)

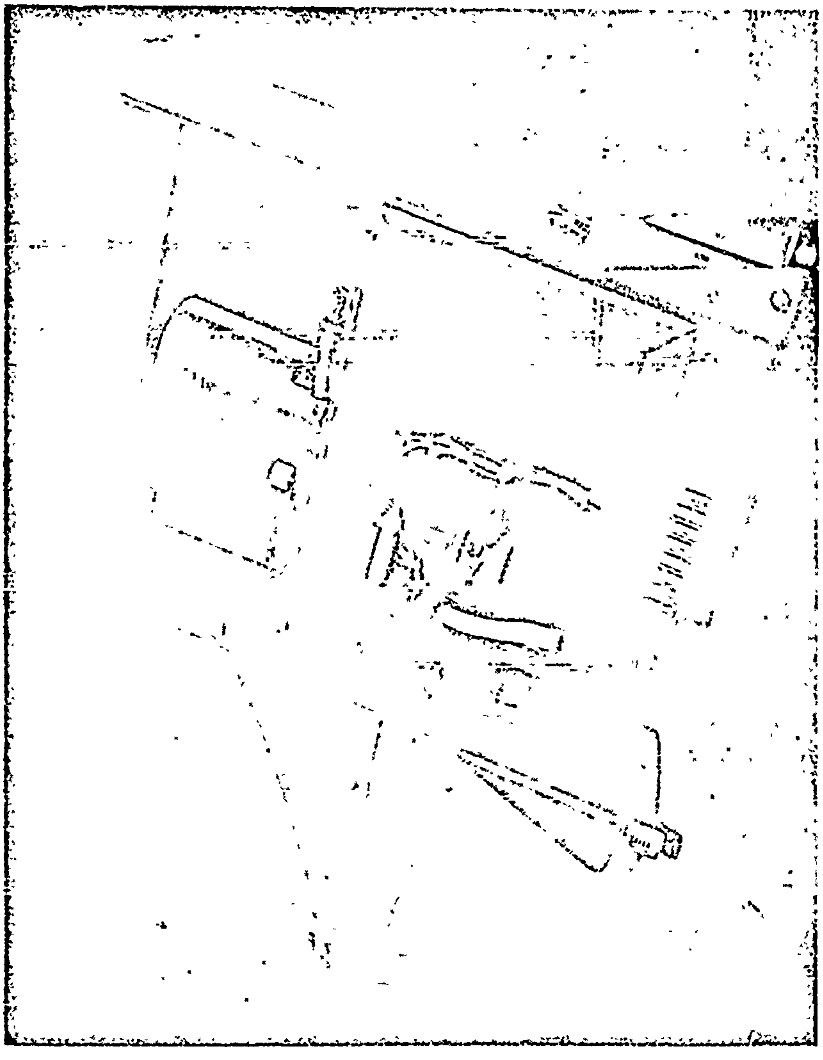

Fig. 6.17—K amplifier.

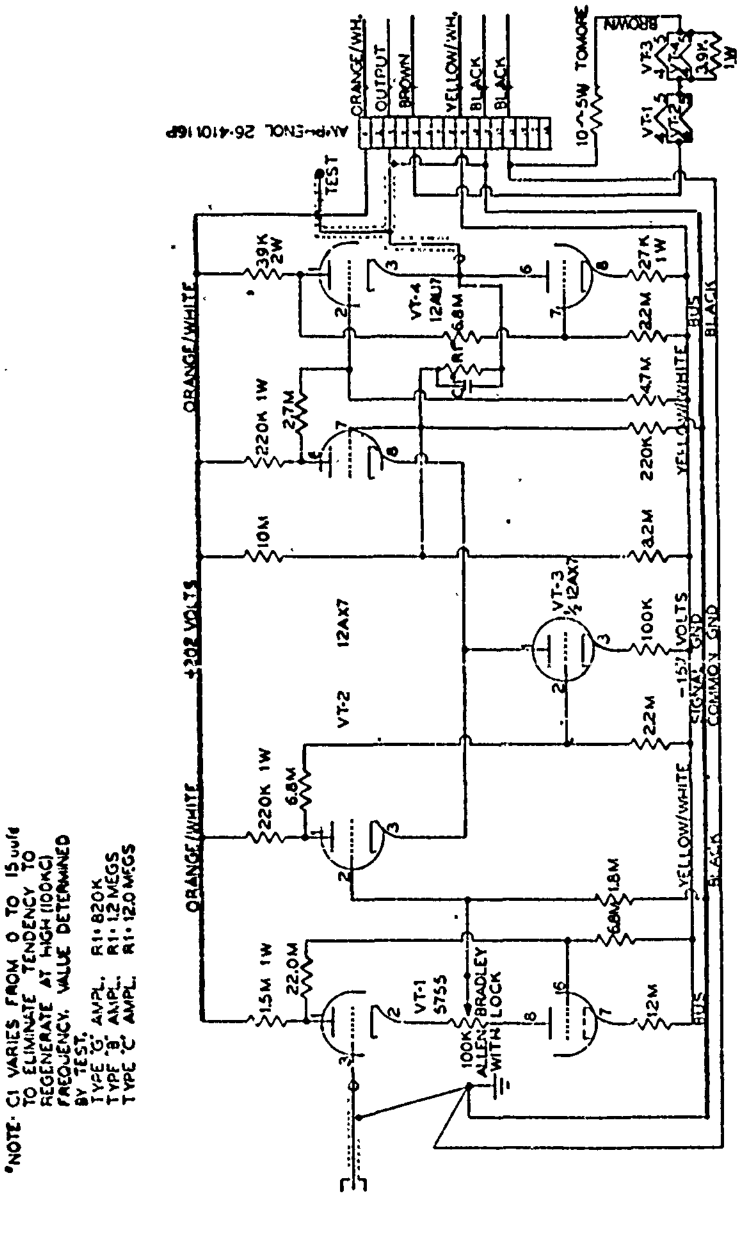

Fig. 6.18—Schematic diagram of the G, B, and C amplifiers.

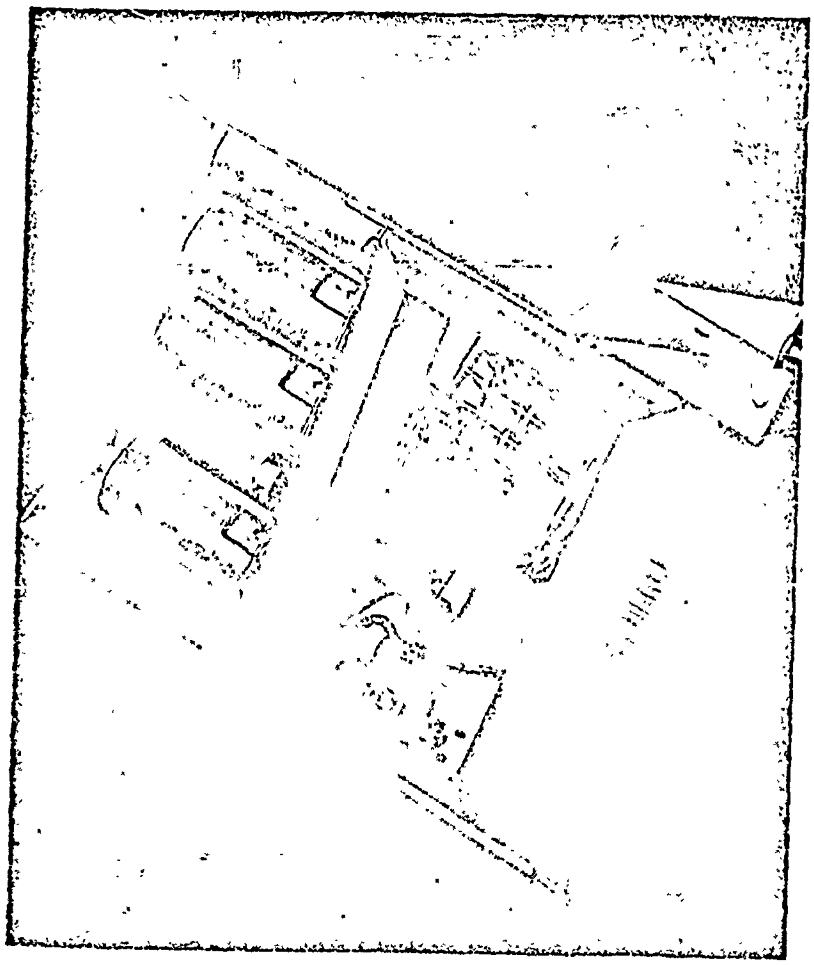

Fig. 6.13—G, B, and C amplifiers.

CONFIDENTIAL

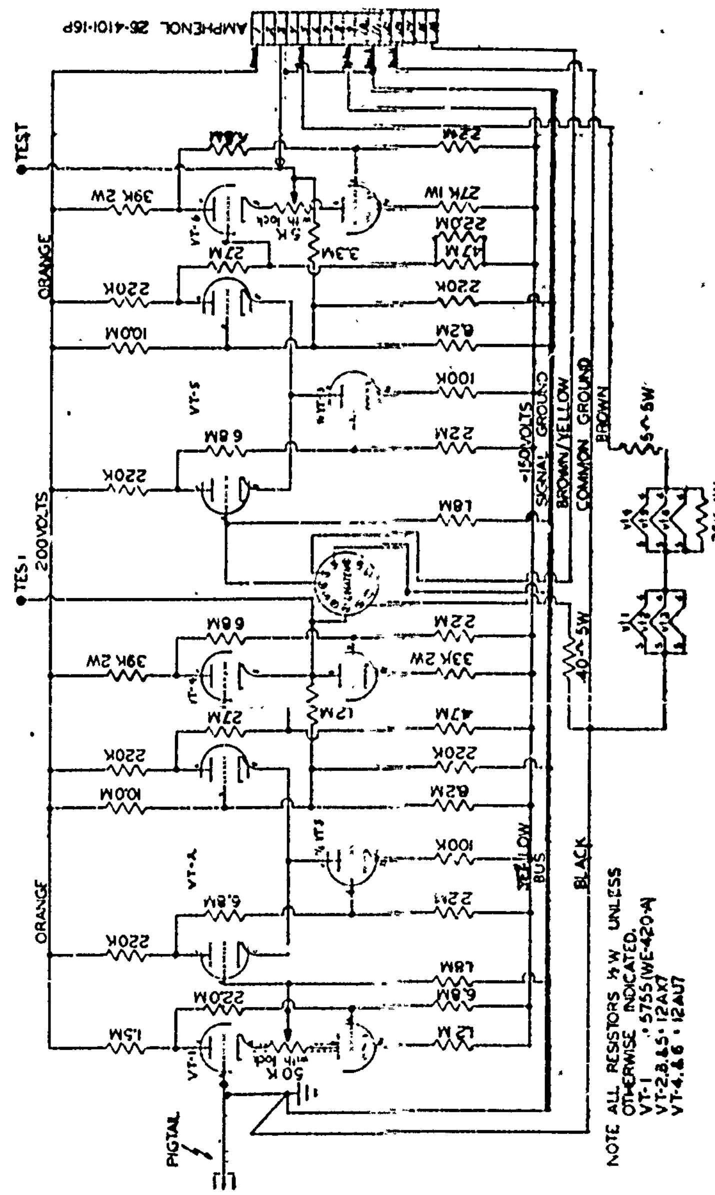

Fig. 6.20—Schematic diagram of the logarithmic amplifier.

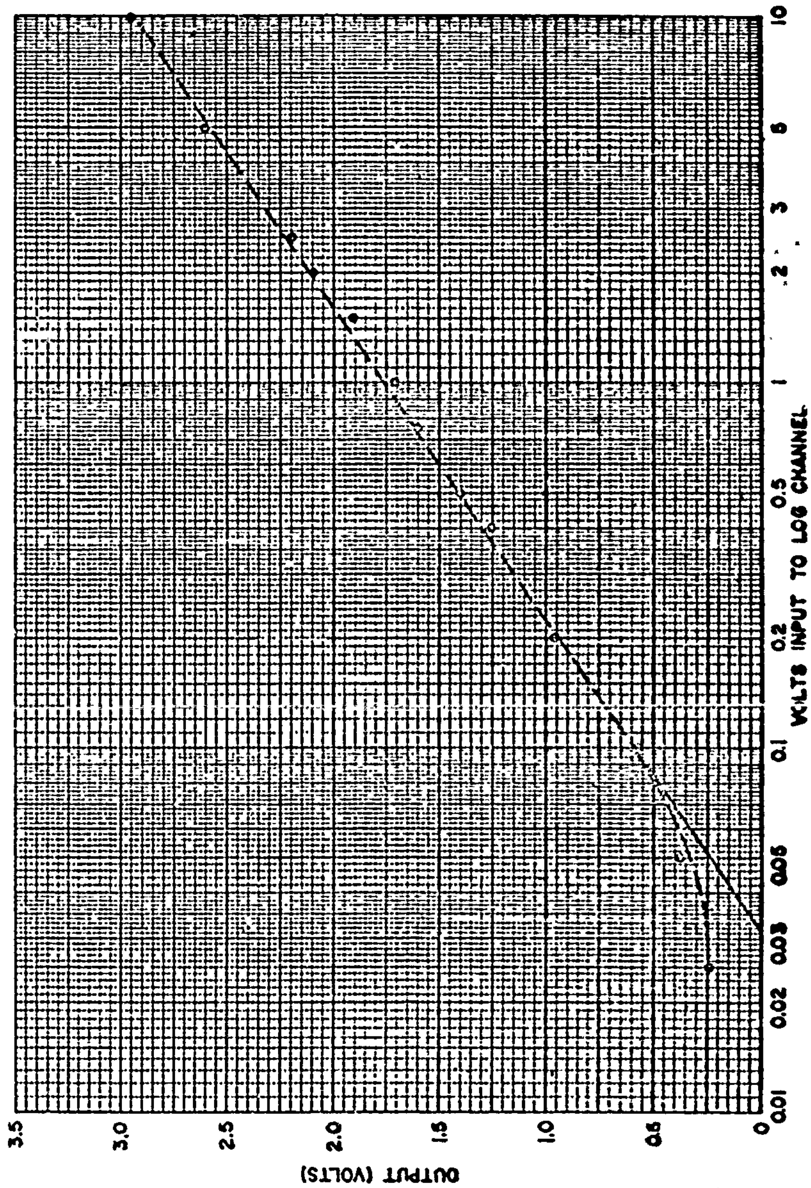

Fig. 6.21 —Gain characteristics of the logarithmic amplifier.

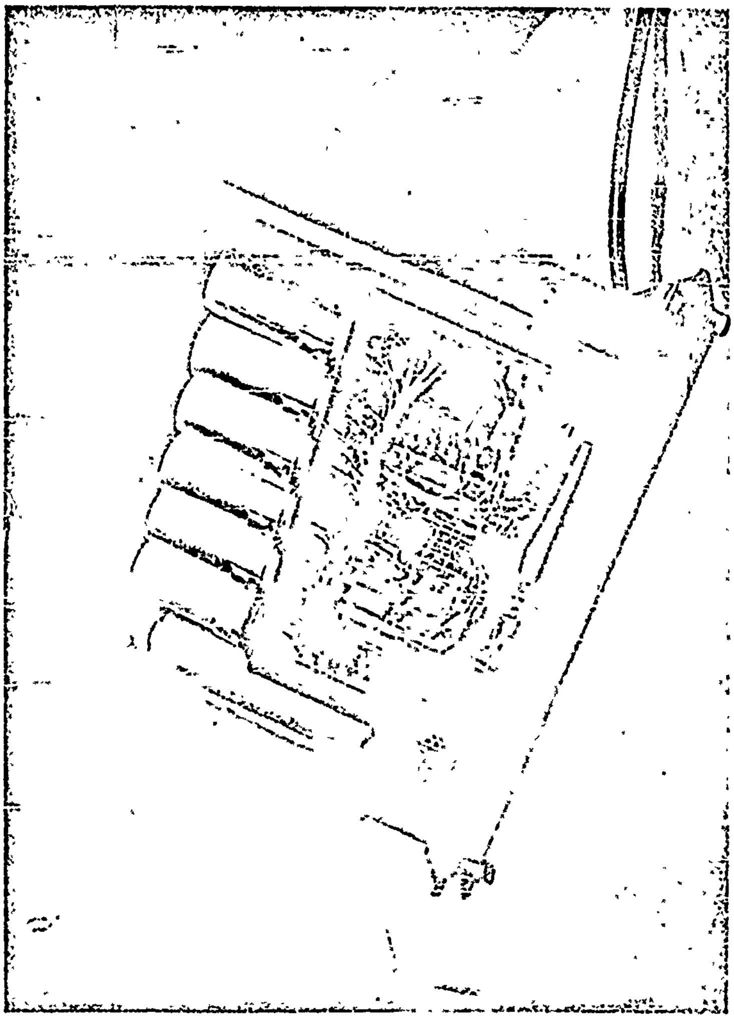

Fig. 6.22—Logarithmic amplifier.

Since the expected data signal was a positive-going voltage and since it was desired to obtain as linear a frequency deviation as possible from the signal, the Davies modulator was biased to operate near one end of its linear curve. Figure 6.23 shows the frequency vs input voltage relation for a typical modulator unit.

After a 15-min warm-up period from a cold start and with a −1.4-volt d-c bias signal at the input (duplicating the data-run conditions), the center frequency of the oscillator was set to 27 kc by adjusting a small trimmer condenser within the unit.

Modulator compensation was used to eliminate an effect known as "drag-out," the rounding off of the leading edge of a sharply rising step function. It is believed that the input capacities of the Davies modulators were responsible for this distortion, and consequently each of the piezoelectric channels was affected to some degree, depending upon the particular modulator used. The compensation consisted of an RC network which acted as the complement of the equivalent modulator input circuit and had to be tailored to the characteristics of each piezoelectric channel.

Laboratory tests showed that the transient response of the modulator, after compensation, was better than 200 μsec and that the over-all frequency drift, after warm-up, was negligible.

The modulator units used with the Ampex recorder were modified slightly to provide increased driving power for the Ampex heads and consisted only of tying together the screen grid and plate of the output tube. A schematic diagram of the Davies modulator is shown in Fig. 6.24, and a picture of the unit is in Fig. 6.25.

6.9 WIANCKO CHANNEL AMPLIFIER

Since the output of the Wiancko gage was already an f-m signal, it needed only a buffer amplifier to raise the signal level to a value high enough to drive the recording heads.

This amplifier was of conventional design and consisted of a dual triode (12AU7); the second half of the tube was connected as a cathode follower. The output of the amplifier was, in the case of the Davies recorders, capacitively coupled to the heads, and transformer coupling was used with the Ampex recorders.

The mechanical design of the amplifier (designated the W amplifier) followed the same pattern of construction as was used with the piezoelectric channel amplifiers.

6.10 CHANNEL ALLOCATIONS

6.10.1 Davies Recorder Systems

The eight Davies recording systems (two each located on the YFNB's 12 and 29 and the LCM's 0-1 and 0-2) were each capable of recording 10 channels of information. Of these 10 channels, only nine were available for recording data; one channel in each system, termed the reference channel, was used exclusively as a check on the tape recording speed (the operation of this will be covered more fully in Sec. 6.13.4). Of the nine channels available for recording data, there were but eight gages monitored—one of the pressure gages fed two amplifiers connected in parallel (refer to the block diagram of the recording system, Fig. 6.1).

6.10.2 Ampex Recorder System

Because there were only seven recording channels available on each of the Ampex tape-transport mechanisms (the Davies recorders each had 10-channel heads), it necessitated the use of three Ampex recorders and consequently the splitting of data among three reels of tape at this station (YFNB-13).

Tables 6.1 to 6.3 are presented to show the relation between the head number, channel number and type, and depth of gage monitored for each recording system. The nominal pressure ranges of the Wiancko gages are also shown.

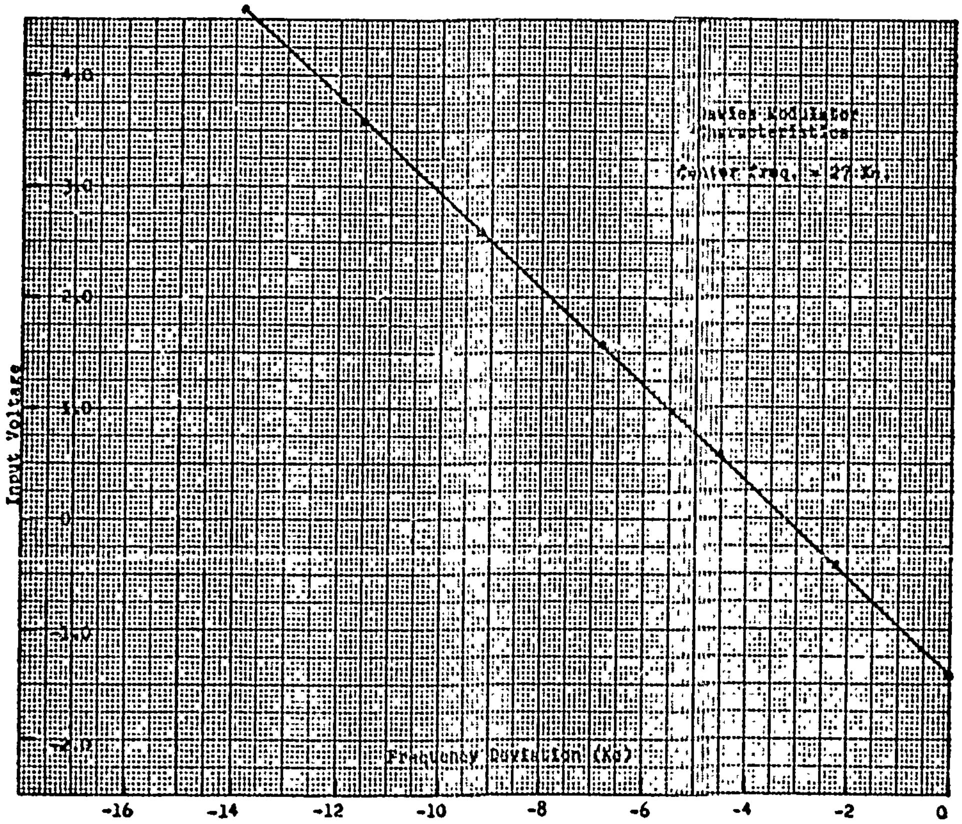

Fig. 6.23—Davies-modulator characteristics.

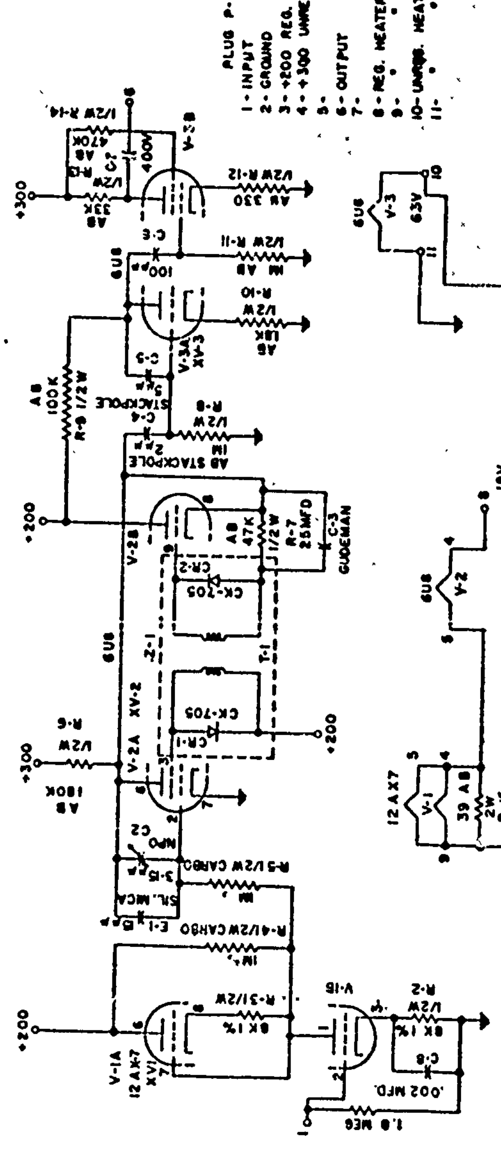

Fig. 6.24—Schematic diagram of the Davies modulator.

Fig. 6.25—Davies-modulator unit.

Table 6.1 —CODE OF GAGE, TAPE, AND RECORDING-HEAD NUMBERS, YFNB-12

Tape E

Head No.	Channel No.	System	Gage No.*	Gage Depth
1	4	E	18206#	200'
2	2	E	1067	25'
3	3	E	1026	50'
4	1**	E	823	200'
5	5-	E	623	1000'
7	7**	E	823	200'
8	8	E	18207#	300'
9	9-	E	623	1000'
10	10	E	18209##	500'

Tape F

Head No.	Channel No.	System	Gage No.*	Gage Depth
1	1**	F	891	25'
2	2	F	1029	100'
3	3	F	1031	200'
4	4	F	18196#	200'
5	5	F	825	500'
7	7**	F	891	25'
8	8	F	893	1000'
9	9	F	18212##	500'
10	10	F	18213##	1000'

* Gage numbers larger than 10,000 indicate Wiancko Gages

** Data channels No. 1 and 7 have a common sensing unit but different amplifiers.

\- Data channels No. 5 and 9 have a common sensing unit but different amplifiers.

\# Gage Range 1000 psi

\#\# Gage Range 1500 psi

Table 6.2—CODE OF GAGE, TAPE, AND RECORDING-HEAD NUMBERS, YFNB-29

Tape G

Head No.	Channel No.	System	Gage No.*	Gage Depth
1	1**	G	821	200'
2	2	G	17159#	100'
3	3	G	17161#	200'
4	4	G	1034	25'
5	5	G	902	500'
7	7**	G	821	200'
8	8	G	1066	1000'
9	9	G	18195##	300'
10	10	G	18200##	1000'

Tape H

Head No.	Channel No.	System	Gage No.*	Gage Depth
1	1**	H	817	25'
2	2	H	17160#	200'
3	3	H	18194##	500'
4	4	H	1036	50'
5	5	H	1035	200'
7	7**	H	817	25'
8	8	H	896	1000'
9	9	H	18198##	500'
10	10	H	18205##	1000'

* Gage numbers larger than 10,000 indicate Wiancko gages.
** Data channels No. 1 and 7 have a common sensing unit but different amplifiers.
\# Gage Range 750 psi
\#\# Gage Range 1000 psi

Table 6.3—CODE OF GAGE, TAPE, AND RECORDING-HEAD NUMBERS, YFNB-13

Tape I					Tape J					Tape K				
Head No.	Channel No.	System	Gage No*	Gage Depth	Head No.	Channel No.	System	Gage No*	Gage Depth	Head No.	Channel No.	System	Gage No*	Gage Depth
1	1**	I	1064	25'	1	1	J	1065	200'	1	8**	I	1064	25'
2	2	I	18192#	100'	2	2	J	1	500'	2	9	I	1033	200'
4	3	I	18199#	200'	4	3	J	811	1000'	4	8-	J	1085	200'
5	4	I	18214##	1000'	5	4	J	810	50'	5	9	J	815	1000'
6	5	I	1032	25'	6	5	J	18197#	500'	6	10	J	18193#	200'
7	7	I	18202#	500'	7	7	J	18216##	1000'	7	10	I	18204#	300'

* Gage numbers larger than 10,000 indicate Wiancko gages.
** Data channels No. 1 and 8 (System I) have a common sensing unit but different amplifiers.
\- Data channels No. 1 and 8 (System J) have a common sensing unit but different amplifiers.
\# Gage Range 1000 psi
\## Gage Range 1500 psi

CONFIDENTIAL

6.11 POWER SUPPLIES

For ease of treatment, this section is divided into parts covering (1) the primary power sources (the batteries) and (2) the electronic power supplies located within the recording equipment itself.

6.11.1 Nickel-Cadmium Batteries

Both weight and space limitations made the use of standard lead-acid storage cells as well as silver-cadmium cells impractical at the two buoy locations. Instead, nickel-cadmium cells (type B cells purchased from Sonotone, Inc., Elmsford, N. Y.) were chosen because of their many advantages over the other batteries tested. It was thought that some of the more important points in favor of the nickel-cadmium cells were: They were relatively lightweight, they could be stored in either a charged or uncharged state without harming the cells, they were capable of an indefinite number of charge-discharge cycles (in excess of 1000), and they had a nearly constant voltage output up to the time the cells approached the discharged condition. In addition, the energy stored per unit volume was considered to be high in relation to that obtainable from the lead-acid batteries. The dimensions of the nickel-cadmium cell are $1\frac{3}{4}$ by $3\frac{3}{16}$ by 9 in.

Since each cell, when charged, produced 1.24 volts, it was necessary to connect 23 cells in series to obtain the required 28 volts for each of the two recording systems per buoy.

After the reception of the −15-min signal, the total current requirement of each recording system was 25 amp. Since the capacity of each nickel-cadmium cell was 30 amp-hr, it was possible to run three complete operating cycles of the equipment before the batteries had to be recharged. Incidentally, at −15 min a dummy load was substituted for the tape-transport power requirement in the Ampex equipment, and thus there was no over-all change in power requirements at −1 min when the tape transport was energized. There was no need for a dummy-load substitution in the Davies systems.

Complete recharging of the nickel-cadmium batteries could be done in a period of about 45 min by using a carbon-pile regulated generator which had been set to deliver 35 volts. The initial charging current was as high as 50 amp but became less as the back electromotive force of the cells was increased. Section 4.2.4 describes the charging generator used, and Sec. 4.3.3 describes the placement of the batteries in the buoy installations. A picture of a nickel-cadmium cell is shown in Fig. 6.26.

6.11.2 Lead-Acid Batteries

In marked contrast to the buoy installations, there was but minor importance attached to either the volume or weight of the batteries used at the three trailer stations. Consequently, it was decided to use standard Navy type lead-acid batteries (model No. 6V-SBMD-130AH), which were rigidly mounted in iron frames at the forward end of the trailers (Sec. 4.5.1). Their ample capacity, 130 amp-hr, ensured about 14 complete operating cycles before they needed recharging. In practice, however, the batteries were placed on trickle charge (about 10 amp) for several hours (or until the specific gravity of the electrolyte reached 1.230) after every two or three operating cycles of the equipment. A total of 10 batteries were used in each trailer, five for each recording system. To obtain the 28 volts for operation, one cell in each bank of five batteries was left disconnected.

6.11.3 Electronic Power Supplies

Design changes of the Operation Castle amplifiers required a regulated negative voltage supply in addition to just the positive supplies used on Castle. This negative supply was necessary since the amplifiers, employing direct coupling between stages, had to have a low d-c output level (−1.4 volts) to match the input circuit of the f-m oscillators (Sec. 6.8) that followed.

In keeping with the general philosophy of "diversification of component responsibility" used throughout the recording system, each electronic power supply was, circuitwise, subdivided into three independent "units." Two of the units each provided an unregulated supply of +300 volts and a regulated supply of +200 volts. The third unit in each system provided two sources of a regulated supply of −160 volts. If a failure had occurred within the power supply or, more likely, within the recording system itself and had disrupted the normal operation of the power supply, only half of the recording system would have been affected.

The circuit for the positive supplies was, essentially, the same as that used in Castle (Sec. 4.3.3 of the Castle report[1]) with but a few minor changes. The complete schematic diagram of the Wigwam power supply is shown in Fig. 6.27 of this report. Laboratory measurements showed that the regulated supplies had a static output impedance of the order of 0.2 ohm.

Mechanically, the Wigwam power supplies (Fig. 6.28) were completely redesigned to fit within the Davies recorders. Thirty-two 22½-volt Mini-Max batteries, used as voltage references, were wax sealed into a separate can, which was, in turn, fastened into the main power-supply chassis with Spring-Lock connectors. The use of Spring-Lock connectors (Simmons Fastener Corp., Albany, N. Y.) permitted easy removal for inspection or replacement.

Initial operation of the power supplies mounted within the Davies recorders led to a high rate of power-tube failures within the power supplies themselves. This was soon traced to excessive heat and was remedied by installing a small centrifugal blower and vent holes in each of the Davies recorders.

6.12 INTEGRATED SYSTEM

6.12.1 Unitized Construction

The mechanical redesign of the recording equipment used on Castle was undertaken to reduce the over-all size of the equipment and to facilitate its servicing. The new design made extensive use of unitized construction, i.e., as many individual units as possible within the recording equipment were mechanically constructed to have the same outside dimensions. The result was a high degree of interchangeability between the individual units within the equipment and, of course, an increased over-all system flexibility. Reference to the photographs in Figs. 6.17, 6.19, and 6.22, for instance, will show the mechanical similarity between the six types of amplifiers used.

The individual units within the recording system—amplifiers, timers, and fiducial generator—were plugged into a master aluminum panel that had been prewired, and thus the need for interconnecting cables was eliminated. Each unit was securely fastened to the panel by means of Quick Lock connectors (Simmons Fastener Corp., Albany, N. Y.). In addition to eliminating the problem of losing or dropping bolts and nuts into the equipment, which might cause short circuits (considerable time was spent salvaging "lost" bolts on Operation Castle), the units could be unplugged and changed within a few seconds. This type of construction also made it possible to have all the components readily accessible for testing while the equipment was in operation.

The aluminum panel with its associated amplifier and timer units mounted on it was, in turn, bolted to an aluminum framework which supported the tape-transport mechanism. Two such frameworks, each with its complete recording system, were bolted back to back and thus provided a dual recording system for each Davies-recorder station. Figure 6.29 shows the assembled recording system and the placement of the individual components. The Ampex recorders were mounted on a different type of framework due to their heavier weight and different suspension requirements. All the electronic plug-in units were anodized (each type a different color) which served as protection from corrosion as well as an easy means of identification.

6.12.2 Test Equipment

System test sets used for checking the electrical performance of the recording equipment were found to be extremely useful throughout the entire operation. The additional test equipment, designed to fulfill a specific need, was used in conjunction with and to supplement the standard equipment normally used (vacuum-tube voltmeters and oscillators).

Fig. 6.26—Nickel-cadmium cell.

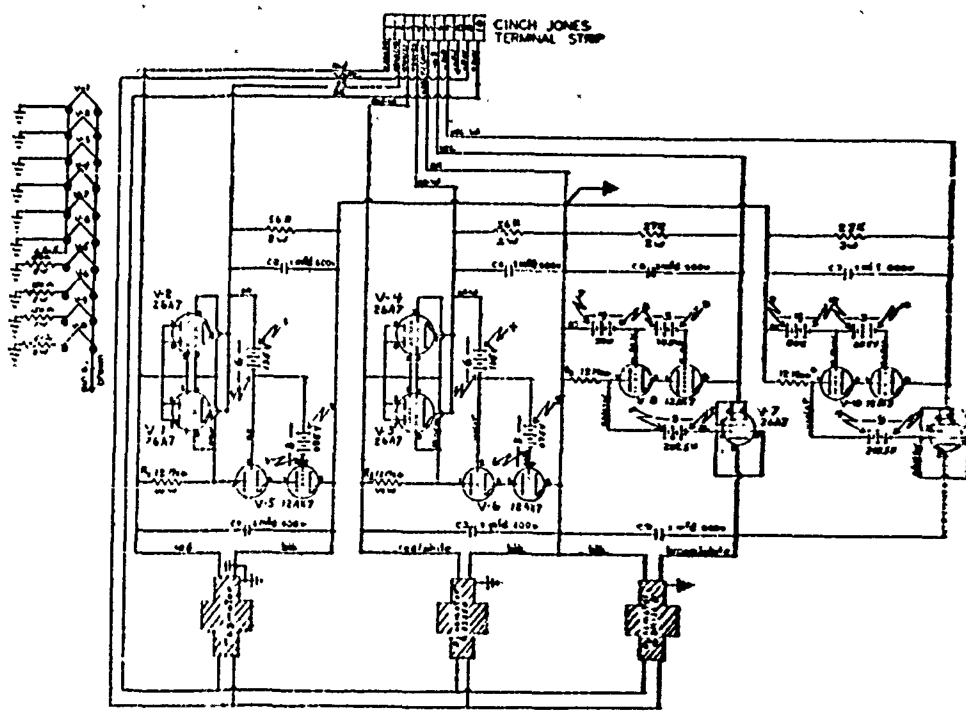

NOTE -Z- INDICATES BATTERY BOX
CONNECTOR-CANNON NO DA-15P

Fig. 6.27—Schematic diagram of the power supply.

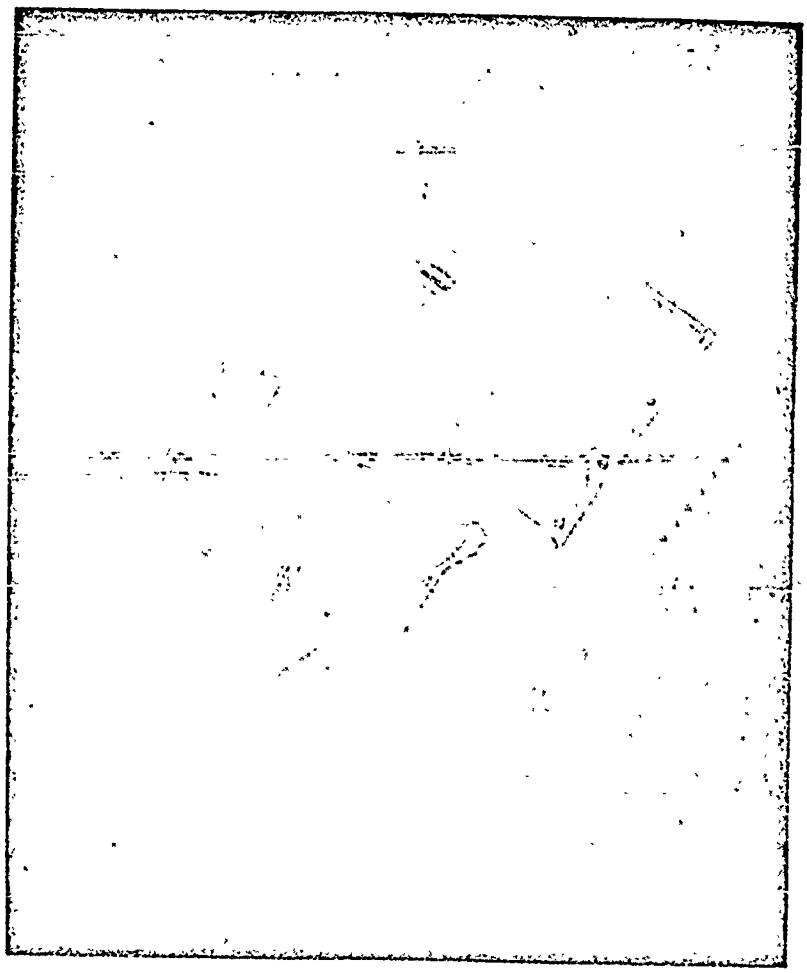

Fig. 6.28—Electronic power supply.

CONFIDENTIAL

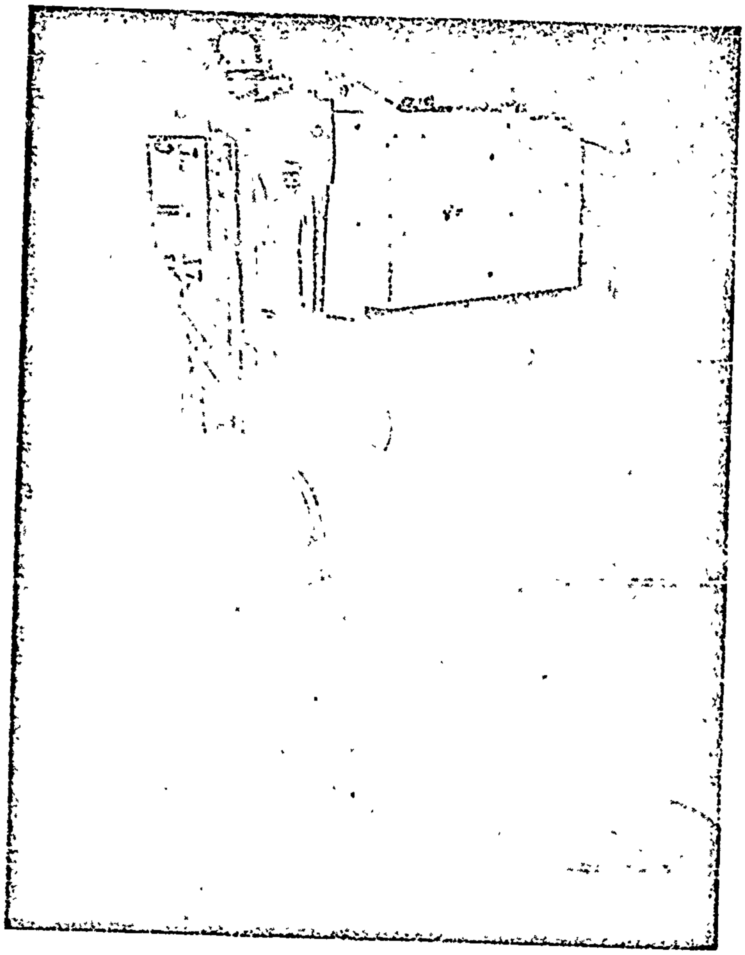

Fig. 6.29—Assembled Davies recording system.

SECRET—RESTRICTED DATA

CONFIDENTIAL

The most versatile of the units was the test box, which by means of switches controlled any or all of the functions normally performed by the two-out-of-three box, the sequence timer, and the calibration-voltage generator. For instance, by the proper selection of the switches within the test box, each of the voltages produced by the calibration-voltage generator could be "called for" and measured. The test box was also capable of simulating a zero-time fiducial signal for purposes of testing. All these functions could be performed by inserting just one multiconnector cable into a test connector plug mounted on the frame of each recording system and another smaller cable into the two-out-of-three box.

In addition to the test box, there was a power-supply tester, which provided a quick check on the operation of the electronic power supplies. By simply pushing buttons, one was able to simulate the no-load and full-load conditions imposed upon the power supply by the recording equipment and, at the same time, to check the change in output voltages produced by these different load conditions. This measurement indicated how well the power supply was regulating. Provisions were also made for checking each of the eight reference voltages supplied by the dry cells sealed into the reference-voltage box.

Two other pieces of specialized test equipment, the recording-head monitor switch and the amplifier output-level checker, were designed to simplify checking of the recording equipment. The recording-head monitor switch enabled one to quickly "tap" into any of the recording heads in the system and monitor the head current (by measuring the voltage across a small resistor placed in series with the head). The amplifier output-level checker, on the other hand, provided an easy way of determining when the d-c output level of the amplifiers (−1.4 volts) was properly set. It essentially provided a −1.4-volt bucking voltage and indicated, by a null detector, when the amplifier output was equal to its internal voltage, thus providing an infinite-impedance-measuring device.

Pictures of the four pieces of test equipment are shown in Fig. 6.30.

6.13 PLAYBACK SYSTEM

The Wigwam playback system was, in many respects, similar to that used on Castle. There were, however, a few important differences; these will be discussed in the sections that follow.

6.13.1 Davies System

The main difference between the playback system used on Castle and that of Wigwam was the addition of two new Davies type discriminators and the use to which the old Castle discriminators were put. The old discriminator originally used for the data channel in Castle was, in Wigwam, used for the fiducial (timing) channel, and the other Castle discriminator (originally used for both the reference and servo channels) was used only for the servo channel. The two new discriminators purchased for Wigwam were used for the data and reference channels, respectively. Timing on Castle was put on during the playback and required no discriminator.

As was the case in Castle, the playback speed was reduced by a factor of 10 to 1 (to 3 in./sec) because of the limited high-frequency response (around 600 cycles) of the Century string oscillograph.

6.13.2 Ampex System

On Castle, electronic compensation was not used with the Ampex recorders to reduce the effects of recording-tape speed variations. It was, however, used on Wigwam and reduced the noise from tape flutter by about a factor of 5. In addition, the use of electronic compensation served to make the data amplitude independent of the capstan drive speed. Since the Ampex heads are not all in the same line (as are the Davies heads), the amount of compensation possible varied from head to head and depended upon the relative position of the data head with respect to the one used for the reference channel (head No. 3).

Electrically, the techniques used for playing back data from the Ampex recorders were the same as those used with the Davies recorders.

CONFIDENTIAL

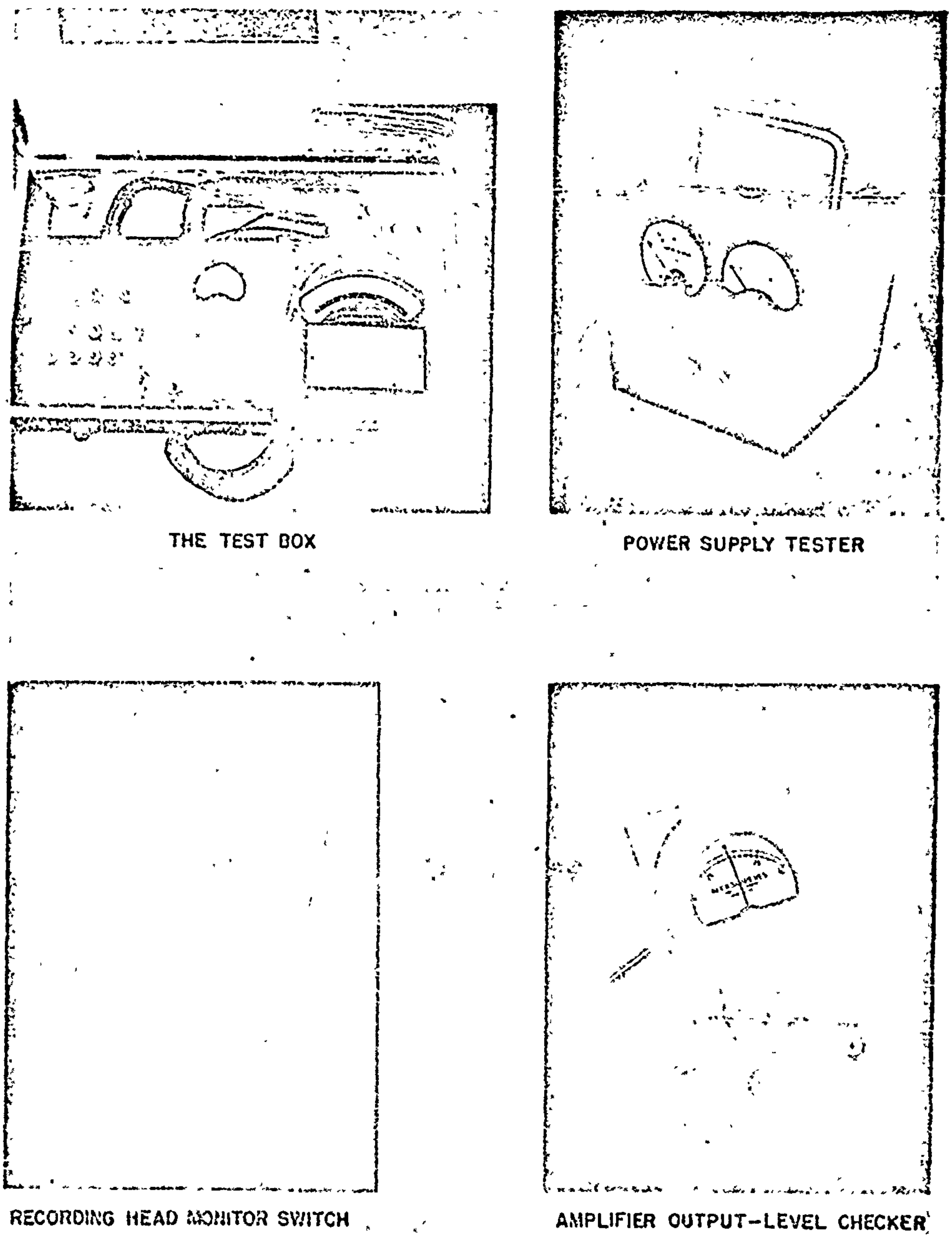

Fig. 6.30--Wigwam test equipment.

SECRET - RES ICTED DATA

CONFIDENTIAL

6.13.3 Timing

The amplitude-modulated output of the 2000-cycle timing oscillator (Secs. 6.6.2 and 6.6.3) was superimposed on the frequency-modulated carrier of a Wiancko channel at the time the data were recorded. Later, during playback, the two frequencies were separated by the use of a 500-cycle low-pass filter. The timing signal was then amplified and fed directly to the Century string oscillograph, the end recording instrument; however, since the playback speed was $\frac{1}{10}$ the recording speed, the frequency of the timing oscillator, when played back, was only 200 cycles.

6.13.4 Reference Oscillator

In addition to the tuning-fork and L-C oscillators mentioned in Secs. 6.6.2 and 6.6.3, there was a crystal oscillator which can, in a broad sense, be considered as a part of the over-all timing system. Its function was to supply a standard frequency (33.3 kc) and was recorded on what was termed the "reference channel" of each recording system throughout its complete operating cycle. Later, during playback, this recorded frequency of the crystal oscillator was compared with another standard, and any deviations from the original frequency were interpreted as a shift in tape speed. The error voltage thus produced by the frequency deviation of the reference channel contained only the "noise" component (produced by both low- and high-frequency tape-speed variations) of the recorded data signal. The high-frequency noise as obtained from the reference channel was shifted 180° and then added electronically to the signal, thus canceling the high-frequency component of the noise voltages. This produced an over-all improvement in signal-to-noise ratio of about 5 to 1.

Long-term tape-speed drift was compensated for by using a separate discriminator and feeding just the low-frequency components of the noise voltage to an electromechanical servo system which, in turn, changed the playback speed to match that of the original recording.

The compensation system as used on Castle and that of Wigwam were essentially the same electrically. However, in Wigwam an additional discriminator was used for the servo link. The difference is shown in Fig. 6.31.

The principle of the playback system is discussed more fully in Appendix A of the Castle report.[1]

6.13.5 Cross Talk

Signal interference between adjacent channels proved to be much more serious in Wigwam than in Castle, even though identical recording heads were used because of the low signal level recorded on Castle. In some cases the recorded signal from an adjacent channel was actually stronger than that produced by the directly recorded signal and was a function of both the recording frequencies and their amplitudes. Laboratory tests later showed that some heads were driven to as much as two and three times saturation, although this was not considered to be the prime cause of the cross talk.

In all cases, however, the interfering signals were attenuated by employing selective filters.

6.13.6 Record Reproduction

Preliminary data records were reproduced on a cathode-ray oscilloscope and a Sanborn recorder as a check on over-all amplifier gain and record running times. The Sanborn pen movement was capable of reproducing signals of up to only 50 cycles and thus indicated only the general character of the recorded signals.

The final records were reproduced on a model 408-X Century string oscilloscope using only four of the recording strings. The records, produced on 8-in. high-contrast paper, had the fiducial and $\frac{1}{2}$-sec radio time signals recorded on a channel near the top edge of the paper, the data record near the center, and the coded timing signal (scaler output) near the bottom edge. The fourth channel was left unenergized and served only to produce a reference base line from which amplitude measurements were made. An attenuator panel was inserted between

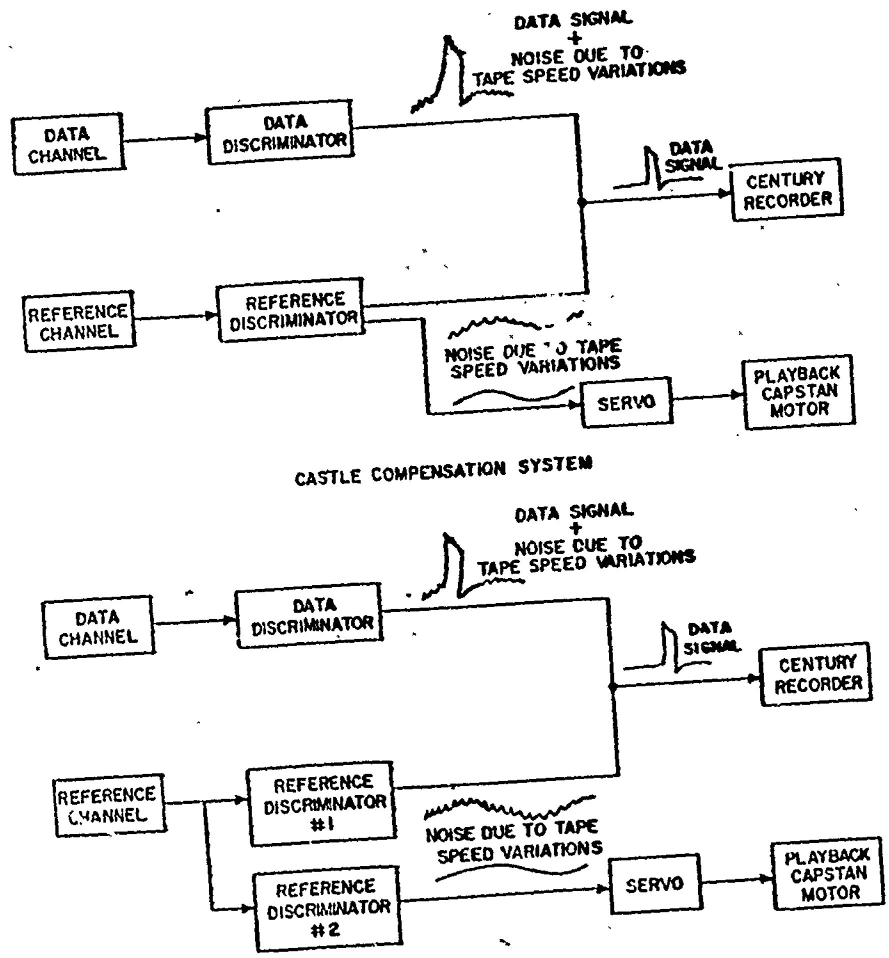

Fig. 6.31—Castle and Wigwam compensation systems.

the string galvanometers and their respective driving sources to provide a means of matching impedances and controlling signal amplitudes.

Paper speeds varied from ¾ to 12 in./sec, depending upon the degree of resolution desired. Records that contained bubble-pulse data were run from zero time up to as much as +100 sec to ensure the inclusion of this information on the final record.

A block diagram of the playback system is given in Fig. 6.32.

6.14 SYSTEM ACCURACY

As was true in the Castle test, the major factor affecting the over-all system accuracy was the signal-to-noise ratio. Other factors contributing to inaccuracies were the amplifier gain drift, circuit nonlinearities, and calibration inaccuracies. In Wigwam, however, these last factors were small and considered to be negligible in respect to the noise figures.

6.14.1 Piezoelectric Linear Channels

Measured values of noise appearing on the linear amplifier channels seemed to fall within 2 to 4 per cent of the peak values of the pressures measured for the initial shock wave. This value of noise was by no means constant and varied quite widely from even one part to another of a particular record. In general, the records obtained from the Ampex recorders had less noise than those from the Davies recorders; this was due, for the most part, to the inherently lower flutter components of the Ampex system.

The use of d-c coupling throughout the amplifiers (except for the input circuit) reduced errors arising from the fact that the RC time constant of the system was not infinite. These errors were found to be quite small—of the order of ½ per cent at most.

In general, the over-all accuracy from the linear amplifier channels of the Davies recorders was probably within 4 per cent, and those obtained from the Ampex were, because of the lower values of tape flutter, no doubt better than this.

6.14.2 Piezoelectric Logarithmic Channels

Nearly all the reduced data were obtained from either the linear amplifier or Wiancko channels since the desired data fell within one or more of the ranges covered by these channels. Consequently, there were but few figures available for logarithmic channel accuracy comparisons.

It may be said, however, that high accuracy was not a prime requirement in the use of the logarithmic channels. Their only purposes were to serve as a backup for the other channels and as protection against large prediction errors. Gain drift, alone, in the Logatens would prevent measurements being made to an accuracy of better than about 10 per cent of full scale.

6.14.3 Wiancko Channels

Noise measurements on the Wiancko channels showed a greater background hash than the linear amplifier channels. This can be accounted for by the fact that the linear range of the Wiancko oscillators was reduced by the static pressure of the water to which they were subjected. The upper limit of this noise was, in general, around 6 per cent of the peak pressures of the initial shock wave. Here, again, there were wide variations from point to point within a given record. However, the over-all accuracy of the Wiancko channels was probably only a little less than that of the piezoelectric linear amplifier channels since there were several sources of inaccuracies in the latter (amplifiers and RC time constants) which were not applicable to the Wiancko channels.

6.14.4 Summary of System Accuracy and Errors

A summary of the various sources of errors for the two recording systems used (Ampex and Davies) and their various channels (linear, logarithmic, and Wiancko) is given in Table 6.4.

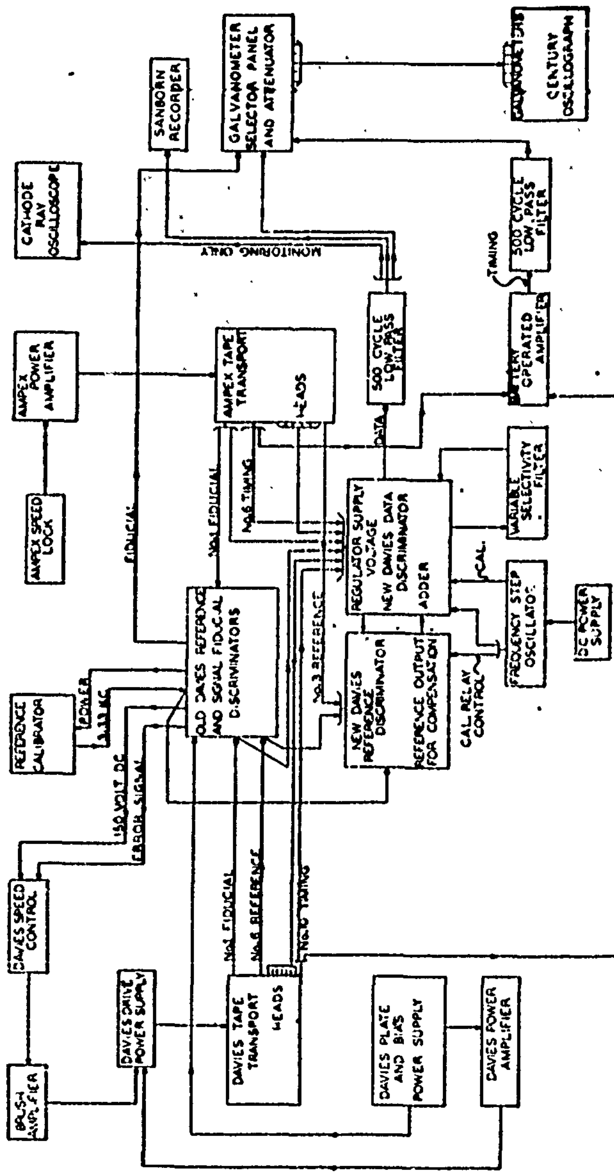

Fig. 6.32—Playback system.

Table 6.4—SUMMARY OF INSTRUMENTATION AND READING ERRORS

Recorder	Gage	Type System	Percentages* Errors from Sig.-to-Noise	Calib. Errors	Errors from non-linearities	Drift Errors	Total Error***
Davies	PE	Linear	4 1/2	1	--	--	4 1/2
	PE	Logarithmic	4**	2	4	10	12
	Wiancko	--	6	2	--	--	6 1/2
Ampex	PE	Linear	3 1/2	1	--	--	3 1/2
	PE	Logarithmic	4**	2	4	10	12
	Wiancko	--	5 1/2	2	--	--	6

* To nearest 1/2 per cent of full scale error.

** Noise measured on high-gain (linear) part of logarithmic curve and compared to peak pressures falling on low-gain part of curve.

*** Square root of the sum of the Squared Errors.

Although some of the information concerning the percentage errors is based on data taken in the laboratory, it must be emphasized that the remainder is based only on the best estimates which can be obtained from the design characteristics of the recording and playback equipment.

In cases where an error is considered to be small compared to the other entries for the same system, it has been omitted.

The table shows that, in general, the Ampex system is a little better than the Davies system (because of the lower noise components due to reduced tape flutter) and that the piezoelectric linear channels are slightly superior to the others. The logarithmic channels are the least accurate.

6.15 CONCLUSIONS AND RECOMMENDATIONS

Electronically, operation of the equipment on Wigwam proved to be a successful undertaking. There were a few instances, though, in which experience with the operation of the recording equipment and its construction would dictate some changes. These are listed below for reference purposes:

1. Calibration-voltage generator: It is suggested that a ground or zero voltage be interposed between each of the calibration steps. Such a calibration sequence would offer two advantages over the present system, namely, (1) eliminate the cumulative effect of a positive (or negative) charge on the input circuit with the consequent introduction of the RC time-constant error at this point and (2) facilitate in some cases the determination of the calibration step being read during the final data analysis. Unfortunately, unless other changes were made, the introduction of a ground between each calibration step would halve the number of available steps and possibly introduce a larger source of error in the data analysis.

2. Timing system:

a. The proven accuracy of the L-C timing oscillator (Sec. 6.6.2) militates against the use of a tuning-fork oscillator in all but data-recording systems having a great many channels.

b. The use of the scaler (Sec. 6.6.3) has shown the need for extensive redesign to increase both its reliability and type of coding to facilitate reading of the finished records.

3. Amplifiers:

a. In Wigwam as in Castle, drift of the logarithmic amplifier gain proved to be excessive. This can probably be reduced by allowing even a longer warm-up time than the 45 min used in Wigwam, but it is doubtful if it would be a practical solution. The substitution of more linear amplifiers covering an over-all greater dynamic range may prove to be more feasible.

b. A better design (or closer quality control) of the oscillators in the Wiancko gages would permit the recording heads to be driven directly by the output of the gage oscillator and eliminate the need for the buffer amplifier used on Wigwam.

4. Unitized construction: It is felt that when a large number of similar items (over 20) are to be built, considerable time and expense can be saved through the use of unitized construction. The equipment for Wigwam was a major step in this direction. However, even better uniformity of construction and ease of servicing can be achieved through the use of printed circuitry. A good deal of time was spent circuit tracing the Wigwam equipment to find initial wiring errors.

5. Playback system: The playback system, at best, was found to be cumbersome and inflexible. The system required rather extensive changes whenever it was desired to change the basic type of record being reproduced, i.e., from a Davies recorder to an Ampex recorder or from a piezoelectric gage record to a Wiancko gage record. Time did not permit the installation of switches to facilitate these changes and so connections had to be laboriously changed by hand each time, with the added possibility of making mistakes.

Newer recording systems are being developed which will materially increase the over-all accuracy and frequency response of the entire recording and playback system, necessitating the complete redesign of the playback system.

REFERENCE

1. C. J. Aronson, E. J. Culling, and J. P. Slifko, Underwater Pressure Measurements, Operation Castle Project 1.4 Report, WT-908 (NOL portion), NOLR-1209, October 1955.

CHAPTER 7

LOCATION OF GAGES

7.1 GENERAL APPROACH TO PROBLEM

To interpret the data obtained at various recording stations, it was necessary to know the distance of the station or gage from the explosive charge. Since the array was considerably distorted by wind and waves and the rate of tow was low, the distances could not be estimated with sufficient accuracy from the amount of tow cable between stations, the lengths of the barges, and measurements on deck. To circumvent this unexpected gap in the data, several indirect methods were used to determine the radial distances from the YC-473 and, as required, the relations of one vessel to another.

Probably the most accurate, most convenient, and most comprehensive information could have been obtained from an aerial mosaic made at the time of the explosion. However, such a mosaic was not available, although mosaics were made 30, 40, and 50 min before the shot. Photographs of parts of the array were made at zero time by cameras located on the YFNB-13 and YFNB-29. Accurate data on the time of arrival of the shock wave at certain positions in the array were available. From the latter two sources it was possible to reconstruct the configuration of the major elements of the array, using the time of arrival to determine their distance from SZ and using the photographs to determine their angular relations. A check on the distances between YFNB's was also made by measuring the height of their masts in the photographs. The calculated general configuration of the array at shot time was checked against the available mosaics and wire tow-cable lengths to be sure there were no impossible arrangements of elements. The calculated configuration is possible and is reasonably consistent with all data available to Project 1.2.

7.2 PROCEDURE USED

The primary method of shock-arrival ranging was based on the following information and assumptions:

1. The sound velocity vs depth information, Table 7.1, calculated from information supplied by the Scripps Institution of Oceanography (see reference 1).
2. Depth of charge, 2000 ft (see reference 2).
3. Time from zero fiducial mark until explosion, 13 msec (see discussion below).
4. Time vs distance data for the shock wave up to 1975 ft from the charge (see the preliminary version of reference 3 and also see reference 4).
5. Excess of shock velocity over acoustic velocity in accordance with reference 5.
6. Arrival time of shock wave at the gages of Projects 1.2 (see Chap. 8) and 1.3 at certain nominal depths.

Table 7.1—DEPTH VS SOUND VELOCITY COMPUTED FROM SCRIPPS INSTITUTION OF OCEANOGRAPHY LETTER OF OCT. 25, 1955, TO NOL

Depth (ft)	Velocity (ft/sec)	Depth (ft)	Velocity (ft/sec)
0	4942.2	1010	4969.7
49.2	4943.2	1332	4855.6
98.4	4946.8	1660	4854.9
147.6	4946.4	1992	4851.9
196.9	4948.4	2615	4852.3
246.1	4948.4	3245	4856.2
295.3	4947.7	3908	4860.1
344.5	4947.7	4871	4869.7
377.3	4948.4	6473	4889.3
426.5	4951.0	8275	4917.9
541.4	4921.2	10105	4948.4
669	4904.8	11963	4980.2
833	4883.4	13839	5014.0

7. The assumption that the bending of the shock-wave path by the hydrographic structure introduced negligible changes in the distances traveled by the shock wave from those of straight ray paths out through the region in which the NOL electronic pressure-time gages were located.

The first operation was to determine the location of the shock front during its first 370 msec of travel. Porzel (preliminary version of reference 3) reported the time of arrival relative to an electromagnetic disturbance (presumably the detonation) at distances from the charge from 14 to 1226 ft. Cunningham[4] reported the arrival time relative to the EG&G fiducial mark at nominal distances 800 to 1975 ft from the charge. Although the two sets of instrumentation providing these data were not on a common support cable, they were probably close enough together that their arrival time vs distance curve should be reasonably smooth. In plotting the two sets of data together (Fig. 7.1), it was found that to obtain a smooth curve it was necessary to assume that the fiducial mark occurred 13 ± 1 msec before the explosion. A detailed discussion of the reasoning is given in Sec. 5.1 of reference 4.

The next step was to compute the shock-wave velocity in all regions of interest so that the position of the shock wave at various times could be calculated. Figure 7.2 is a replotting of the data of reference 5 to a suitable scale for the range of pressures to be found in these regions. From Fig. 7.2 and the expected (or measured) shock-wave decay with distance, Fig. 7.3 was constructed.

In Fig. 7.3 the distance from 1000 to 13,000 ft from the charge was divided into 16 regions (Table 7.2), in each of which the extra velocity due to shock pressure decreased by 0.2 per cent. The hydrographic data on sound velocity, Table 7.1, were plotted (Fig. 7.4), and average velocities in eight zones of depth were determined. A large graph was made showing the arrangement of zones of depth and regions of distances from the charge. The shock-wave velocity in each zone-region was then computed and tabulated (Table 7.2). Appropriate rays were drawn on the large graph, and the position of the shock wave after each 0.1 sec was calculated (Table 7.3). A section of the large graph is reproduced in Fig. 7.5 to show the method of use.

A large chart of the array was then prepared, showing the positions of certain elements at various times as determined from the aerial mosaics. The location of the YFNB-29 was measured and plotted for the times −50, −40, and −30 min. From the sonic ranging calculations an arc was plotted representing the possible positions of the NOL gage string on the YFNB-29 at zero time. The heading of the YFNB-29 was determined from photographs taken from its stern by a camera which had its optical axis aligned parallel to the center line of the barge. Since a line from the cameras on the YFNB-29 to the YC-473 was not necessarily colinear with the basic grid line of the aerial mosaics, a position was selected for the YFNB-29 consistent with locations shown in the mosaics but with a distance determined by shock-wave ranging and a heading determined by surface photographs. The exact orientation of the photomosaic grid was not known to Project 1.2. The grid was merely convenient for comparing the relative motions of the barges during the hour preceding shot time. Project 1.5 (reference 7) has determined the actual bearing of the YFNB-29 from the YC-473 to be about 003°T, but this does not affect the relations calculated in this chapter.

By the use of angles determined from the YFNB-29 photographs and of distances determined from sonic ranging, the positions of the YFNB's 13 and 12 were plotted. The angles obtained from photographs of the YFNB's 29 and 13 and the shock-wave arrival times at the stern of the SQUAWs then determined the rough locations of pontoons, SQUAW-29, and the LCM's. The headings of the YFNB's 12 and 13 were checked by angles from the YFNB-29 and arrival times at the NEL and NOL electronic gage strings.

7.3 POSITIONS OF ARRAY ELEMENTS

Figure 7.6 shows the estimated positions of the YFNB's 12, 13, and 29 at various times as shown in the chart of the array. The shifts of position indicate that the elements of the array were moving relative to one another and that perhaps the whole instrumentation end of

(Text continues on page 163.)

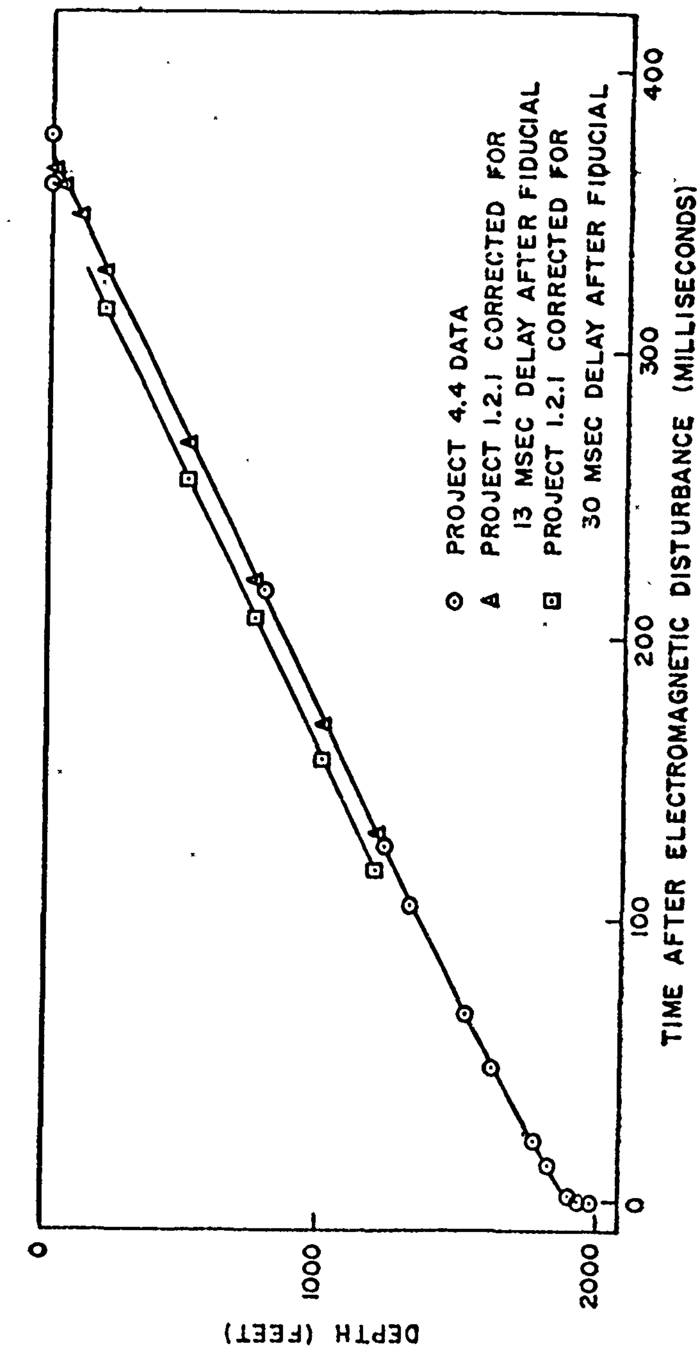

Fig. 7.1—Time of arrival of shock wave, 2000- to 0-ft depth.

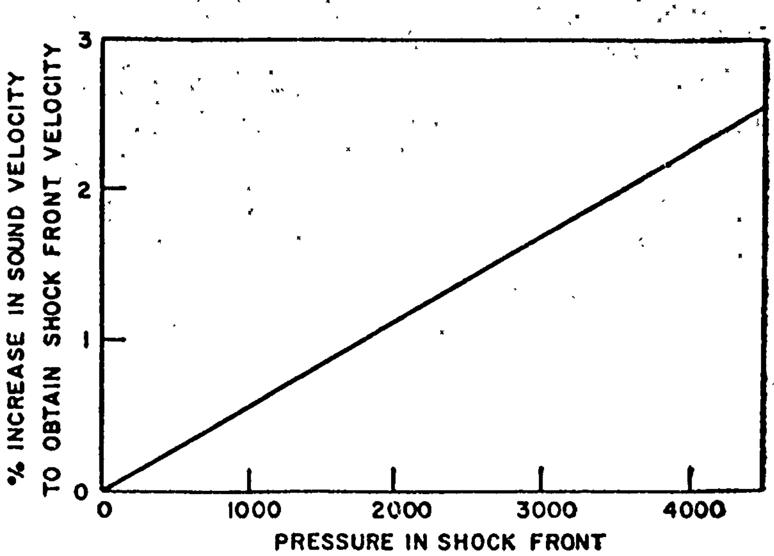

Fig. 7.2—Pressure vs increase in sound velocity due to shock pressure.

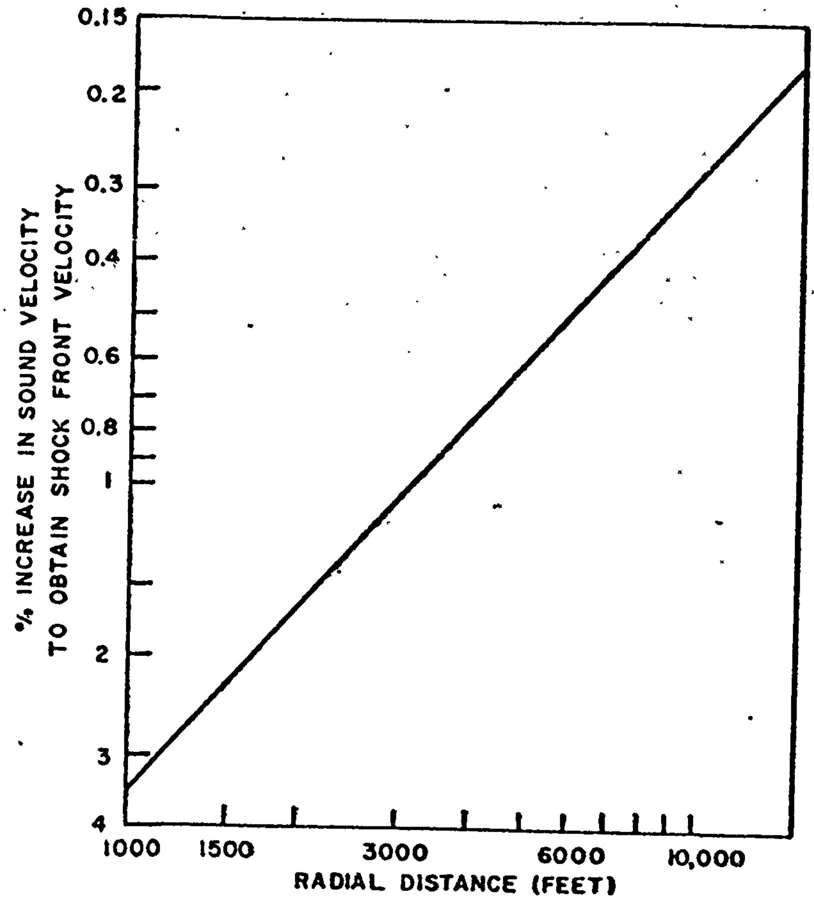

Fig. 7.3—Radial distance vs increase in sound velocity to obtain shock-front velocity.

CONFIDENTIAL

Table 7.2—SHOCK-WAVE VELOCITIES BY DISTANCE (REGION) AND DEPTH (ZONE)*

	Radial Distance from	Radial Distance to	% of Sound Velocity	Zone or Depth 2000	A	B	C	D	E	F	G	H
Mean Sound Velocity				4852	4855	4864	4878	4893	4909	4925	4944	4947
Depth			from to		2000 1300	1300 1000	1000 800	800 700	700 600	600 500	500 400	400 0
Region												
1	1030	1100	103.3	5012	5015	5025	5039					
2	1100	1160	103.1	5002	5006	5015	5029					
3	1160	1230	102.9	4993	4996	5005	5019	5035				
4	1230	1320	102.7	4983	4986	4995	5010	5925	5042			
5	1320	1420	102.5	4973	4976	4986	5000	5015	5032	5048		
6	1420	1530	102.3	4964	4967	4976	4990	5006	5022	5038	5058	5061
7	1530	1690	102.1	4954	4957	4966	4980	4996	5012	5028	5048	5051
8	1690	1860	101.9	4944	4947	4956	4970	4986	5002	5019	5038	5041
9	1860	2060	101.7	4934	4938	4947	4961	4976	4992	5009	5028	5031
10	2060	2320	101.5	4925	4928	4937	4951	4966	4983	4999	5018	5021
11	2320	2680	101.3	4915	4918	4927	4941	4957	4973	4989	5008	5011
12	2680	3120	101.1	4905	4908	4918	4932	4947	4963	4979	4998	5001
13	3120	3850	100.9	4896	4899	4908	4922	4937	4953	4969	4988	4992
14	3850	5000	100.7	4886	4889	4898	4912	4927	4943	4959	4979	4982
15	5000	7100	100.5	4876	4879	4888	4902	4917	4934	4950	4969	4972
16	7100	13000	100.3	4867	4870	4879	4893	4908	4924	4940	4959	4962

* All velocities in feet per second -- all distances in feet

SECRET – RESTRICTED DATA

CONFIDENTIAL

CONFIDENTIAL

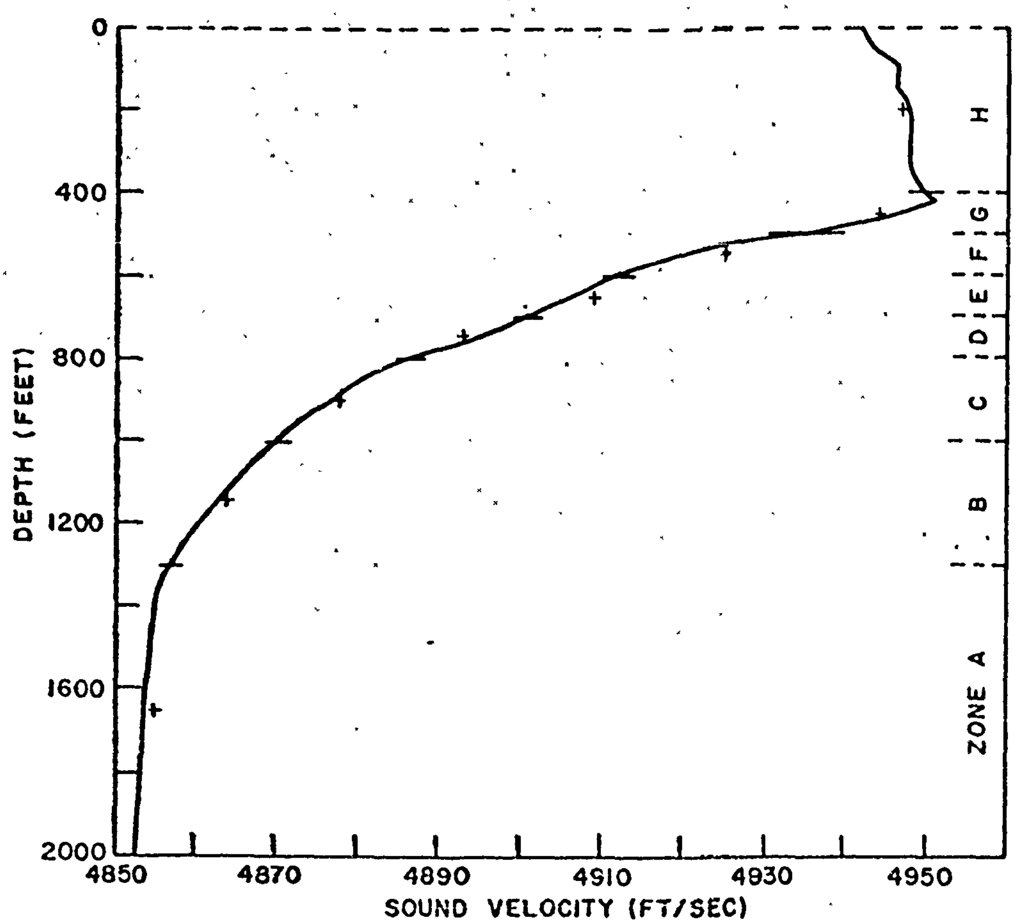

Fig. 7.4—Hydrosonic structure.

SECRET—RESTRICTED DATA

CONFIDENTIAL

Table 7.3—SHOCK-WAVE POSITIONS ON VARIOUS RAYS (DISTANCES IN FEET)

Ray Angle above Horizontal	0°	5° 39'	9° 44'	13° 22'	19° 28'	30° 5'
Ray Number	I	III	V	VII	X	XII
Time in sec after detonation						
.2	1152	1152	1152	1152	1152	1152
.3	1647.7	1647.4	1647.4	1647.4	1647.4	1647.7
.4	2141.1	2140.5	2140.5	2140.5	2140.5	2142.7
.5	2632.8	2632.6	2632.6	2632.6	2633.5	2638.8
.6	2123.6	3122.4	3122.4	3122.4	3125.4	3132.3
.7	3613.2	3612.3	3612.3	3613.2	3617.6	3630.4
.8	4102.3	4102.6	4102.6	4103.5	4110.1	4129.0
.9	4590.9	5591.5	4592.4	4593.8	4605.0	4627.2
1.0	5079.3	5080.2	5082.0	5084.8	5102.1	
1.1	5566.9	5568.1	5570.8	5575.8	5599.3	
1.2	6054.5	6056.0	6060.0	6085.5	6096.5	
1.3	6542.1	6543.9	6550.2	6563.0	6593.7	
1.4	7029.1	7031.8	7040.4	7059.5		
1.5	7516.5	7519.7	7531.1	7555.8		
1.6	8003.2	8007.6	8022.9	8052.0		
1.7	8489.3	8495.5	8516.0	8548.2		
1.8	8976.6	8983.4	9010.5	9044.4		
1.9	9463.3	9471.3	9506.4	9540.6		
2.0	9950.0	9959.2	10002.6			
2.1	10436.7	10447.9	10498.8			
2.2	10923.4	10937.2	10995.0			
2.3	11410.1	11426.5	11491.2			
2.4	11896.8	11915.8	11987.4			
2.5	12383.5	12405.8	12483.6			
2.6	12870.2	12896.6	12979.8			

ARRIVAL TIMES AT NEL AND NOL GAGES
CORRECTED TO TIME SCALE SHOWN

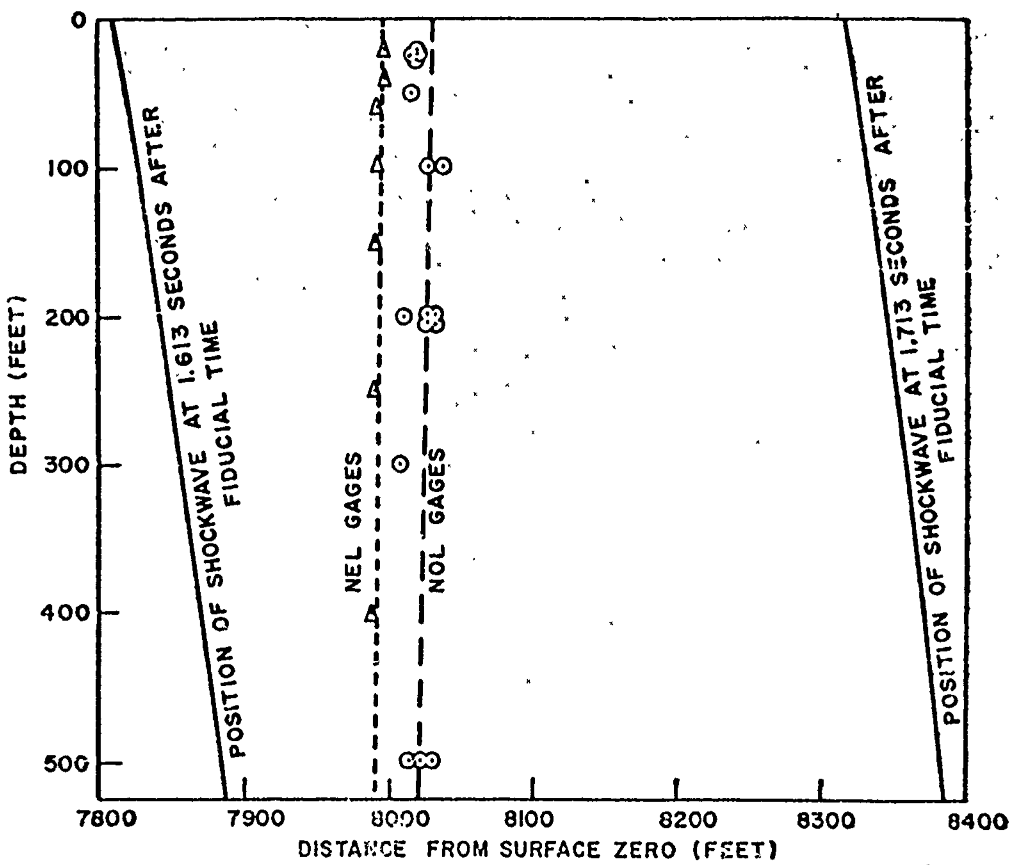

Fig. 7.5—Gage locations relative to position of shock wave (YFNB-13).

CONFIDENTIAL

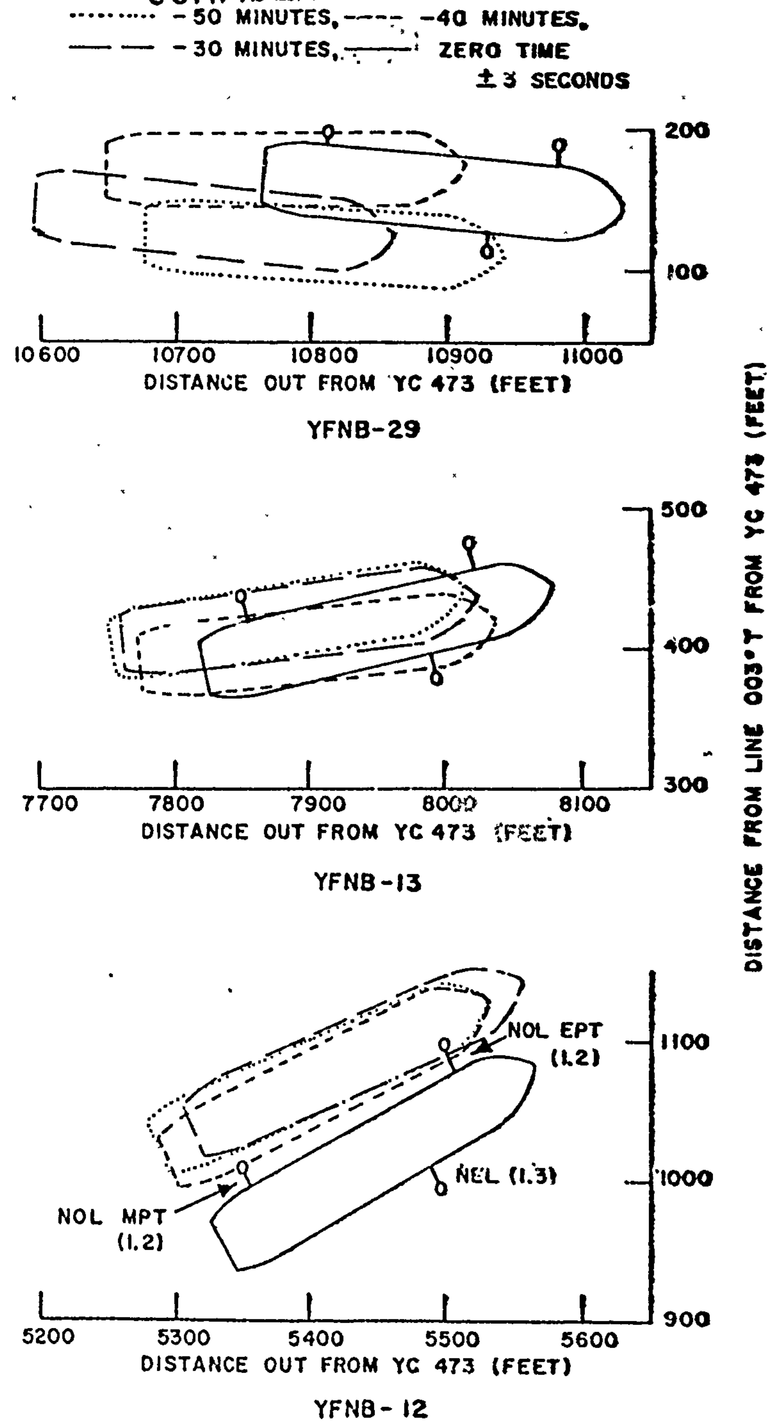

Fig. 7.6—Locations of YFNB's.

SECRET - RESTRICTED DATA

CONFIDENTIAL

Table 7.4—BEST ESTIMATES OF EQUIPMENT LOCATION (VALUES ROUNDED TO NEAREST 5 FT)

Item Measured	Depth	On Aerial Photo. Grid Out	On Aerial Photo. Grid Off to Side	Radial Dist. from Surface Zero	Slant Range from Charge
YFNB-29 EPT String	25	11030	190	11030	11205
	50			11025	11200
	100			11030	11190
	200			11025	11175
	300			11025	11155
	500			11025	11125
	1000			11020	11065
YFNB-13 EPT String	25	8020	470	8035	8275
	50			8035	8270
	100			8035	8255
	200			8030	8230
	300			8030	8205
	500			8020	8160
	1000			8005	8065
YFNB-12 EPT String	25	5505	1095	5600	5940
	50			5600	5930
	100			5600	5915
	200			5600	5880
	300			5590	5845
	500			5585	5780
	1000			5560	5650
YFNB-12 MPT-BC	0	5350	1000	5440	
YFNB-13 MPT-BC	0	7850	430	7860	
YFNB-29 MPT-BC	0	10865	200	10865	
MPT-Buoy No. 1	0	2730	345	2900*	
YFNB-12-NEL-EPT	0	5495	1000	5585	
YFNB-13-NEL-EPT	0	7990	380	7995	
YFNB-13-NEL-EPT	0	10980	115	10980	
MPT-Buoy No. 2	--	--	--	8700*	

* By Method of Section 8.2.6

Table 7.5 — RECOVERY DATA ON BUOYS AND OTHER OBJECTS

Item Description	Original Position Along Tow From Zero	Date-Time# Group of Sighting (May 1955)	Position Relative to Zero##		Radiation Level mr/hr		Ship Reporting	
			Degrees	Miles	Object	Background	No.	Name
1. MPT* Yellow Wooden Buoy	4300'	151258T	238.5(T)	3.6	2	3	ATF 92	USS TAWASA
2. MPT* Yellow Wooden Buoy	2900'	151559T	236.5(T)	3.4	200	1	do	do
3. EPT** Yellow Steel Buoy (O-1)	~2400'	151729T	231 (T)	4.5	0	1	do	do
4. B/C Rubber Buoy	3500'	151737T	238 (T)	25.2***	100	0	do	do
5. Black Rubber Buoy	?	151940T	238 (T)	10.4	100	0	do	do
6. Black & Yellow Rubber Buoy	?	160850T	216.5(T)	7.8	600	1	do	do
7. EPT** Yellow Steel Buoy (O-2)	~4100'	161207T	218.5(T)	5.6	0	1	do	do
8. LCM A-2	~4000'	151720(?)	201 (T)	31	2500	0	DD 723	USS WALKE
9. Black Rubber Buoy	?	160122Z	248	214	25	0	DDR 838	USS SMALL
10. Bumper Buoy	?	151655T	230	220	--	--	DD 752	USS A.B. CUNNINGHAM
11. Rubber Buoy	?	160859T	226	242***	150	0	DD 744	USS BLUE
12. Buoy 88	?	161309T	239	230***	0	0	do	do

* Instrumentation String Recovered
** Instrumentation String on Buoy but not recovered (Both these Buoys broke free from LCM's before zero time.)
*** Distance value seems inconsistent with others recovered by same ship at nearly the same time.
\# Zero Time 12h 59m 59.88s PDT on 14 May 1955
\#\# Zero Location 28° 44'N 126° 16'W

the array was surging slightly. The array seems straighter at zero time than at −30 min. The differences between the zero-time plot and the aerial mosaic plots seem consistent with the shifts during the 10-min intervals between mosaics.

From the large graph of arrival time vs location and the large chart of the array, Table 7.4 was compiled. It shows various distances relative to the charge and the grid for a number of gages and stations.

It is evident from these time-of-arrival data that the NOL electronic gage strings slanted slightly toward the charge from the surface. This does not agree with an informal communication from Horrer[8] of Scripps which indicated that at a depth of 1000 ft the NOL piezoelectric and Wiancko line had a starboard excursion of about 25 ft and a forward excursion of about 10 ft. However, the deviation from the vertical in either event was not serious since a moderate surge in the array could reasonably slant the gage cables as indicated.

Some items could not be located by the methods described in this chapter. The NOL mechanical pressure-time gage buoy No. 2 was not detected in any photographs, and the location of the mechanical pressure-time gage buoy No. 1 from photographs only gave its position ½ hr before zero. However, a technique described in Sec. 8.2.6 gave the accepted values listed in Table 7.4. The NOL ball-crusher buoys on the tow cable did not yield data, and no serious attempt was made to locate them. The 0-1 electronic pressure-time gage buoy broke free about 4 hr before shot time, and the 0-2 buoy broke free during the night before D-day. An unsuccessful attempt was made to locate them in photographs to find out what pressure they withstood during the shot. Data on where floating objects were recovered are fragmentary (Table 7.5) and inconclusive, although all NOL buoys with deep gage strings were found in the same general area. Table 7.5 was compiled from information submitted by various patrol and search ships.

In summary, it may be stated that data from surface photographs, arrival times, and aerial mosaics yield a chart of the instrumentation array of reasonable configuration and consistency. Although means of checking all points are lacking, the locations of the electronic gages given herein should not be in error by more than ½ per cent in the region 3000 to 12,000 ft from the charge.

REFERENCES

1. P. L. Horrer, Scripps Institution of Oceanography, Unclassified letter of 25 October 1955, to NOL, attention: C. J. Aronson.
2. NEL Special Projects Unit Secret memo 973.1, Ser 00608, to Dist. of 25 May 1955, on Preliminary Data for Project Use.
3. F. B. Porzel, Close-in Time of Arrival of Underwater Shock Wave, Operation Wigwam Project 4.4 Report, WT-1034 (in preparation).
4. C. B. Cunningham, Free-field Pressures, Station Zero, Operation Wigwam Project 1.2.1 Report, WT-1006, December 1955.
5. J. M. Richardson, A. B. Arons, and R. R. Halverson, Hydrodynamic Properties of Sea Water at the Front of a Shock Wave, Table 1, J. Chem. Phys., 15: 788 (1947).
6. T. McMillian, Free-field Pressure Measurements, Operation Wigwam Project 1.3 Report, WT-1007.
7. G. A. Young, J. F. Goertner, and R. L. Willey, Photographic Measurements of Surface Phenomena, Operation Wigwam Project 1.5 Report, WT-1009 (in preparation).
8. P. L. Horrer, Scripps Institution of Oceanography, Unclassified letter of 19 March 1956, to NOL, attention: C. J. Aronson.

CHAPTER 8

RESULTS AND ACCURACIES

8.1 BALL-CRUSHER-GAGE RESULTS AND CONCLUSIONS

Tables 8.1 and 8.2 summarize the results. Each table lists block number, depth, deformation of each gage in the block, slant range, the average deformation of the block, and the peak pressure calculated from the average deformation. In several instances one deformation was considerably less than the other three deformations from the same block. It is presumed that the low deformations were a result of gage leakage before the shot. The low defor—tion was discarded, and the average deformation was calculated from the remaining three.

In Figs. 8.1 and 8.2 the ball-crusher peak pressures are plotted against depth nese plots show a large scatter in the peak pressures near the surface. The cause of this scatter is not known. Between the 400- and 700-ft depths both positions showed significantly high peak pressures. The electronic gage results also showed trends to higher pressures at these depths. These higher peak pressures were probably due to refraction of the shock wave by a cold-water layer (see Sec. 9.8).

Peak pressures from the $\frac{3}{8}$-in. gages were consistently higher than those from the $\frac{5}{32}$-in. gages. Ball-crusher gages have always shown this discrepancy in the region of pressure where the two sizes overlap. The discrepancy was probably due to the fact that the calibration curves of the copper spheres were not absolutely linear.

There was no systematic trend of peak pressure with depth along either of the gage strings except that attributed to refraction (see Sec. 9.8). Any increase in peak pressure due to a decrease in slant range from the top to the bottom of the string would have been too small to be indicated by the gages. The ball-crusher peak pressures agreed fairly well with the peak pressures from the electronic gages.

The method of waterproofing was satisfactory. Only about 4 per cent of the gages that were recovered had leaked. The general agreement of ball-crusher peak pressures with electronic gage results and the lack of any trend of ball-crusher peak pressures with depth indicated that the correction for hydrostatic loading was satisfactory.

Mooring of the gage strings could have been improved for those gage strings hung from flotation buoys by modeling the ball-crusher rig after the mooring system used on the mechanical pressure-time gages.

8.2 MECHANICAL PRESSURE-TIME GAGE RESULTS

8.2.1 Record Interpretation

A photograph of a typical record as it appears on the drum is shown in Fig. 8.3. The lowest trace was the timing trace. The record started at the left by closing of the blast switch and

(Text continues on page 173.)

Table 8.1 —BALL-CRUSHER DEFORMATIONS AND PEAK PRESSURES FROM YFNB-13

Block	Depth (ft)	Slant Range (ft)	Deformations (in.)		Avg. Def. (in.)	$P_{max}(P_1)$ (psi)
344*	1002	7923	.0121 .0115	.0121 .0117	.0119	673
1180	953	7929	.0256 .0254	.0258 .0255	.0256	581
81	905	7936	.0247 .0248	.0257 .0248	.0250	572
451	856	7943	.0248 .0254	.0242 .0252	.0249	578
1137	807	7951	.0248 .0254	.0252 .0254	.0252	596
235	758	7958	.0263 .0256	.0257 .0259	.0259	626
1154*	709	7966	.0110 .0108	.0113 .0115	.0112	675
1206	660	7974	.0248 .0256	.0248 .0244	.0249	614
76	611	7982	.0257 .0259	.0266 .0266	.0262	662
1164	561	7990	.0259 .0256	.0259 .0259	.0258	660
1133	512	7999	.0252 .0260	.0253 .0259	.0256	663
116	464	8009	.0207** .0259	.0259 .0256	.0258	678
123*	417	8018	.0121 .0109	.0107 .0110	.0112	727
1233	369	8028	.0232 .0225	.0231 .0229	.0229	609
1159	322	8037	.0222 .0222	.0209 .0212	.0216	579
75	275	8047	.0217 .0222	.0207 .0210	.0214	582
1166	265	8049	.0129** .0201	.0211 .0202	.0205	558
1157	255	8051	.0211 .0211	.0199 .0206	.0207	566

* 3/8-in. gage

** Deformation is low - This value was not used in computing average.

Table 8.1 —(Continued)

Block	Depth (ft)	Slant Range (ft)	Deformations (in.)		Avg. Def. (in.)	$P_{max}(P_1)$ (psi)
1152*	245	8053	.0097 .0089	.0091 .0094	.0093	621
1132	235	8055	.0194 .0207	.0216 .0215	.0208	572
1139	225	8057	.0211 .0121**	.0218 .0208	.0212	586
1169	215	8060	.0206 .0214	.0201 .0209	.0208	576
1196	205	8062	.0202 .0210	.0188 .0205	.0201	557
237	195	8064	.0204 .0135**	.0200 .0234	.0212	592
No No.*	185	8066	.0087 .0086	.0082 .0096	.0088	596
1148	175	8068	.0199 .0208	.0199 .0152**	.0202	565
1160	165	8071	.0198 .0190	.0200 .0190	.0197	552
253	155	8073	.0213 .0200	.0185 .0198	.0199	560
25	145	8076	.0195 .0201	.0205 .0208	.0202	571
1156*	135	8078	.0100 .0090	.0090 .0105	.0096	662
1235	125	8080	.0230 .0236	.0232 .0264	.0240	687
1221	115	8083	.0234 .0227	.0215 .0215	.0223	639
172	105	8085	.0217 .0205	.0205 .0209	.0209	559
1147	95	8087	.0201 .0205	.0200 .0231	.0209	601
1226	85	8090	.0210 .0170	.0161 .0212	.0188	540
1237*	75	8092	.0101 .0092	.0102 .0099	.0099	895

* 3/8-inch gage
** Deformation is low - This value was not used in computing average.

Table 8.1 — (Continued)

Block	Depth (ft)	Slant Range (ft)	Deformations (in.)		Avg. Def. (in.)	$P_{max}(P_1)$ (psi)
1050	65	8094	.0177 .0215	.0142** .0204	.0199	577
1165	55	8097	.0184 .0178	.0179 .0196	.0184	535
1101	45	8100	.0166 .0189	.0185 .0182	.0181	528
1136	35	8102	.0211 .0202	.0199 .0238	.0212	622
1150	25	8104	.0202 .0196	.0190 .0208	.0199	589
1234	15	8107	.0160 .0178	.0188 .0196	.0180	533
18	5	8109	.0129 .0126	.0127 .0120	.0125	370
1142	5	8109	.0140 .0165	.0161 .0161	.0157	465

* 3/8-in. gage

** Deformation is low - This value was not used in computing average.

Table 8.2—BALL-CRUSHER DEFORMATIONS AND PEAK PRESSURES FROM YFNB-29

Block	Depth (ft)	Slant Range (ft)	Deformations (in.)	Adv. Def. (in.)	P_{max} (P_1) (psi)
332	1002	10,911	.0217	.0218	459
			.0215		
			.0219		
			.0220		
1134	952	10,916	.0219	.0219	471
			.0225		
			.0220		
			.0211		
1158	903	10,921	.0210	.0210	454
			.0206		
			.0215		
			.0209		
1167	853	10,926	.0208	.0210	463
			.0207		
			.0207		
			.0219		
1207	2204	10,931	.0036**	.0208	467
			.0210		
			.0205		
			.0209		
1171*	754	10,937	.0091	.0097	560
			.0100		
			.0095		
			.0101		
1130	705	10,942	.0218	.0226	538
			.0238		
			.0221		
			.0226		
1116	655	10,948	.0209	.0215	514
			.0215		
			.0218		
			.0218		
1231	606	10,954	.0299	.0298	769
			.0107**		
			.0289		
			.0305		

* 3/8-in. gages
** Deformation is low - This value was not used in computing averages.

Table 8.2—(Continued)

Block	Depth (ft)	Slant Range (ft)	Deformations (in.)	Adv. Def. (in.)	P_{max} (P_1) (psi)
1138	556	10,960	.0249 .0258 .0268 .0257	.0258	660
1163	508	10,967	.0178 .0191 .0196 .0182	.0187	459
1187*	458	10,974	.0083 .0082 .0080 .0087	.0083	511
1151	408	10,981	.0172 .0166 .0160 .0177	.0169	424
1041	358	10,989	.0149 .0027** .0148 .0156	.0151	380
1113	309	10,996	.0156 .0165 .0157 .0149	.0157	408
1	259	11,004	.0150 .0144 .0149 .0154	.0149	393

* 3/8-in. gages
** Deformation is low - This value was not used in computing average.

CONFIDENTIAL

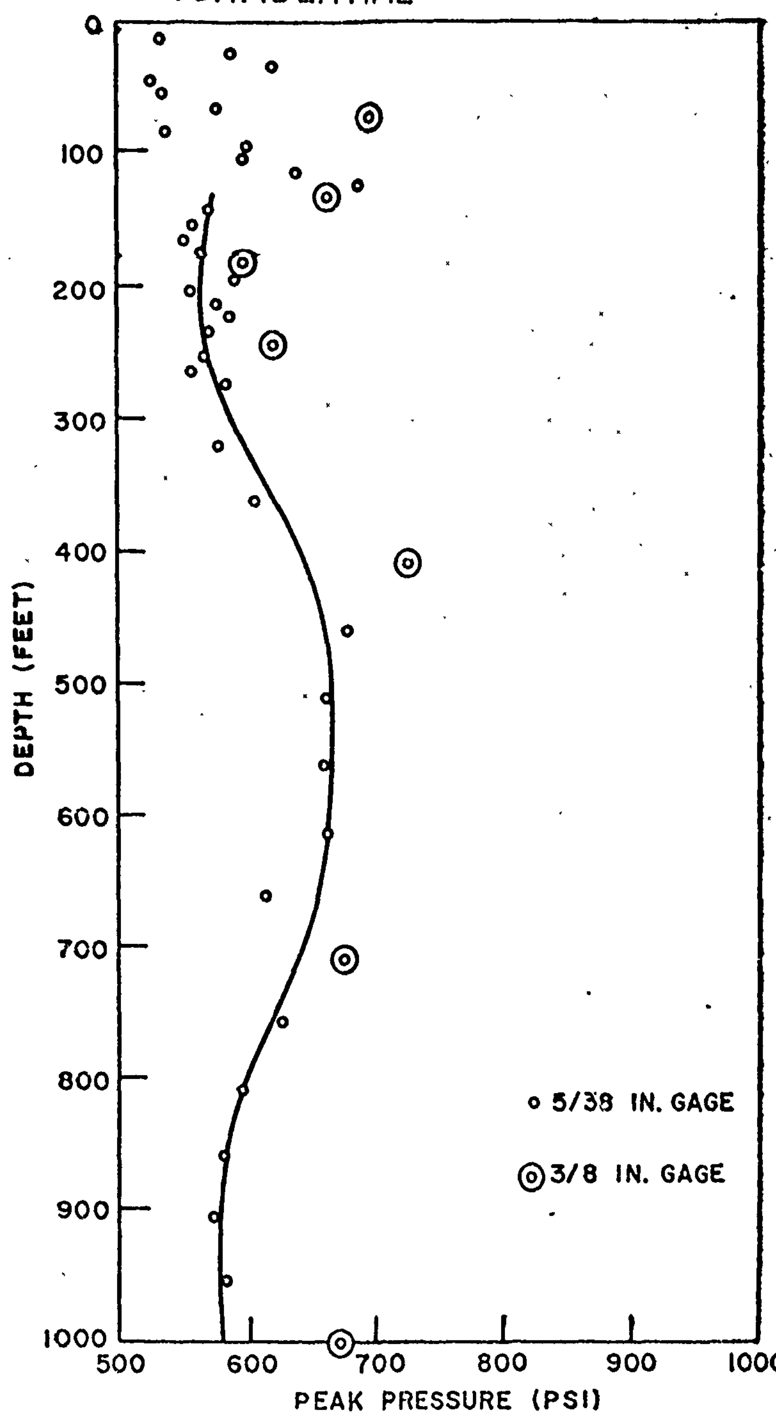

Fig. 8.1—Ball-crusher peak pressure vs depth, YFNB-13.

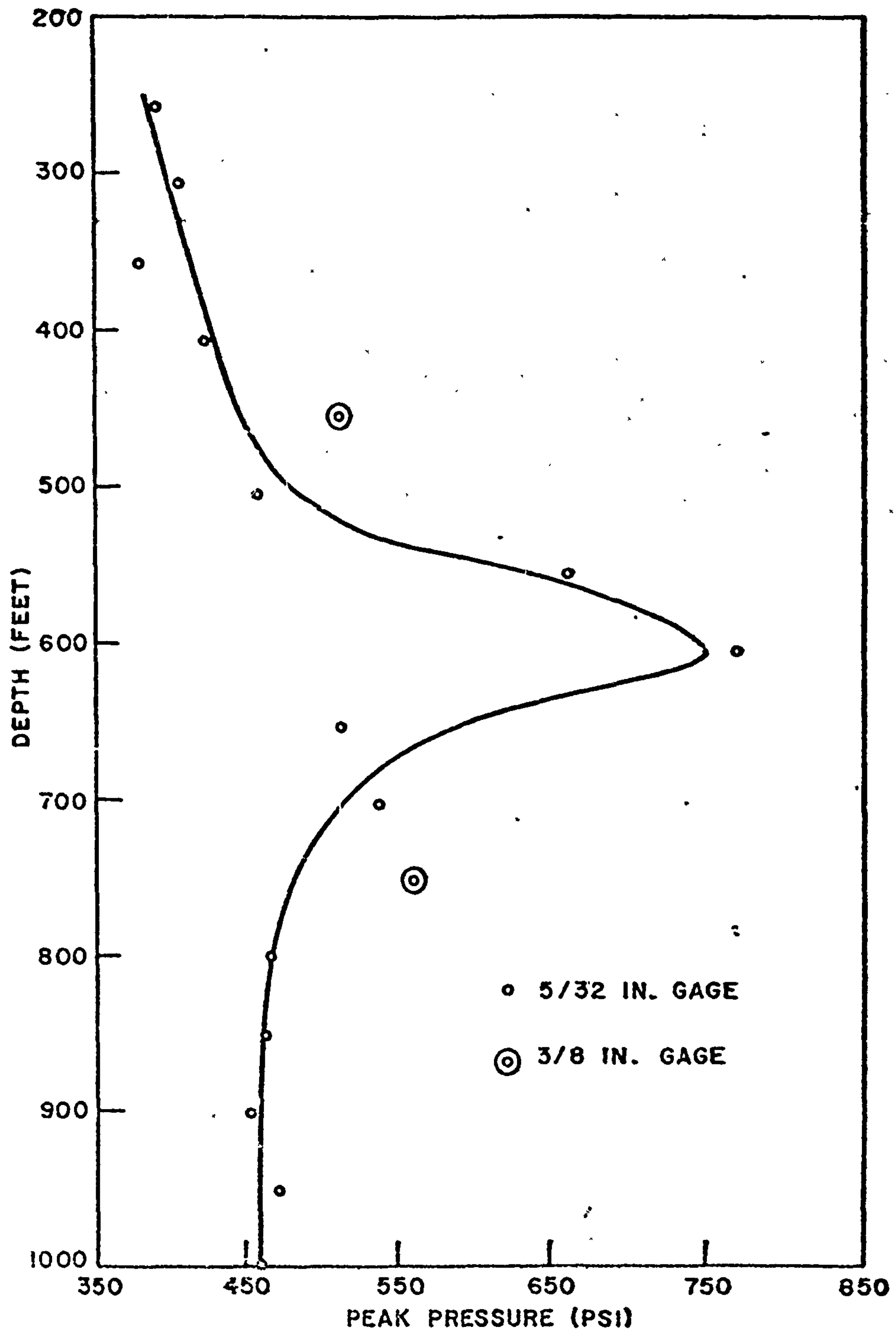

Fig. 8.2—Ball-crusher peak pressure vs depth, YFNB-29.

CONFIDENTIAL

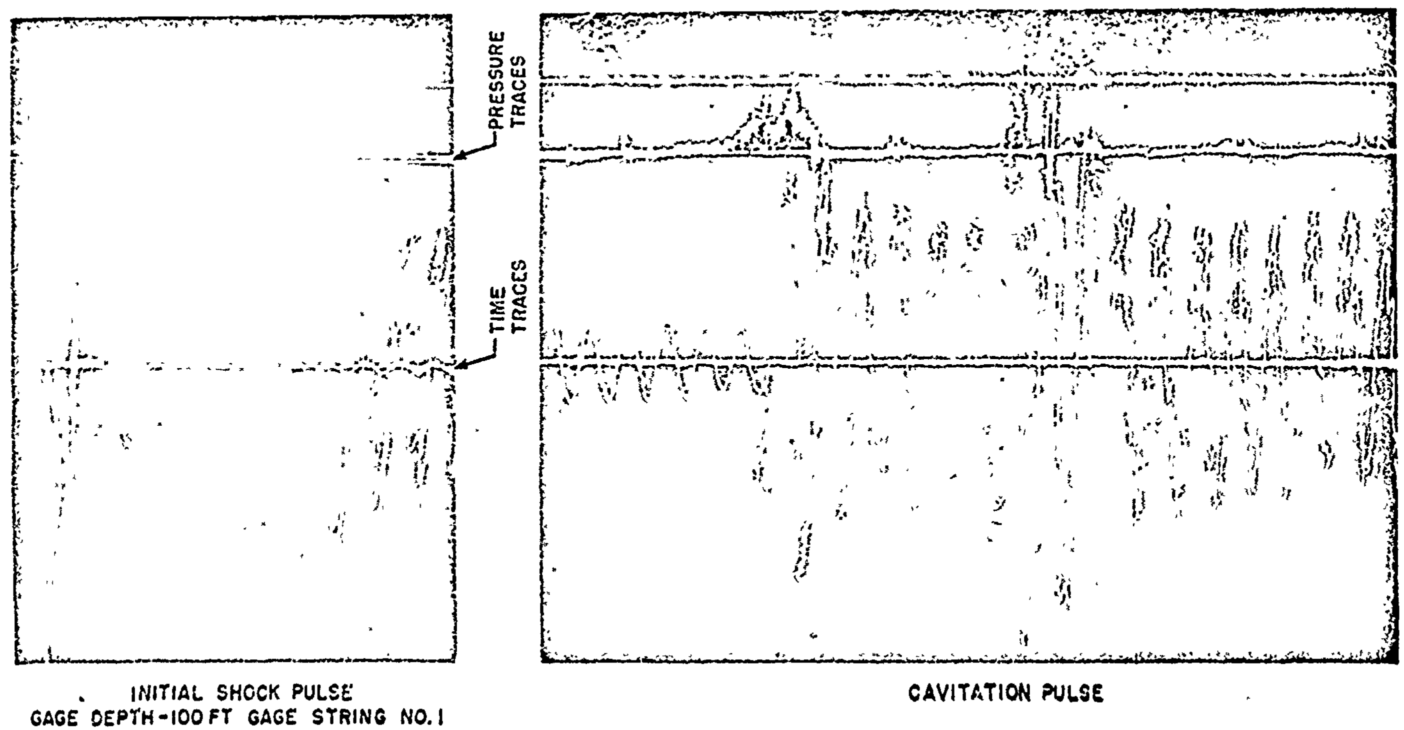

Fig. 8.3—Typical mechanical pressure-time gage record.

traveled for approximately 80 msec before shock arrival started the timing reed. This oscillation (20 msec per cycle) gradually decayed for about 530 msec, at which time the timing trace shows that the gages were shocked by something, perhaps by a tug of the cable, since no significant pressure appeared on the pressure trace at that time. About 120 msec later the gage was struck by the peak of the cavitation pulse.

The timing trace then gradually decayed until it was again shocked by the first bubble pulse and by following shocks. These oscillations could be counted over much of the record and provided a reasonably accurate time measurement.

There was considerable harmonic distortion in the timing trace at the time of heavy shock. This made it impossible to determine the speed regulation, using the timing trace, for periods shorter than 1 cycle or 20 msec. Some information could be obtained, however, from the pressure trace, especially if the pressure wave shape was assumed to be known a priori.

The pressure trace showed a conventional water shock wave. The distortion on the pressure-decay trace was probably caused by high-frequency speed variations originating with the escapement and amplified by axial play of the worm shaft. The double base line to the left of the pressure rise is a measure of friction in this gage. There was more friction in this particular gage than in any other. The usual amount was one line width. After the pressure decayed, the lower line showed the pressure cutoff by cavitation. This gage, being at the 100-ft depth, showed about 44 plus 15 psi, or 59 psi, below hydrostatic pressure until the cavitation closed and created a positive pressure pulse. The pressure signals after the cavitation pulse were bottom reflections and second or third bubble pulses, which occurred much later and showed up on this part of the record because the drum revolved for $2\frac{1}{2}$ revolutions. The first bubble did not occur on the part of the record shown in this photograph.

8.2.2 Timing Calibration

After the operation a preliminary calibration of each timing reed was made at San Diego with a Strobotac. The frequencies obtained were accurate to 2 per cent.

Subsequent to this, each timing reed was again calibrated, this time at NOL, by recording on the drum, for comparison, a trace made by a phonograph cutter-head stylus. The head was driven by a tuning fork. The clock motor was replaced by an electric motor to give higher drum speeds and resolution. By this means the reed frequency was determined to within 0.1 per cent. An unsuccessful effort was made to improve the reading of the timing signal during the shock phase by a study of the harmonic distortion of the reed.

The net result of this calibration was that the time could be read with a precision of 1 part in 1000 only if no shock was present during that time and if the timing trace was continuous for over 100 cycles. Shock tests indicated that, although shock caused a phase shift in the timing reed, time could be determined to within 5 msec at each shock. This error, of course, could accumulate if there were several shocks.

8.2.3 Pressure Calibration

After the Operation each gage was statically calibrated twice, once before removal of the sensing element from its recorder and once after removal. In general, these calibrations showed linearity and lack of friction of the same excellence as that which existed before the shot.

After its return to NOL, each element was dynamically tested to determine the degree of damping. Previous work had been limited to only a few elements.

The dynamic calibration pulse was obtained by using one to three ND 24 detonators in the explosion chamber described in Chap. 3. The pulse was characterized by a rise time of $\frac{1}{10}$ msec and an exponential decay of about 20 per cent in 2 msec.

From these tests it was found that, although some were properly damped, most of the elements were rather seriously underdamped. Figure 8.4 shows typical records. Measurements were made on all gages which were still operable (about 18 out of 26) to obtain the amount of overshoot of each stylus.

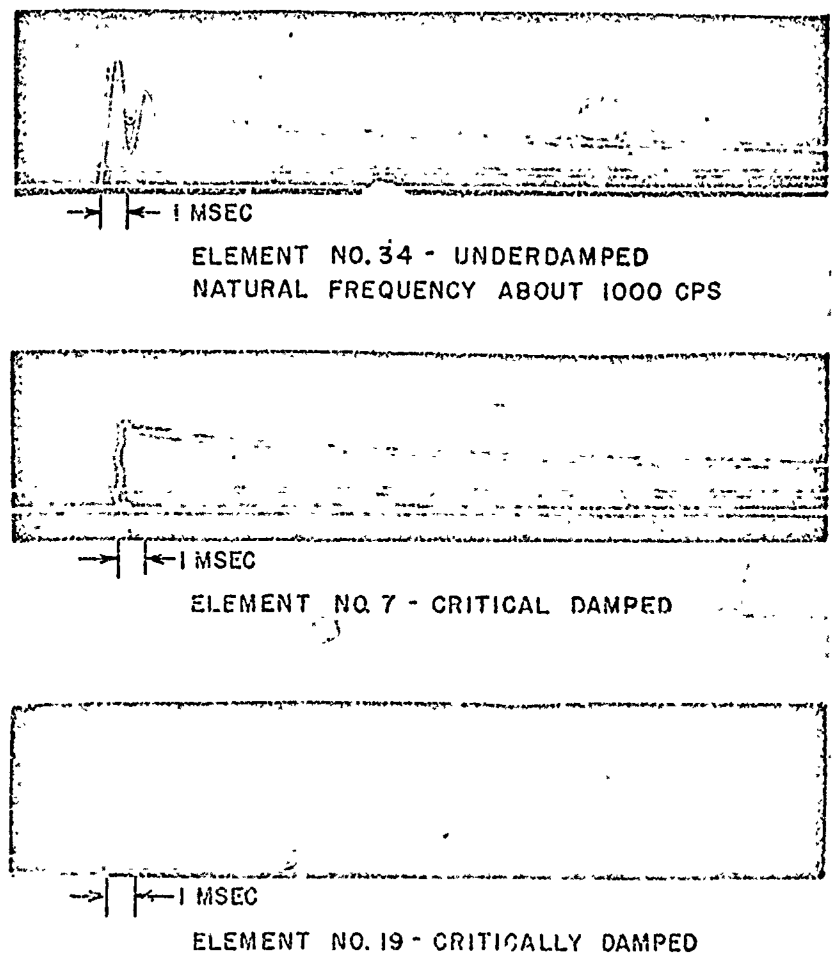

Fig. 8.4—High-speed mechanical pressure-time gage calibration records made to determine amount of overshoot.

A dynamic pressure calibration was then made on the elements for the 50- and 500-ft gages of buoy string No. 1. This could not be done on the 100- and 300-ft gages because of leaks which developed after the shot. Because each calibration took about two weeks, it was considered to be warranted only on the gages of string No. 1 since this string was located in a region where no other pressure gages were.

The dynamic calibration pulse was obtained using ND 24 detonators in a pressure chamber as before, but this time much effort was spent on the electronic recording to ensure a precisely calibrated record (Fig. 8.5) from the strain gage. The two dynamic calibration curves obtained are shown in Figs. 8.6 and 8.7.

The curves showed that dynamic sensitivity was lower than static sensitivity by about 10 per cent. The reason for this was unknown but was believed to arise from hysteresis of the Wiancko twisted-tube part of the sensing element.

No tests were made to determine the duration of this apparent hysteresis. This meant that the dynamic curve could only be used with confidence for step pressures. The amount that the hysteresis changed during the time from pressure rise to cutoff may have been anything from 0 to 10 per cent of the pressure; therefore the cutoff pressures could not be measured so well as pressure rises.

8.2.4 Buoy String No. 1

Records were obtained from the five uppermost gages. The 750- and 1000-ft gages were lost for some unknown reason. The 50-, 100-, 300-, and 500-ft gages gave pressure-time records. Both blast switches operated properly. The 200-ft gage ran prematurely and yielded only a peak-pressure record. Figures 8.8 to 8.10 show photographic prints of the principal shock, the cavitation pulse, and the first bubble pulse on each gage. There were many other pulses on the record which are not presented here. Pressure and time data are given in Tables 8.3, 8.5, and 8.6. No results are given for the YFNB-12 (Table 8.4) because the string was not lowered.

Pressure values based on dynamic calibration curves were obtained for the 50- and 500-ft gages. For the 100-, 200-, and 300-ft gages, all pressures were based on the static calibration curve for each gage and increased 10 per cent.

Of course, the validity of the assumption that the results of tests on two gages applied to all others was questionable; however, this was considered to be a justifiable attempt to get the most accurate data from the records.

Peak pressures were obtained from the records by replotting the curves on semilog paper so that the exponential decay showed up as a straight line. Values of θ were obtained by noting the time at which the pressure had dropped to $1/e$ of its peak.

The estimated over-all accuracy of pressure measurements was 12 per cent.

Positive durations (t_2)* were obtained as follows:

1. The displacement of the drum was measured for several cycles of the timing trace which were made at the time of the shock pulse.
2. An average speed of the drum was determined.
3. The displacement of t_2 on the pressure trace was measured and then divided by the average drum speed to obtain the duration.

Values of t_2 were believed to be correct within 3 msec.

Photographs of the principal shock, Fig. 8.8, showed a repeating step effect on the pressure decay. This may have been caused by the stop-and-go action of the escapement-controlled motor. A similar effect was noticed in calibration work, but the number of steps which showed up during the decay cannot be determined sufficiently to check the positive duration. From the appearance of the record, there seemed to be a noticeable variation in speed, which might have been partly caused by worm-shaft play. This should have averaged out for the longer pulses so that this error would not be expected to accumulate.

(Text continues on page 185.)

*Such quantities are listed in the data tables and are illustrated in Fig. 8.12.

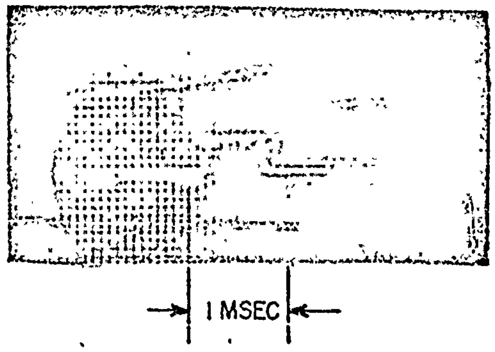

STRAIN GAGE RECORD, CALIBRATION STEPS, AND TIMING TRACE
PRESSURE AT 1 MSEC = 1150 PSI

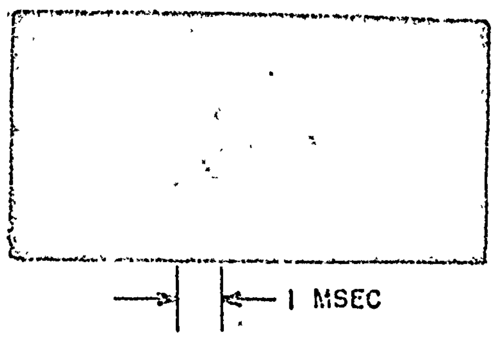

MECHANICAL GAGE TRACE
DEFLECTION AT 1 MSEC = 16.2 MILS

Fig. 8.5 — Typical set of mechanical pressure-time gage dynamic calibration records.

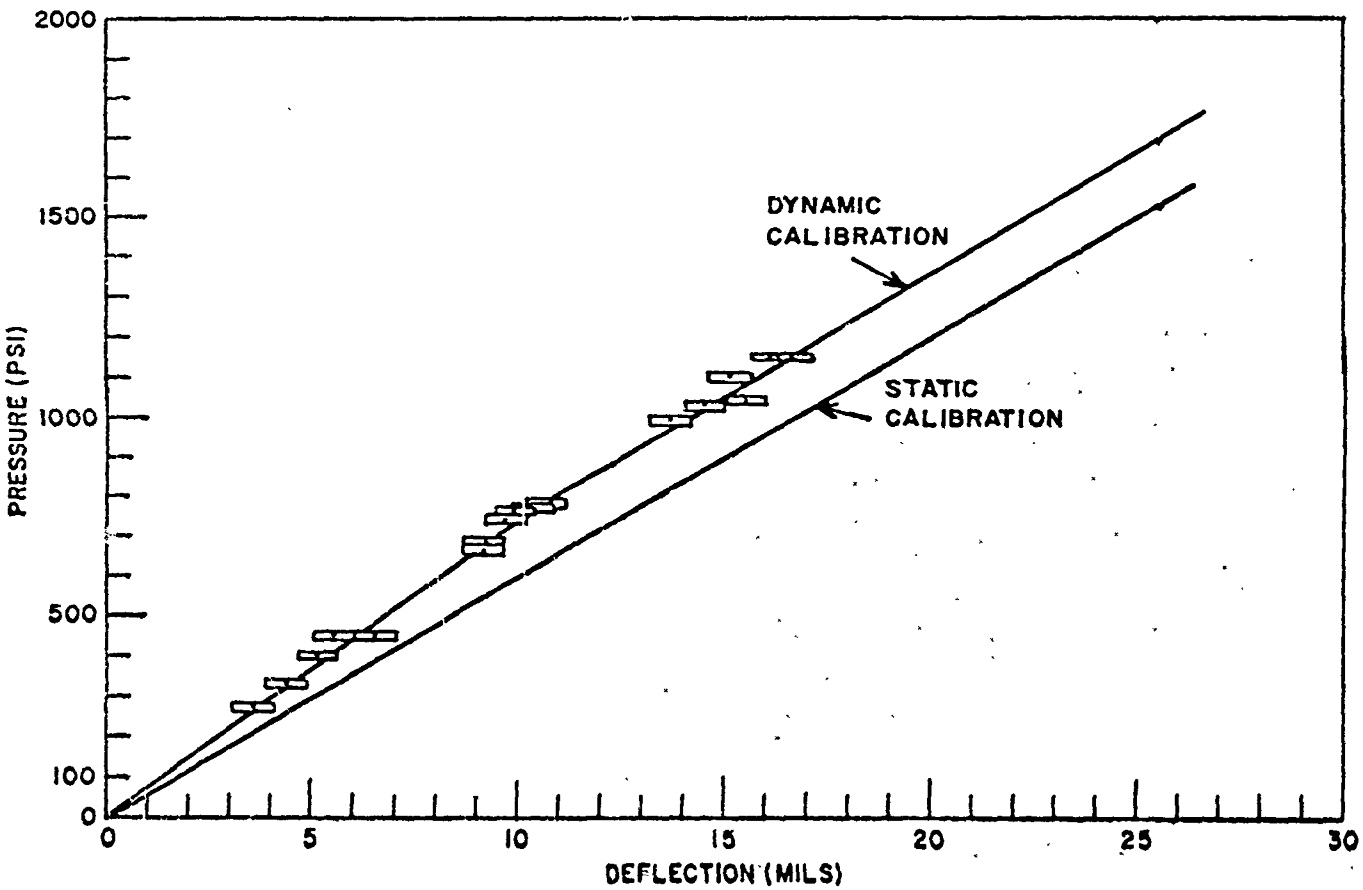

Fig. 6.0—Dynamic and static calibration curves for mechanical pressure-dms gage No. 4, element No. 49.

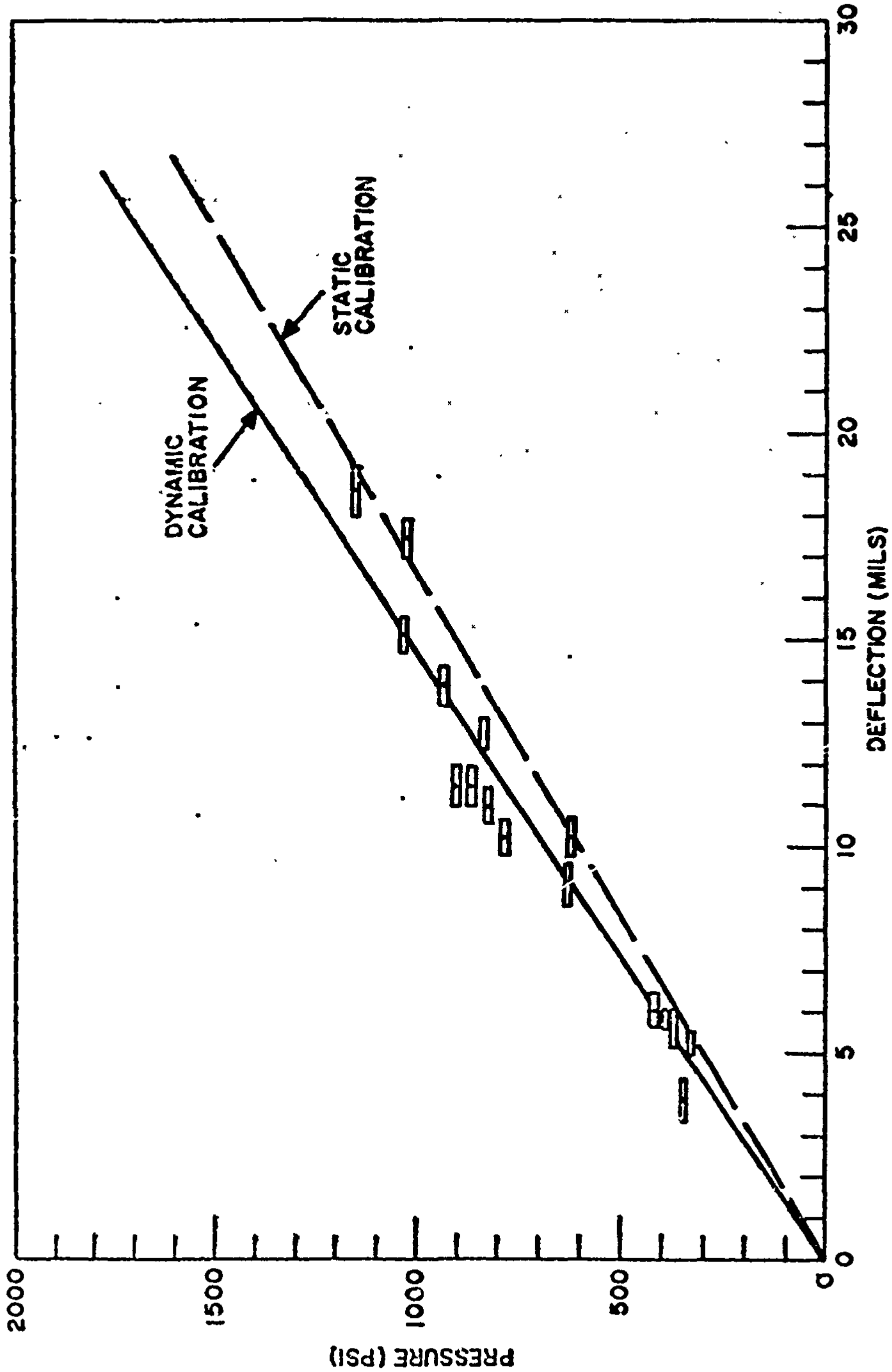

Fig. 8.7—Dynamic and static calibration curves for mechanical pressure-time gage No. 28, element No. 27.

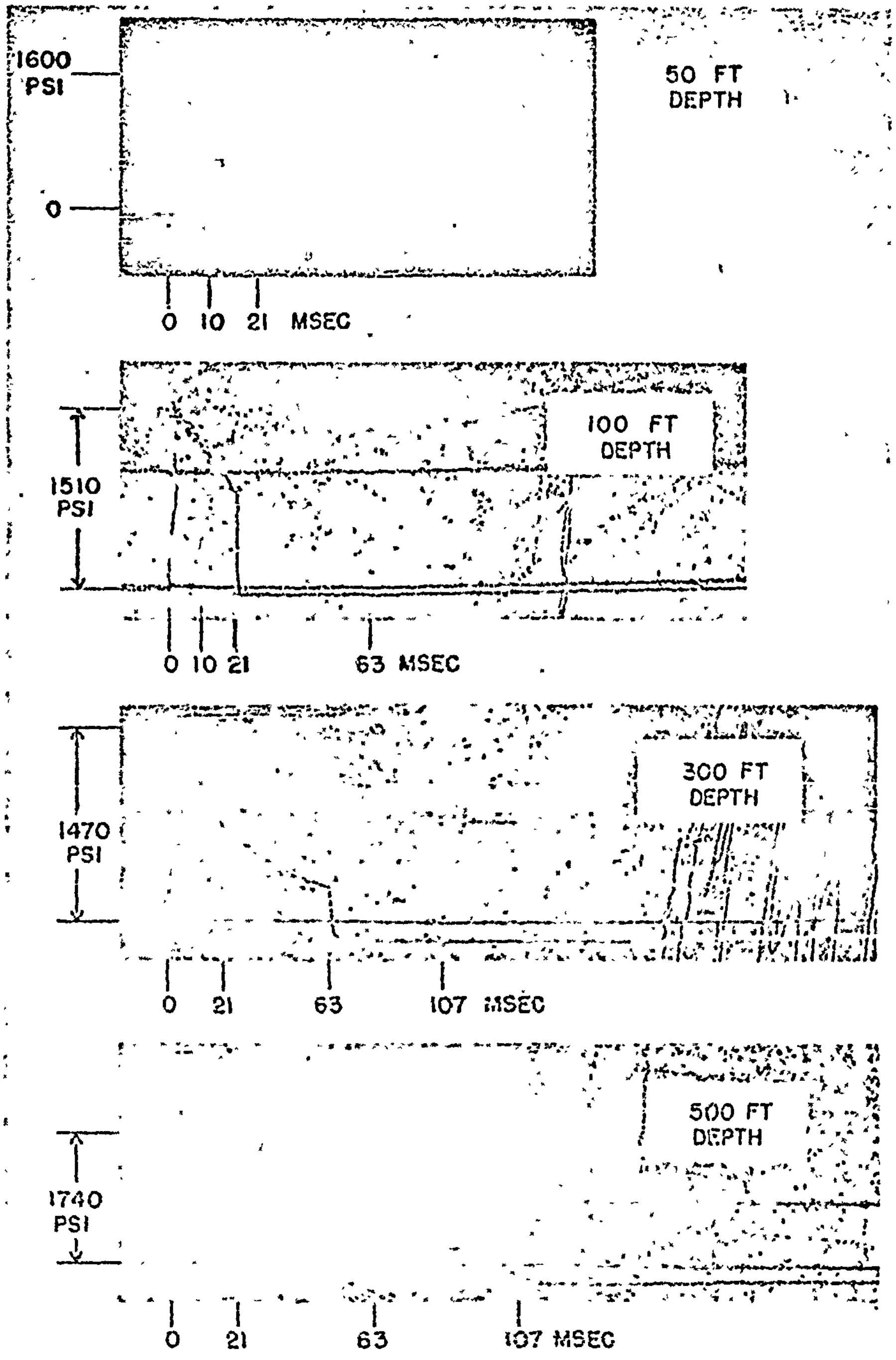

Fig. 8.3—Principal pulses from mechanical pressure-time gages on buoy string No. 1.

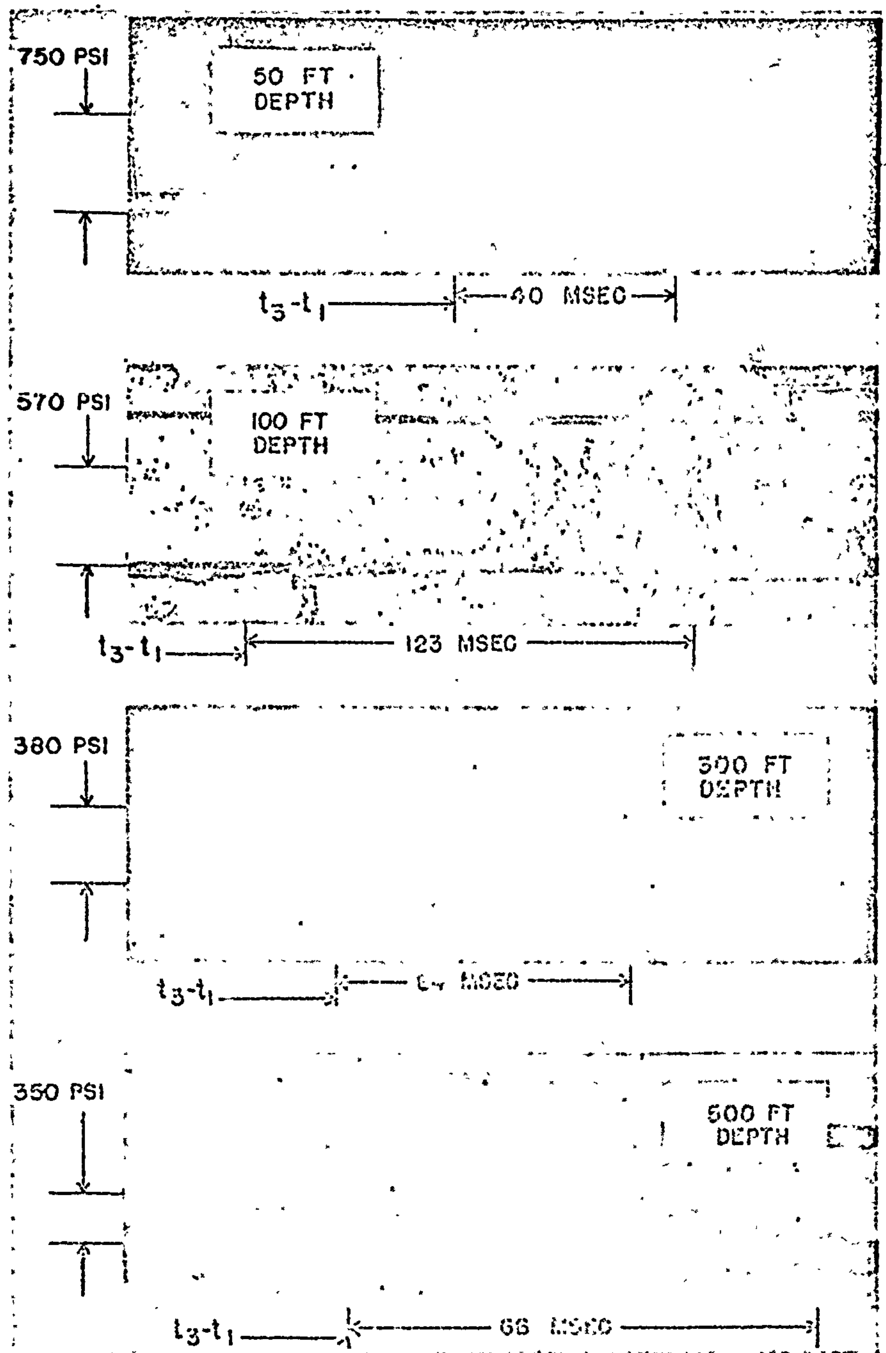

Fig. 8.9—Cavitation closure pulses from mechanical pressure-time gages on buoy string No. 1.

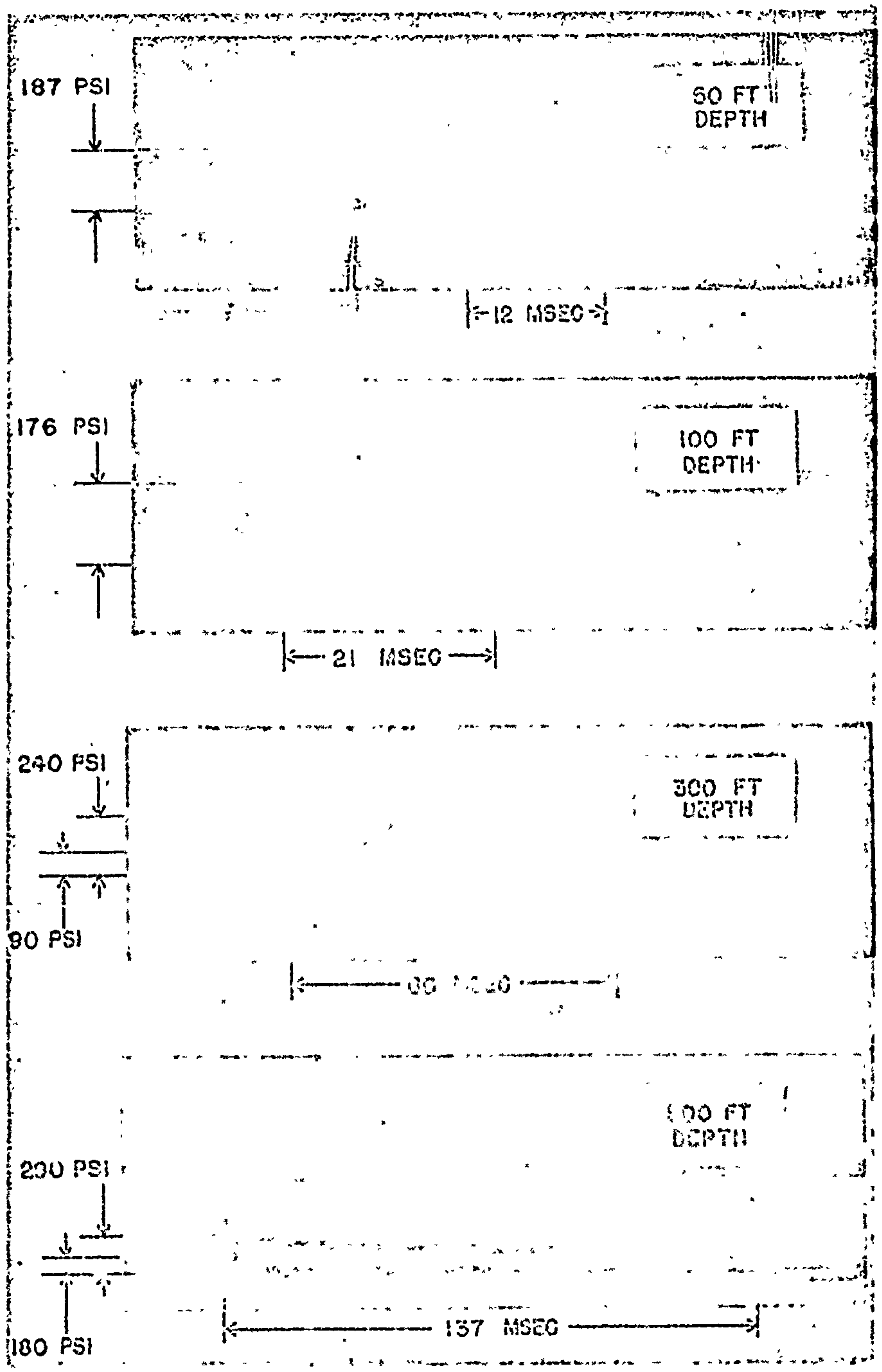

Fig. 8.10—First bubble pulses from mechanical pressure-time gages on buoy string No. 1.

Table 8.3—MECHANICAL PRESSURE-TIME GAGE RESULTS (BUOY STRINGS)

Location	Gage No.	Sensing Element No.	Sensing Element Range (psi)	Depth (ft)	Slant Range (ft)	Horizontal Range (ft)	P_1 psi	P_2 psi	t_2 msec	t_5-t_1 msec	P_4 psi	t_4 msec	t_3-t_1 msec
Buoy String No. 1	4	49	1000	50	3490	2900	1600	1170	10	2780	750	40	770
	13	18	500	100	3460	2900	1510	810	21	2780	570	180	650
	26	50	1000	200	3410	2900	1520	—	—	—	—	—	—
"	27	19	500	300	3360	2900	1470	310	63	2760	380	340	730
"	28	27	1000	500	3270	2900	1740	160	107	2830	350	400	810
Buoy String No. 2	40	17	300	50	8650	8700	540	500	6	2800	—	—	—
	32	45	500	100	8640	8700	—	—	—	—	—	—	—
	33	29	300	200	8600	8700	500	—	—	—	—	—	—
"	34	21	500	300	8580	8700	610	380	16 to 20	2850	—	—	—
"	36	28	750	500	8550	8700	460–580	—		—	—	—	—
"	38	20	500	750	8500	8700	740	130	56	2750	—	—	—
"	39	22	500	1000	8450	8700	876	—	—	—	—	—	—

Location	Gage No.	Sensing Element No.	Sensing Element Range (psi)	Depth (ft)	Slant Range (ft)	Horizontal Range (ft)	θ msec	back pressure psi	P_5	P_6	t_6	t_3-t_0
Buoy String No. 1	4	49	1000	50	3490	2900	31	1000	—	190	12	1415
	13	18	500	100	3460	2900	34	1000	—	180	21	1290
	26	50	1000	200	3410	2900	—	1000	—	—	—	—
"	27	19	500	300	3360	2900	27	1000	90	240	60	1352
"	28	27	1000	500	3270	2900	27	1000	180	290	137	1412
Buoy String No. 2	40	17	300	50	8650	8700	—	600	—	—	—	—
	32	45	500	100	8640	8700	—	1000	—	—	—	—
	33	29	300	200	8600	8700	—	600	—	—	—	—
"	34	21	500	300	8580	8700	—	1000	—	—	—	—
"	36	28	750	500	8550	8700	—	1000	—	—	—	—
"	38	20	500	750	8500	8700	—	1000	—	—	—	—
"	39	22	500	1000	8450	8700	—	1000	—	—	—	—

Location	Gage No.	Sensing Element No.	Sensing Element Range (psi)	Depth (ft)	Slant Range (ft)	Horizontal Range (ft)	$t_1 - t_0 = t_s$* msec	From Table 7.3
Buoy String No. 1	4	49	1000	50	3490	2900	645	35°.3 Ray
	13	18	500	100	3460	2900	640	" "
	26	50	1000	200	3410	2900	—	" "
"	27	19	500	300	3360	2900	622	" "
"	28	27	1000	500	3270	2900	606	28°.6 Ray
Buoy String No. 2	40	17	300	50	8650	8700	—	—
	32	45	500	100	8640	8700	—	—
	33	29	300	200	8600	8700	—	—
"	34	21	500	300	8580	8700	—	—
"	36	28	750	500	8550	8700	—	—
"	38	20	500	750	8500	8700	—	—
"	39	22	500	1000	8450	8700	—	—

*$t_s = t_1 - t_0$ where t_0 = 13 (NRL) msec t_s = shock travel time

CONFIDENTIAL

Table 8.4—YFNB-12 RESULTS

Gage Type	Tape and Head No.	Foot Notes	Gage No.	Depth	Range Slant	Range Horiz.	Pressures in psi P_o	P_1	P_2	P_3	P_4	P_5	P_6	P_1 (j)
PE	E-2	e, d	1067	25	5940	5600	—	920	805	-22	—	—	—	—
PE	F-1	c, h	891	25	5940	5600	—	—	—	—	—	—	—	—
PE	F-7	c, e	891	25	5940	5600	—	865	—	—	83	—	—	—
PE	E-3	d	1026	50	5930	5600	—	915	710	-18	80	—	—	—
PE	F-2	d	1029	100	5915	5600	—	922	—	—	255	—	—	—
PE	E-4	a, h	823	200	5880	5600	—	—	—	—	—	—	—	—
PE	E-7	a, d	823	200	5880	5600	—	905	462	-80	99	—	—	—
PE	F-3	d	1031	200	5880	5600	—	910	—	—	116	—	—	—
W	E-1		18206	200	5880	5600	84	855	452	-93	105	—	—	960
W	F-4		18196	200	5880	5600	79	855	482	-104	152	—	—	960
W	E-8		18207	300	5845	5590	124	873	316	-142	—	—	—	980
PE	F-5		825	500	5780	5585	—	990	—	—	129	—	—	—
W	E-10		18209	500	5780	5585	222	970	193	-220	—	35	105	1090
W	F-9		18212	500	5780	5585	218	930	185	-216	115	25	75	1100
PE	E-5	b, d	623	1000	5650	5560	—	940	55	—	—	—	—	—
PE	E-9	b, i	623	1000	5650	5560	—	—	—	—	—	53	118	—
PE	F-8	d	893	1000	5650	5560	—	950	—	—	—	—	—	—
W	F-10		18213	1000	5650	5560	426	848	72	-236	92	60	130	965

Average for 1000 ft gages (PE and corrected Wiancko) P_1 = 951

a. Channels having a common indicating mark were recorded from the same gage.
b. Channels " " " " " " " " " " "
c. Channels " " " " " " " " " " "
d. Records compensated for drag-out.
e. Data reworked and extrapolated to t = 0 with θ = 35
h. Bad Calibration
i. Too High Gain
j. Wiancko corrected pressures, see Section 9.2 and Tables 5.1, 6.1, 6.2, and 6.3.

Gage Type	Tape and Head No.	Foot Notes	Gage No.	Depth	Range Slant	Range Horiz.	Times are in msec t_1 (f)	t_2	t_3	t_4	t_5	t_6	t_7	t_8
PE	E-2	e, d	1067	25	5940	5600	1181	3	—	—	—	—	—	—
PE	F-1	c, h	891	25	5940	5600	1181	3	—	—	—	—	—	—
PE	F-7	c, e	891	25	5940	5600	1181	2.8	1396	57.5	—	—	—	—
PE	E-3	d	1026	50	5930	5600	1179	6.2	1394	52.8	—	—	—	—
PE	F-2	d	1029	100	5915	5600	1177	12.6	1396	54	—	—	—	—
PE	E-4	a, h	823	200	5880	5600	1170	24.4	—	—	—	—	—	—
PE	E-7	a, d	823	200	5880	5600	1170	24.5	1414	77.5	—	—	—	—
PE	F-3	d	1031	200	5880	5600	1171	24	1415	94	—	—	—	—
W	E-1		18206	200	5880	5600	1170	23.9	1414	81.5	3980	—	5875	6118
W	F-4		18196	200	5880	5600	1170	24.1	1414	104	—	—	—	—
W	E-8		18207	300	5845	5590	1164	36.2	—	—	—	—	—	—
PE	F-5		825	500	5780	5585	1154	61	1469	54	3955	—	—	—
W	E-10		18209	500	5780	5585	1152	61.5	—	—	3965	49.5	5815	6055
W	F-9		18212	500	5780	5585	1152	60	1467	54	3957	49.4	—	—
PE	E-5	b, d	623	1000	5650	5560	1128	127.5	—	—	—	—	—	5762
PE	E-9	b, i	623	1000	5650	5560	1129	127.4	1566	77.5	3936	104.5	5728	5965
PE	F-8	d	893	1000	5650	5560	1129	127.6	—	—	3941	105.5	—	5934
W	F-10		18213	1000	5650	5560	1129	127.5	1566	83	3932	104	—	5924

Average for 1000 ft gages (PE and corrected Wiancko) P_1 = 951

a. Channels having a common indicating mark were recorded from the same gage.
b. Channels " " " " " " " " " " "
c. Channels " " " " " " " " " " "
d. Records compensated for drag-out.
e. Data reworked and extrapolated to t = 0 with θ = 35
h. Bad Calibration
i. Too High Gain
f. $t_s = t_1 - t_o$ where t_o = 13 msec t_s = shock travel time

Table 3.4—(Continued)

Gage Type	Tape and Head No.	Foot Notes	Gage No.	Depth	Range Slant	Range Horiz.	t_9	t_{10}	t_{11}	t_{12}	t_{13}	t_{14}	t_{15}	t_{16}
							Times are in msec							
PE	E-2	e, d	-1067	25	5940	5600	—	—	—	—	—	—	—	—
PE	F-1	c, h	891	25	5940	5600	—	—	—	—	—	—	—	—
PE	F-7	c, e	891	25	5940	5600	—	—	—	—	—	—	—	—
PE	E-3	d	1026	50	5930	5600	—	—	—	—	—	—	—	—
PE	F-2	d	1029	100	5915	5600	—	—	—	—	—	—	—	—
PE	E-4	a, h	823	200	5880	5600	—	—	—	—	—	—	—	—
PE	E-7	a, d	823	200	5880	5600	—	—	—	—	—	—	—	—
PE	F-3	d	1031	200	5880	5600	—	—	—	—	—	—	—	—
W	E-1		18206	200	5880	5600	5960	6486	6500	6603	6636	~7850	—	8445
W	F-4		18196	200	5880	5600	—	—	—	—	—	—	—	—
W	E-8		18207	300	5845	5590	—	—	—	—	—	—	—	—
PE	F-5		825	500	5780	5585	—	—	—	6602	—	—	—	—
W	E-10		18209	500	5780	5585	6020	6477	6492	6593	6629	7650	7925	8440
W	F-9		18212	500	5780	5585	—	—	—	6610	—	—	—	—
PE	E-5	b, d	623	1000	5650	5560	—	—	—	6615	—	—	—	—
PE	E-9	b, i	623	1000	5650	5560	6108	6469	6492	6595	6629	7575	7982	8433
PE	F-8	d	893	1000	5650	5560	—	—	—	6601	—	—	—	—
W	F-10		18213	1000	5650	5560	—	—	—	6601	—	—	—	—

Average for 1000 ft gages (PE and corrected Wiancko) $P_1 = 951$

a. Channels having a common indicating mark were recorded from the same gage.
b. Channels " " " " " " " " " " "
c. Channels " " " " " " " " " " "
d. Records compensated for drag-out.
e. Data reworked and extrapolated to $t = 0$ with $\theta = 35$
h. Bad Calibration
i. Too High Gain

Gage Type	Tape and Head No.	Foot Notes	Gage No.	Depth	Range Slant	Range Horiz.	t_{17}	t_{18}	t_5-t_1	t_3-t_1	t_e (g)	t_s (f)	t_3-t_o	t_{B1}
							Times are in msec							
PE	E-2	e, d	1067	25	5940	5600	—	—	—	—	—	1168	—	—
PE	F-1	c, h	891	25	5940	5600	—	—	—	—	—	1168	—	—
PE	F-7	c, e	891	25	5940	5600	—	—	—	215	—	1168	1382	—
PE	E-3	d	1026	50	5930	5600	—	—	—	215	—	1166	1381	—
PE	F-2	d	1029	100	5915	5600	—	—	—	219	12.6	1164	1383	—
PE	E-4	a, h	823	200	5880	5600	—	—	—	—	—	1157	—	—
PE	E-7	a, d	823	200	5880	5600	—	—	—	244	24.5	1157	1401	—
PE	F-3	d	1031	200	5880	5600	—	—	—	244	24	1158	1402	—
W	E-1		18206	200	5880	5600	8522	—	2810	244	23.9	1157	1401	—
W	F-4		18196	200	5880	5600	—	—	—	244	24.1	1157	1401	—
W	E-8		18207	300	5845	5590	—	—	—	—	36.2	1151	—	—
PE	F-5		825	500	5780	5585	—	—	2801	315	50	1141	1456	—
W	E-10		18209	500	5780	5585	8516	59	2813	—	24	1139	—	2864
W	F-9		18212	500	5780	5585	—	49	2805	315	27.5	1139	1454	2854 to
PE	E-5	b, d	623	1000	5650	5560	—	to 59	2818	—	35	1115	—	2859
PE	E-9	b, i	623	1000	5650	5560	8517	—	2807	437	—	1116	1553	—
PE	F-8	d	893	1000	5650	5560	—	—	2812	—	30	1116	—	—
W	F-10		18213	1000	5650	5560	—	8	2803	437	30	1116	1553	2838

Average for 1000 ft gages (PE and corrected Wiancko) $P_1 = 951$

a. Channels having a common indicating mark were recorded from the same gage.
b. Channels " " " " " " " " " " "
c. Channels " " " " " " " " " " "
d. Records compensated for drag-out.
e. Data reworked and extrapolated to $t = 0$ with $\theta = 35$
f. $t_s = t_1 - t_o$ where $t_o = 13$ msec t_s = shock travel time
g. t_o = Time to which θ was measured
h. Bad Calibration
i. Too High Gain

CONFIDENTIAL

Table 8.4—(Continued)

Gage Type	Tape and Head No.	Foot Notes	Gage No.	Depth	Range		Times are in msec					lb-sec/in.^{2}	in.-lbs/in.^{2}
					Slant	Horiz.	t_{B2}	t_{B3}	t_8-t_1	$t_{12}-t_1$	θ	I	E
PE	E-2	e, d	1067	25	5940	5600	—	—	—	—	—	—	—
PE	F-1	c, h	891	25	5940	5600	—	—	—	—	—	—	—
PE	F-7	c, e	891	25	5940	5600	—	—	—	—	—	—	—
PE	E-3	d	1026	50	5930	5600	—	—	—	—	26	—	—
PE	F-2	d	1029	100	5915	5600	—	—	—	—	33.6	—	—
PE	E-4	a, h	823	200	5880	5600	—	—	—	—	—	—	—
PE	E-7	a, d	823	200	5880	5600	—	—	—	—	34	—	—
PE	F-3	d	1031	200	5880	5600	—	—	—	—	34.2	—	—
W	E-1		18206	200	5880	5600	—	—	4948	5433	37.2	—	—
W	F-4		18196	200	5880	5600	—	—	—	—	37.1	—	—
W	E-8		18207	300	5845	5590	—	—	—	—	35.6	19.8	1980
PE	F-5		825	500	5780	5585	—	—	—	5448	33.5	27.9	2820
W	E-10		18209	500	5780	5585	—	—	4903	5441	32.5	27.2	2670
W	F-9		18212	500	5780	5585	—	—	—	5458	32.5	27.5	2870
PE	E-5	b, d	623	1000	5650	5560	—	—	4634	5487	32.8	31.8	2640
PE	E-9	b, i	623	1000	5650	5560	—	—	4836	5466	—	—	—
PE	F-8	d	893	1000	5650	5560	—	—	4805	5472	32.5	32.6	2717
W	F-10		18213	1000	5650	5560	2700	1900	4795	5479	42.2	35.2	2735

Average for 1000 ft gages (PE and corrected Wiancko) P_1 = 951, θ = 35.8, I = 33.2, (K) E = 2697

a. Channels having a common indicating mark were recorded from the same gage.
b. Channels " " " " " " " " " " "
c. Channels " " " " " " " " " " "
d. Records compensated for drag-out.
e. Data reworked and extrapolated to t = 0 with θ = 35
h. Bad Calibration
i. Too High Gain
k. Geometrical average

Average for all gages θ = 34.1

Bubble periods were obtained by counting cycles of the timing reed, which fortunately was sufficiently excited for the necessary time by action of the cavitation closure pulse. The accuracy of these measurements was believed to be ±½ per cent.

There were several other pulses on the records which were not presented or measured for this report. These records will be available for further analysis if this should become necessary.

8.2.5 Buoy String No. 2

Good pressure-time records were obtained from three gages. The remaining four failed to start because the blast-switch cable was accidentally cut during installation by the screws of the USS Bolster. These gages yielded peak pressure only.

All pressures were obtained from the static calibration curves and then increased by 10 per cent. Pressure-time records at 50-, 300-, and 750-ft depths were replotted on semilog paper to obtain peak-pressure values as was done for string No. 1. The estimated accuracy was 12 per cent. Peak pressures from the remaining gages were obtained by applying the overshoot factor measured as described in Sec. 8.2.3. The estimated accuracy was 15 per cent.

Positive durations (t_2) were obtained as before. The 300-ft measurement was somewhat uncertain and may have been anywhere from 16 to 24 msec. The other values were believed to be correct within 3 msec.

Bubble-period measurements for all three gages were poor because of discontinuous timing trace. The reeds were quiet for up to 50 per cent of the records because of the absence of any sizable cavitation pulse. To obtain timing values, it was necessary to estimate the speed

(Text continues on page 195.)

Table 8.5 — YFNB-13 RESULTS

Gage Type	Tape and Head No.	Foot Notes	Gage No.	Depth	Range: Slant	Range: Horiz.	Pressures in psi: P_o	P_1	P_2	P_3	P_5	P_6	P_1 (h)	msec (f): t_1
PE	I-1	a, e	1064	25	8275	8035	—	—	—	—	—	—	—	1653
PE	K-1	a, d	1064	25	8275	8035	—	595	555	-12	—	—	—	1652
PE	I-6	d	1032	25	8275	8035	—	630	582	-25	—	—	—	1653
PE	J-5	c, d	810	50	8270	8035	—	607	525	-29	—	—	—	1652
MPT	46		10	50	8100	7860	—	580	510	—	—	—	—	—
W	I-2		18192	100	8255	8035	36	540	482	-52	—	—	607	1653
MPT	8		11	100	8090	7860	—	580	520	—	—	—	—	—
PE	J-1	b, e	1065	200	8230	8030	—	—	—	—	—	—	—	1647
PE	K-4	b	1065	200	8230	8030	—	615	415	-100	—	—	—	1650
PE	K-2		1033	200	8230	8030	—	618	422	-100	—	—	—	1650
W	I-4		18199	200	8230	8030	86	595	402	-97	—	—	670	1651
W	K-6		18193	200	8230	8030	81	570	400	-100	—	—	640	1651
MPT	33		14	200	8050	7860	—	—	—	—	—	—	—	—
W	K-7		18204	300	8205	8030	140	578	328	-139	—	—	650	1643
MPT	9		15	300	8030	7860	—	570	325	—	—	—	—	—
PE	J-2		1	500	8160	8020	—	740	221	-150	—	—	—	1640
W	I-7		18202	500	8160	8020	224	685	231	-189	—	—	770	1640
W	J-6		18197	500	8160	8020	224	720	228	-188	—	—	810	1642
MPT	48		18	500	8000	7860	—	650	210	—	—	—	—	—
MPT	52		19	750	7950	7860	—	620	130	—	—	—	—	—
PE	J-4		811	1000	8065	8005	—	640	81	-150	—	—	—	1625
PE	K-5		815	1000	8065	8005	—	625	80	-147	—	—	—	1624
W	J-7		18216	1000	8065	8005	452	600	91	-238	25	75	682	1622
W	I-5		18214	1000	8065	8005	—	—	—	—	—	—	—	—
MPT	24		20	1000	7920	7860	—	690	85	—	—	—	—	—

Average for 1000 ft gages (PE and corrected Wiancko) P_1 = 649; with MPT P_1 = 660

a. Channels having a common indicating mark were recorded from same gages.
b. Channels " " " " " " " " "
c. Records compensated for drag-out.
d. Data reworked and extrapolated to $t = 0$ with $\theta = 35$.
e. Bad Calibration
f. $t_s = t_1 - t_o$ where t_o - 13 (NRL) msec
h. Wiancko corrected pressures, see Section 9.2 and Tables 5.1, 6.1, 6.2 and 6.3

CONFIDENTIAL

Table 8.5—(Continued)

Gage Type	Tape and Head No.	Foot Notes	Gage No.	Depth	Range Slant	Range Horiz.	t_2	t_5	t_6	t_7	t_8	t_9	t_{10}	t_{11}	t_{12}
							Times are in msec								
PE	I-1	a, e	1064	25	8275	8035	2.1	—	—	—	—	—	—	—	—
PE	K-1	a, d	1064	25	8275	8035	1.8	—	—	—	—	—	—	—	—
PE	I-6	d	1032	25	8275	8035	2	—	—	—	—	—	—	—	—
PE	J-5	c, d	810	50	8270	8035	3.8	—	—	—	—	—	—	—	—
MPT	46		10	50	8100	7860	4	—	—	—	—	—	—	—	—
W	I-2		18192	100	8255	8035	8.3	4473	—	6114	6292	6266	6992	7004	7104
MPT	8		11	100	8090	7860	10	—	—	—	—	—	—	—	—
PE	J-1	b, e	1065	200	8230	8030	15.6	—	—	—	—	—	—	—	—
PE	K-4	b	1065	200	8230	8030	15.4	—	—	—	—	—	—	—	—
PE	K-2		1033	200	8230	8030	15.6	—	—	—	—	—	—	—	—
W	I-4		18199	200	8230	8030	15.9	—	—	—	—	—	—	—	—
W	K-6		18193	200	8230	8030	15.8	—	—	—	—	—	—	—	—
MPT	33		14	200	8050	7860	—	—	—	—	—	—	—	—	—
W	K-7		18204	300	8205	8030	23.3	—	—	—	—	—	—	—	—
MPT	9		15	300	8030	7860	—	—	21	—	—	—	—	—	—
PE	J-2		1	500	8160	8020	38	—	—	—	—	—	—	—	—
W	I-7		18202	500	8160	8020	37.9	4462	30	6040	6208	6336	6980	6995	7102
W	J-6		18197	500	8160	8020	38.3	4462	32	6040	6208	6336	6980	6995	7102
MPT	48		18	500	8000	7860	—	—	32	—	—	—	—	—	—
MPT	52		19	750	7950	7860	—	—	62	—	—	—	—	—	—
PE	J-4		811	1000	8065	8005	84.1	—	67	—	—	—	—	—	—
PE	K-5		815	1000	8065	8005	84.2	—	64.2	—	—	—	—	—	—
W	J-7		18216	1000	8065	8005	84.2	4453	—	5957	6110	6350	6972	6993	7092
W	I-5		18214	1000	8065	8005	—	—	—	—	—	—	—	—	—
MPT	24		20	1000	7920	7860	—	—	70	—	—	—	—	—	—

Average for 1000 ft gages (PE and corrected Wiancko) $P_1 = 649$; with MPT $P_1 = 660$

a. Channels having a common indicating mark were recorded from same gages.
b. Channels " " " " " " " " "
c. Records compensated for drag-out.
d. Data reworked and extrapolated to $t = 0$ with $\theta = 35$.
e. Bad Calibration

Table 8.5 — (Continued)

Gage Type	Tape and Head No.	Foot Notes	Gage No.	Depth	Range: Slant	Range: Horiz.	Times are in msec: t_{13}	t_{14}	t_{16}	t_{17}	t_{18}	t_5-t_1	θ	t_θ (g)
PE	I-1	a, e	1064	25	8275	8035	—	—	—	—	—	—	—	—
PE	K-1	a, d	1064	25	8275	8035	—	—	—	—	—	—	—	—
PE	I-6	d	1032	25	8275	8035	—	—	—	—	—	—	—	—
PE	J-5	c, d	810	50	8270	8035	—	—	—	—	—	—	—	—
MPT	46		10	50	8100	7860	—	—	—	—	—	2800	—	—
W	I-2		18192	100	8255	8035	7146	—	—	9045	—	2820	54	8.3
MPT	8		11	100	8090	7860	—	—	—	—	—	2840	—	—
PE	J-1	b, e	1065	200	8230	8030	—	—	—	—	—	—	—	—
PE	K-4	b	1065	200	8230	8030	—	—	—	—	—	—	—	—
PE	K-2		1033	200	8230	8030	—	—	—	—	—	—	40.7	15.6
W	I-4		18199	200	8230	8030	—	—	—	—	—	—	38.7	15.9
W	K-6		18193	200	8230	8030	—	—	—	—	—	—	44	15.8
MPT	33		14	200	8050	7860	—	—	—	—	—	—	—	—
W	K-7		18204	300	8205	7860	—	—	—	—	—	—	51	10
MPT	9		15	300	8030	8020	—	—	—	—	—	2890	—	—
PE	J-2		1	500	8160	8020	—	—	—	—	—	2808	25.2	7.5
W	I-7		18202	500	8160	8020	7140	7835	8958	9040	—	2822	30	15
W	J-6		18197	500	8160	8020	7140	7835	8958	9040	—	2820	30.7	17.5
MPT	48		18	500	8000	7860	—	—	—	—	—	2820	—	—
MPT	52		19	750	7950	7860	—	—	—	—	—	2780	—	—
PE	J-4		811	1000	8065	8005	—	—	—	—	—	2827	45	22.5
PE	K-5		815	1000	8065	8005	—	—	—	—	—	—	47.7	25
W	J-7		18216	1000	8065	8005	7132	7710	8933	9015	57 to 87	2831	50.9	30
W	I-5		18214	1000	8065	8005	—	—	—	—	—	—	—	—
MPT	24		20	1000	7920	7860	—	—	—	—	—	2780	—	—

Average for 1000 ft gages (PE and corrected Wiancko) $P_1 = 649$; with MPT $P_1 = 660$, $\theta = 47.8$

a. Channels having a common indicating mark were recorded from same gages.
b. Channels " " " " " " " " " "
c. Records compensated for drag-out.
d. Data reworked and extrapolated to $t = 0$ with $\theta = 35$.
e. Bad Calibration
g. t_θ = Time to which θ was measured

Average for all gages $\theta = 41.6$

Table 8.5 — (Continued)

Gage Type	Tape and Head No.	Foot Notes	Gage No.	Depth	Range Slant	Range Horiz.	lbs-sec/in.^{2} I	in.-lbs/in.^{2} E	Back Pressure	Sensing Element Range (psi)
PE	I-1	a, e	1064	25	8275	8035	—	—	—	—
PE	K-1	a, d	1064	25	8275	8035	—	—	—	—
PE	I-6	d	1032	25	8275	8035	—	—	—	—
PE	J-5	c, d	810	50	8270	8035	—	—	—	—
MPT	46		10	50	8100	7860	—	—	1000	500
W	I-2		18192	100	8255	8035	—	—	—	—
MPT	8		11	100	8090	7860	—	—	600	300
PE	J-1	b, e	1065	200	8230	8030	—	—	—	—
PE	K-4	b	1065	200	8230	8030	—	—	—	—
PE	K-2		1033	200	8230	8030	—	—	—	—
W	I-4		18199	200	8230	8030	—	—	—	—
W	K-6		18193	200	8230	8030	—	—	—	—
MPT	33		14	200	8050	7860	—	—	400	200
W	K-7		18204	300	8205	8030	10.5	866	—	—
MPT	9		15	300	8030	7860	—	—	600	300
PE	J-2		1	500	8160	8020	15.9	1301	—	—
W	I-7		18202	500	8160	8020	15.2	1180	—	—
W	J-6		18197	500	8160	8020	16.9	1304	—	—
MPT	48		18	500	8000	7860	—	—	600	300
MPT	52		19	750	7950	7860	—	—	600	200
PE	J-4		811	1000	8065	8005	23.7	1575	—	—
PE	K-5		815	1000	8065	8005	23.6	1550	—	—
W	J-7		18216	1000	8065	8005	23.7	1517	—	—
W	I-5		18214	1000	8065	8005	—	—	—	—
MPT	24		20	1000	7920	7860	—	—	1000	500

Average for 1000 ft gages (PE and corrected Wiancko) P_1 = 649; with MPT P_1 = 660, I = 23.6 (h) and E = 1547

a. Channels having a common indicating mark were recorded from same gages.
b. Channels " " " " " " " " " "
c. Records compensated for drag-out.
d. Data reworked and extrapolated to t = 0 with θ = 35.
e. Bad Calibration
h. Geometrical Average

Table 8.5—(Continu~d)

Gage Type	Tape and Head No.	Foot Notes	Gage No.	Depth	Range: Slant	Range: Horiz.	$t_s(f)$	t_{B1}	t_{B2}	t_{B3}	t_8-t_1	$t_{12}-t_1$
PE	I-1	a, e	1064	25	8275	8035	1640	—	—	—	—	—
PE	K-1	a, d	1064	25	8275	8035	1639	—	—	—	—	—
PE	I-6	d	1032	25	8275	8035	1640	—	—	—	—	—
PE	J-5	c, d	810	50	8270	8035	1639	—	—	—	—	—
MPT	46		10	50	8100	7860	—	—	—	—	—	—
W	I-2		18192	100	8255	8035	1640	—	—	—	4639	5451
MPT	8		11	100	8090	7860	—	—	—	—	—	—
PE	J-1	b, e	1065	200	8230	8030	1634	—	—	—	—	—
PE	K-4	b	1065	200	8230	8030	1637	—	—	—	—	—
PE	K-2		1033	200	8230	8030	1637	—	—	—	—	—
W	I-4		18199	200	8230	8030	1638	—	—	—	—	—
W	K-6		18193	200	8230	8030	1638	—	—	—	—	—
MPT	33		14	200	8050	7860	—	—	—	—	—	—
W	K-7		18204	300	8205	8030	1630	—	—	—	—	—
MPT	9		15	300	8030	7860	—	—	—	—	—	—
PE	J-2		1	500	8160	8020	1627	—	—	—	—	—
W	I-7		18202	500	8160	8020	1627	—	—	—	4568	5462
W	J-6		18197	500	8160	8020	1629	—	—	—	4566	5460
MPT	48		18	500	8000	7860	—	—	—	—	—	—
MPT	52		19	750	7950	7860	—	—	—	—	—	—
PE	J-4		811	1000	8065	8005	1612	—	—	—	4482	5505
PE	K-5		815	1000	8065	8005	1611	—	—	—	—	—
W	J-7		18216	1000	8065	8005	1609	2881 to 2911	2600	2000	4468	5450
W	I-5		18214	1000	8065	8005	—		—	—	—	—
MPT	24		20	1000	7920	7860	—	—	—	—	—	—

Average for 1000 ft gages (PE and corrected Wiancko) P_1 = 649; with MPT P_1 = 660

a. Channels having a common indicating mark were recorded from same gages.
b. Channels " " " " " " " "
c. Records compensated for drag-out.
d. Data reworked and extrapolated to t = 0 with θ = 35.
e. Bad Calibration
f. $t_s = t_1 - t_o$ where t_o = 13 (NRL) msec (t_s = shock travel time)

Table 8.8—YFNB-29 RESULTS

Gage Type	Tape and Head No.	Foot Notes	Gage No.	Depth	Range		Pressures in psi								msec
					Slant	Horiz.	P_o	P_1	P_2	P_3	P_5	P_6	P_1(i)	t_1(g)	t_2
PE	H-1	a	817	25	11205	11030	—	374	362	-5	—	—	—	2254	1.1
PE	H-7	a, d	817	25	11205	11030	—	380	358	-4	—	—	—	2253	1.1
PE	G-4	d	1034	25	11205	11030	—	382	359	-5	—	—	—	2254	1.1
PE	H-4	c,. d	1036	50	11200	11025	—	350	308	-7.5	—	—	—	2252	2.8
MPT	11		1	50	11060	10865	—	410	—	—	—	—	—	—	—
W	G-2		17159	100	11190	11030	46	373	335	-40	—	—	415	2247	5
MPT	38		3	100	11020	10865	—	430	—	—	—	—	—	—	—
PE	G-1	b, e	821	200	11175	11025	—	—	—	—	—	—	—	2249	10.2
PE	G-7	b	821	200	11175	11025	—	332	280	-29	—	—	—	2248	10
PE	H-5	f	1035	200	11175	11025	—	—	—	—	—	—	—	—	—
W	G-3		17161	200	11175	11025	92	380	324	-58	—	—	423	2251	9.7
W	H-2		17160	200	11175	11025	78	370	328	-29	—	—	412	2251	9.6
MPT	35		5	200	10980	10865	—	320	—	—	—	—	—	—	—
W	G-9		18195	300	11155	11025	125	370	301	-73	—	—	415	2249	14.5
MPT	34		9	300	10980	10865	—	480	—	—	—	—	—	—	—
PE	G-5	d, c	902	500	11125	11025	—	510	253	—	—	—	—	2246	22.5
W	H-3		18194	500	11125	11025	218	484	255	-102	—	—	544	2244	22.5
W	H-9		18198	500	11125	11025	202	472	248	-100	—	—	530	2246	22.8
MPT	10		6	500	10970	10865	—	700	—	—	—	—	—	—	—
MPT	13		7	750	10940	10865	—	700	—	—	—	—	—	—	—
PE	G-8		1066	1000	11065	11020	—	478	113	-124	—	—	—	2241	52.6
PE	H-8		896	1000	11065	11020	—	462	106	-164	—	—	—	2241	53.5
W	G-10		18200	1000	11065	11020	434	425	112	-178	23	60	477	2238	53.2
W	H-10		18205	1000	11065	11020	438	444	112	-182	—	—	500	2241	52.8
MPT	14		8	1000	10910	10865	—	630	—	—	—	—	—	—	—

Average for 1000 ft gages (PE and corrected Wiancko) $P_1 = 480$; with MPT $P_1 = 506$ (Geometrical averages)

a. Channels having a common indicating mark were recorded from same gages.
b. Channels " " " " " " " " " "
c. Records compensated for drag-out.
d. Original data used and extrapolated to $t = 0$ with $\theta = 35$.
e. Bad Calibration
f. Bad Gage
g. $t_s = t_1 - t_o$ where $t_o = 13$ (NRL) msec t_s = shock travel time
i. Wiancko corrected pressures, see Section 9.2 and Tables 5.1, 6.1, 6.2, and 6.3.

Table 8.6—(Continued)

Gage Type	Tape and Head No.	Foot Notes	Gage No.	Depth	Range Slant	Range Horiz.	t_5	t_6	t_7	t_8	t_9	t_{10}	t_{11}	t_{12}	t_{14}	t_{16}
							Times are in msec									
PE	H-1	a	817	25	11205	11030	—	—	—	—	—	—	—	—	—	—
PE	H-7	a, d	817	25	11205	11030	—	—	—	—	—	—	—	—	—	—
PE	G-4	d	1034	25	11205	11030	—	—	—	—	—	—	—	—	—	—
PE	H-4	c, d	1036	50	11200	11025	—	—	—	—	—	—	—	—	—	—
MPT	11		1	50	11060	10865	—	—	—	—	—	—	—	—	—	—
W	G-2		17159	100	11190	11030	5076	—	6436	6519	—	—	—	—	—	—
MPT	38		3	100	11020	10865	—	—	—	—	—	—	—	—	—	—
PE	G-1	b, e	821	200	11175	11025	—	—	—	—	—	—	—	—	—	—
PE	G-7	b	821	200	11175	11025	—	—	—	—	—	—	—	—	—	—
PE	H-5	f	1035	200	11175	11025	—	—	—	—	—	—	—	—	—	—
W	G-3		17161	200	11175	11025	—	—	—	—	—	—	—	—	—	—
W	H-2		17160	200	11175	11025	—	—	—	—	—	—	—	—	—	—
MPT	35		5	200	10980	10865	—	—	—	—	—	—	—	—	—	—
W	G-9		18195	300	11155	11025	—	—	—	—	—	—	—	—	—	—
MPT	34		9	300	10980	10865	—	—	—	—	—	—	—	—	—	—
PE	G-5	d, c	902	500	11125	11025	—	—	—	—	—	—	—	—	—	—
W	H-3		18194	500	11125	11025	5067	16.8	6358	6446	6523	—	—	7693	—	7733
W	H-9		18198	500	11125	11025	—	18	—	6447	—	—	—	7789	—	—
MPT	10		6	500	10970	10865	—	—	—	—	—	—	—	—	—	—
MPT	13		7	750	10940	10865	—	—	—	—	—	—	—	—	—	—
PE	G-8		1066	1000	11065	11020	—	40	—	—	—	—	—	—	—	—
PE	H-8		896	1000	11065	11020	—	—	—	—	—	—	—	—	—	—
W	G-10		18200	1000	11065	11020	5067	—	6257	6346	6640	7588	7602	7711	7835	7750
W	H-10		18205	1000	11065	11020	5130	37.7	—	6413	—	—	—	7814	—	—
MPT	14		8	1000	10910	10865	—	—	—	—	—	—	—	—	—	—

Average for 1000 ft gages (PE and corrected Wiancko) $P_1 = 480$; with MPT $P_1 = 506$ (Geometrical Averages)

a. Channels having a common indicating mark were recorded from same gages.
b. Channels " " " " " " " " " "
c. Records compensated for drag-out.
d. Original data used and extrapolated to $t = 0$ with $\theta = 35$.
e. Bad Calibration
f. Bad Gage

Table 8.6—(Continued)

Gage Type	Tape and Head No.	Foot Notes	Gage No.	Depth	Range Slant	Range Horiz.	t_{17}	t_{18}	t_5-t_1	Θ	$t_Θ$(h)	t_s(g)	t_{B1}	t_{B2}
PE	H-1	a	817	25	11205	11030	—	—	—	—	—	2241	—	—
PE	H-7	a, d	817	25	11205	11030	—	—	—	—	—	2240	—	—
PE	G-4	d	1034	25	11205	11030	—	—	—	—	—	2241	—	—
PE	H-4	c, d	1036	50	11200	11025	—	—	—	—	—	2239	—	—
MPT	11		1	50	11060	10865	—	—	—	—	—	—	—	—
W	G-2		17159	100	11190	11030	—	—	2829	47.9	5	2234	—	—
MPT	38		3	100	11020	10865	—	—	—	—	—	—	—	—
PE	G-1	b, e	821	200	11175	11025	—	—	—	—	—	2236	—	—
PE	G-7	b	821	200	11175	11025	—	—	—	59.7	10	2235	—	—
PE	H-5	f	1035	200	11175	11025	—	—	—	—	—	—	—	—
W	G-3		17161	200	11175	11025	—	—	—	68.2	9.7	2238	—	—
W	H-2		17160	200	11175	11025	—	—	—	74.5	9.6	2238	—	—
MPT	35		5	200	10980	10865	—	—	—	—	—	—	—	—
W	G-9		18195	300	11155	11025	—	—	—	85.9	12.5	2236	—	—
MPT	34		9	300	10980	10865	—	—	—	—	—	—	—	—
PE	G-5	d, c	902	500	11125	11025	—	—	—	32.5	22.5	2233	—	—
W	H-3		18194	500	11125	11025	—	—	2823	34	10	2231	—	—
W	H-9		18198	500	11125	11025	—	—	2824	36.5	10	2233	—	—
MPT	10		6	500	10970	10865	—	—	—	—	—	—	—	—
MPT	13		7	750	10940	10865	—	—	—	—	—	—	—	—
PE	G-8		1066	1000	11065	11020	—	—	—	57.5	12.5	2228	—	—
PE	H-8		896	1000	11065	11020	—	—	—	62.5	15	2228	—	—
W	G-10		18200	1000	11065	11020	9630	60 to 65	3829	126(j)	20	2225	2889 to 2894	2660
W	H-10		18205	1000	11065	11020	—	—	2889	49	10	2228	—	—
MPT	14		8	1000	10910	10865	—	—	—	—	—	—	—	—

Average for 1000 ft gages Θ = 56.3, Average for all gages Θ = 55.3

a. Channels having a common indicating mark were recorded from same gages.

b. Channels " " " " " " " " " , "

c. Records compensated for drag-out.

d. Original data used and extrapolated to t = 0 with Θ = 35.

e. Bad Calibration

f. Bad Gage

g. $t_s = t_1 - t_o$ where t_o = 13 (NRL) msec t_s = shock travel time

h. $t_Θ$ = Time to which Θ was measured.

j. 126 value not used in averages.

CONFIDENTIAL

Table 8.6 — (Continued)

Gage Type	Tape and Head No.	Foot Notes	Gage No.	Depth	Range Slant	Range Horiz.	lbs-sec/in.^{2} I	in.-lbs/in.^{2} E	Back Pressure	Sensing Element Range (psi)	Times are in msec t_{B3}	t_8-t_1	$t_{12}-t_1$
PE	H-1	a	817	25	11205	11030	—	—	—	—	—	—	—
PE	H-7	a, d	817	25	11205	11030	—	—	—	—	—	—	—
PE	G-4	d	1034	25	11205	11030	—	—	—	—	—	—	—
PE	H-4	c, d	1036	50	11200	11025	—	—	—	—	—	—	—
MPT	11		1	50	11060	10865	—	—	600	300	—	—	—
W	G-2		17159	100	11190	11030	—	—	—	—	—	4272	—
MPT	38		3	100	11020	10865	—	—	300	150	—	—	—
PE	G-1	b, e	821	200	11175	11025	—	—	—	—	—	—	—
PE	G-7	b	821	200	11175	11025	—	—	—	—	—	—	—
PE	H-5	f	1035	200	11175	11025	—	—	—	—	—	—	—
W	G-3		17161	200	11175	11025	—	—	—	—	—	—	—
W	H-2		17160	200	11175	11025	—	—	—	—	—	—	—
MPT	35		5	200	10980	10865	—	—	300	150	—	—	—
W	G-9		18195	300	11155	11025	5.15	300	—	—	—	—	—
MPT	34		9	300	10980	10865	—	—	400	200	—	—	—
PE	G-5	d, c	902	500	11125	11025	8.38	561	—	—	—	—	—
W	H-3		18194	500	11125	11025	8.02	520	—	—	—	4201	5449
W	H-9		18198	500	11125	11025	8.03	518	—	—	—	4201	5543
MPT	10		6	500	10970	10865	—	—	600	300	—	—	—
MPT	13		7	750	10940	10865	—	—	600	300	—	—	—
PE	G-8		1066	1000	11065	11020	15.1	838	—	—	—	—	—
PE	H-8		896	1000	11065	11020	14.6	820	—	—	—	—	—
W	G-10		18200	1000	11065	11020	14.5	868	—	—	1900	4108	5473
W	H-10		18205	1000	11065	11020	14.6	806	—	—	—	4172	5573
MPT	14		8	1000	10910	10865	—	—	600	300	—	—	—

Average for 1000 ft gages (PE and corrected Wiancko) P_1 = 480 with MPT P_1 = 506, I = 14.7, E = 846 (k)

a. Channels having a common indicating mark were recorded from same gages.
b. Channels " " " " " " " " "
c. Records compensated for drag-out.
d. Original data used and extrapolated to t = 0 with θ = 35.
e. Bad Calibration
f. Bad Gage (k) Geometrical average of or P_1 and I; arithmetic average of E.

SECRET – RESTRICTED DATA

CONFIDENTIAL

of the drum during the period when the reed was still. However, measurements from periods when the reed was moving showed that there was a considerable variation in drum speed, and thus the use of an average was unreliable. The values recorded, therefore, represent the means between maximum and minimum readings and have a spread of 400 msec.

This doubt might have been resolved and the errors reduced by a speed-time calibration for each gage since it was likely that the speed changes would have been reproducible. This work was not undertaken since there were excellent timing results obtained from the electronic gages on the YFNB's.

There were several other pulses on the records which were not measured or presented.

8.2.6 Location of Buoy Strings

As discussed in Chap. 7, the location of buoy string No. 1 was determined from photographs taken ½ hr before shot time. Buoy string No. 2 could not be found in the photographs and therefore must have broken free before the photographs were taken. It was also possible that buoy string No. 1 broke free during the last ½ hr before the shot.

An independent check on position was made by replotting Brockhurst's predicted curves[1] of pulse duration vs range in Fig. 8.11. Measured values from NOL electronic results on the YFNB's are also shown for comparison. In general, the measured durations from the electronic gages were a little longer at a given distance than Brockhurst's. The NOL curves were extrapolated to the buoy string No. 1 position. This was quite risky, and not much faith was put in it. The curves at 300 and 750 ft were interpolated.

The values of t_2 measured by the mechanical pressure-time gages were then located on the NOL data curves. The best value for buoy string No. 1 appeared to be 2900 ft; the best value for buoy string No. 2 was 8700 ft. If a new set of curves based on the technique of reference 1 and the actual temperature gradient existing during Wigwam were available, a slightly better determination of the position of buoy string No. 1 might be made.

8.2.7 YFNB-12

This string was not lowered because of malhandling, and therefore it gave no results. It was realized in advance that even having the ball crushers and the mechanical pressure-time gages on the same string would add to the lowering difficulties. The addition of the camera to this was felt to be quite risky, but it was desired to keep instrument strings from the YFNB's to a minimum to reduce the possibility of their fouling one another. Because the unusually heavy weather required the string to be lowered at night at the last possible minute, there was not time to correct the handling difficulties.

With 1 hr more of time, the mechanical pressure-time and ball-crusher gages could have been lowered from the YFNB-12 without lowering the camera. In fact, at 0600 the first ball crushers and mechanical gages were connected to a spare lowering line, which was powered by the niggerhead of the YFNB tow winch. At this point, power was secured on the YFNB-12 and orders were given to evacuate. Considerable protest was made to the commanding officer, and it was pointed out that, by changing the original 0800 evacuation time, many valuable data would be lost. Nevertheless, the order remained, and the scientists were herded off the vessel at 0630, 5 hr before shot time. On the YFNB-13 the evacuation was made at 0900.

8.2.8 YFNB-13

This string yielded six pressure-time records. Unfortunately, the gages at the 300-, 500-, 750-, and 1000-ft depths all started after shock arrival by 15 to 45 msec. The 300-, 500-, and 1000-ft gages were connected to the EG&G relay that was set to close at zero time; this would have given almost 2 sec of running before shock arrival. The reason for this electrical failure is unknown.

The 750-ft gage was connected to a blast switch at the 300-ft depth, and therefore it was expected to start late if the shock front reached the 750-ft depth ahead of the 300-ft depth. This may have happened, since the pressures were considerably higher at 750 ft than at 300 ft.

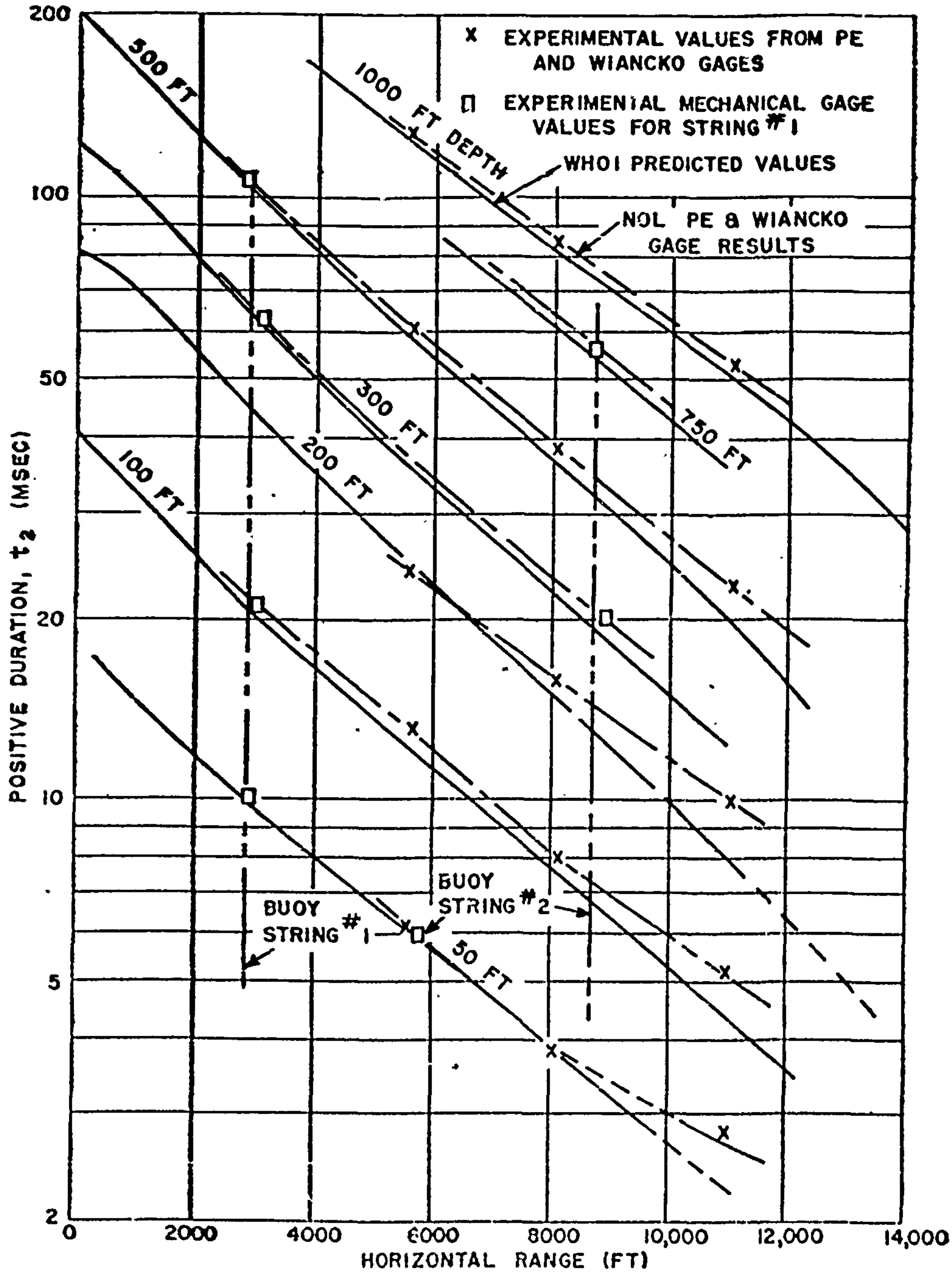

Fig. 8.11—Comparison of Woods Hole Oceanographic Institution predicted values of duration with the experimental values.

The values for p_1 and p_2 for the 50- and 100-ft gages were obtained from the pressure-time curves and the static calibration curves with a 10 per cent dynamic correction added, as was explained previously. For the 750-ft gage the percentage overshoot was obtained from the bubble-pulse record, which was very clear, and was applied to the maximum displacement of the stylus to obtain a peak pressure to which was added the dynamic correction. No calibration was made on this element because of corrosion damage.

Peak pressures for the 300-, 500-, and 1000-ft gages were obtained by reconstructing the record on semilog paper in such a position that the cutoff (t_2) was as recorded by electronic gages on the YFNB-13. The slope of the pressure-decay curve was then extrapolated to zero time and read for peak pressure. Then the dynamic correction was added as for other gages. Cutoff pressure values were also increased by 10 per cent. This method seemed satisfactory for the 300- and 500-ft gages which were not delayed much in starting; however, there was so much latitude in extrapolating the curve for the 1000-ft gage that results from the latter might be as much as 20 per cent off. The other pressure values were believed to be within 12 per cent of the true value.

Bubble periods (t_{B1}, t_{B2}, and t_{B3}; or $t_5 - t_1$ in the case of mechanical pressure-time gages) were determined by counting timing-reed cycles on the records from the 50-, 100-, and 750-ft-depth gages; on records from the other gages the periods were determined by a combination of counting cycles and estimating speed when the reed was still. The values for the former were believed to be accurate to within 40 msec. The values for the latter could be off as much as 100 msec.

There were several other pulses, evident on all the records from this string, which were quite distinct and which might be compared with those from electronic gages. Such a comparison was considered unnecessary for this report.

8.2.9 YFNB-29

Seven peak-pressure records were obtained from this location. None of the gages operated to give pressure-time records because of electrical failure, probably in the splices in the cable. The blast-switch and explosive triggers were tested after recovery and found satisfactory. Testing of the EG&G relay system was not possible, and testing of the cable continuity after lowering was not practicable for lack of time. The molded rubber covering of one of the splices was found damaged. This was probably caused by air pressure leaking from one of the gages through the stuffing gland and up into the cable, where it probably blew up the splice cover like a balloon. The fact that the charging pressure of 600 psi had all leaked out of the 50-ft gage supports this theory.

The elements of the 50-, 100-, 200-, 300-, and 500-ft gages were tested with the explosion chamber to determine the degree of overshoot. The peak deflection was corrected by this factor before obtaining a pressure from the static calibration curve. It was not possible to test the 750- and 1000-ft gages in this manner. These pressure values, therefore, were not corrected for overshoot. All values obtained were believed to be accurate to ±15 per cent.

8.2.10 Conclusions

Although there were many casualties due to heavy weather and development was incomplete, the results showed that the mechanical pressure-time gages actually accomplished the purpose for which they were designed, i.e., to back up electronic instrumentation. A great deal of interesting and useful information was obtained by buoy string No. 1, which became especially valuable because of the failure of other systems in the region between the YFNB-13 and the YC-976.

No small credit for the success of this string was due to the method used for attaching the string to the towline. There was evidence that the solid-wooden-buoy design was much superior to either the steel-buoy or rubber-buoy design. The 150-ft spar showed itself to be quite seaworthy and effective in separating the buoy string from the towline.

A great deal of experience was obtained in rigging and handling floating objects in a seaway which is not reported here. In general, however, it was once again demonstrated that inertia forces in a seaway are great and that much wear and breakage result if the design is not flexible where connections are made. Steel cable or chain should never be allowed to rub against hard surfaces. Safety and ease of handling were greatly improved by the provision of handling lines long enough so that connections could be made on the deck of the M-boats.

The blast-switch starter system was fundamentally successful. It was reliable and fast. Casualties were principally due to the heavy weather. The switch could have been packaged better, however, to facilitate electrical checks. More care in rigging the starter for buoy string No. 2 could have prevented the cable from being cut. In the case of the YFNB's, not much could have been done to improve the starting time because of the position of the string. If the string had been forward on the vessel, the starter could have been aft and adequate starting time would have been possible. The electrical failures were probably attributable to the rush and the lack of time to make continuity checks after submersion.

Peak-pressure measurements were obtained from pressure-time records that, in general, were believed to be within 12 per cent of the correct values, as indicated by comparison with other gage results. An accuracy of 5 per cent would have been obtained for nearly all the gages if development and testing difficulties could have been eliminated a little sooner. It appeared that this mechanical gage was capable of measuring pressure as accurately as the Wiancko electronic gage, since the principal errors in electronic gage measurement appeared to be caused by mechanical difficulties such as hysteresis.

Pressure distortion due to shock was small and caused no difficulty. The balanced stylus with bearing support seemed to work out fine.

Friction was low, usually causing not over one line width ($\frac{1}{2}$-mil error). The record reading accuracy was therefore within 1 per cent for most values of peak pressure.

An apparent hysteresis was the predominant error mechanism, and more study is needed to understand and eliminate the trouble. This can be corrected by dynamic calibration using a step pressure pulse, but after the step rise the magnitude of the correction is difficult to measure, especially for decaying pulses.

Pressurizing the gage cases turned out to be a nuisance on this test, mostly because of its effect on leaky sensing elements and cable stuffing glands. It was not needed because predicted values were accurate. If predictions had been low by 50 to 100 per cent, it would have saved many records. The sensitivity advantage obtained was of little value because of the apparent hysteresis shown by the dynamic calibration.

Timing-measurement accuracies were not quite so good as desired; however, they are probably satisfactory for cavitation studies and damage predictions, and in this regard the mechanical pressure-time gage system was quite valuable. These measurements may not have been good enough for confirmation of some theoretical predictions.

The clock motor was reliable, but it was deficient in speed control. This, however, would not have mattered for long time measurements if a self-excited timing reed had been provided. Short time measurements would have been better if the harmonics had been eliminated by redesign of the timing reed.

The fact that the drum turned $2\frac{1}{2}$ revolutions caused the styluses to retrace, which in turn caused some confusion in record reading, as was expected. A spiral feed would have solved this but would have complicated the design and introduced more backlash. A larger drum could be used at the cost of some increase in over-all size. A slower speed would have reduced the time resolution. A compromise was necessary to obtain 12 sec of recording time and good pulse-duration resolution. The best answer would have been to reduce the recording-time requirement to 5 sec, which could have been done in 1 revolution, and to use a +2-sec EG&G signal for starting on the YFNB's.

Recording on soot-coated glass with a diamond stylus tip gave good legibility and ease in obtaining photographic enlargements of records. Part of this success was because of the lead and rubber shock mounts which performed excellently in reducing the shock on the recorder. Without the shock mounts some distortion would have been introduced because of chipping of the glass under the stylus tip.

To summarize, the Wigwam test showed that this mechanical pressure-time gage did:

1. Measure step pressure rises with an over-all accuracy better than 12 per cent.

2. Respond to step pressure pulses in a little less than 1 msec, when critically damped.
3. Respond to step pressure pulses in about ½ msec with 0.7 critical damping.
4. Measure pulse durations with a distortion of about ±2 msec.
5. Measure time between events over 1 sec apart with an accuracy of 1 per cent when the timing reed was kept in oscillation.
6. Produce records which could be quickly and easily read and reproduced.
7. Operate satisfactorily under conditions of heavy shock without damage.

In addition, the experience obtained showed that, with a reasonable amount of further development:

1. For short pulses a time resolution of ¼ msec can be obtained by increasing the recording speed by about eight times for gages located near the surface. In addition, the escapement control can be eliminated in favor of a viscous brake, and the worm-shaft play can be lessened.
2. Time resolution of ½ per cent for periods about 1 sec long can be obtained and made certain by using a cam-excited, rotary timing-signal generator, designed to minimize shock-excited harmonics.

Further development might also give better pressure accuracy by virtue of a better understanding of the apparent hysteresis effect of the twisted tube. The lack of a proved standard makes this work difficult.

The addition of an oscillator-driven magnetic stylus might improve the timing resolution for short pulses.

In conclusion, this backup system, consisting of mechanical recorders, blast switches, wooden buoys, and 150-ft spars, was successful in obtaining reasonably accurate data under severe weather difficulties.

8.3 ELECTRONIC PRESSURE-TIME GAGE RESULTS

8.3.1 Use of Wiancko Gages on Wigwam

Thirty-two Wiancko gages were set in the water on Operation Wigwam at depths of 200, 300, 500, and 1000 ft at recording stations 0-1, 0-2, YFNB-12, YFNB-13, and YFNB-29 and at the 100-ft depth on the latter two stations. The pressure rating of the gages used at each of the above locations was determined by the hydrostatic pressure and the predicted values of the shock-wave peak pressure, with the result that the actual total pressure on the gages was between 60 and 100 per cent of the pressure rating of the gages. No performance data on the gages on stations 0-1 and 0-2 were obtained since the recording equipment did not operate and the gages were never recovered. However, all gages were operating satisfactorily at the last check made before setting the gages into the water a few days before shot time. Pressure-time records were obtained on 21 of the 22 gages used on the three YFNB stations, and a direct comparison of results with tourmaline gages was obtained at depths of 200, 500, and 1000 ft.

8.3.2 Comparison of Peak Pressures from Wiancko and Tourmaline Gages

An idealized sketch of a Wigwam pressure-time record showing the quantities measured and defining terms is given as Fig. 8.12. (A portion of an actual Wiancko record is reproduced as Fig. 9.12.) A comparison of peak-pressure results (see Tables 8.4 to 8.6) showed that the values obtained with 14 Wiancko gages were between 90 and 99 per cent of the peak-pressure values obtained with tourmaline gages at the corresponding locations. However, two Wiancko gage peak-pressure values were 114 and 111 per cent of the peak pressure recorded with a tourmaline gage at the same location. These large values were contrary to the consistently low values obtained in the shock-wave performance tests (see Table 5.1). Although no reason for this behavior can be given, it should be mentioned that these large values were compared with a single tourmaline gage value which was unusually low. Furthermore, the two Wiancko gages were never subjected to the shock-wave performance tests. Excluding the two large values, the Wiancko gages recorded, on the average, 94 per cent of the peak shock-wave pressures recorded with tourmaline gages. This value is several per cent larger than the average pressure ratios obtained in the shock-wave performance tests.

DEFINITIONS

- SHOCK TRAVEL TIME = $t_s = t_1 - t_c$
- FIRST BUBBLE PERIOD = $t_{B1} = t_5 - t_1 + t_{18}$
- SECOND BUBBLE PERIOD = $t_{B2} = (t_{10} \rightarrow t_{13}) - (t_5 + t_{18})$
- THIRD BUBBLE PERIOD = $t_{B3} = (t_{16} \rightarrow t_{17}) - (t_{10} \rightarrow t_{13})$
- t_{18} = INTERVAL BETWEEN t_5 AND OCCURRENCE OF MINIMUM VOLUME OF FIRST BUBBLE AS DETERMINED BY RECONSTRUCTION OF COMPLETE PULSE
- t_0 = 29 MSECS (EG+G) OR 13 MSECS (NRL)
- P_0 = HYDROSTATIC PRESSURE (ALL PRESSURES MEASURED FROM P_0)

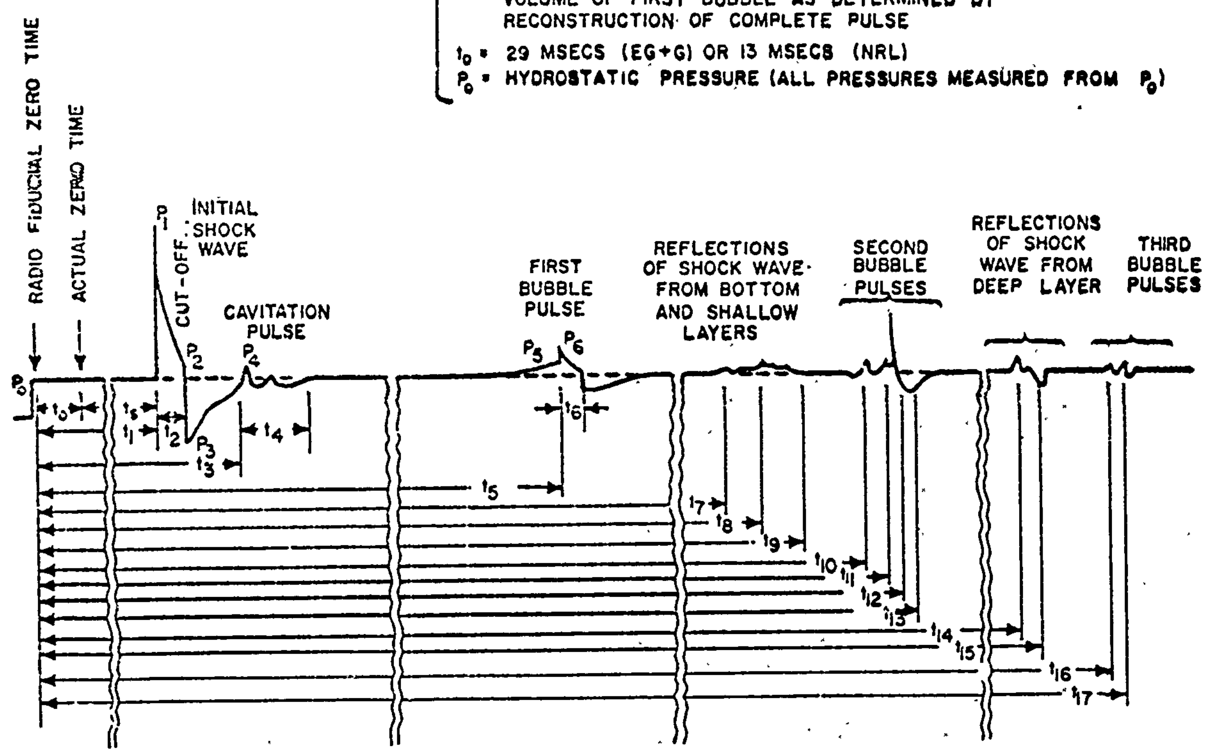

Fig. 8.12—Quantities measured on Wigwam underwater pressure-time records.

8.3.3 Impulse Comparisons

CONFIDENTIAL

A comparison of the reduced impulse (momentum) in the shock wave (the positive area under the shock-wave pressure-time curve) was obtained at depths of 500 and 1000 ft on the three YFNB stations and showed that, in general, the results from the Wiancko gages were again smaller (average value was 97 per cent, excluding two comparisons) than the results from the tourmaline gages at corresponding locations. Possible reasons why the Wiancko gage impulse results were not quite so low, compared with the tourmaline results, as were the corresponding peak-pressure results are that the pressures recorded with tourmaline gages may have decayed too rapidly or that the Wiancko gages may have exhibited hysteresis during the recording of the shock wave, or both. Since several effects, although each may be small, may cause the pressures recorded with tourmaline gages* to decay too rapidly and since hysteresis in the Wiancko gages, although small, may cause the recorded pressures to decay too slowly, it is surprising indeed that the difference between the impulse comparison (97 per cent) and the peak pressure comparison (94 per cent) was so small.

Although no accurate measurement of the mean frequency (gage submerged and under hydrostatic pressure) of the Wiancko gages was possible immediately before and after the Wigwam shot to determine the "permanent" change in frequency, comparisons of the hydrostatic calibrations before and after the shot showed that the mean frequency (at atmospheric pressure) changed by 50 cycles or less on all gages but one. This particular gage, which gave a higher value in the momentum comparison (106 per cent) than was obtained for Wiancko gages on the average, produced an increase of 375 cycles in the mean frequency. Hysteresis in the Wiancko gages was again observed in the hydrostatic calibration after the Wigwam shot. The magnitude of the hysteresis was approximately the same as that discussed above.

8.3.4 Wigwam Signal Rise Times on Wiancko Gages

The rise times recorded with Wiancko gages on the Wigwam shot were between 1 and 2 msec. The accuracy in reading the rise times was determined primarily by the time resolution on the pressure-time records, which was about ½ msec. These rise times were large compared with those recorded in the shock-wave performance tests, the increase in the rise times being caused by the filter used in the playback equipment. This filter was necessary in order to reduce the high-frequency components of flutter and noise recorded from the magnetic tape. Although the slow rise times caused an error in the recorded peak pressures, the results entered in Tables 8.4 to 8.6 were corrected for this error by reading the peak pressure at the intersection of the line representing zero time and the extrapolated straight line on the constructed log pressure vs time plot.

8.3.5 Damage to Wiancko Gages

The 22 Wiancko gages used on the three YFNB stations were calibrated and examined for possible damage after the Wigwam shot. Four gages were found to behave erratically during calibration, but only one of these failed to produce a pressure-time record. Broken wire leads at the pin connection in the glass seal and a shorted power-supply lead caused the gage oscillators in three gages to stop oscillating during calibration.

Although these three gages produced what seemed to be a pressure-time curve without distortion, one of these gages recorded a very low peak-pressure value (90 per cent) but a high value of momentum (109 per cent) when compared with values obtained with the tourmaline gages at the same position. The gage that failed to record pressures produced a gage-oscillator signal that varied considerably in amplitude and frequency during calibration. The gage cases and seals held up very well for there was no evidence of water in any of the gage cases.

*These effects are discussed in the tourmaline gage section in Chap. 5. The Wiancko gages did not show these effects and were capable of maintaining the frequency constant (within the limits of stability of the oscillator) when the applied pressure was held constant.

8.3.6 Other Electronic Pressure-Time Gage Results

Since the electronic pressure-time gages were considered to be the primary instrumentation, with the ball-crusher gages and mechanical pressure-time gages as backup instrumentation, most of the electronic gage results are discussed in Chap. 9. In general, however, conclusions about these gages may be summarized as follows:

1. Both Wiancko and tourmaline gages were rugged, and they operated satisfactorily.
2. They gave peak-pressure results which agreed without correction to about 6 per cent.
3. Agreement between them on impulse measurements was within 3 per cent, on the average.
4. The Wiancko gages apparently remained stable to within 50 cycles of their mean frequency or to within about 2 per cent of their full-scale deviation.
5. Wiancko gages recorded rise times of about $1\frac{1}{2}$ msec on Wigwam because of playback limitations; however, they were capable of rise times as fast as 0.3 msec on high-explosive trials where the playback did not limit the response.
6. Tourmaline gage cable signal was estimated to be less than 0.2 per cent of the recorded shock-wave signal on Wigwam.
7. Dynamic calibrations of the tourmaline gages gave values agreeing with static calibrations to within 7 per cent. These dynamic calibrations were used.
8. Other effects from which tourmaline gages suffer, such as high- and low-frequency distortion, pyroelectric effect, and first-time gage effect, were negligible as determined by field and laboratory tests or were corrected for by suitable calibration or aging techniques.

REFERENCE

1. R. R. Brockhurst, Predictions of the Effect of Refraction on Peak Pressure and Duration of Explosion Pressure Waves, Woods Hole Oceanographic Institution Report 54-14, March 1955.

CHAPTER 9

ANALYSES

9.1 INTRODUCTION

The purpose of this chapter is to present a brief analysis of the data obtained by Project 1.2 from Operation Wigwam. The data discussed in this chapter were presented in Chap. 8 and, where appropriate, were limited to the 1000-ft gages located at the instrumentation stations on the YFNB's 12, 13, and 29. It was felt that the data from these gages (rather than those at more shallow depths) were the only data capable of providing free-field information since they were, by comparison, relatively free from such phenomena as reflection and refraction effects. In other portions of the discussion, data from shallower gages and other stations were used.

9.2 PRESSURE VS DISTANCE CURVES AND TNT EQUIVALENTS

Figure 9.1 shows the peak-pressure measurements obtained at the three YFNB stations for the individual 1000-ft-depth gages. It should be noted that the pressures obtained from the Wiancko gages were usually lower than those from the piezoelectric gages. It is believed that such a systematic difference, although not thoroughly understood, existed fairly consistently whenever the two types of gages were used dynamically. In other words, as was discussed in Sec. 5.1.6, if pressures measured during a dynamic calibration of Wiancko gages were calculated on the basis of static calibration data, the piezoelectric gages read higher by about 10 per cent. If the dynamic calibration procedure was warranted at all, it was necessary to disregard the differences resulting from the use of the static calibration constants (or curves) and use the dynamic calibrations, at least for shock peak pressures. At the time of writing, there was no firm conviction that the Wiancko pressures were "right" and the piezoelectric pressures were "wrong" or vice versa; however, since many of the data were to be compared directly or indirectly with TNT effects, it was decided arbitrarily to consider the piezoelectric measurements as "correct" and to adjust the Wiancko Wigwam data, which had been calculated by the use of static calibration constants, by correction factors* that had been determined during the dynamic calibration process. The choice of piezoelectric over Wiancko measurements was justified since the great bulk of high-explosive data on underwater shock pressures was determined by piezoelectric gages and many empirical relations for pressure and other quantities were based on such data.

Tables 8.4 to 8.6 give the Wiancko pressures before and after correction.

The equivalent value of 46.2×10^6 lb of TNT to produce the same measured peak pressures as were found in Wigwam was obtained by taking the geometric average of the measured

*These correction factors appeared to be 4 or 5 per cent too large in view of the actual Wigwam results.

CONFIDENTIAL

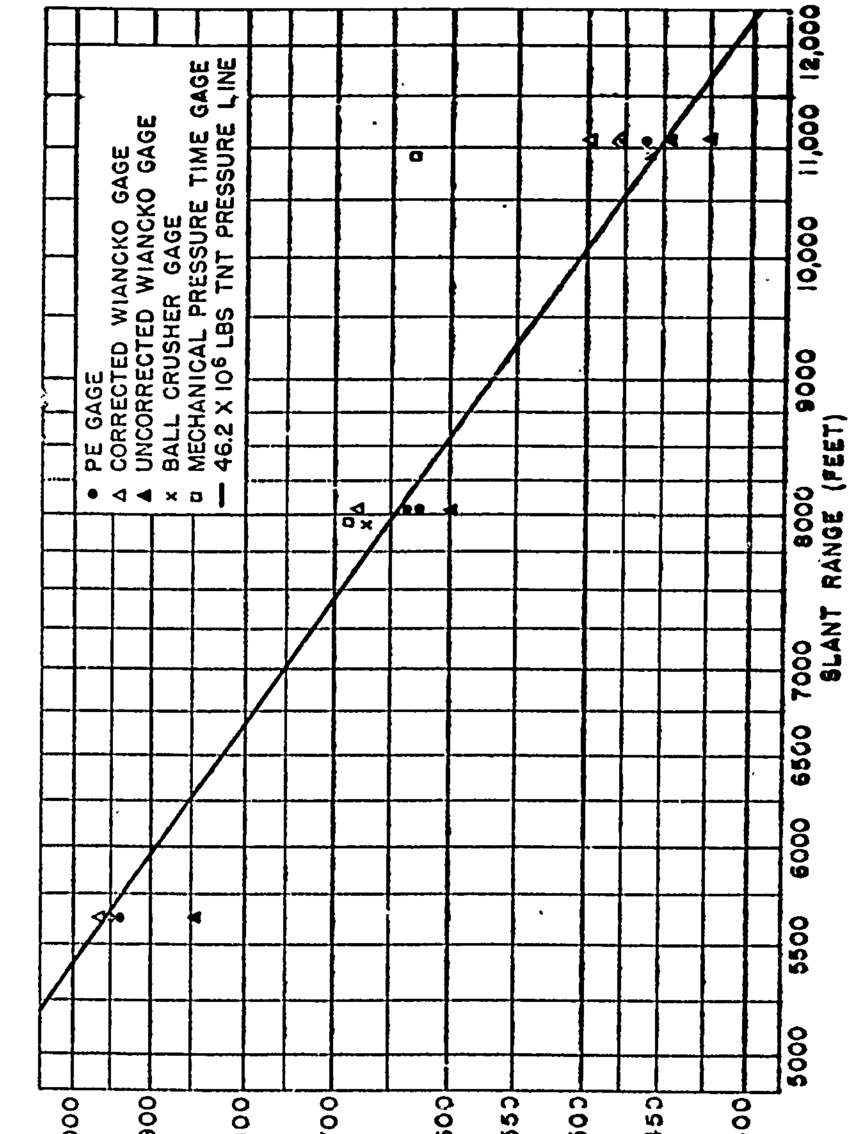

Fig. 9.1—Wigwam peak pressures at 1000-ft depth (YFNB's 12, 13, and 29), showing individual gage data points.

pressures for the 1000-ft-depth gages at the YFNB-12 and YFNB-13 stations and then computing the equivalent weight of TNT by inserting it in the empirical TNT equation:[5]

$$P = 2.16 \times 10^{4} \left(\frac{W^{1/3}}{r}\right)^{1.13} \quad \text{or} \quad W = r^{3}\left(\frac{P}{2.16 \times 10^{4}}\right)^{2.65}$$

where W is the weight of TNT in pounds, P is the pressure in pounds per square inch, and r is the slant range in feet. The pressures obtained at the YFNB-[illegible] station were not used in this determination because it was thought that, at this greater distance error would be introduced from refraction effects (see Sec. 9.8).

Figure 9.2 shows how the averaged (geometric) data from both the NRL[2] and the deep NOL stations compare with the computed 46.2×10^6 lb of TNT pressure line.

At this point it was of interest to investigate the TNT efficiency of the Wigwam shot as far as pressure-distance relations were concerned. In the Project 1.2 preliminary report a value of 40×10^6 lb of TNT was presented; however, upon rereading the data and taking account of various instrumentation errors discussed in previous chapters, the value of 46.2×10^6 lb was found to be a more accurate figure. This figure compares extremely well with the equivalent TNT value of 45.76×10^6 lb predicted by Snay in reference 3. In October 1955, at a meeting of Project Officers in San Francisco, the following radiochemical yield figures were given:

LASL:	32 metric kt	Radiochemistry
NRL:	34 metric kt	
ARF:	30.5 metric kt	Hydrodynamic

where 1 metric kt equals 2.205×10^6 lb of TNT at 1000 cal/g. Alternatively, 1 metric kt equals 10^{12} g-cal or 4.2×10^{19} ergs. Informal talks with Peter King of NRL revealed that the difference between the LASL and NRL figures arose not from a difference in experimental procedures but from the fact that LASL incorporated a number of correction factors unavailable to NRL and based on LASL's extensive experience in this work. Therefore the "efficiency figure" for Wigwam which may be defined as

$$\frac{\text{Yield (shock wave)}}{\text{Yield (radiochemistry)}}$$

becomes

$$\frac{46.2 \times 10^6}{32 \times 2205 \times 10^3} = \frac{46.2 \times 10^6}{70.6 \times 10^6} = 0.65$$

9.3 ENERGY AND IMPULSE VS DISTANCE CURVES

Reference to Fig. 9.3 shows the relation existing between the measured energy at each of the YFNB locations and that which would have been obtained if 46.2×10^6 lb of TNT had been detonated. The shock-wave energy (strictly speaking, this is the shock-wave energy flux) for 46.2×10^6 lb of TNT was computed from the empirical relation[1]

$$E_{TNT} = 2.44 \times 10^{3} (W^{1/3}) \left(\frac{W^{1/3}}{r}\right)^{2.04}$$

where W is in pounds of TNT, r is the slant range in feet, and E, which is integrated out to a time equivalent to 6.7θ, is in inch-pounds per square inch. The experimental points on this graph are again the geometric averages of the energies measured by each of the 1000-ft-depth gages.

Since surface cutoff made it impossible to measure the energy out to 6.7θ, an equivalent TNT energy line, which is shown adjacent to each of the data points, was obtained by determining what the TNT energy would have been if it had been measured only out to the same

CONFIDENTIAL

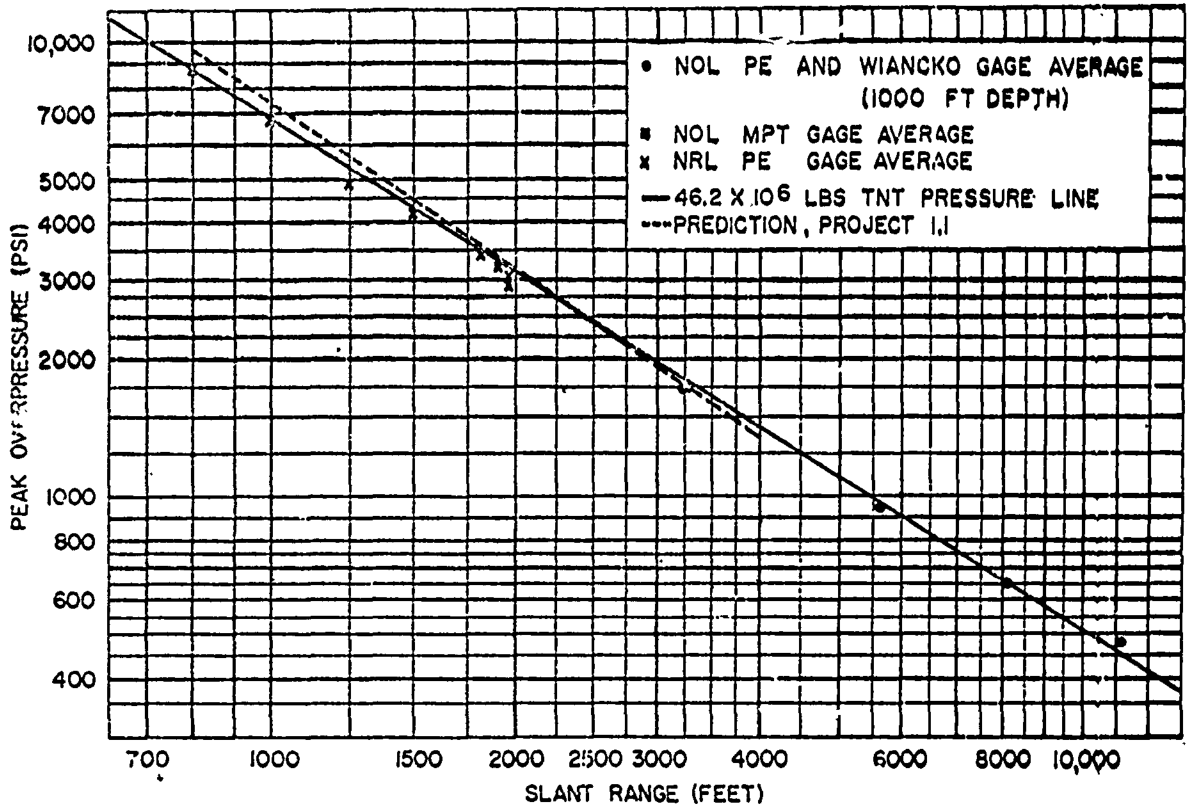

Fig. 9.2—Averaged Wigwam peak pressures compared with those for TNT.

CONFIDENTIAL

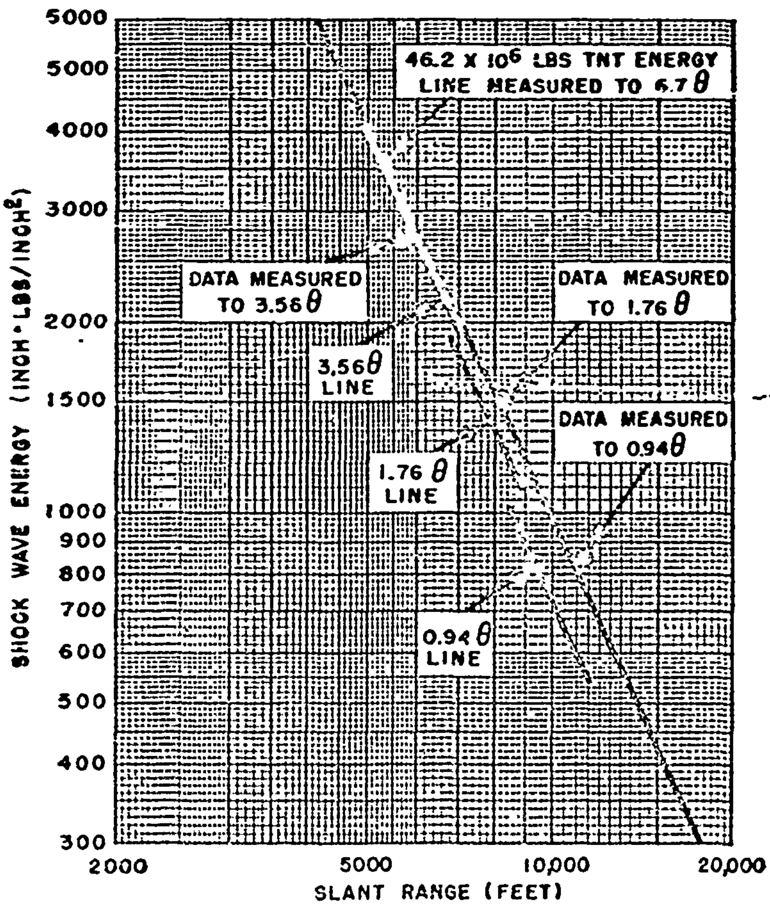

Fig. 9.3—Averaged Wigwam shock-wave energies measured at 1000-ft depth (YFNB's 12, 13, and 29).

time, i.e., to the same number of θ's, as each of the 1000-ft data points. The curve showing the relation of the total energy vs the number of θ's to which the measurement was made is shown in Fig. 9.4. This correction procedure is based upon two arbitrary assumptions: (1) the curve showing the percentage of total energy vs the time to which the measurement was made is the same for TNT as for HBX-2 (the data from which the curve in Fig. 9.4 was compiled) and (2) that the shape of the underwater pressure-time curve generated by the Wigwam bomb was the same as that produced by TNT. It is, at present, thought that there will be no essential differences between the energy-θ curve as obtained from the HBX-2 data and that obtained from TNT. Indications are, however, that the pressure-time relation, and hence the total energy obtained in a nuclear-generated shock wave, may be different from that obtained from a TNT-generated shock wave.

In the range from 1000 to about 15,000 psi (the usual range of measurements), the shock wave from a high-explosive detonation decays exponentially out to a time equal to or greater than the time constant θ (as defined in Sec. 9.4). The decay of Wigwam pressure-time curves could be examined only for the deeper gage positions where surface cutoff did not occur until a time at least as great as θ. For these deeper gages the shock-wave decay was similar to that of a TNT shock wave at the YFNB-12 position. At the YFNB-13 position the shock-wave decay rate deviated from the initial θ value at a time equal to about $\frac{1}{2}\theta$ after the peak pressure; at the YFNB-29 position the deviation occurred even earlier.

Similarly, the shock-wave decay rate of TNT perhaps deviates from the initial θ values at peak-pressure values of about 500 psi since an analysis of high-explosive data on the relation of the duration of the initial exponential decay rate relative to the value of θ in the range 1000 to 15,000 psi indicates that this deviation is possible. However, since no high-explosive data are readily available for direct comparison in the pressure ranges measured at the YFNB-13 and YFNB-29, the TNT and Wigwam integrals at the two greater distances are not necessarily comparable. In other words, if TNT pressure-time curves at all pressure ranges decay exponentially to at least a time θ at their original decay rate, then Wigwam pressure-time curves are not similar to those from TNT. However, it is entirely possible that the decay characteristics of TNT pressure-time curves for pressures less than 1000 psi are not similar to those of TNT at pressure ranges above 1000 psi. If this is so, then the Wigwam decay characteristics may be similar to those of TNT. In either case the effect of refraction on the Wigwam values has to be considered.

Because of these considerations, it is considered coincidental that the measured energies fall so closely to the theoretical 6.7θ line for an equivalent amount of TNT (as determined from peak-pressure measurements). Since no account has been taken in the above analysis of the possible effect of refraction (see Sec. 9.8), the agreement may even be more coincidental than it appears at this time.

Figure 9.5 shows the comparable impulse-distance relation which existed at the three YFNB stations. The construction of this curve followed very closely the same procedures as were outlined for the energy-distance curve and was based upon the same assumptions and limitations. The equation used for the reduced impulse from TNT was

$$I_{TNT} = 1.46W^{1/3}\left(\frac{W^{1/3}}{r}\right)^{0.89}$$

where W is in pounds of TNT, r is the slant range in feet, and I is the impulse in pound-seconds per square inch.[1]

The curve showing the relation of the total impulse of HBX-2 vs the number of θ's to which the measurement was made is shown in Fig. 9.6.

9.4 TIME CONSTANT (θ) VS DISTANCE CURVE

The data plotted in Fig. 9.7 indicate a rather wide variation between the measured time constants and those which could be expected if the Wigwam bomb had been equivalent to a TNT detonation of 46.2×10^6 lb. The equation for TNT which was used was

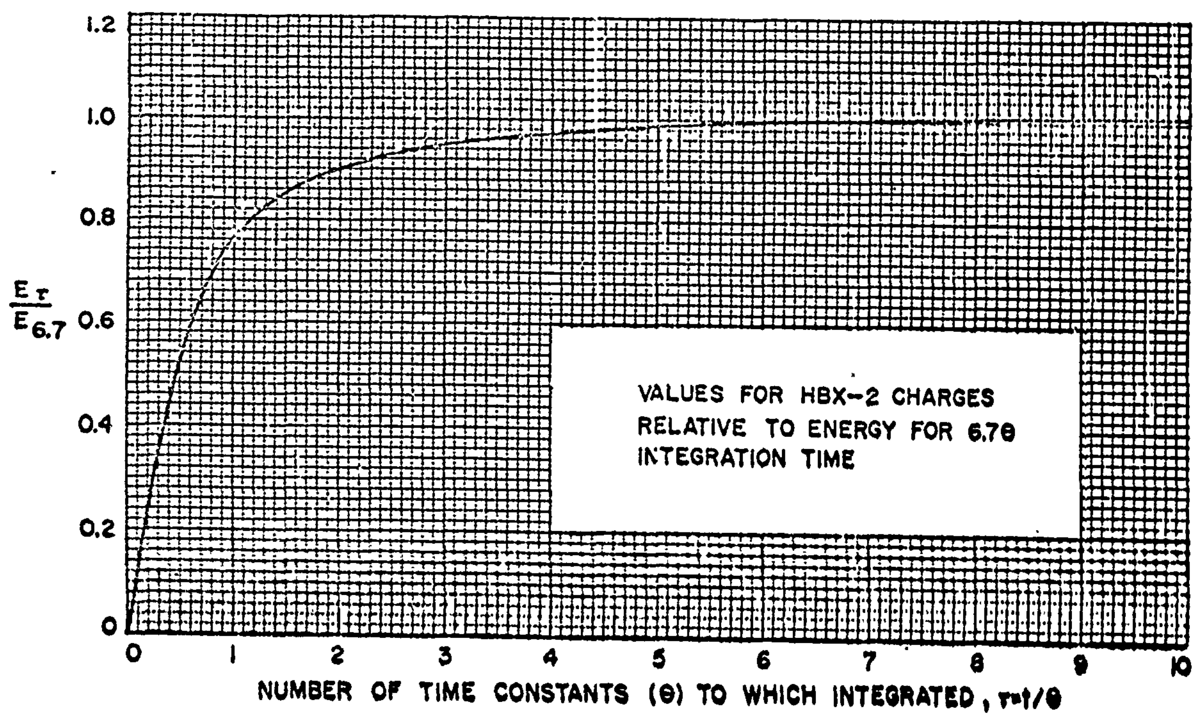

Fig. 9.4—Variation of underwater shock-wave energy, E, with time of integration.

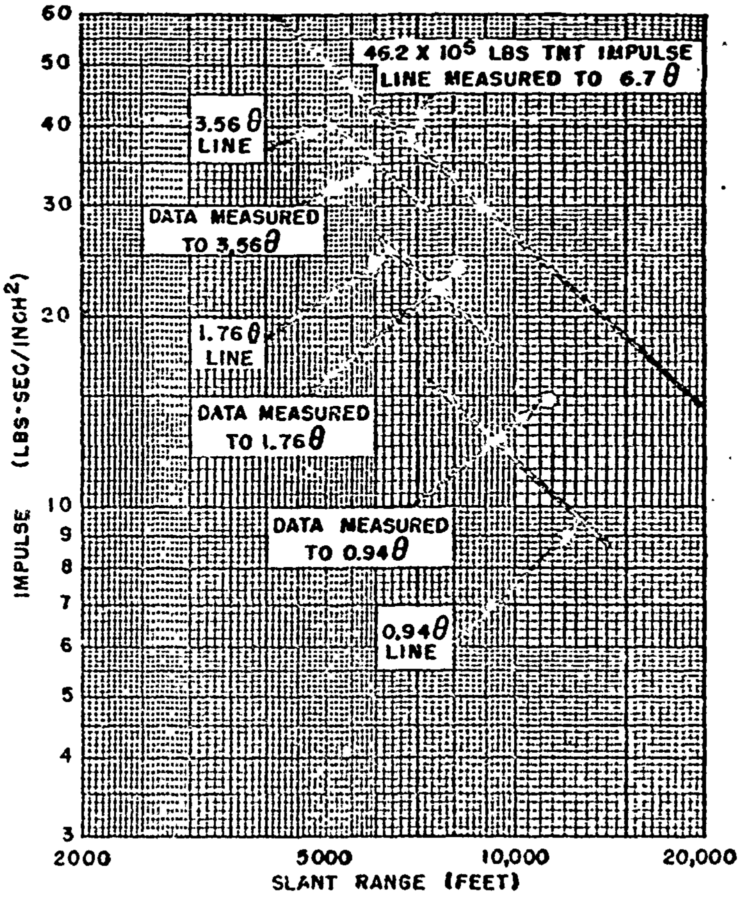

Fig. 9.5—Averaged Wigwam impulses measured at 1000-ft depth (YFNB's 12, 13, and 29).

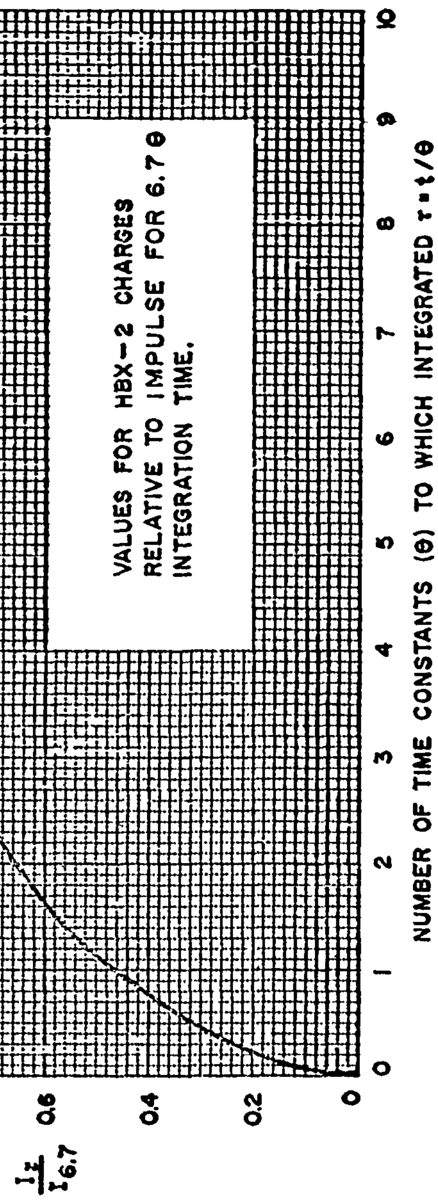

Fig. 9.6—Variation of underwater shock-wave impulse, I_τ with time of integration.

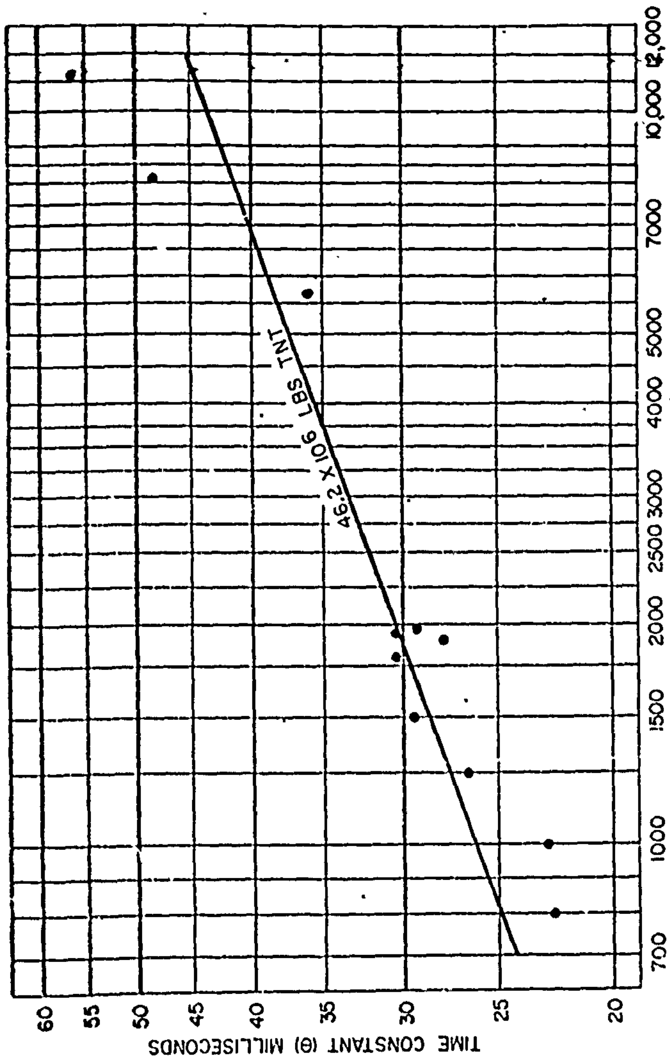

Fig. 9.7—Averaged Wigwam time constants for NOL and NRL stations.

CONFIDENTIAL

$$\theta_{TNT} = 0.058W^{1/3}\left(\frac{W^{1/3}}{r}\right)^{-0.22}$$

where θ is the time in milliseconds for the pressure to fall to $1/e$ of its peak value, assuming that the initial decay was maintained out to this time; W is in pounds of TNT; and r is the slant range in feet.[4]

The NRL values of θ which are plotted in Fig. 9.7 are the geometric averages of the data given in reference 2 for each slant distance. On the other hand, the NOL θ values are the averages for the 1000-ft gages on single strings. To see if θ varied with depth in any simple fashion, some rough plots of θ vs depth for each YFND string showed that θ seemed largest at about 300 ft and smallest at 500 ft, with the values at 200 ft and shallower and at 1000 ft falling between the 300- and 500-ft values. It was suggested that, if refraction were indeed causing this variation, then large θ values should correspond to small peak pressures and vice versa. To test this, p/θ vs depth was plotted for each string; but these values also varied with depth, with a sharp change in the curve at 500 ft. At any rate it was concluded that the discrepancy might well be attributed to refraction effects or to a real difference between the nature of a TNT blast and that produced by the Wigwam weapon as discussed above. It is well to remember the fact that the experimental determination of θ is made graphically and is subject to error, as can be seen by the scatter in the values of θ presented in Tables 8.3 to 8.6. For this reason no great reliability can be placed on the accuracy of those values; however, it might be noted that the differences become somewhat smaller at the closer-in stations (those measured by NRL[2]).

9.5 BUBBLE

From the electronic pressure-time gage records it was possible to speculate about certain bubble characteristics. The following information was desired:

1. The bubble period for each pulsation.
2. The bubble migration between bubble minima.
3. The amplitude of at least the first pulse.
4. An interpretation of the wave shapes observed in the various pulses.

Measurement and analysis of the data showed the above items to be interdependent. For example, a knowledge of the shape of the first bubble pulse was needed in order to measure either the period or the pressure. Some correction was made for the fact that the gage location affected the magnitude and arrival time of the surface cutoff on the bubble pulse; however, no correction to "free-water values" was made for the fact that the bubble migration affected the shape of the pulse.

9.5.1 Bubble Period

The electronic pressure-time gage records of the first bubble pulse showed a sharp-fronted wave at the end of a long, gradual rise in pressure (Fig. 9.8). Shortly thereafter the negative reflection of the sharp-fronted wave from the surface was evident (see Fig. 9.8a). Since there was some doubt that the sharp-fronted wave occurred at the time of the bubble's true minimum volume, the bubble pulse as it would appear at the recording gage if no surface reflection were present was reconstructed using the point-by-point system described on pages 381 and 382 in Cole.[5]

The usual problems of bubble-pulse reconstruction were present in abundance, plus those introduced by additional pressure pulses from cavitation closures during the negative phase following the shock wave. It should be remembered that an additional reason for the low overall accuracy of the bubble reconstruction was that the Wiancko gages supplying the records used in these reconstructions were responding to transient pressures which generated signals almost at the noise level of the recording system during most of the bubble pulse. The records read were selected on the basis of the d-c response of the Wiancko gage. The recording systems used with piezoelectric gages were thought to have poor response to negative pressures, and

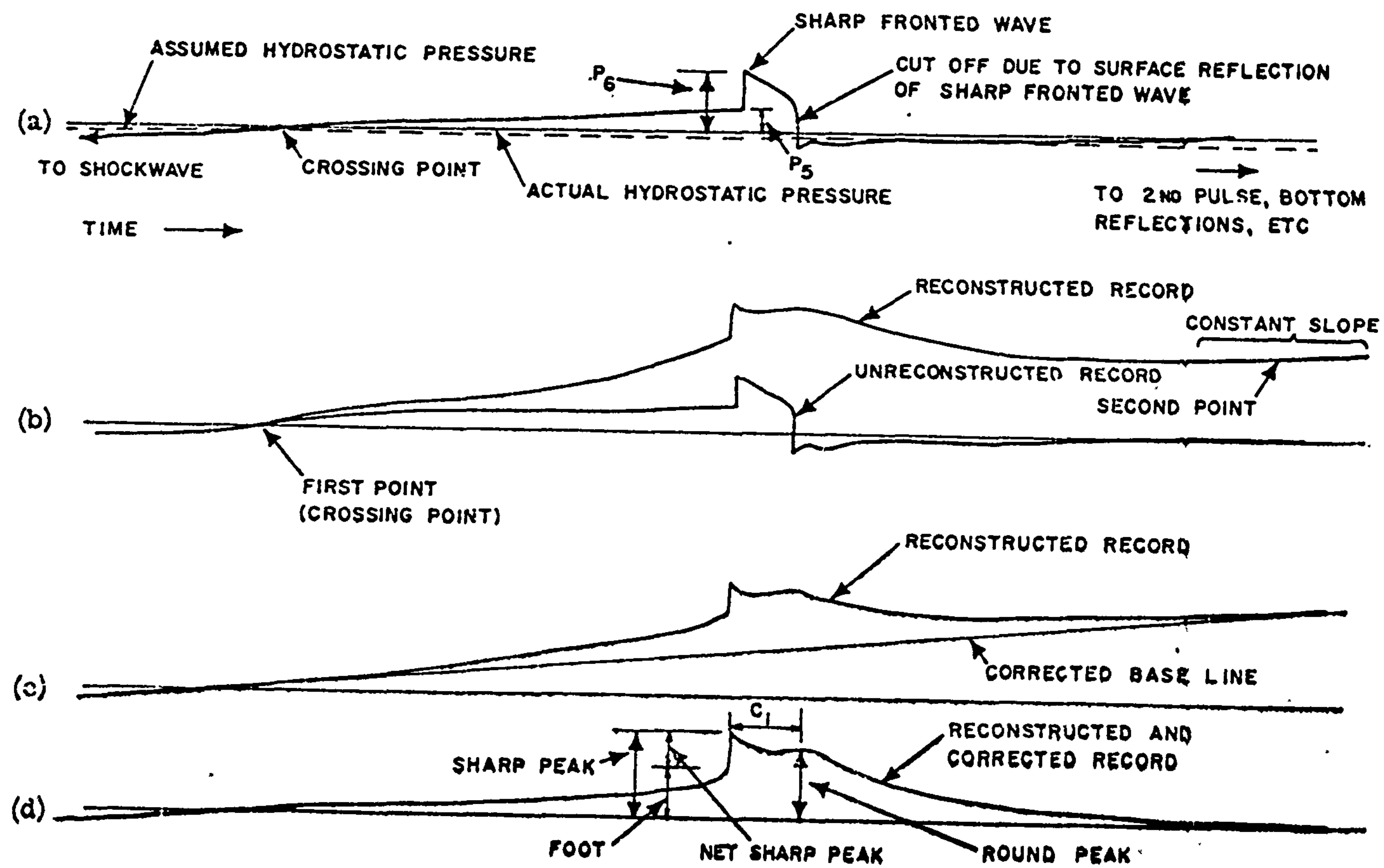

Fig. 9.8—Sample bubble-pulse record and stages of reconstruction.

furthermore it was not desired to have to consider gage time-constant effects in the bubble-reconstruction work. Actually, some of the piezoelectric gage channels might have yielded good data, but it was not considered warranted to expend the large effort required to read all the piezoelectric gage records available. One piezoelectric channel was interpreted as a check; it had a high sensitivity and was designed to yield a large bubble signal. The bubble records were reconstructed by applying corrections for the increased path of the reflected wave over the direct wave and for drift due to incorrect assumption of the hydrostatic level. Figure 9.8b shows a bubble record before and after reconstruction with correction for drift. Figure 9.8c shows the corrected base line, and Fig. 9.8d shows the completely corrected reconstruction. The corrected base line slanted up or down because of the repetitive addition of a small error, depending on whether the assumed hydrostatic pressure was low or high. If the negative reflection from the surface were acoustic, the entire pressure-time history starting with the shock wave could probably be accurately reconstructed; however, this was not the case. Because of nonlinear cutoff the negative phase was distorted, and the reconstruction of the bubble was affected by reflections and nonlinearities which carried over from the shock wave and the negative phase.

Selection of the points between which to draw the corrected base line was based on changes in curvature of the reconstructed record relative to the assumed base line. The point after the peak of the bubble pulse where the slope of the reconstruction was about constant, either upward or downward, was selected as the second point; and the assumed crossing point (Fig. 9.8b) was selected as the first point. On most records analyzed, the second point was found to occur as long after the bubble peak as the first was before the peak, indicating a reasonable symmetry of pressure on either side of the peak, except for the sharp-fronted wave. No attempt was made to correct the reconstruction for the effects (if any) of bubble migration.

The reconstructed pulse showed that the sharp-fronted wave occurred slightly before the time of the bubble's minimum volume. From the reconstructed pressure-time history it was apparent that the sharp-fronted wave was of lower net amplitude than the main bubble pulse, and, although the former did reach the greater pressure, it was not nearly so significant as it first appeared. Table 9.1 is a summary of the various pressures measured on the first bubble pulse.

By use of the reconstructed bubble pulse it was possible to correct the bubble period $(t_5 - t_1)$ as shown in Fig. 8.12 by the quantity C_1 (Fig. 9.8d). These corrections are listed in Table 9.2. An additional correction, C_2, which is caused by the migration of the bubble and the difference between the propagation velocity of the bubble pulse and that of the shock wave (because of the different paths and pressures), also is shown. The sum of $C_1 + C_2 = t_{B}$. The actual time between the explosion and the first-bubble maximum pressure, the so-called "bubble minimum," is considered to be the corrected first bubble period shown in Table 9.2 as t_{B1}. The average value of this for Wigwam was 2.878 sec, uncorrected for the presence of the ocean surface or bottom (reference 3, Sec. 3.3). From this was calculated the equivalent TNT yield, in terms of the bubble period, using the relation

$$T = 4.36 \frac{W^{1/3}}{(H + 33)^{5/6}}$$

where T is the period of oscillation in seconds, W is the charge weight in pounds, and H is the depth of the charge in feet.[1] This gives a value of W equal to 53.6×10^6 lb of TNT. Finally, from the relation[1]

$$A_{max} = 12.6 \frac{W^{1/3}}{(H + 33)^{1/3}}$$

the maximum bubble radius (A_{max}) was computed to be 375 ft. These data agree remarkably well with the predictions of reference 3, namely, T = 2.88 sec and A_{max} = 376 ft.

Table 9.1 — PRESSURES MEASURED ON THE FIRST BUBBLE PULSE

Channel (Tape & Head)	Gage Type	Depth	Horizontal Distance	Unreconstructed			Reconstructed and Corrected			
				Foot	Sharp Peak	Net Peak	Foot	Sharp Peak	Round Peak	Net Sharp Peak
E-10	W	500	5585	35	105	70	165	237	202	72
F-9	W	500	5585	25	75	50	200	270	235	70
E-9	PE	1000	5560	53	118	66	128	202	172	74
F-10	W	1000	5560	60	130	70	169	228	202	59
J-7	W	1000	8005	25	75	50	104	139	121	35
G-10	W	1000	11020	23	60	37	70	109	92	39

Pressures in psi -- Distances in feet

Table 9.2 — BUBBLE PERIODS AND CORRECTIONS

Channel Tape & Head	c_1	c_2	t_{12}	t_{B1}	t_{B2}	t_{B3}
E-10	.070	-.011	.059	2.572		
F-9	.060 to .065	-.011	.049 to .054	2.854 to 2.859		
F-10	.035	-.027	.003	2.811	2.7	1.9
J-7	.060 to .090	-.003	.057 to .087	2.888 to 2.918	2.6	2.0
G-10	.060 to .065	--	.060 to .065	2.889 to 2.894	2.6	1.9
Averages	--	--	--	2.878	2.6	1.9

Times in seconds

The sharp peak on the first pulse may be analogous to the "anomalous" pulse often encountered in conventional explosives testing, which may be caused by a jet of water rising through the bubble and impinging upon the top surface of the bubble from within. Such an impact would tend to unstabilize the bubble, perhaps leading to irregular later pulses.

The later bubble periods were measured without correction (Table 9.3); their peaks were assumed to be at the time of maximum signal. They are shown as t_{B2} and t_{B3} and are equal, respectively, to (t_{18} to t_{13}) – ($t_5 + t_{18}$) and (t_{16} to t_{17}) – (t_{18} to t_{13}). The range of values of the second and third pulses was caused by the fact that their maximum signal was diffuse and complex and no actual peak seemed to occur. The points selected were chosen only because they were detectable at several gage stations and appeared about in the middle of the disturbances caused, respectively, by the second and third pulses.

9.5.2 Bubble Migration

If the arrival time of a definite pressure transient is known at various gage locations on a string and if certain other data are available, it is possible to calculate the location of the source of the transient. Each bubble pulse displayed discontinuities or pips of sufficient sharpness to permit ranging if the arrival times and other data were known with sufficient accuracy. In this case the effective base line for the ranging did not exceed 975 ft, the maximum distance between gages on a single string. If the discontinuity were reflected from the water surface and if the resulting negative pressure were identifiable on the record, an effective base line over twice as long (2000 ft) would be available. Only the first of the bubble pulses provided such a reflection.

An approximate formula has been derived for either method of calculation using the following data:

a = distance, in feet, between gages or gage and image gage
V_1 = velocity, in feet per second, of propagation from source to nearer gage
V_2 = velocity, in feet per second, of propagation from source to farther gage (or image gage)
m = horizontal distance, in feet, from source to gage line

The equation is:

$$X = \frac{a \pm \sqrt{a^2 - \left(\frac{V_2^2}{V_1^2} - 1 + \frac{V_2^2\Delta}{V_1 m}\right)\left[\left(\frac{V_2^2}{V_1^2} - 1\right) m^2 + V_2^2\Delta\left(\Delta + \frac{2m}{V_2}\right) - a^2\right]}}{\frac{V_2^2}{V_1^2} - 1 + \frac{V_2^2\Delta}{V_1 m}}$$

where Δ is the time interval, in seconds, between the arrival at two gages on a string or between the arrival of the positive wave and its cutoff at one gage and X is the depth, in feet, of the source from the nearer gage; X is negative if the source is above the nearer gage.

Application of the above formula involves several quantities, all of which were approximate and some of which were derived from measurement of the shock-wave phenomena. The distance between two gages on the same string was known to better than 1 per cent; however, the distance between a gage and its image was not known so well because the gage line may have been inclined to the surface and the actual depth of the gage would be uncertain. The horizontal standoff was determined by arrival time and sonic ranging of the shock wave (see Chap. 7). If two gages were used, the slope of the gage line was important since the minimum standoff was roughly six times the base line (975 ft was the maximum between gages). Error in the horizontal standoff was important in all cases because, in the equation (as used here), the depth (X) was a function of the sum or difference of large numbers or their squares or products and most of the numbers were of the same order of magnitude. The accuracy of the two propagation velocities used was rather low.

These propagation velocities were estimated by calculating the average sound velocity from an assumed source of the pulse to the gage and then correcting this velocity to take account of the increased velocity associated with the pressure of the pulse. Successive approximations of the path (or source location) were made until the calculated and assumed positions of the source were reasonably close together.

Table 9.3 — VARIOUS TIME INTERVALS MEASURED FOR BUBBLE RANGING (INTERVALS IN SECONDS)

Description	YFNB-12	YFNB-13	YFNB-29
t_2	.1275	.0844	.0535
t_6	.1045	.068	.0377
t_5 (1000' gage) $-t_5$(200' gage)	.044		
t_5 (1000' gage) $-t_5$(100' gage)		.030	.010
t_{10} (1000' gage) $-t_{10}$ (200' gage)	.017		
t_{10} (1000' gage) $-t_{10}$ (100' gage)		.011	*
t_{11} (1000' gage) $-t_{11}$ (200' gage)	.008		
t_{11} (1000' gage) $-t_{11}$ (100' gage)		.011	*
t_{12} (1000' gage) $-t_{12}$ (200' gage)	.008		
t_{12} (1000' gage) $-t_{12}$ (100' gage)		.014	*
t_{13} (1000' gage) $-t_{13}$ (200' gage)	.007		
t_{13} (1000' gage) $-t_{13}$ (100' gage)		.012	*
t_{16} (1000' gage) $-t_{16}$ (200' gage)	.012		
t_{16} (1000' gage) $-t_{16}$ (100' gage)		.024	*
t_{17} (1000' gage) $-t_{17}$ (200' gage)	.005		
t_{17} (1000' gage) $-t_{17}$ (100' gage)		.005	*

* Pip not identifiable at shallow gage.

9.5.3 Bubble-migration Results

The ranged depth, 1000 + X, was determined by use of the cutoff times from the first bubble pulse, as measured at the 1000-ft gages on the YFNB-12, and the following data:

$a = 2000$ ft
$V_1 = 4894$ ft/sec
$V_2 = 4936$ ft/sec
$m = 5560$ ft
$\Delta = 0.1045$ sec

This gave X = 594 ft, and a ranged depth of 1594 ft; hence the migration was about 400 ft.

Alternatively, by use of the arrival times at the 1000- and 25-ft gages on the YFNB-12, the ranged migration was downward; however, when account was taken for an assumed slope toward the charge of 40 ft per 1000 ft in the gage line, the migration was calculated to be 70 ft upward. The expected errors in this case were so large that further calculations were considered futile. Similarly, any ranging of the later pulses would be hopelessly inaccurate. It should be noted that only the source of the sharp pip was ranged. This does not mean that the center of gravity of the bubble had migrated 400 ft.

The time intervals in Table 9.3 are given to illustrate the reason for abandoning the computation of the later migrations of the bubble. As later and later pips were considered, the intervals became increasingly smaller (which indicated migration in this case) and the errors in the measurement of time increased, as did the uncertainties in the calculation of the propagation velocity. The angle of the gage string became important when the surface cutoff was unidentifiable. To check the method, the location of the charge was calculated from the t_2 values measured at the YFNB-12. V_1 was used in measuring the location of the gage in the sonic ranging method. It was used again here. V_2 was calculated using the same method as that used in the bubble ranging formula, from which the depth of the charge was calculated to be 1950 ft. A difference of only about 25 ft/sec in either propagation velocity would have made a difference of about 50 ft in ranged charge depth. A 1-msec error in the arrival time would have yielded an error of 18 ft. At best, it seemed that this approach to ranging was good to about 50 ft in depth; at worst, the errors ran into hundreds of feet and the method was useless.

9.6 BOTTOM REFLECTIONS AND LATER BUBBLE PULSES

9.6.1 Description of Records

The Project 1.2 electronic pressure-time records showed a fairly large number of complex waves following after, but not adjacent to, the first bubble pulse. After careful comparison, certain waves or pips were identified on gage records at all YFNB's and at all depths on each string, except that some of the points were unidentifiable at the shallow gages on the farthest YFNB (YFNB-29). Although there were many other identifiable points associated with those selected, representative members of each wave train were used. For example, even though the points at t_{10}, t_{11}, and t_{12} were prominent and easily followed, no particular significance was attached to their individual characteristics. On the other hand, the pressure waves at t_7, t_8, and t_{14} represented different phenomena, and their arrival times and amplitudes were significant.

The arrival times of various pips at different places are tabulated in Table 9.4. The arrival times at the 1000-ft gages on the three YFNB's are plotted in Fig. 9.9. It can be seen that most of the pulses arrived from the direction of the charge since their times of arrival fall on lines nearly parallel to that of the initial shock. Three pulses arrived from almost below the array, and they have been identified as bottom reflections of the shock wave. The shock wave, first bubble pulse, and second bubble pulse were clear and distinct, and, although the second pulse was irregular in amplitude, it followed at a logical time. The pips tentatively identified as the third pulse (t_{16} and t_{17}) seemed to have the same characteristics as those of the second pulse, although they were weaker. Following them was a dip in pressure which has not been identified, and it persisted about 0.7 sec. The arrival of the center of this dip is noted

CONFIDENTIAL

Table 9.4—ARRIVAL TIMES* OF PRESSURES AT VARIOUS POINTS

Item	Code**	YFNB-12			YFNB-13			YFNB-29		
	Tape	E-1	E-10	E-9	I-2	I-7,J-6	J-7	G-2	H-3	H-10
	Depth	200'	500'	1000'	100'	500'	1000'	100'	500'	1000'
Shock Wave	t_1	1.170	1.152	1.129	1.653	1.640	1.622	2.247	2.244	2.238
First Bubble Pulse	t_5	3.980	3.965	3.936	4.473	4.462	4.453	5.076	5.067	5.067
Bottom Reflection (Bottom)	t_7	5.875	5.815	5.728	6.114	6.040	5.957	6.436	6.358	6.257
Bottom Reflection (Sub-bottom)	t_8	6.118	6.055	5.965	6.292	6.208	6.110	6.519	6.446	6.346
Bottom Reflection Cutoff	t_9	5.96	6.020	6.108	6.266	6.336	6.350		6.523	6.640
Second Bubble Pulse	t_{10}	6.486	6.477	6.469	6.992	6.980	6.972			7.588
Second Bubble Pulse	t_{11}	6.500	6.492	6.492	7.004	6.995	6.993			7.602
Second Bubble Pulse	t_{12}	6.603	6.593	6.595	7.104	7.102	7.092		7.693	7.711
Second Bubble Pulse	t_{13}	6.636	6.629	6.629	7.146	7.140	7.132			
Bottom Reflection (Deep Sub-bottom)	t_{14}	~7.85	7.65	7.575		7.835	7.710			~7.835
Bottom Reflection Cutoff	t_{15}		7.925	7.982						
Third Bubble Pulse(?)	t_{16}	8.445	8.440	8.433		8.958	8.933		7.733	7.750
Third Bubble Pulse(?)	t_{17}	8.522	8.526	8.517	9.045	9.040	9.015			9.630

* Relative to EG&G Fiducial Time (Seconds) Average of Available Data
** See Figure 8.12

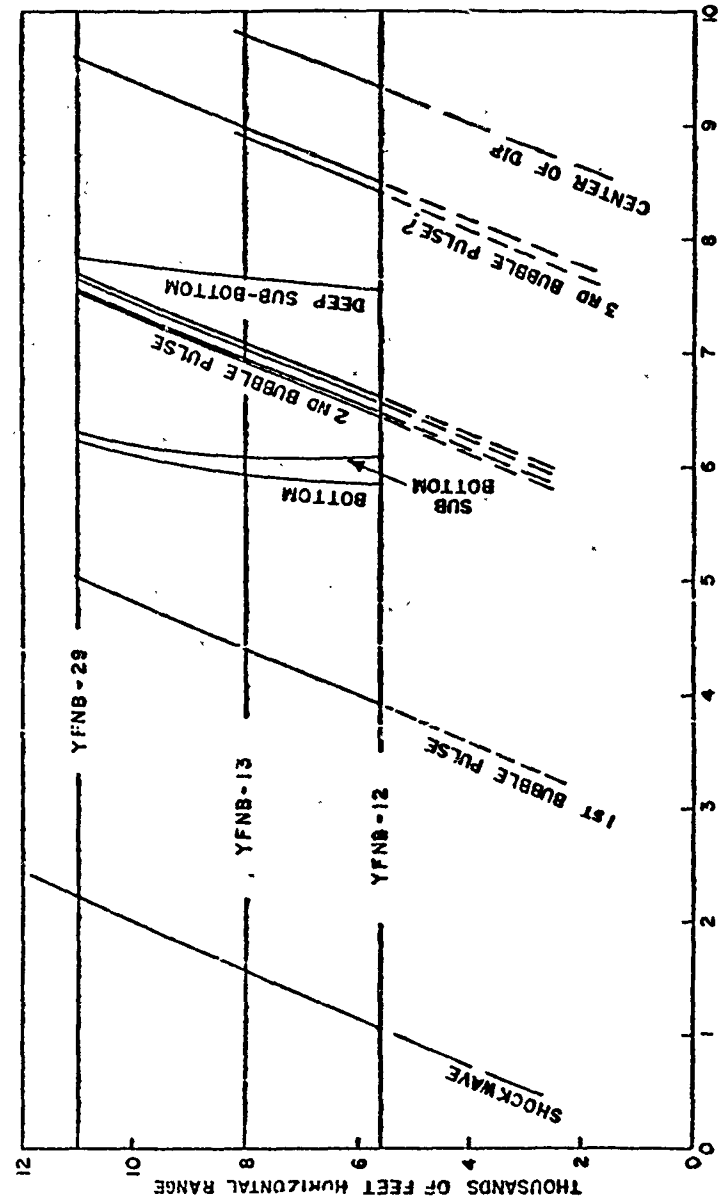

Fig. 9.9—Arrival times of pressures at 1000-ft gages on YFNB's.

in Fig. 9.9. The time of the dip did not seem to correspond exactly with the venting of the bubble or the origin of the plume observable in the surface-phenomena photographs and movies. However, the surface phenomena deep inside the spray dome and plume are not well understood, and the phase of the bubble at venting was uncertain; therefore the dip may have actually originated then.

Careful interpretation of the bottom-reflection data indicated three things: first, the bottom was irregular, sloping downward from SZ toward the YFNB's; second, there were several significant layers in the bottom; and third, all significant reflections were from the initial shock rather than the bubble.

9.6.2 Structure of Sea Bottom

Using arrival times and the shock-velocity structure of the water, it was possible to ascertain the distance and the direction of the image of the charge in the bottom by a process of ranging. In order for the arrival times (t_7) to check and to have the source correspond with the charge, it was necessary to postulate a sloping bottom at the depths shown in Fig. 9.10. In order to account for the major peak (t_8) following the first arrival, a subbottom as shown was necessary. To account for the last observed pulse (t_{14}), a deep subbottom was postulated. Alternatively, t_{14} could have been caused by the first bubble pulse, but, if the bottom was as postulated for the shock-wave reflection, the bubble pulse would have had to originate at a depth of 7000 ft. The bottom topography represented in Fig. 9.10 could be reconciled with the bottom contours supplied by Project 2.8 in its preliminary version of reference 6 if SZ were displaced about 10,000 ft from their stated SZ on the 020° contour away from San Francisco.

The layers and associated arrival times have tentatively been identified as sediments (t_7), basalt (t_8), and ultrabasic rock (t_{14}). The thickness of the basaltic rock could have been about 21,000 ft if the propagation velocity in it were about 22,000 ft/sec.

Figure 9.10 shows the position of the bomb relative to the Project 1.2 electronic gages and the bottom. In addition to the bottom, subbottom, and deep subbottom proposed because of t_7, t_8, and t_{14}, there was some evidence of layering within the various major layers. For instance, there were noticeable pulses occurring after t_8, which could account for a bottom shown as "possible approximate bottom of sediments" in Fig. 9.10. Unfortunately, the pulses were partially masked by the surface cutoff of preceding pressures and were not identifiable at enough gages for good ranging. It should be pointed out that there were discrepancies in the times of arrival or time differences for t_7, t_8, and t_{14} which were probably caused by inaccuracies in the record reading and method of obtaining a time base. There were enough coherent data to establish the identity of the three reflections that were studied.

The data on layering given here depend on reflection from one small area of bottom. For comparison, three estimates of bottom structure are included in Fig. 9.10. The first[7] applied to the Pacific Ocean between New Guinea and Berkeley, Calif., and was obtained by studies of Love-wave dispersion of earthquake tremors. The velocities given are shear-wave velocities. The second[8] applied to the Nares Basin in the Atlantic Ocean northeast of Puerto Rico. The velocities given are for a pressure wave. The structure was obtained by the study of the refraction of waves from a small explosion in the ocean. The last (Raitt, as quoted in reference 8) applied to the Pacific Ocean between Hawaii and San Diego and was based on refraction studies of earthquake tremors. Though the Project 1.2 data did not provide velocity data for the shock-wave travel in rock of any type, a reasonable structure resulted when velocities obtained from the refraction studies of Raitt were used in computing the position of the deep subbottom.

9.6.3 Slicks and Spray Domes

Several slicks seen in the aerial photographs of Project 1.5 have been identified with pressure-time phenomena of known origin. Slick 1 was caused by the direct shock wave. Slick 2 was caused by the bottom reflection from the shallow sedimentary layers. Slick 3 was caused by reflection from the deep layer. The exact arrival time and the pressure at the ocean surface probably varied from place to place, depending on the bottom topography. Slick 4, which was observable on some aerial color movies, has not been identified on the Project 1.2 records.

CONFIDENTIAL

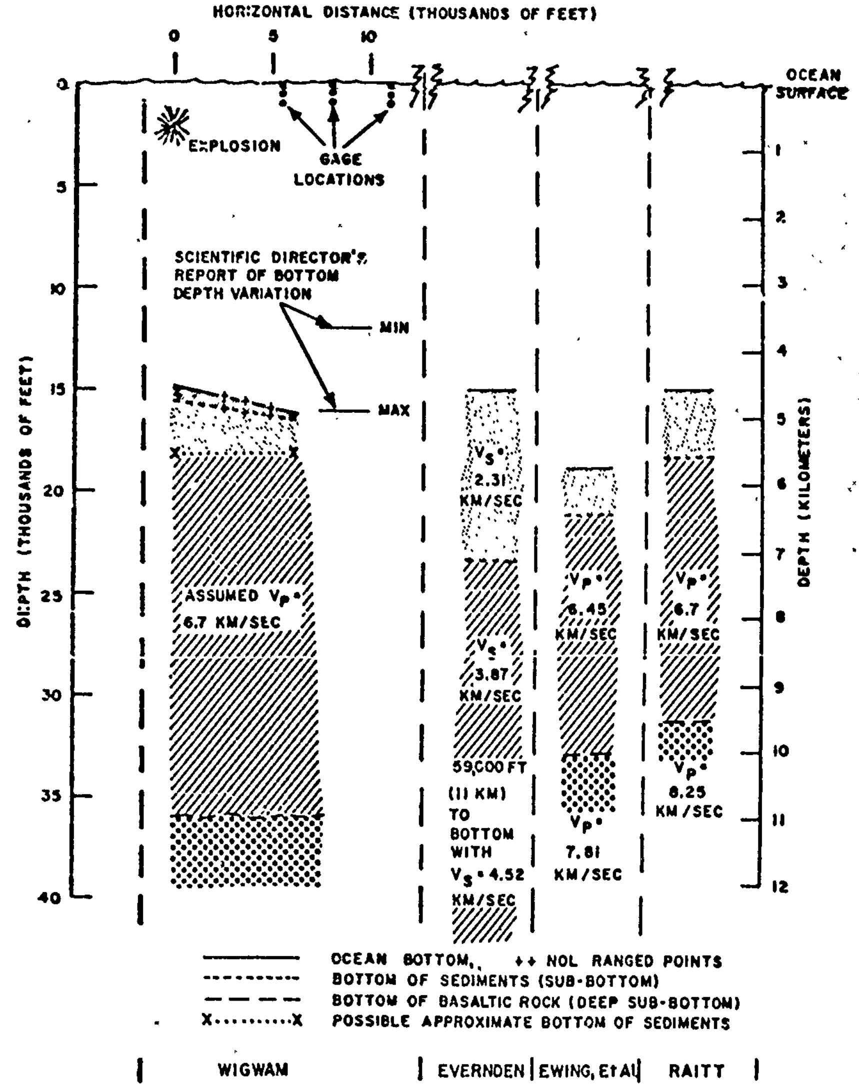

Fig. 9.10—Wigwam bottom structure and comparison with other locations and methods.

SECRET – RESTRICTED DATA

CONFIDENTIAL

The movies did not show the YFNB area in sufficient detail to determine whether slick 4 existed in that area.

Figures 9.11a to h show rough plots of pressure vs gage location. Figure 9.11a shows the shock wave; Figs. 9.11b, d, and e show measured bubble pulses; Fig. 9.11c shows the first bubble pulse reconstructed, and Figs. 9.11f to h show bottom reflections. It may be noted that the data in Figs. 9.11a and g may not agree to better than 20 per cent with the shock-wave peak-pressure values given in Tables 8.4 to 8.6. This arises from the fact that the values plotted in Figs. 9.11a and g were read from the same records as those which were played back so as to get the most accurate values of the bubble and reflected pressures. These latter pressures were low compared to the initial shock pressures, which on this playback fell so nearly off-scale that they could not be read as accurately as when played back in the manner used to obtain the values tabulated in Tables 8.4 to 8.6. The only reason for rereading the initial shock pressures and plotting them in Figs. 9.11a and g was to present for comparison the values as actually obtained from the same records as those used to determine the bubble and reflected pressures. The significance of the initial shock-wave pressures in Figs. 9.11a and g is, therefore, limited to rough comparisons with the corresponding reflected and bubble pressures.

The shock wave produced a spray dome extending from SZ to about 7500 ft, at which point the pressure was about 550 psi with a vertical component of about 160 psi. Presumably any pressure wave striking the surface with a vertical component of over 160 psi could produce a spray dome. A vertical component of 160 psi corresponds to a tensile strength of water (T) of 320 psi, which may be compared with the value of 300 to 900 estimated from conventional charge experiments using the same method of calculation. See Table IX of reference 9.

The vertical component of all bubble pulses was far below the minimum level for spray-dome formation under the Wigwam conditions at the YFNB locations. The probable maximum radius of the first-bubble-pulse spray dome was about 3500 ft, based on extrapolated values of the reconstructed bubble pulse (Fig. 9.11c). This was visible as a higher but narrower spray dome within the shock-wave spray dome. If extrapolation of the unreconstructed-bubble-pulse peak pressure had been used, the radius would have been smaller. The later bubble pulses, originating even closer than the first to the surface because of migration, would have produced even smaller diameter spray domes. No later bubble-pulse spray domes could be positively identified on Wigwam since the shock-wave spray dome still covered a larger area than the maximum that any bubble pulse could have produced when they did exist.

Study of the bottom reflections, however, indicated that pressures from them large enough to cause spray or slick formation could exist at great distances from SZ. If the formation of spray depends on the gross pressure wave rather than on the net portion remaining after surface cutoff, then the reflection from the subbottom (Fig. 9.11g) should have caused spray to form ahead of the YFNB-29, that is, slightly farther out from SZ. Examination of the Project 1.5 records (J-4, 30-30 RKF 632) and (J-1, 30-30 MZF-72) showed a definite small patch of spray 500 to 4000 ft ahead of the YFNB-29, an amazing and fortuitous confirmation of the prediction since the patch was small in area and the total number of such patches was small. It is safe to say that the criterion of a 165-psi vertical component is good to 20 per cent under the Wigwam conditions. The only way that the maximum pressure in any spray area caused by bottom reflection could be estimated was by calculating the velocity of a spray droplet necessary to project it into the air for the observed duration of the spray. Since the spray was retarded by air resistance, since visible patches of foam might have remained on the surface after all the spray had fallen back, and since any spray phenomena might have been caused by multiple or prolonged reflection, the estimated maximum values were probably too large. However, the peak vertical component in any patch was probably bracketed by the 165-psi minimum value and the calculated maximum value. Several patches were measured for duration, and the results are shown in Table 9.5. The spray numbered 4 is believed to be located ahead of the YFNB-29.

The following formula used in these calculations was adapted from reference 9.

$$\frac{tg}{2} = \frac{2}{\rho U}\left(Pm_v - \frac{T}{2}\right)$$

CONFIDENTIAL

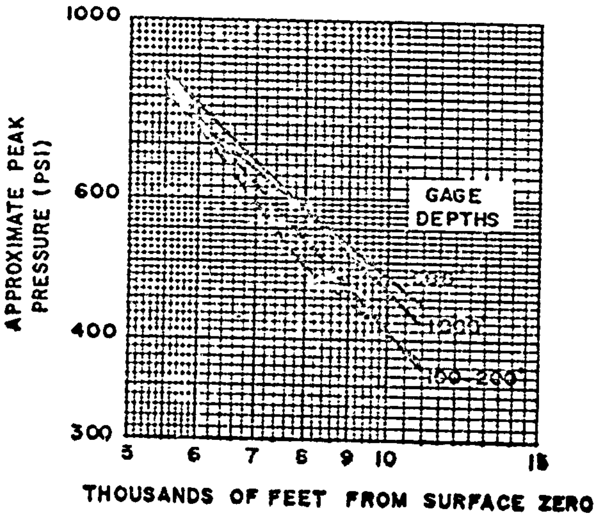

Fig. 9.11a—Primary shock wave as read from bubble records.

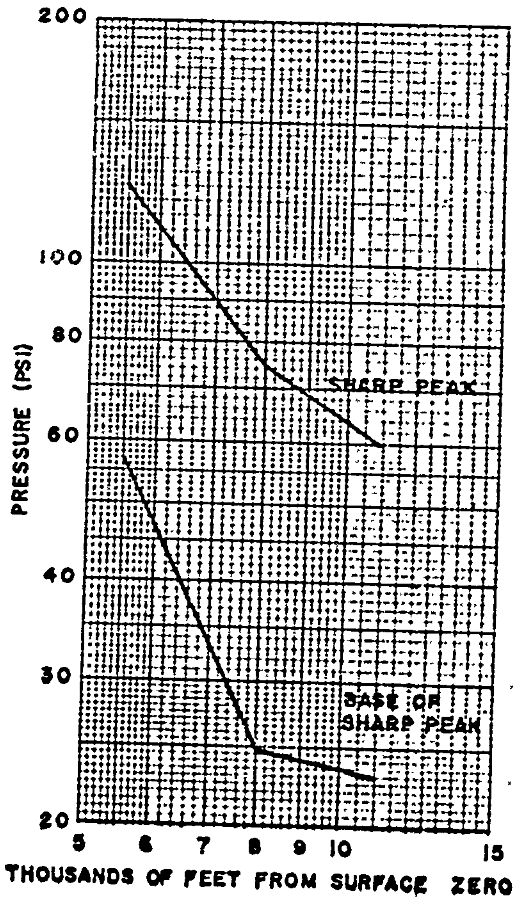

Fig. 9.11b—Unreconstructed first bubble pulse, 1000-ft-deep gages only.

SECRET – RESTRICTED DATA

CONFIDENTIAL

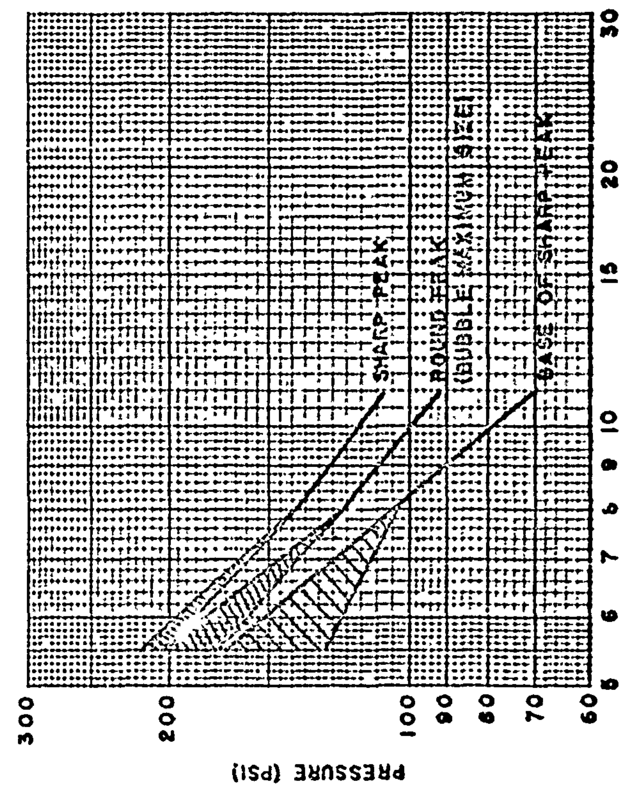

Fig. 9.11c—Reconstructed and corrected first bubble pulse, 1000-ft-deep gages only.

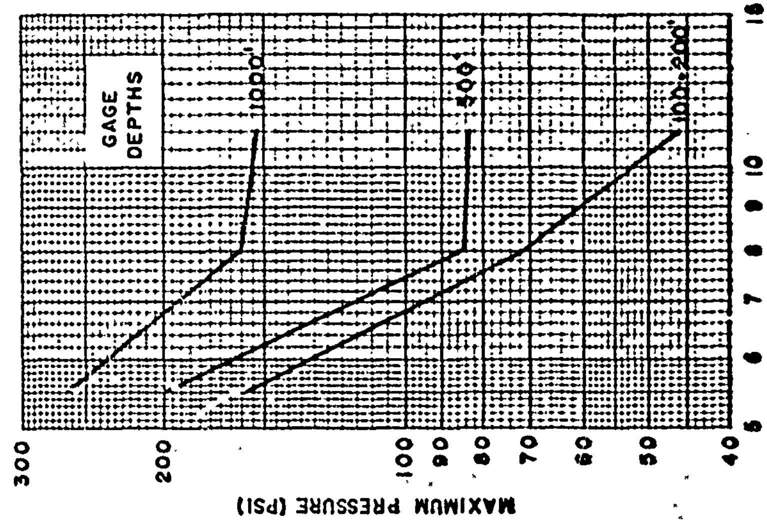

Fig. 9.11d—Second bubble pulse.

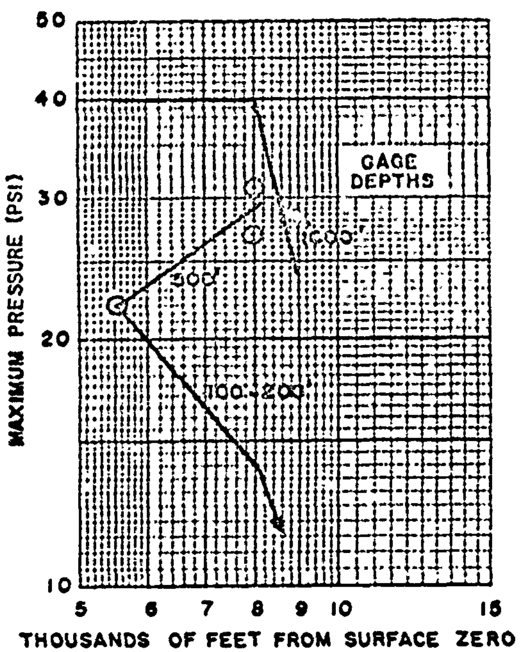

Fig. 9.11e—Third bubble pulse.

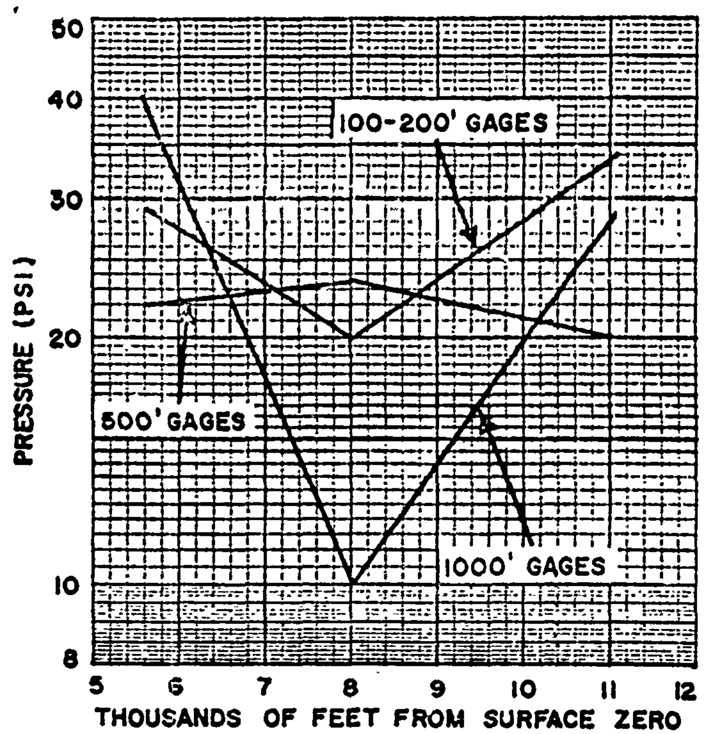

Fig. 9.11f—Bottom reflection.

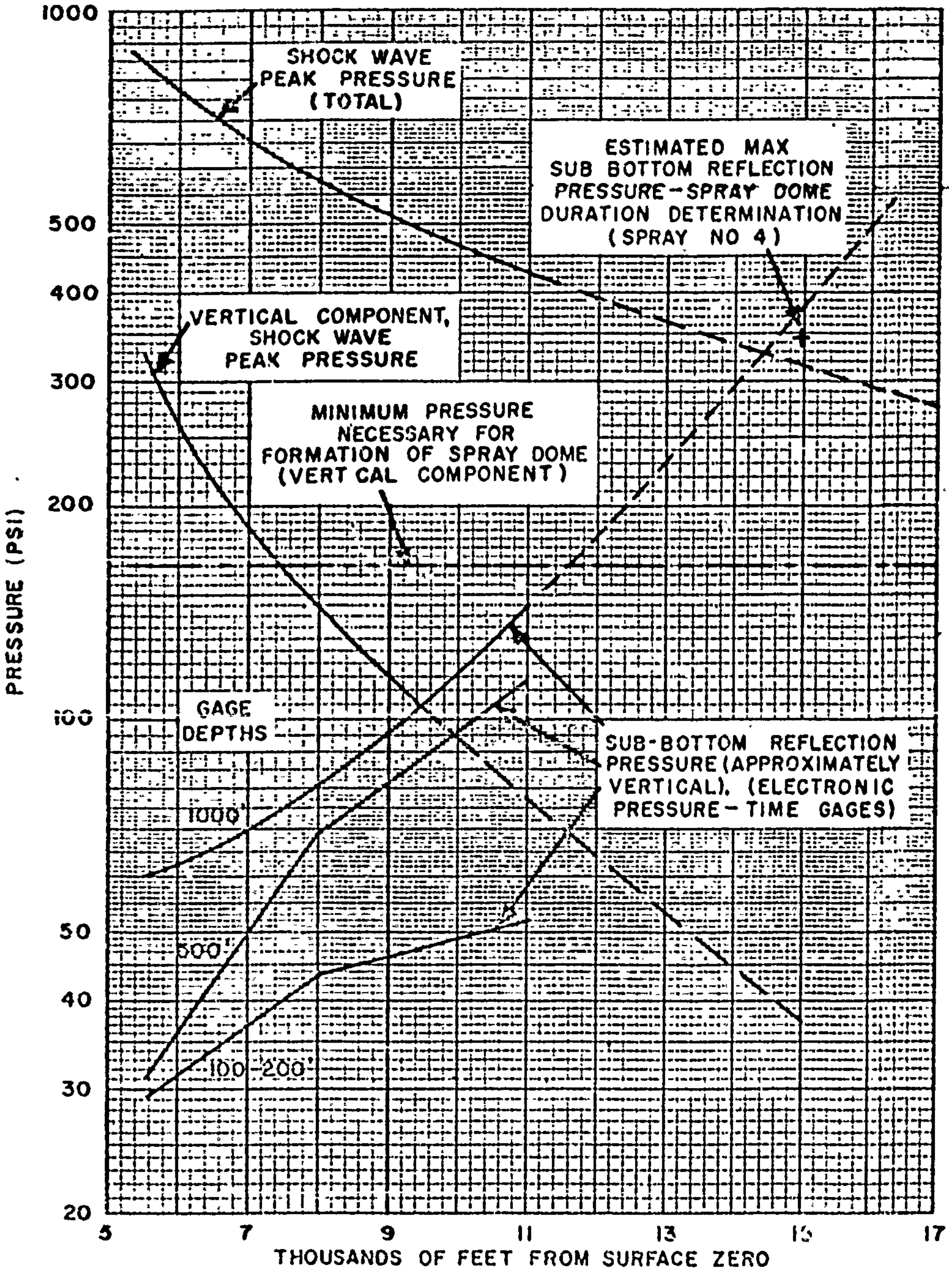

Fig. 9.11g—Subbottom reflection.

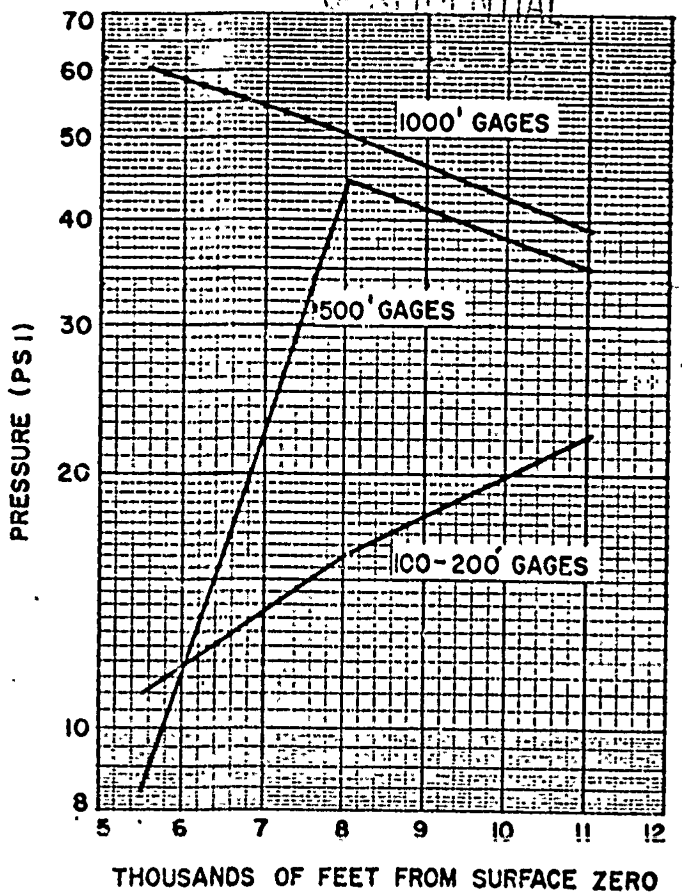

Fig. 9.11h—Deep subbottom reflection.

Table 9.5—CALCULATED PRESSURES FROM BOTTOM REFLECTIONS CAUSING SPRAY PHENOMENA

Spray No.	Est. Radial Distance, ft.	Start of Spray Rise, sec. after Fiducial	Spray Duration secs.	Mim.Vert. Pressure Component psi	Max.Vert. Pressure Component psi
1	11,000	6.24	.25	165	300
2	14,000	6.28	.15	165	240
3	16,000	6.74	.32	165	340
4	15,000	6.74	.34	165	350
5	16,000	6.90	.77	165	580
6	17,000	7.82	.48	165	420
7	15,000	7.03	1.19	165	810
8	17,000	7.12	.42	165	390

where t = time spray is in air, in seconds

g = acceleration due to gravity (32.2 ft/sec^2)

ρU = density times shock propagation velocity (68.4 for average sea water)

Pm_v = maximum vertical pressure component, in pounds per square inch

$T/2$ = pressure required to overcome tensile strength of sea water (165 psi under these conditions)

9.6.4 Conclusions on Reflections and Bubble Pulses

The first bubble pulse produced a fairly smooth, rounded pulse with a sharp peak, probably caused by impact of the lower and upper surfaces during some type of vortex action in the collapse. The later bubble pulses produced multiple spikes, some of considerable amplitude but with small energy content. The reflections from the ocean bottom of the primary shock wave indicated good reflection from the bottom and from several lower levels in the rock. Slicks and scattered spray patches subsequent to the primary shock phenomena were caused only by the bottom reflections of the primary shock since their reflections approached the surface at an angle such that maximum vertical movement of the water resulted. No surface phenomena or bottom reflections from bubbles were detected beyond the region covered by the spray dome from the initial shock. Considerable work on the interpretation of the spray phenomena caused by the bottom reflections could provide data on the distribution of dangerous pressure areas around deep explosions. This could probably be extrapolated to different types of bottom and depths of water and should be considered in the tactical use of this type of weapon.

9.7 CAVITATION

Cavitation occurs when the tension created by the reflection of the shock wave from the surface exceeds the sum of the hydrostatic pressure plus that of the decaying pressure wave from the principal shock by an amount greater than the tensile strength of the water. This phenomenon, which is part of the formation process of the spray dome, has been observed frequently in high-explosive explosions[5,10] and was indicated in the Crossroads Baker records of the University of Washington report[11,12] where it was recorded to a distance of 3700 ft.[13] Wigwam records showed what appeared to be measurable cavitation out at least as far as 5600 ft, but it was most obvious on the mechanical pressure-time gages at 2900 ft.

The appearance of what is believed to be the cavitation pulse can be seen in Fig. 8.9, as recorded on the mechanical pressure-time gages for several depths at a horizontal range of 2900 ft, and in Fig. 9.12, as recorded on a Wiancko gage at a depth of 500 ft and a horizontal range of 5585 ft. Quantitative measurements from these and other gages on the same strings are given in Table 9.6. Inspection of these figures and the table reveals that at the 2900-ft string the cavitation period was first apparent about $\frac{3}{4}$ sec after the arrival of the initial shock, arriving first at the 100-ft depth. The pressure magnitude at this distance was from $\frac{1}{5}$ to $\frac{1}{2}$ that of the primary shock. At the 5600-ft string, the first cavitation arrivals were at the gages located at depths of 100 ft or shallower. The magnitudes at this string varied from less than $\frac{1}{10}$ to $\frac{1}{4}$ the pressure of the primary shock. The duration of this effect varied rather widely, i.e., from 40 to 400 msec at the close-in string but only from 52 to 104 msec at the 5600-ft string. Before further consideration is given these data, it is important to realize that their precision is quite low because their characteristics made it impossible to select the times of appearance and disappearance with much assurance. Furthermore, the pulses were irregular in form, having multiple peaks. These characteristics probably arose from three basic properties of the cavitation phenomenon:

1. It occurred over a widespread area, so that some gages may actually have been within the cavitation volume.
2. The pulses that generated the pressure signals probably arose as portions of the cavitation volume collapsed at different times depending on their thickness.
3. There was probably some surface cutoff of these pressures.

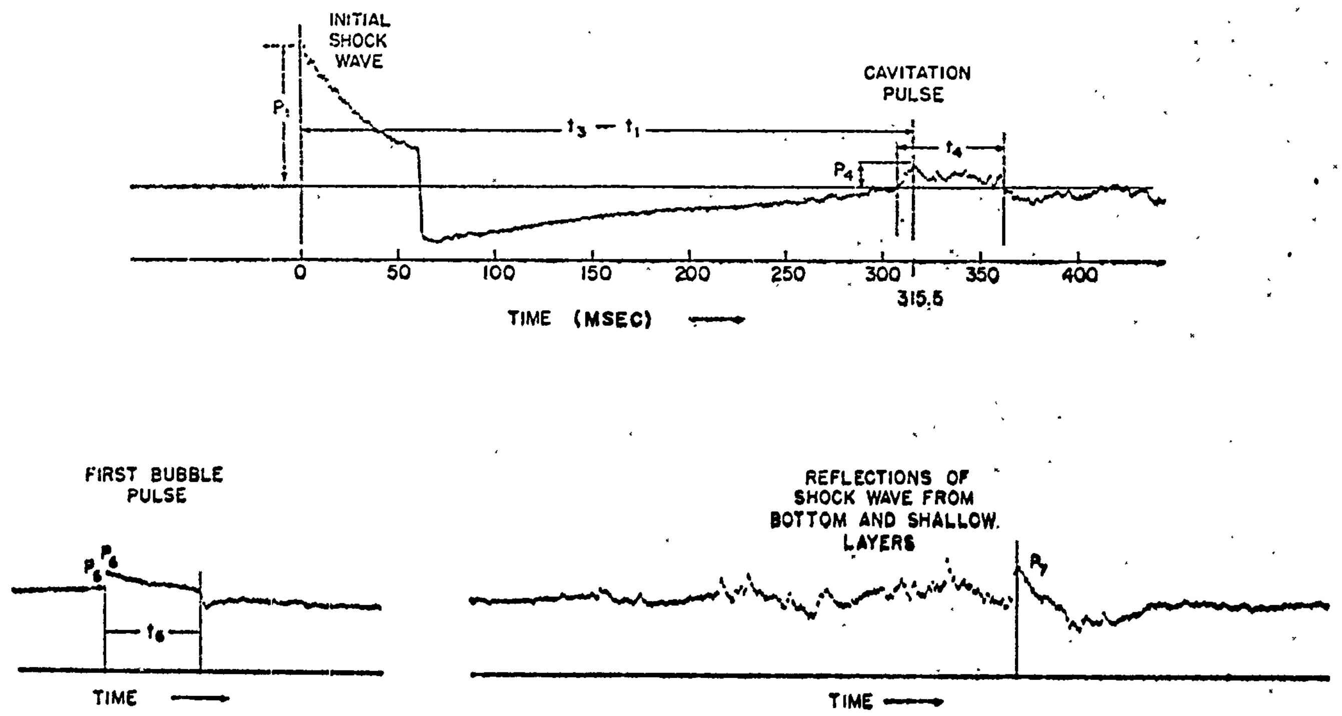

Fig. 9.12—Reproduction of sections of an actual pressure-time record from a Wiancko gage; tape F, head 9.

CONFIDENTIAL

Table 9.6—CAVITATION-PULSE DATA

Gage Type and Record No.	Horizontal Range and Depth (ft)	Arrival Time After Initial Shock (msec) t_3-t_1	Approx. Duration of Cavitation (msec) t_4	Estimated Absolute Arrival Time (msec) t_3-t_0	Ratio of Cavitation Pressure to Shock Pressure P_4/P_1	Cavitation Pressure (psi) P_4
MPT 4	2900 50	770	40	1415	0.468	750
MPT 13	2900 100	650	180	1290	0.378	570
MPT 27	2900 300	730	340	1352	0.259	380
MPT 28	2900 500	810	400	1412	0.201	350
PE F-7	5600 25	214.25	57.5	1382	0.096	83.0
PE E-3	5600 50	214.75	52.8	1381	0.087	80.0
PE F-2	5600 100	219.0	54.0	1383	0.277	255
PE E-7	5600 200	244.0	77.5	1401	0.109	99.0
PE F-3	5600 200	244.0	94.0	1402	0.128	116.0
W** F-4	5600 200	244.0	104	1401	0.22	171***
W** E-1	5600 200	244.0	81.5	1401	0.169	118***
W* F-9	5585 500	315.5	54.0	1454	0.175	131***
PE F-5	5585 500	315.0	54.0	1456	0.130	129.0
W* F-10	5560 1000	436.7	83.0	1553	0.142	105***
PE E-9	5560 1000	436.7	77.5	1553	--	--

* Wiancko Gage Range 1500 psi -- correction factor = 0.88

** Wiancko Gage Range 1000 psi -- correction factor = 0.89

*** Corrected values i.e. Wiancko values as read were divided by correction factors to bring them in line with PE values -- see Chapter 5.

SECRET – RESTRICTED DATA

CONFIDENTIAL

The problem was further complicated by the fact that there probably were localized cavitation closures that produced spikelike pressures of durations too short for the gage to follow. Such durations were indicated by the fact that the timing stylus of the mechanical gages started a violent bouncing before there was any significant pressure rise and continued after the pressure decayed to zero. The duration values in Table 9.6 for the mechanical gages represent the periods during which the bouncing of the timing reed stylus was apparent; however, since there were no mechanical styluses on the Wiancko gages, the durations measured by the Wiancko gages represented the time during which a measurable pressure was on the record. The net result of all these effects was to render impossible the accurate ranging of the source of the cavitation pulses, although an attempt was made to do so.

The technique tried was as follows (refer to Table 9.6): A plot of arrival time vs distance was made, using NRL data from the zero barge[2] and the NOL data from the YFNB-12. Between the slant ranges of about 2000 ft, where the NRL data ended, and 5600 ft, where the YFNB-12 (NOL) data began, arrival times for the 30.5° ray were plotted from Table 7.3 (since this ray corresponded most closely to the 2900-ft string). This enabled the arrival time of the initial shock at the mechanical gages at 2900 ft to be estimated. Such values were added to the $t_3 - t_1$ column to get the estimated absolute arrival time $(t_3 - t_0)$ for the mechanical gages. The value of $t_3 - t_0$ for the Wiancko gages was calculated directly. A plot of absolute arrival times $(t_3 - t_0)$ was then made (Fig. 9.13). This seemed to indicate the source to be at less than a 100-ft depth; but no exact ranging was warranted since it was unlikely that the arrival times plotted were from the identical portions of the diffuse source.

Although these data are essentially only qualitative, it appears likely that the long-duration cavitation pressures and their associated effects might be potent sources of damage to targets reasonably close to the surface, where the primary shock suffers from early surface cutoff.

9.8 REFRACTION EFFECTS

Brockhurst, in reference 14, presents a number of predictions of the effect of refraction on peak pressure, travel time, and pulse duration out to a range of 30,000 ft from an explosive source at a depth of 2000 ft. Such refraction was assumed to have arisen from the presence of a thermal structure in the water. Two such thermal structures, each typical of the Pacific Ocean southwest from San Diego, were used as the basis for two sets of predictions. Although the actual thermal structure as measured on Operation Wigwam (Table 7.1) was different from each of those used by Brockhurst, it most closely resembled the one designated by him as MIT 408. The predictions based on his MIT 408 calculations were, therefore, compared with some of the actual Wigwam data.

First of all, pressure contours based on this were plotted (Fig. 9.14). These were calculated from Figs. 12 and Ia through Ii of reference 14, assuming a TNT yield of 43.8×10^6 lb of TNT. (As discussed in Sec. 9.2, a better equivalent to Wigwam would have been 46.2×10^6 lb of TNT. However, Fig. 9.14 had been prepared before this value was arrived at, and in view of the small differences between the thermal structure of MIT 408 and the actual one, a revision was not deemed to be worth while.) For comparison with this prediction, the Wigwam experimental data were used as a basis for the contours shown in Fig. 9.15. Although they are by no means identical contour plots, it is obvious that the similarities between Figs. 9.14 and 9.15 are sufficient to confirm the predictions of Brockhurst qualitatively and perhaps even quantitatively. The principal difference seems to be in the shape of the 1500- and 900-psi contours.

A second comparison of interest between Brockhurst's work and the Wigwam data results when the positive durations of the initial shock wave are plotted together as shown in Fig. 9.16. On this plot, in addition to the NOL data from the YFNB stations, NEL data from approximately the same locations are shown. The straight line gives the approximate expected positive duration as a function of depth for a homogeneous medium, and the curved solid line is based on Fig. 14 of reference 14.

A third comparison can be seen in Fig. 9.17, where experimental pressures vs depth have been plotted for comparison with Brockhurst's prediction and with the pressures to be expected

CONFIDENTIAL

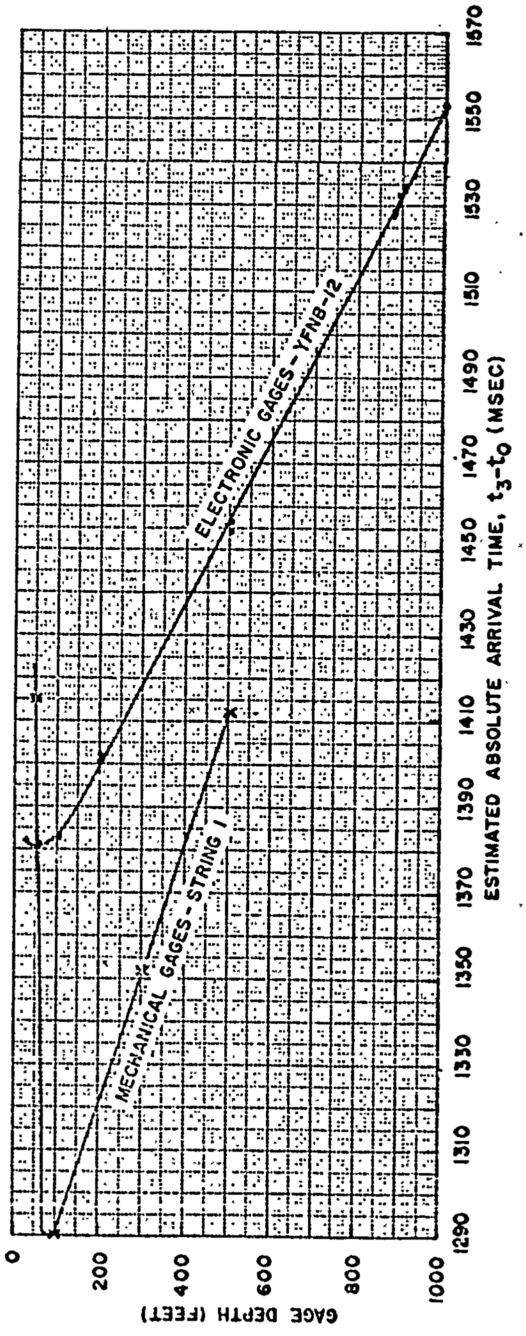

Fig. 9.13—Arrival times of cavitation pulse.

SECRET — RESTRICTED DATA

CONFIDENTIAL

CONFIDENTIAL

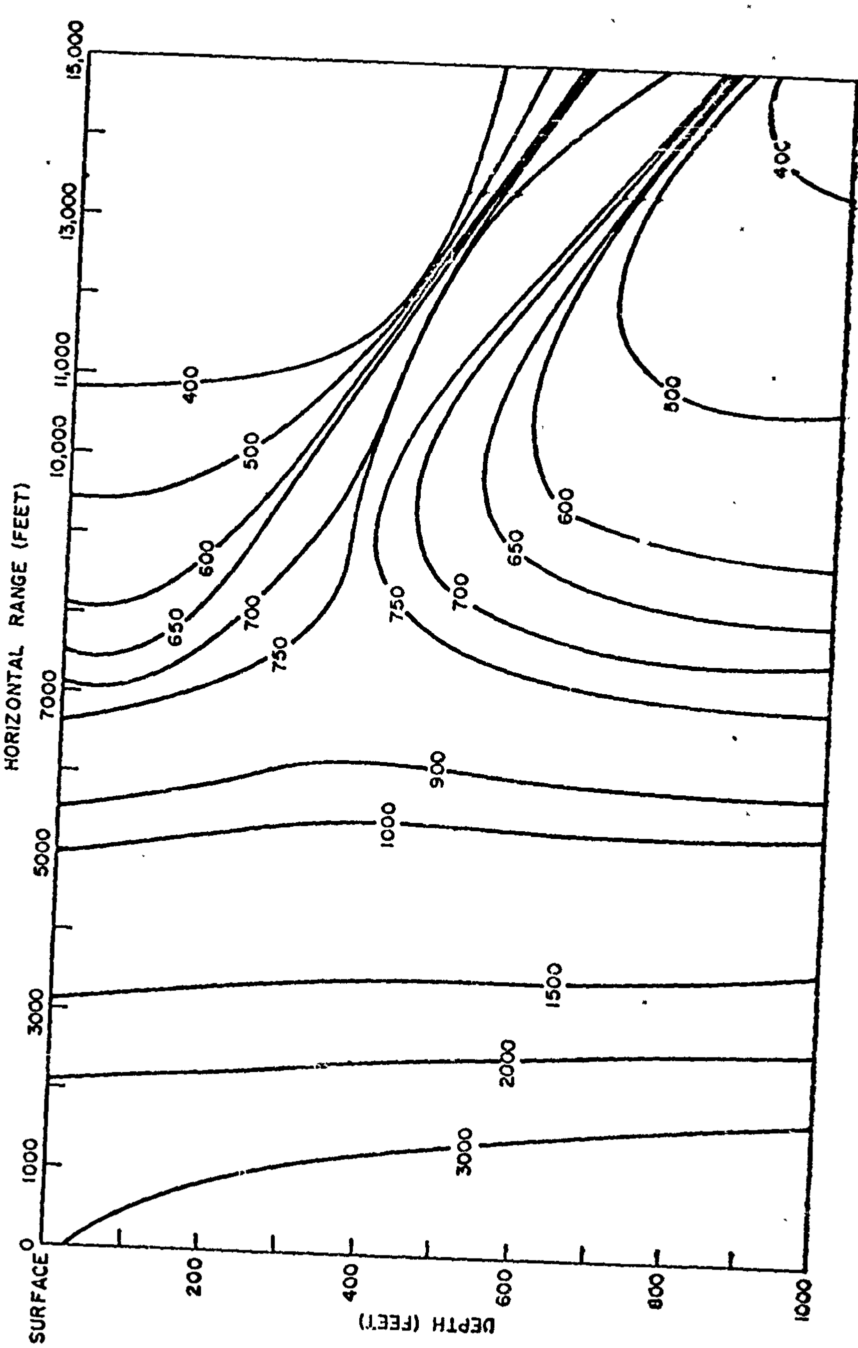

Fig. 9.14—Isobars (pounds per square inch) calculated from Brockhurst.

CONFIDENTIAL

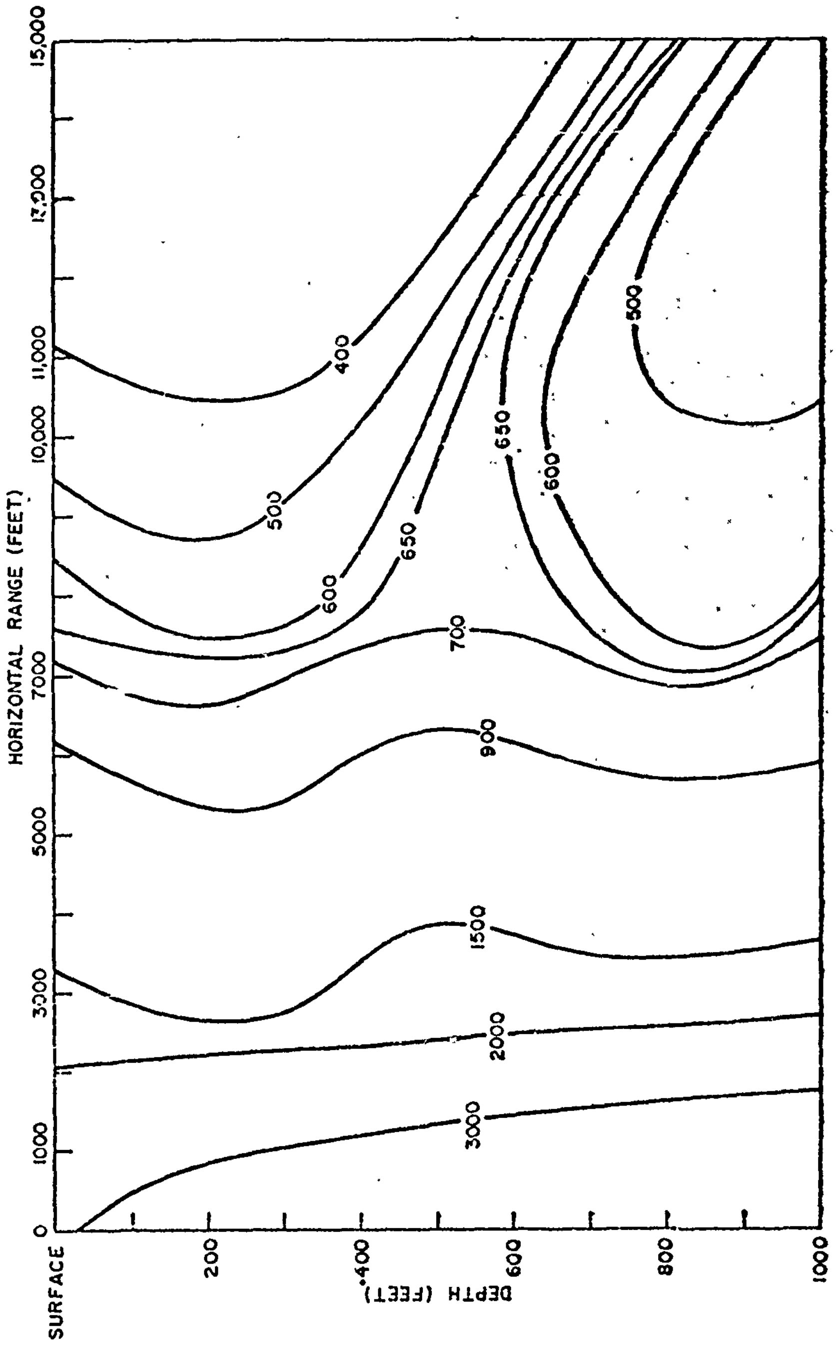

Fig. 9.15—Smoothed isobars (pounds per square inch) based on NOL and NRL Wigwam data.

CONFIDENTIAL

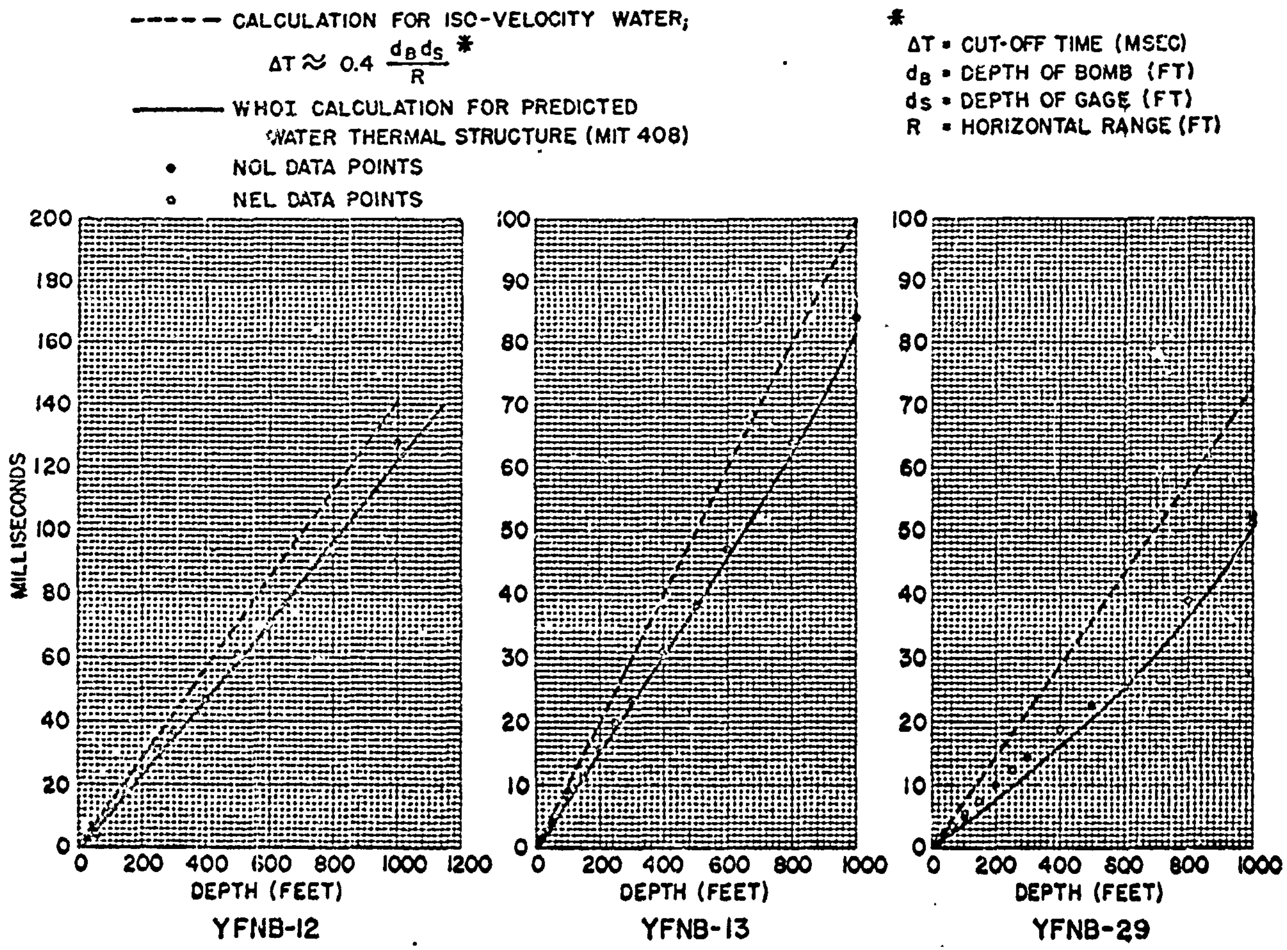

Fig. 9.16—Cutoff times for initial shock.

CONFIDENTIAL

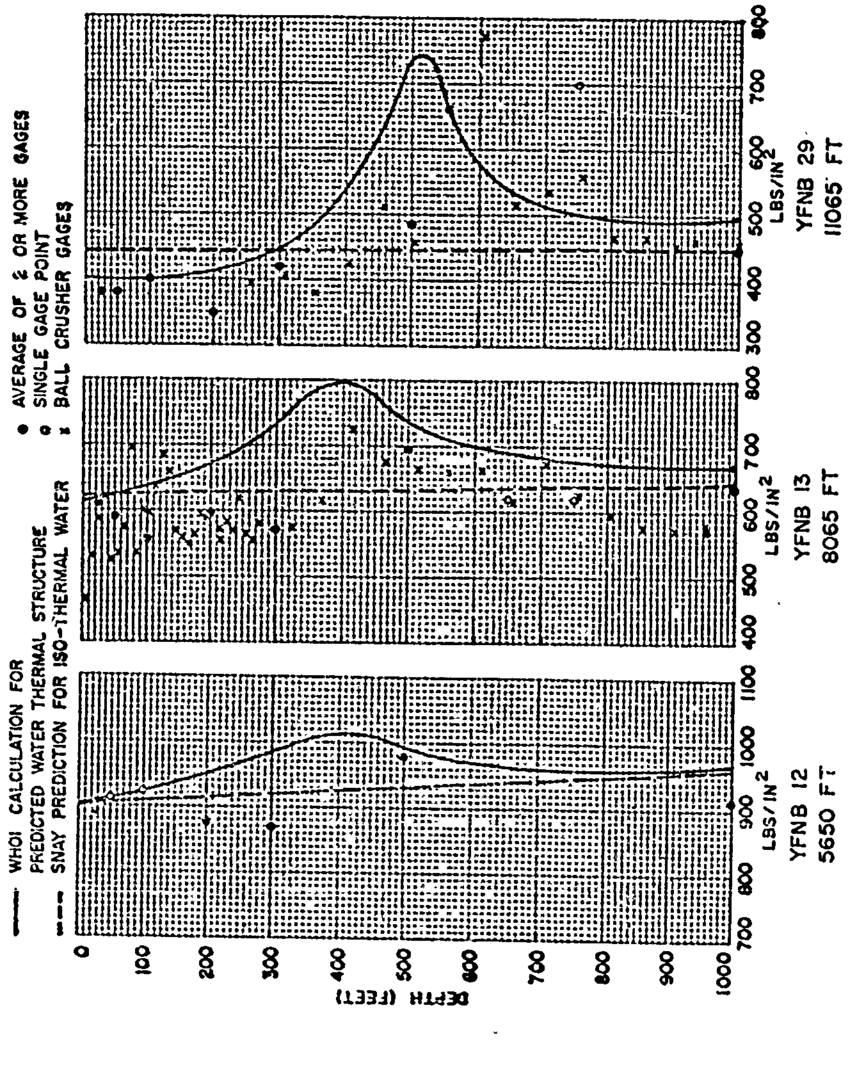

Fig. 9.17—Peak pressure vs depth.

in a homogeneous medium. Although there were some differences, it is apparent that the predicted refraction effect was substantially correct. Probably the principal evident difference was that the experimental pressure peaks occurred 100 to 200 ft lower than predicted. (The Wiancko gage values used in this figure were not corrected by the technique described in Sec. 9.2.)

9.9 WIGWAM COMPARED WITH CROSSROADS BAKER AND CASTLE

A comparison of the underwater peak pressure–distance curves from Wigwam, Crossroads Baker, and several Castle shots is presented in Fig. 9.18, all reduced to 1 kt (radiochemical yield). The Wigwam data used in this graph, which are also given in Table 9.7, were calculated from reference 2 and from Tables 8.3 to 8.6 by cube-root scaling from 32 kt (radiochemical yield). The Crossroads data were calculated by cube-root scaling from Table 6 of Enclosure C of Volume I of reference 15, assuming a 19-kt radiochemical yield. The Castle data represent coarse averages given in Table 7.7 of reference 16. The straight lines through the Castle and Crossroads data were fitted by eye. The line through the Wigwam data is the free-field curve (see Sec. 9.2 for the equation) for 1.44×10^6 lb of TNT. This value was arrived at from the data in Sec. 9.2 as follows:

$$\frac{\text{Best TNT yield as fitted to data}}{\text{Radiochemical yield}} = \frac{46.2 \times 10^6 \text{ lb}}{32 \text{ kt (radiochemical yield)}}$$

$$= 1.44 \times 10^6 \text{ lb of TNT per kiloton (radiochemical yield)}$$

Before further discussion of the significance of Fig. 9.18, the following few remarks on the nature of the Crossroads Baker and Castle data are appropriate.

As was stated in Sec. 2.2.5, the method of waterproofing used on Crossroads may have affected the response of the ball-crusher gages. Because the tests made for Wigwam on waterproofing did not simulate the Crossroads conditions adequately, it is impossible to say whether the Crossroads data required correction. It is entirely possible, however, that Operation Hardtack, which is to be conducted under conditions similar to Crossroads, will provide a definite answer to the question. In other words, on Hardtack it is planned to use some gages waterproofed in the Crossroads manner to obtain data for comparison with data from gages waterproofed in the Wigwam manner and from gages with no waterproofing. These results may enable the Crossroads data, which depend heavily on ball-crusher measurements, to be modified and may lead to improved Crossroads underwater pressure results.

The Crossroads Baker shot was fired at about mid-depth (90 ft) in Bikini Lagoon and had a radiochemical yield of 19 kt, according to reference 15.

The Castle data represent averaged values from four large surface shots (yields from 1.7 to 15.5 Mt) as measured at various depths in the lagoon (180 ft deep). The underwater pressures as measured by both pressure-time and peak-pressure gages were of the order of magnitude of the air blast at the surface of the lagoon. The origin of the peak value was sometimes seismic "rumble" and sometimes air blast, but no true underwater shock wave could be definitely isolated.

The principal point of interest of Fig. 9.18 is the indication it presents of the attenuation of pressure arising from the presence of the top and bottom surfaces. As may be seen, the Wigwam points, which were selected to be as free as possible from reflection and refraction effects, fall along the TNT pressure-distance decay curve (slope 1.13); whereas the Crossroads data decay much more rapidly (slope 1.7). The Castle data, which are not indicative of true underwater pressures or any other single phenomenon because of their heterogeneous origin, decay with a slope of approximately 2. In addition to this, the region of conventional target interest, say 600 to 1000 psi, extends out approximately twice as far for the Wigwam as for the Crossroads Baker geometry. As far as the Castle data are concerned, no experimental points were measured which even approached this region of conventional target interest. Although this graph (Fig. 9.18) only points out the obvious, it may be of value to have on a single sheet a

CONFIDENTIAL

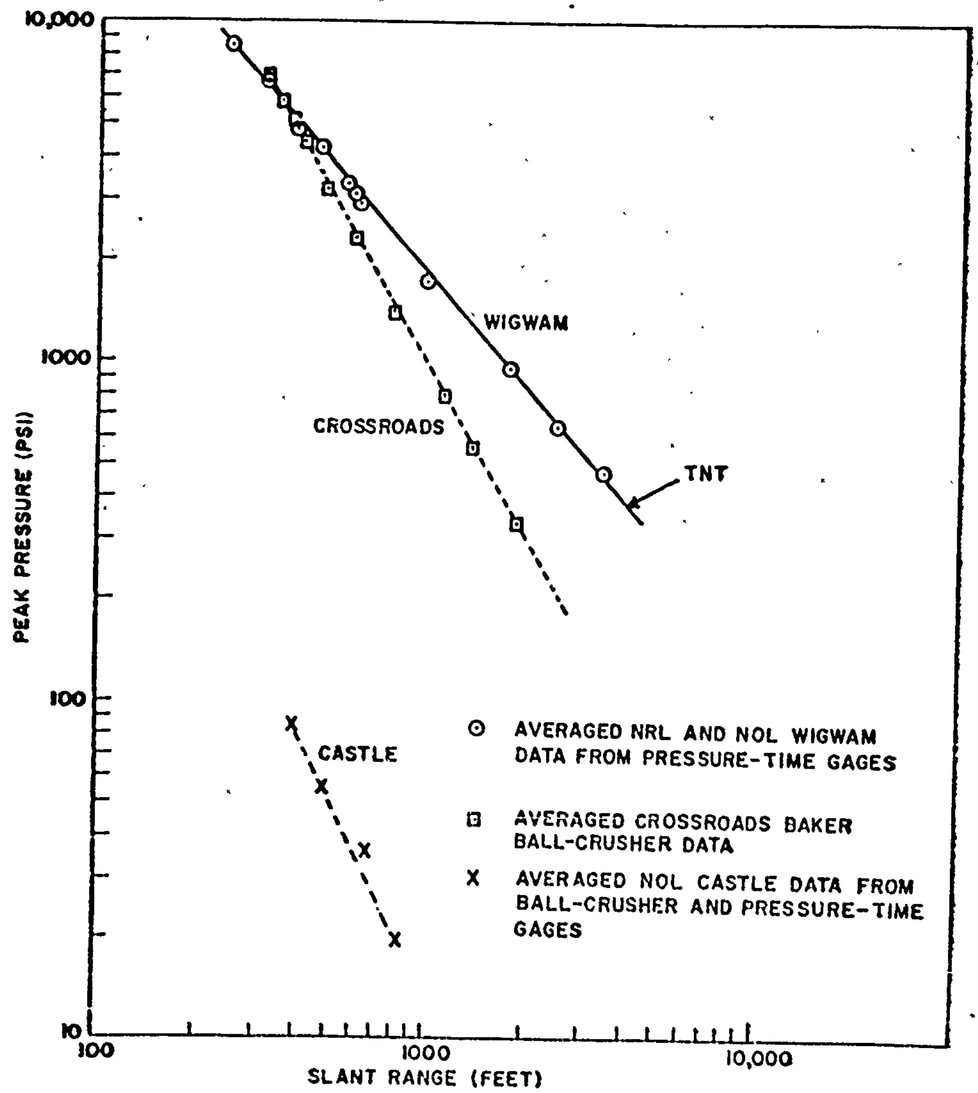

Fig. 9.18—Crossroads Baker, Wigwam, and Castle underwater peak pressures vs distance, reduced to 1 kt (radiochemical yield).

Table 9.7—PEAK PRESSURES VS DISTANCE, REDUCED TO 1 KT (RADIOCHEMICAL YIELD)

	Range in ft for 1 KT(RC)	Peak Pressure in PSI	Source of Data
CROSSROADS	312	7000	Ball Crusher Results at Mid-Depth from Table 6, Enclosure C of Vol. I - "Report of the Technical Director Operation CROSSORADS", SRD, 1 Dec. 1946 (Calculated from Yield of 19 KT(RC))
	347	5900	
	373	5200	
	405	4400	
	478	3200	
	582	2300	
	772	1400	
	1140	800	
	1386	560	
	1870	330	
WIGWAM	242	8586	Averaged Values (Geometric) from WT-1006 - Operation WIGWAM - Project 1.2.1 "Free Field Pressures, Station Zero", SRD, Dec. 1955 (Calculated from Yield of 32 KT(RC))
	304	6700	
	378	4877	
	455	4253	
	546	3384	
	576	3129	
	592	3051	
	599	2932	
	954	1740	Average Values (Geometric) from Table 8.3, 8.4, 8.5 and 8.6 of this Report (Calculated from Yield of 32 KT(RC))
	1710	951	
	2440	649	
	3340	480	
CASTLE	391	~86	From Table 7.7 of WT-908 (NOL portion) Operation CASTLE - Project 1.4 "Underwater Pressure Measurements", SRD, Oct. 1955 (Calculated from Yields of various CASTLE shots)
	485	~56	
	675	~36	
	836	~19	

SECRET - RESTRICTED DATA

CONFIDENTIAL

handy comparison of nearly all the significant underwater pressure measurements made on nuclear bursts to date.

REFERENCES

1. Explosion Effects Data Sheets, NAVORD Report 2986, U. S. Naval Ordnance Laboratory, White Oak, Md., 14 June 1955.
2. Free-field Pressures, Station Zero, Operation Wigwam Project 1.2.1 Report, WT-1006.
3. H. G. Snay et al., Predictions of Underwater Explosion Phenomena, Operation Wigwam Project 1.1 Report, WT-1004.
4. A. B. Arons, J. Acoust. Soc. Amer., 26: 343 (1954).
5. R. H. Cole, "Underwater Explosions," Princeton University Press, 1948.
6. Physical Oceanography of the Test Area, Operation Wigwam Project 2.8 Report, WT-1019.
7. J. F. Evernden, Love-Wave Dispersion and the Structure of the Pacific Basin, Bull. Seism. Soc. Am., 44: 1-5 (1954).
8. M. Ewing, G. H. Sutton, and C. B. Officer, Jr., Seismic Refraction Measurements in the Atlantic Ocean, Part VI; Typical Deep Stations, North American Basin, Subb., Bull. Seism. Soc. Am., 44: 21-38 (1954).
9. D. A. Wilson, B. A. Cotter, and R. S. Price, The Determination of Peak Pressure of an Underwater Explosion from a Study of the Initial Dome Velocity, BuOrd NAVORD Report 13-47.
10. E. H. Kennard, Underwater Explosions: A Summary of Results, DTMB Report C-334, February 1951.
11. J. E. Henderson et al., University of Washington Crossroads Technical Instrumentation Report, Tests Able and Baker, Vol. IV, Original Data, Linear Time Axis Recorder.
12. Ibid., Vol. V, Original Data, Logarithmic Time Axis Recorder.
13. C. W. Nelson and C. F. Garland, Analysis of Underwater Explosion Data — Test Baker, Progress Report No. 5, University of California, Contract NObs-47436, June 1951.
14. R. R. Brockhurst, Predictions of the Effect of Refraction on Peak Pressure and Duration of Explosion Pressure Waves, Woods Hole Oceanographic Institution Report, 54-14, March 1955.
15. Report of the Technical Director, Operation Crossroads, 1 December 1946.
16. C. J. Aronson, E. J. Culling, and J. P. Slifko, Underwater Pressure Measurements, Operation Castle Project 1.4 Report, WT-908 (NOL portion), NOLR-1209, October 1955.

SECRET – RESTRICTED DATA

CONFIDENTIAL

CHAPTER 10

SUMMARY OF RESULTS

This Chapter is designed to serve as a handy summary of the data presented and the conclusions reached in the body of the report.

10.1 SUMMARY OF INSTRUMENTATION PERFORMANCE

10.1.1 Ball-crusher Gages

1. Results from the YFNB stations indicated satisfactory operation and agreement with electronic gages.
2. The free-floating buoy support system for the ball crushers was unsatisfactory, and all stations of this nature were lost.
3. The waterproofing technique and hydrostatic loading correction were satisfactory.
4. The results of the $\frac{3}{8}$-in. gages were higher than for the $\frac{5}{32}$-in. gages.

10.1.2 Mechanical Pressure-Time Gages

1. These gages satisfactorily backed up the electronic gage system, particularly in the region between the zero barge and the YFNB-12, where no other gages operated successfully.
2. The free-floating wooden buoy and spar support system for the mechanical pressure-time gages was successfully used.
3. Peak-pressure measurements from mechanical pressure-time gage records were believed to be good to 12 per cent.
4. Pressure distortion from shock caused no difficulty in the mechanical pressure-time records.
5. Although there was some apparent hysteresis, the mechanical recording features were successful; for example, response to step pressure pulses was less than 1 msec.
6. Timing-measurement accuracies over short periods were good to ± 2 msec. Over periods greater than 1 sec, a timing accuracy of about 1 per cent was achieved.

10.1.3 Electronic Pressure-Time Gages

1. The tourmaline piezoelectric and the Wiancko electromechanical gages operated satisfactorily and gave consistent results to within a few per cent.
2. Rise times from Wiancko gages of about $1\frac{1}{2}$ msec were realized, although the gage itself was capable of rise times of about 0.3 msec.
3. The piezoelectric gage records were judged to be essentially free from such effects as cable signals, pyroelectric effects, first-time gage effects, and frequency distortions.

4. The Wiancko gage records were judged to be essentially free from acceleration effects and hysteresis. (See Sec. 10.1.4 for other comments pertinent to electronic pressure-time gages.)

10.1.4 Electronic Recording System

1. The Ampex system gave slightly better accuracy than the Davies system.
2. The piezoelectric linear channels, with an estimated accuracy of between $3\frac{1}{2}$ and $4\frac{1}{2}$ per cent, were superior to the estimated accuracy for the Wiancko channels of 6 to $6\frac{1}{2}$ per cent and to the estimated accuracy for the piezoelectric log channels of about 12 per cent.
3. The calibration-voltage generator might have been improved by use of a ground or zero voltage between each step.
4. The L-C timing oscillator was satisfactory, and the tuning fork did not seem to be needed.
5. The scaler, which gave coded timing marks, was unsatisfactory.
6. The use of more linear (piezoelectric) amplifiers with wide ranges would have been better than the use of the log channels.
7. If the Wiancko oscillators, although satisfactory, had been improved, they could have eliminated the requirement for the buffer amplifier.
8. Unitized construction was a valuable technique, and it might be improved by the use of printed circuits.
9. The playback system was too cumbersome and inflexible.

10.1.5 Mechanical Arrays

1. The suspension system used on the modified LCM's was unsuccessful. Its failure was attributed to the fact that the weather was more severe than was contemplated by the designers.
2. Attachment of buoys to the tow cable must be easier and sturdier than on Wigwam so that chafing can be completely eliminated.
3. LCM's were, in general, satisfactory instrumentation platforms but not so satisfactory as the ships were.
4. The trailers in the YFNB's were highly satisfactory instrumentation shelters, and the YFNB winch systems performed smoothly with good control.
5. The YFNB booms were slightly too short to completely eliminate cable chafing.

10.2 SUMMARY OF DATA

10.2.1 Gage Locations

1. The distances of the electronic gages from SZ were determined to within $\frac{1}{2}$ per cent, in the region 3000 to 12,000 ft from the charge, by means of surface photographs, shock arrival times, and aerial mosaics.
2. The array was surging slightly as indicated by comparison of aerial mosaics taken at −50, −40, and −30 min before zero time. Additional surging was indicated by the shock arrival data.
3. The NOL electronic gage strings slanted slightly toward the charge from the surface, according to time-of-arrival data.

10.2.2 Characteristics of Pressure-Time Signals

Although there was considerable variation among the pressure-time records, they had the following general characteristics in order of time:

1. An initial shock wave with a surface cutoff, followed by a negative phase.
2. A cavitation pulse which approximated in magnitude the initial shock close-in but which became negligible beyond about a mile from SZ.
3. The first bubble pulse which, uncorrected, had a single sharp pip after a slow rise.

4. Multiple peaked low-amplitude reflections of the initial shock wave from the bottom and shallow sublayers.

5. Multiple peaked pulses from the second bubble.

6. Multiple peaked low-amplitude reflections of the primary shock wave from deep subsurface layers.

7. Small signals perhaps arising from third bubble pulses.

10.2.3 Free-field Shock Effects Vs Distance

1. The pressure-distance curve for free water as determined by the 1000-ft electronic gages on the YFNB's 12 and 13 appeared similar to that predicted by Project 1.1 and to that from TNT.

2. The reduced energy flux density vs distance curve appeared to agree well with a curve calculated for the same yield of TNT as would make the pressure-distance curves agree. However, this was fortuitous since the TNT curve was integrated over a longer interval than the Wigwam curves. This indicated that the pressure-time curves for Wigwam and TNT may not have been similar or that refraction effects were present.

3. The same conclusion as in 2 above was reached when the reduced impulse from Wigwam was compared with that from TNT.

4. Although time constants were measured, no great reliability can be assigned to them because of the scatter existing in the data and the fact that they varied with depth. Furthermore, the shock-wave decay rates at the YFNB's 13 and 29 deviated from their initial values at times equal to $\theta/2$ or less. This also indicated a possible difference between TNT and Wigwam pressure-time curves.

10.2.4 Bubble Effects

1. The first bubble pulse, after reconstruction to eliminate the effects of surface reflection, showed that the sharp-fronted wave, so obvious in the uncorrected records, occurred before the bubble minimum and was of lower net amplitude than the main bubble pulse.

2. Second and third bubble pulses were measured without correction.

3. Average bubble periods were t_{B1} = 2.878 sec, t_{B2} = 2.6 sec, and t_{B3} = 1.9 sec.

4. The maximum amplitude, as measured on the deep gages from the YFNB-12, of the corrected bubble pulse was about 25 per cent of that of the peak of the shock wave.

5. The maximum bubble radius was calculated to be 375 ft, based on the first bubble period.

6. Migration up to the time of the emission of the sharp pip on the first bubble pulse was measured to be about 400 ft. No satisfactory migration measurements were made for the later pulses.

7. No surface phenomena or bottom reflections from bubbles were detected beyond the region covered by the spray dome from the initial shock.

10.2.5 Reflections

1. There were at least three bottom reflections, all of them attributable to the primary shock.

2. This led to the conclusion that the primary shock was reflected (1) off the sediments forming the regular bottom at about 15,000 ft, (2) off a subbottom of basalt starting at about 16,000 ft and extending about 21,000 ft, and (3) off an ultrabasic layer below the basalt.

3. A vertical pressure component of over 160 psi was necessary to produce a spray dome. On this criterion a patch of spray was predicted and found to occur from a subbottom reflection farther out from SZ than the YFNB-29.

10.2.6 Cavitation Effects

1. Apparent evidence of cavitation occurred on strings located at 2900 ft and 5600 ft from surface zero.

2. The ratio of cavitation peak pressure to shock peak pressure was from $\frac{1}{6}$ to $\frac{1}{2}$ at 2900 ft and from $\frac{1}{13}$ to $\frac{1}{4}$ at 5600 ft.

3. The duration ranged from 40 to 400 msec.

4. No ranging of the cavitation pulses was possible.

10.2.7 Refraction Effects

1. The effect of the temperature structure of the water in refracting the shock wave was essentially as predicted on peak pressure and pulse duration as far out as the measurements extended (about a 12,000-ft range).

2. The result was that the pressures at depths of 400 to 700 ft at the ranges of the YFNB's were greater than they were at other depths on the same gage strings.

3. Positive shock durations were appreciably shortened from those to be expected in a homogeneous medium.

10.2.8 Comparisons with Underwater Pressures from Other Nuclear Tests

1. The Wigwam pressure-distance curve in the region of target interest and at depths not seriously affected by refraction fell off at a rate of 1.13 (similar to that from TNT), compared with 1.7 from Crossroads Baker and 2.0 from Castle. Differences were attributed to surface and bottom effects.

2. The pressure region of 600 to 1000 psi extended out twice as far on Wigwam as on Crossroads Baker when data for both were reduced to 1 kt (radiochemical yield). Reduced Castle data were not measured in close enough to be within the 600-psi region.

10.2.9 TNT Equivalents

1. From shock-wave peak pressure vs distance, 46.2×10^6 lb of TNT.

2. From bubble-period measurements, 53.6×10^6 lb of TNT.

3. From LASL radiochemical measurements, 32 metric kt (radiochemical yield) = 70.6×10^6 lb of TNT.

4. Hence:

$$\frac{46.2}{70.6} = 0.65 = \text{shock-wave efficiency}$$

and

$$\frac{53.6}{70.6} = 0.76 = \text{bubble efficiency}$$

10.2.10 Summary of Averaged Values

Averaged values of certain quantities of interest, which were measured by the 1000-ft electronic gages on the YFNB's, are listed below:

	YFNB-12	YFNB-13	YFNB-29
P_1 (arithmetic), psi	951	649	479
P_1 (geometrical), psi	951	649	480
θ (arithmetic) (msec)	35.8	47.8	56.3
I (geometrical) (lb-sec/in.^{2})	33.2	23.7	14.7
E (arithmetic) (in.-lb/in.^{2})	2697	1547	645.5

APPENDIX A

EFFECTS ON SONAR

Although it is beyond the scope of this report and the function of Project 1.2, some information on the effect of the Wigwam shot on sonar gear has been made available to the authors as a result of inquiries to the vessels present in the vicinity of the Operation. Since this information is not generally known, it is included here because it is the type of data needed for the design of tactics to be used with atomic depth charges.

Each of 12 ships was queried for information on the following points:

1. The distance that the ship was from the center of burst.
2. Type of sonar gear on the ship at the time of the test.
3. Time before zero that the sonar was turned off.
4. Time after zero that the sonar was turned on.
5. Condition of reception at the time sonar was turned on after time zero.
6. Time after zero that sonar would have been operable in the detection of a target.
7. Estimation of the area blanketed by the burst.
8. Any effects noted on the operation of the ship's fathometer.

Of the replies received at this time, only those from the USS Blue (DD-744), the USS Walke (DD-723), and the USS McKean (DDR-784) are of interest, since their sonar gear was not turned off. Their answers are given in Secs. A.1 to A.3.

A.1 USS BLUE (DD-744)

The following answers were submitted by the USS Blue (DD-744):

1. The USS Blue (DD-744) was 25 miles from the center of the burst.
2. QHBa sonar gear was on the ship at the time of the burst.
3. Sonar was switched from "Echo Ranging" to "Listen" 30 min prior to zero time.
4. Sonar was switched from "Listen" to "Echo Ranging" 30 min after zero time.
5. The reception was good at the time the sonar gear was switched to "Echo Ranging" after zero time.
6. It is believed that the sonar equipment would have been operable in the detection of a target 5 min after zero time.
7. We were unable to estimate the area blanketed by the burst since this ship's area was not affected.
8. The fathometer was not in operation at the time of the burst.

The following additional observations were noted:

1. Twenty-seven seconds after zero time the blast was heard on the speakers on sonar.
2. Approximately 5 sec later one-half of the scope blanked out for about 1½ sec.

A.2 USS WALKE (DD-723)

In answer to the queries the following information was submitted:

1. The USS Walke bore 315°T at a distance of 6 miles from SZ at explosion time.
2. The USS Walke was then equipped with QHBa sonar.
3. The sonar equipment was not secured at any time during the test. At zero time the QHBa was on "Listen," and the gain was on a medium setting (5). Immediately after the explosion the gain was turned to minimum setting. The entire scope was blanked by the initial shock wave and remained completely clouded for approximately 13 to 15 sec. The initial sound received was a deafening roar much greater in intensity but not unlike that of a depth charge exploding nearby. The scope cleared somewhat after 15 sec, but the effect of the explosion continued for 60 to 80 sec. The noise remained quite audible despite the minimum gain setting, and bright crackling pips of light similar to those made by porpoises appeared on the scope. Sonar operators observed three distinct shock waves.
4. After 90 sec the QHBa presentation returned to normal, and it would have been possible to detect targets nearby after this interval of time had elapsed.
5. The scope was entirely blanked by the initial blast. No wedge-shaped noise spoke was ever discernible. Within the limits of QHBa sonar (3750 yards), no water disturbance was in evidence. The Walke can make no reliable estimate of the ocean area blanked by the burst.
6. The ship's fathometer was not in operation at zero time.
7. The AN/UQC-1B underwater telephone was energized and adjusted to a full gain setting at blast time. A noise similar in every respect to that received on the QHBa was heard on the UQC. The gain was immediately cut to 0, but the noise persisted.

The Walke forwarded enclosures (1) and (2)* for their possible scientific value. The grid viewer for BT #685 was included. The BT has since been lost at sea. The Walke made one drop (drop 20) 7 min prior to zero time; unfortunately, the slide has since been destroyed. The recorded sonar message was sonar long 300/25 Mike. BT slides 21 through 35 were forwarded. Slide 21 was in the water 1 min after zero time, and slide 35 was dropped 2 hr 30 min after zero time. It should be noted that the times inscribed on the slides are in hours and minutes after zero time and not in local or Greenwich hours. The Walke's position was relatively constant during drops 20 through 35. Sonar conditions were unusually good during Operation Wigwam and were not apparently adversely affected by the atomic explosion. The Walke consistently held contact on ships of the array at ranges greater than 3000 yards.

Other than during the initial shock wave, the Walke believed that there was no effect on echo ranging by an atomic blast of the Wigwam caliber at a distance of 6 miles or greater. Any other opinions expressed would be pure conjecture; however, it was thought that echo ranging would be possible at ranges considerably closer than 6 miles within 90 sec after the initial explosion of a Wigwam-caliber bomb.

A.3 USS McKEAN (DDR-784)

This ship supplied the information requested, as follows:

1. This ship was 10,000 yards from the center of burst.
2. The sonar equipment was type QHBa.
3. The sonar equipment was in operation during the entire period of the test.
4. Not applicable.
5. Reception was good before and after the burst. The scope was blanked for a short period by turbulence immediately following the burst.
6. The sonar could have detected a target between 1500 and 2000 yards within 45 sec after the burst.

---

*Enclosures (1) and (2) were bathythermograph (BT) slides and a viewer. These were forwarded to A. B. Focke, the Scientific Director.

7. The entire field of the scope was blanked for about 30 sec, gradually clearing on the side away from the burst and clearing enough for detection within 45 sec.

8. No effects were noted on the operation of the ship's fathometer.

DISTRIBUTION

Military Distribution Categories 5-23 and 5-60

ARMY ACTIVITIES

Asst. Dep. Chief of Staff for Military Operations, D/A, Washington 25, D.C. ATTN: Asst. Executive (R&SW)	1
Chief of Research and Development, D/A, Washington 25, D.C. ATTN: Atomic Division	2
Chief of Ordnance, D/A, Washington 25, D.C. ATTN: ORDTX-AR	3
Chief Signal Officer, D/A, P&O Division, Washington 25, D.C. ATTN: SIGRD-8	4–6
The Surgeon General, D/A, Washington 25, D.C. ATTN: Chief, R&D Division	7
Chief Chemical Officer, D/A, Washington 25, D.C.	8–9
The Quartermaster General, D/A, Washington 25, D.C. ATTN: Research and Development Div.	10
Chief of Engineers, D/A, Washington 25, D.C. ATTN: ENGNB	11–15
Chief of Transportation, Military Planning and Intelligence Div., Washington 25, D.C.	16
Commanding General, Headquarters, U. S. Continental Army Command, Ft. Monroe, Va.	17–19
President, Board #1, Headquarters, Continental Army Command, Ft. Sill, Okla.	20
President, Board #2, Headquarters, Continental Army Command, Ft. Knox, Ky.	21
President, Board #4, Headquarters, Continental Army Command, Ft. Bliss, Tex.	22
Commanding General, U.S. Army Caribbean, Ft. Amador, C.Z. ATTN: Cml. Off.	23
Commander-in-Chief, European Command, APO 128, New York, N.Y.	24
Commander-in-Chief, Far East Command, APO 500, San Francisco, Calif. ATTN: ACofS, J-3	25–26
Commanding General, U.S. Army Europe, APO 403, New York, N.Y. ATTN: OPOT Div., Combat Dev. Br.	27–28
Commanding General, U.S. Army Pacific, APO 958, San Francisco, Calif. ATTN: Cml. Off.	29–30
Commandant, Command and General Staff College, Ft. Leavenworth, Kan. ATTN: ALLLS(AS)	31–32
Commandant, The Artillery and Guided Missile School, Ft. Sill, Okla.	33
Secretary, The Antiaircraft Artillery and Guided Missile School, Ft. Bliss, Tex. ATTN: Maj. Gregg D. Breitegan, Dept. of Tactics and Combined Arms	34
Commanding General, Army Medical Service School, Brooke Army Medical Center, Ft. Sam Houston, Tex.	35
Director, Special Weapons Development Office, Headquarters, CONARC, Ft. Bliss, Tex. ATTN: Capt. T. E. Sibarer	36
Commandant, Walter Reed Army Institute of Research, Walter Reed Army Medical Center, Washington 25, D.C.	37
Superintendent, U.S. Military Academy, West Point, N.Y. ATTN: Prof. of Ordnance	38
Commandant, Chemical Corps School, Chemical Corps Training Command, Ft. McClellan, Ala.	39
Commanding General, Research and Engineering Command, Army Chemical Center, Md. ATTN: Deputy for RW and Non-Toxic Material	40
Commanding General, Aberdeen Proving Grounds, Md. (inner envelope) ATTN: for Director, Ballistics Research Laboratory	41–42
Commanding General, The Engineer Center, Ft. Belvoir, Va. ATTN: Asst. Commandant, Engineer School	43–45

UNCLASSIFIED

CONFIDENTIAL

Commanding Officer, Engineer Research and Development Laboratory, Ft. Belvoir, Va. ATTN: Chief, Technical Intelligence Branch	46
Commanding Officer, Picatinny Arsenal, Dover, N.J. ATTN: ORDBB-TK	47
Commanding Officer, Army Medical Research Laboratory, Ft. Knox, Ky.	48
Commanding Officer, Chemical Corps Chemical and Radiological Laboratory, Army Chemical Center, Md. ATTN: Tech. Library	49–50
Commanding Officer, Transportation R&D Station, Ft. Eustis, Va.	51
Director, Technical Documents Center, Evans Signal Laboratory, Belmar, N.J.	52
Director, Waterways Experiment Station, PO Box 631, Vicksburg, Miss. ATTN: Library	53
Director, Armed Forces Institute of Pathology, Walter Reed Army Medical Center, 6825 16th Street, N.W., Washington 25, D.C.	54
Director, Operations Research Office, Johns Hopkins University, 7100 Connecticut Ave., Chevy Chase, Md., Washington 15, D.C.	55
Commanding General, Quartermaster Research and Development Command, Quartermaster Research and Development Center, Natick, Mass. ATTN: CBR Liaison Office	56–57
Technical Information Service Extension, Oak Ridge, Tenn.	58–64

NAVY ACTIVITIES

Chief of Naval Operations, D/N, Washington 25, D.C. ATTN: OP-36	65–66
Chief of Naval Operations, D/N, Washington 25, D.C. ATTN: OP-03EG	67
Director of Naval Intelligence, D/N, Washington 25, D.C. ATTN: OP-922V	68
Chief, Bureau of Medicine and Surgery, D/N, Washington 25, D.C. ATTN: Special Weapons Defense Div.	69
Chief, Bureau of Ordnance, D/N, Washington 25, D.C.	70
Chief, Bureau of Ships, D/N, Washington 25, D.C. ATTN: Code 348	71
Chief, Bureau of Yards and Docks, D/N, Washington 25, D.C. ATTN: D-440	72
Chief, Bureau of Supplies and Accounts, D/N, Washington 25, D.C.	73
Chief, Bureau of Aeronautics, D/N, Washington 25, D.C.	74–75
Chief of Naval Research, Department of the Navy, Washington 25, D.C. ATTN: Code 811	76
Commander-in-Chief, U.S. Pacific Fleet, Fleet Post Office, San Francisco, Calif.	77
Commander-in-Chief, U.S. Atlantic Fleet, U.S. Naval Base, Norfolk 11, Va.	78
Commandant, U.S. Marine Corps, Washington 25, D.C. ATTN: Code A03H	79–82
President, U.S. Naval War College, Newport, R.I.	83
Superintendent, U.S. Naval Postgraduate School, Monterey, Calif.	84
Commanding Officer, U.S. Naval Schools Command, U.S. Naval Station, Treasure Island, San Francisco, Calif.	85
Commanding Officer, U.S. Fleet Training Center, Naval Base, Norfolk 11, Va. ATTN: Special Weapons School	86
Commanding Officer, U.S. Fleet Training Center, Naval Station, San Diego 36, Calif. ATTN: (SPWP School)	87–88
Commanding Officer, U.S. Naval Damage Control Training Center, Naval Base, Philadelphia 12, Pa. ATTN: ABC Defense Course	89
Commanding Officer, U.S. Naval Unit, Chemical Corps School, Army Chemical Training Center, Ft. McClellan, Ala.	90
Commander, U.S. Naval Ordnance Laboratory, Silver Spring 19, Md. ATTN: EE	91
Commander, U.S. Naval Ordnance Laboratory, Silver Spring 19, Md. ATTN: EH	92
Commander, U.S. Naval Ordnance Laboratory, Silver Spring 19, Md. ATTN: R	93
Commander, U.S. Naval Ordnance Test Station, Inyokern, China Lake, Calif.	94
Officer-in-Charge, U.S. Naval Civil Engineering Res. and Evaluation Lab., U.S. Naval Construction Battalion Center, Port Hueneme, Calif. ATTN: Code 753	95
Commanding Officer, U.S. Naval Medical Research Inst., National Naval Medical Center, Bethesda 14, Md.	96
Director, Naval Air Experimental Station, Air Material Center, U.S. Naval Base, Philadelphia, Pa.	97
Director, U.S. Naval Research Laboratory, Washington 25, D.C. ATTN: Mrs. Katherine H. Cass	98
Commanding Officer and Director, U.S. Navy Electronics Laboratory, San Diego 52, Calif.	99
Commanding Officer, U.S. Naval Radiological Defense Laboratory, San Francisco 24, Calif. ATTN: Technical Information Division	100–101

SECRET—RESTRICTED DATA

CONFIDENTIAL

UNCLASSIFIED

UNCLASSIFIED

CONFIDENTIAL

Commanding Officer and Director, David W. Taylor Model Basin, Washington 7, D.C. ATTN: Library	102
Commander, U.S. Naval Air Development Center, Johnsville, Pa.	103
Commanding Officer and Director, U.S. Naval Engineering Experiment Station, Annapolis, Md. ATTN: Code 705	104
Technical Information Service Extension, Oak Ridge, Tenn. (surplus)	105–111

AIR FORCE ACTIVITIES

Asst. for Atomic Energy, Headquarters, USAF, Washington 25, D.C. ATTN: DCS/O	112
Director of Operations, Headquarters, USAF, Washington 25, D.C. ATTN: Operations Analysis	113
Director of Plans, Headquarters, USAF, Washington 25, D.C. ATTN: War Plans Div.	114
Director of Research and Development, Headquarters, USAF, Washington 25, D.C. ATTN: Combat Components Div.	115
Director of Intelligence, Headquarters, USAF, Washington 25, D.C. ATTN: AFOIN-IB2	116–117
The Surgeon General, Headquarters, USAF, Washington 25, D.C. ATTN: Bio. Def. Br., Pre. Med. Div.	118
Asst. Chief of Staff, Intelligence, Headquarters, U.S. Air Forces Europe, APO 633, New York, N.Y. ATTN: Directorate of Air Targets	119
Commander, 497th Reconnaissance Technical Squadron (Augmented), APO 633, New York, N.Y.	120
Commander, Far East Air Forces, APO 925, San Francisco, Calif. ATTN: Special Assistant for Damage Control	121
Commander-in-Chief, Strategic Air Command, Offutt Air Force Base, Omaha, Nebr. ATTN: Special Weapons Branch, Inspector Div., Inspector General	122
Commander, Tactical Air Command, Langley AFB, Va. ATTN: Documents Security Branch	123
Commander, Air Defense Command, Ent AFB, Colo.	124
Research Directorate, Headquarters, Air Force Special Weapons Center, Kirtland Air Force Base, N. Mex. ATTN: Blast Effects Research	125–126
Assistant Chief of Staff, Installations, Headquarters, USAF, Washington 25, D.C. ATTN: AFCIE-E	127
Commander, Air Research and Development Command, PO Box 1395, Baltimore, Md. ATTN: RDDN	128
Commander, Air Proving Ground Command, Eglin AFB, Fla. ATTN: Adj./Tech. Report Branch	129
Director, Air University Library, Maxwell AFB, Ala.	130–131
Commander, Flying Training Air Force, Waco, Tex. ATTN: Director of Observer Training	132–139
Commander, Crew Training Air Force, Randolph Field, Tex. ATTN: 2GTS, DCS/O	140
Commandant, Air Force School of Aviation Medicine, Randolph AFB, Tex.	141–142
Commander, Wright Air Development Center, Wright-Patterson AFB, Dayton, Ohio ATTN: WCOSI	143–148
Commander, Air Force Cambridge Research Center, LG Hanscom Field, Bedford, Mass. ATTN: CRQST-2	149–150
Commander, Air Force Special Weapons Center, Kirtland AFB, N. Mex. ATTN: Library	151–153
Commander, Lowry AFB, Denver, Colo. ATTN: Department of Special Weapons Training	154
Commander, 1009th Special Weapons Squadron, Headquarters, USAF, Washington 25, D.C.	155
The RAND Corporation, 1700 Main Street, Santa Monica, Calif. ATTN: Nuclear Energy Division	156–157
Commander, Second Air Force, Barksdale AFB, La. ATTN: Operations Analysis Office	158
Commander, Eighth Air Force, Westover AFB, Mass. ATTN: Operations Analysis Office	159
Commander, Fifteenth Air Force, March AFB, Calif. ATTN: Operations Analysis Office	160
Commander, Western Development Division (ARDC), PO Box 262, Inglewood, Calif. ATTN: WDSIT, Mr. R. G. Weitz	161
Technical Information Service Extension, Oak Ridge, Tenn. (surplus)	162–170

UNCLASSIFIED

OTHER DEPARTMENT OF DEFENSE ACTIVITIES

Asst. Secretary of Defense, Research and Development, D/D, Washington 25, D.C. ATTN: Tech. Library	171
U.S. Documents Officer, Office of the U.S. National Military Representative, SHAPE, APO 55, New York, N.Y.	172
Director, Weapons Systems Evaluation Group, OSD, Rm. 2E1006, Pentagon, Washington 25, D.C.	173
Armed Services Explosives Safety Board, D/D, Building T-7, Gravelly Point, Washington 25, D.C.	174
Commandant, Armed Forces Staff College, Norfolk 11, Va. ATTN: Secretary	175
Commander, Field Command, Armed Forces Special Weapons Project, PO Box 5100, Albuquerque, N. Mex.	176–181
Commander, Field Command, Armed Forces Special Weapons Project, PO Box 5100, Albuquerque, N. Mex. ATTN: Technical Training Group	182–183
Chief, Armed Forces Special Weapons Project, Washington 25, D.C. ATTN: Documents Library Branch	184–192
Technical Information Service Extension, Oak Ridge, Tenn. (surplus)	193–199

ATOMIC ENERGY COMMISSION ACTIVITIES

U.S. Atomic Energy Commission, Classified Technical Library, 1901 Constitution Ave., Washington 25, D.C. ATTN: Mrs. J. M. O'Leary (for DMA)	200–202
Los Alamos Scientific Laboratory, Report Library, PO Box 1663, Los Alamos, N. Mex. ATTN: Helen Redman	203–204
Sandia Corporation, Classified Document Division, Sandia Base, Albuquerque, N. Mex. ATTN: H. J. Smyth, Jr.	205–209
University of California Radiation Laboratory, PO Box 808, Livermore, Calif. ATTN: Clovis G. Craig	210–212
Weapon Data Section, Technical Information Service Extension, Oak Ridge, Tenn.	213
Technical Information Service Extension, Oak Ridge, Tenn. (surplus)	214–224

ADDITIONAL DISTRIBUTION

Commander, Operational Development Force, United States Atlantic Fleet, United States Naval Base, Norfolk 11, Va.	225